January 2015

Catalytic Conversion Of Crop Oil To Petrochemical Substitutes And Other Bio-Based Chemicals

Swapnil Liladhar Fegade

CATALYTIC CONVERSION OF CROP OIL TO PETROCHEMICAL SUBSTITUTES
AND OTHER BIO-BASED CHEMICALS

by

Swapnil Liladhar Fegade
Bachelor of Technology in Polymer Engineering,
University of Mumbai, Institute of Chemical Technology, India

A Dissertation

Submitted to the Graduate Faculty

of the

University of North Dakota

in partial fulfillment of the requirements

for the degree of

Doctor of Philosophy

Grand Forks, North Dakota
May
2015

This Dissertation, submitted by Swapnil Liladhar Fegade in partial fulfillment of the requirements for the Degree of Doctor of Philosophy from the University of North Dakota, has been read by the Faculty Advisory Committee under whom the work has been done and is hereby approved.

_____
Dr. Brian Tande Co-Chairperson

_____
Dr. Wayne Seames Co-Chairperson

_____
Dr. Michael Mann   Committee Member

_____
Dr. Evguenii Kozliak Committee Member

_____
Dr. Alena Kubátová   Committee Member

This dissertation meets the standards for appearance, conforms to the style and format requirements of the Graduate School of the University of North Dakota, and is hereby approved.

_____
Dean of the Graduate School

_____
Date

PERMISSION

Title   Catalytic Conversion of Crop Oil to Petrochemical Substitutes and Other
               Bio-Based Chemicals

Department   Chemical Engineering

Degree   Doctor of Philosophy

        In presenting this dissertation in partial fulfillment of the requirements for a
graduate degree from the University of North Dakota, I agree that the library of this
University shall make it freely available for inspection. I further agree that permission
for extensive copying for scholarly purposes may be granted by the professor who
supervised my dissertation work or, in his absence, by the chairperson of the department
or the dean of the Graduate School. It is understood that any copying or publication or
other use of this dissertation or part thereof for financial gain shall not be allowed without
my written permission. It is also understood that due recognition shall be given to me
and to the University of North Dakota in any scholarly use which may be made of any
material in my dissertation.

                                        Signature __Swapnil Fegade_____

                                        Date   ____05/04/2015_____

TABLE OF CONTENTS

LIST OF FIGURES

LIST OF TABLES

ACKNOWLEDGEMENTS

Thanks to my mother (Rajani Liladhar Fegade), father (Liladhar D. Fegade), sister (Sanghavi Chaudhari), and son (Arnav Swapnil Fegade) for continuously supporting me throughout my doctoral studies.

ABSTRACT

A two-step process was developed for the production of aromatic hydrocarbons from triacyl glyceride (TG) oils such as crop oils, algae oils, and microbial oils. In the first step, TG (soybean) oil was non-catalytically cracked to produce an organic liquid product (OLP). The resulting OLP was then converted into aromatic compounds in a second reaction using a zeolite catalyst, HZSM-5. In this second reaction three main factors were found to influence the yield of aromatic hydrocarbons, namely the SiO_2:Al_2O_3 ratio in the HZSM-5, the reaction temperature and the OLP-to-catalyst ratio. Upon optimization, up to 58 wt% aromatics were obtained. Detailed analyses revealed that most of the alkenes and carboxylic acids, and even many of the unidentified/unresolved compounds which are characteristic products of non-catalytic TG cracking, were reformed into aromatic hydrocarbons and *n*-alkanes. Instead of BTEX compounds that are the common products of alkene reforming with HZSM-5, longer-chain alkylbenzenes dominated the reformate (along with medium-size n-alkanes). Another novel feature of the two-step process was a sizable (up to 13 wt%) yield of alicyclic hydrocarbons, both cyclohexanes and cyclopentanes. At optimum conditions, the yields of coke (5 wt%) and gaseous products (14 wt%) were found to be lower than those in a corresponding one-step catalytic cracking/aromatization process. Thus this novel two-step process may provide a new route for the production of renewable aromatic hydrocarbons.

Aromatization of propylene was performed in a continuous reactor over HZSM-5 catalysts. A full-factorial design of experiments (DOE) methodology identified the effects of temperature (400-500 °C), Si:Al ratio (50-80), propylene feed concentration (8.9-12.5 mol%), and catalyst amount (0.2-1.0 g) on propylene conversion as well as the yields of benzene, toluene, *p*-xylene, *o*-xylene (BTX), and total BTX. The Si:Al ratio and amount of the HZSM-5 catalyst influenced all of the responses, while temperature impacted all the responses except the yield of *p*-xylene. An increase in feed concentration significantly increased the yields of benzene, toluene, and total BTX. An interaction between propylene feed concentration and catalyst amount influenced the yields of benzene, toluene, and total BTX. This interaction indicated that a higher feed concentration promotes aromatization at higher catalyst concentrations. By contrast, the interaction of Si:Al ratio with propylene feed concentration was found significant for *p*-xylene and *o*-xylene yields, but not for benzene and toluene, suggesting that xylenes are synthesized on different sites than those for benzene and toluene. These interaction effects demonstrate how the use of DOE can uncover significant information generally missed using traditional experimental strategies.

The catalytic conversion of propylene to BTX (benzene, toluene, xylenes) over nanoscale HZSM-5 zeolite was studied. A full-factorial design of experiments (DOE) methodology identified three factors which significantly affected the aromatization process: temperature (400-500 °C), propylene feed concentration (8.9-12.5 mol%), and catalyst amount (0.2-1.0 g). An increase in all three factors significantly increased the

yields of benzene, toluene, and total BTX but decreased the yield of xylene. A DOE method was used to determine significant interaction effects which may be missed using parametric experimental strategies. The observed effects showed that nanoscale HZSM-5 catalyst is better suited for facilitating cracking rather than aromatization reactions presumably due to the smaller pore availability compared to micro-sized zeolites. Select experiments in a batch reactor with soybean oil as a feedstock showed that the nanoscale zeolite strongly retained large amounts of water, presumably within its pores, despite prior high temperature calcinations.

CHAPTER I

INTRODUCTION AND BACKGROUND

Project Motivation

Fossil fuels, such as crude oil and natural gas, are the primary source for many of the world's most important chemicals, polymers, and composite materials. Petroleum is the only source of petrochemicals. Although most crude oil is refined into products for the transportation fuels market, a notable portion of it is used as a feedstock for aromatic compounds and monomers for plastics and composites [1, 2]. However, there is consensus in the scientific community that global climate change is and will continue to occur due to the vast emission of fixed carbon into the atmosphere due to the extensive use of fossil fuels [1, 3, 4]. Previous research at the University of North Dakota (UND) [5, 6] and elsewhere [7-9] has led to the successful development processes that can generate replacements for petroleum based fuels. However, there is still a need to identify ways to use renewable feedstocks for producing chemicals and materials, which could potentially replace petroleum derived chemicals and plastics materials.

Prior work performed under UND's Sustainable Energy Research Initiative and Supporting Education (SUNRISE) program has shown that during the non-catalytic (thermal) cracking of TAG oil, gaseous hydrocarbons such as methane, propane, propylene are generated [10] Similarly, during a single-step catalytic cracking of TAG oil a major gaseous product was propylene. So, the first task of this research was to explore the conversion of TAG oil cracking-derived propylene into aromatic compounds.

The organic liquid products (OLP's) obtained from the non-catalytic cracking of TAG oils consists primarily of alkanes and carboxylic acids, both of which can be processed and separated into various transportation fuels (e.g. jet fuel, diesel) and other by-products (e.g. naphtha). However, 10-20 % (wt % of feed oil) of these OLP's was found to be medium chain length (C_6-C_{12}) olefins [11, 12]. These olefins are undesirable for fuels applications. They need to be converted into more valuable products because it isn't possible to separate them from the alkanes reasonably and they led to oxidative stability problems in the fuel.

Hypotheses

In a previous catalytic cracking study at (UND SUNRISE) using a zeolite catalyst to convert TAG oil into an OLP, it was found that unacceptable levels of coke were formed resulting in catalyst deactivation. It was postulated [13] that the coke formation was primarily occurring as a secondary reaction due to the formation of radical intermediates during the initial TAG decomposition reactions. If true, then these reactions compete with secondary aromatization reactions while also inhibiting the ability of the catalyst to facilitate the desired reaction pathways. **The primary objective of the work presented in this dissertation was to test this hypothesis.**

To test this hypothesis and to develop a reaction sequence that would minimize catalyst deactivation due to coke formation on the catalyst surface, a two-step process was proposed [13]. In this proposed process the TAG oil is cracked non-catalytically under conditions favoring olefin formation in the first step. Any coke/tar formed due to secondary reactions of decomposition radicals would then occur in the absence of a catalyst. Techniques to minimize coke deposition onto reaction surfaces and to

2

collect/process tars produced in this first reactor are the subject of study by other UND students and thus are outside of the scope of this dissertation.

The first reaction step is followed by intermediate purification steps to remove highly volatile compounds (herein known as "gases" or "non-condensable") from the OLP that include compounds targeted from conversion into aromatics. This step is followed by a second reaction step in which the OLP from the cracking reaction is catalytically reformed to generate aromatics. Since the first step was well established previously, the primary emphasis in the work documented by this dissertation was placed on the second reaction step.

Previous studies [10] have also shown that a high concentration of propylene, ethylene, and butylene is present in the gases produced during the initial non-catalytic cracking reaction. These compounds are common feedstock chemicals for the production of simple aromatics and thus could also be exploited to increase the aromatics production from TAG oil.

A series of studies were performed to evaluate the production of aromatics from the products of the initial TAG decomposition reactions. First, model alpha olefins were chosen and reforming reactions to generate aromatics were studied for each compound separately. Light alkenes present in the cracking reaction gases were represented by propylene, while 1-tetradecene, 1-hexene, 1-octene, and 1-decene were used to represent the alkenes present in the OLP. Finally the reforming of an actual alkene-rich heterogeneous organic liquid product generated by non-catalytic TAG oil cracking was studied.

Background

Catalytic Reforming

Aromatic compounds such as benzenes, toluene and xylenes (BTX) are of great importance to the petrochemical industry because they are starting materials for manufacturing polymers, resins, and elastomers. They are also used as solvents or as additives to gasoline to increase its octane rating. Chemical grade aromatics, such as for use in polymer production are usually produced from propylene and other light alkenes that originate from natural gas; petroleum refineries produce aromatics from light straight run naphtha for motor gasoline blend stock [14].

Reforming is a process in which hydrocarbon molecules are rearranged and reconstructed into more complex molecules. When reforming is facilitated by catalytic action, the process is called catalytic reforming. The liquid products obtained by reforming are known as reformates. Reforming is the primary method used in the production of BTX [15, 16] when it is often known as "aromatization" [17]. In this process, lighter hydrocarbon molecules are also produced as unwanted byproducts, but they do have some value as energy feedstocks [16].

In 1949, Universal Oil Products (UOP LLC) commercialized a catalytic reforming process called 'Platforming'. In this process, light naphtha feedstocks are converted into aromatic rich high octane liquid products while generating byproducts such as hydrogen, propane, butane, and other lighter gases. As the name suggests, it is a '**Plat**inum' based catalytic 're**forming**' process.

The first improvement to this process was to introduce a bimetallic catalyst containing platinum and rhenium which enabled operation of the reformer at lower

4

pressures while yielding a higher octane rated reformate. Unfortunately, catalyst coking was a problem. As this problem could not be solved by catalyst development alone, UOP eventually commercialized the CCR (continuous catalyst regeneration) Platforming process, in which catalyst is taken out of the reformer continuously, regenerated and then returned to the reformer. As the coke was burned off continuously, catalyst deactivation due to coke deposition was minimized and longer run times between catalyst change outs were possible. This process increased the liquid products and aromatics yields compared to the original process [1].

Several other commercialized reforming processes for the production of aromatic rich liquid products have been developed [1, 2]:

1) Magnaforming by Engelhard Minerals and Chemicals Corporation.

2) Powerforming by ExxonMobil.

3) Hydroforming by Standard Oil Development Co.

4) Rheniforming by Chevron.

5) Ultraforming by Amoco.

6) Thermofor catalytic reforming.

7) Houdriforming by Houdry Division of Air Products and Chemicals, Inc.

8) M2 forming process by Mobil (now ExxonMobil).

9) Aroforming by Salutec Australia and IFP France.

10) Cyclar process by BP-UOP.

From a review of the published reforming catalyst studies, it is clear that almost all the commercialized (aromatization) reforming catalysts include either an individual

metallic active agent or single/bimetallic active agents supported by Al_2O_3. The metals are typically platinum (Pt), rhenium (Re), and/or tin (Sn). A few processes also reportedly use chromium oxide and molybdenum oxide as catalysts [2, 18].

Catalytic reforming is a complex process that involves many reactions. A summary of a few reactions involved is as follows [2, 19, 20]

1) *Dehydrogenation.* The initial step in reforming is known as the activation step. During this step, dehydrogenation via C-H bond scissioning of the feed molecules occurs, resulting in the formation of double bonds in the linear or cyclic molecules which eventually lead to aromatics formation. As the double bonds are formed, hydrogen is released. Several studies had been conducted in order to understand the mechanism of dehydrogenation. C-H bond scission either happens because of an adsorption-desorption phenomena of feed molecules on the catalyst surface or by collision between molecules (Zaera 2002). In short, dehydrogenation is the loss of hydrogen from a molecule. During this step, radical intermediates are formed.

2) *Hydrocracking.* The hydrogen generated in dehydrogenation and dehydrocyclization, at elevated temperatures and pressures, converts and cracks the feed into smaller saturated hydrocarbon molecules. This is called hydrocracking.

3) *Cyclization / Dehydrocyclization.* During cyclization step, linear open chain radical intermediates are converted into cyclic closed chain molecules. When cyclization couples with dehydrogenation of terminal hydrogen of a linear molecule, the reaction is called dehydrocyclization.

4) *Isomerization / dehydroisomerization.* Isomerization is the reaction in which a molecule rearranges into another molecule without changing the number of atoms in it. In the reforming process, isomerization couples with dehydrogenation (called dehydroisomerization) and converts cyclic compounds into aromatics keeping the number of carbon atoms same. e.g. methylcyclopentane through dehydroisomerization gets converted into benzene.

5) *Hydrogenolysis.* In the hydrogenolysis reaction, C-C bonds are broken and C-H bonds are formed. Although this is similar to hydrocracking, the product distribution is different. In the reforming process, where the objective is to produce aromatics-rich liquid products, hydrogenolysis is an unwanted reaction as it generates low-value gaseous compounds.

6) *Coke deposition.* The deposition of carbonaceous (coke) material on the catalyst surface is called coke deposition. This blocks the active sites on a catalyst and hence is the major reason for undesired catalyst deactivation, resulting in the decrease or complete loss of catalytic activity.

Dissertation Outline

This dissertation is written as a series of journal papers and is divided into multiple chapters. The first chapter is an overall introduction to this research and provides background for the results of this work. Chapter 2 is a paper on the aromatization of propylene over commercially available zeolite catalysts. The third chapter is a research manuscript on the performance of a nano-sized HZSM-5 on propylene aromatization. Chapter 4 is a manuscript on the catalytic conversion of 1-tetradecene to aromatic

compounds. Chapter 5 mainly focuses on a two step process for the conversion of triacyl glyceride (TAG) oil to aromatics and other chemicals that can replace their petroleum-derived analogs. TAG oils are most commonly produced by plants and are known as crop or vegetable oils.   They can also be produced by algae (algal oil) or bacteria. Conclusions and recommendations for future studies appear in the sixth chapter. The appendices contain detailed procedures, equipment details, and additional original information to support this dissertation. Appendices also include raw statistical data used for the preparation of manuscripts listed in this dissertation. Unused data and the results of additional experimental runs are also included. Appendices end with published preprints based on additional experimentation and data.

CHAPTER II

AROMATIZATION OF PROPYLENE OVER HZSM-5

Introduction

Short chain (light) aliphatic hydrocarbons are abundant products of the petrochemical industry that can be readily converted into valuable aromatic hydrocarbons, such as benzene, toluene, and xylenes (BTX). Several companies, including ExxonMobil and UOP, have developed and commercialized processes to aromatize LPG and other light aliphatic hydrocarbons, e.g., propylene. While reforming processes are important and well established in petroleum refining, they are also relevant to the production of gasoline-like biofuels, where significant amounts of propylene can be produced as a co-product.[21]

In addition to being an industrially important process, the aromatization of light hydrocarbons over zeolites has been the subject of numerous studies.[22-32] The aromatization of propane and propylene has been studied over several types of zeolites, including zeolite beta, zeolite HY, and ZSM-5.[33-38]

Only limited mechanistic information has been obtained on propylene aromatization over ZSM-5. Lukyanov et al., based on developed kinetic models, [34], proposed that alkenes first form oligomers which yield dienes via a hydride transfer. These dienes then form cyclic compounds, which are converted to aromatics through another hydride transfer. Hydride transfer reactions were found to be catalyzed by

zeolitic protons.[35] Zeolites with a higher bulk Al content showed a greater alkane aromatization capability than those with a lower Al content.

For propylene and *n*-butene aromatization, the aromatics distribution was found to be similar.[35-38] This observation indicated that a simple scheme involving alkene oligomerization followed by aromatization does not account for all steps of this complex process. Significant transfer of small hydrocarbon fragments appears to occur, thus yielding similar-size final products upon the conversion of different-size substrates.

The presence of gallium within the zeolite was also shown to increase the aromatics selectivity. [36] This catalyst exhibited a high alkene aromatization activity due to the presence of gallium and strong protonic acid sites. The product selectivity and aromatics' distribution were similar for both propylene and *n*-butene transformation reactions. *Para*-xylene was the primary aromatic hydrocarbon formed and, depending upon reaction time, the aromatics' distribution was controlled by several reactions, such as alkylation/dealkylation, isomerization and other inter-aromatics transformation.

n-Hexane, substituted cyclohexanes and trimerization products were found to be important intermediates during propylene aromatization over HZSM-5.[39] Apparently, zeolites combine and detach, i.e., 're-shuffle' C_1 and C_2 fragments in small aliphatic molecules either prior to or concomitantly with cyclization.[40] observed that HZSM-5 had a higher aromatization activity than that of alkali-exchanged ZSM-5 catalysts. The authors proposed that propylene transformation on alkali-exchanged ZSM-5 proceeds via oligomerization and then, after the dehydrocyclization step, the reaction directly routes to benzene formation where Lewis acid and weakly basic sites are reactive instead of Brønsted acid sites. A recent review summarizes the current state of understanding of

propane aromatization over HZSM-5, including experimental, theoretical, and modeling insights.[41]   It is thought that light alkanes are activated by HZSM-5 via penta-coordinated carbonium-ion-like transition states, which result in neutral surface alkoxide species. These intermediates are believed to subsequently react via carbenium-ion transition states.

The major (upon addition of C_2 fragments) and potential minor synthetic paths, based on the current literature, are shown in Scheme 1. The system's complexity significantly complicates both the optimization of the process and determination of its mechanism. Only applying a number of independent mechanistic tools and approaches may lead to developing greater understanding of this multifactorial system with multiple interactions and feedback loops.

Missing from the literature is the use of a systematic statistical approach. In this present study, our main objective was to prepare a statistical model for this catalytic reforming process for the purposes of optimizing the reaction conditions. DOE methodology has been used in the optimization of many industrial processes.[31]. A two-level factorial design allows one to determine the relative influence of several factors in this process, within the studied range, while requiring fewer experimental runs than traditional experimental methodology. Systematic errors can also be eliminated by using a DOE approach. In this study, all the data, figures, information is generated with only 16 experimental runs.

However, in addition to process optimization, a significant benefit of the DOE approach is the ability to identify significant *interactions* between factors. These interactions are usually not found using a more traditional approach to experimentation,

11

yet they can play an important role in the optimization of a process. Thus, the novel second objective of this study was to apply a factorial design of experiments (DOE) strategy to this process as a mechanistic tool, i.e., to determine which factors and interactions exert the greatest influence on the aromatization of propylene to BTX. We postulated that the consideration of these factors and their interactions may provide insight into some mechanistic details of such a complex process as propylene conversion to aromatics, particularly the diversity of active sites producing different-size aromatic products.

Obviously, the results obtained by DOE alone cannot be used as evidence proving the occurrence of certain pathways; the current study could not provide definitive answers to key mechanistic questions. Yet, the application of DOE led to several mechanistic insights which can be used in future detailed studies in combination with the other methods. In the current study, we matched our key DOE results with those published in the literature, i.e., obtained by other experimental or theoretical methods. Evidence was obtained to support the hypothesis that some BTX products are assembled on different active sites.

Experimental

Materials

ZSM-5 zeolite catalysts featuring Si:Al ratios of 50 and 80 were obtained in the powder form from Zeolyst International (Conshohocken, PA). Activation of ZSM-5 was achieved by calcination at 500 °C for 5 hours in air to convert the ammonium form into HZSM-5[37]. Ultra high purity propylene and nitrogen gases were obtained from Praxair.

12

Catalytic Activity Tests

Catalytic activity tests to produce aromatic compounds from propylene were carried out in a continuous, downflow reactor having an inner diameter of 1 cm and a length of 25.4 cm. Fig. 1 shows a schematic diagram of the experimental setup.
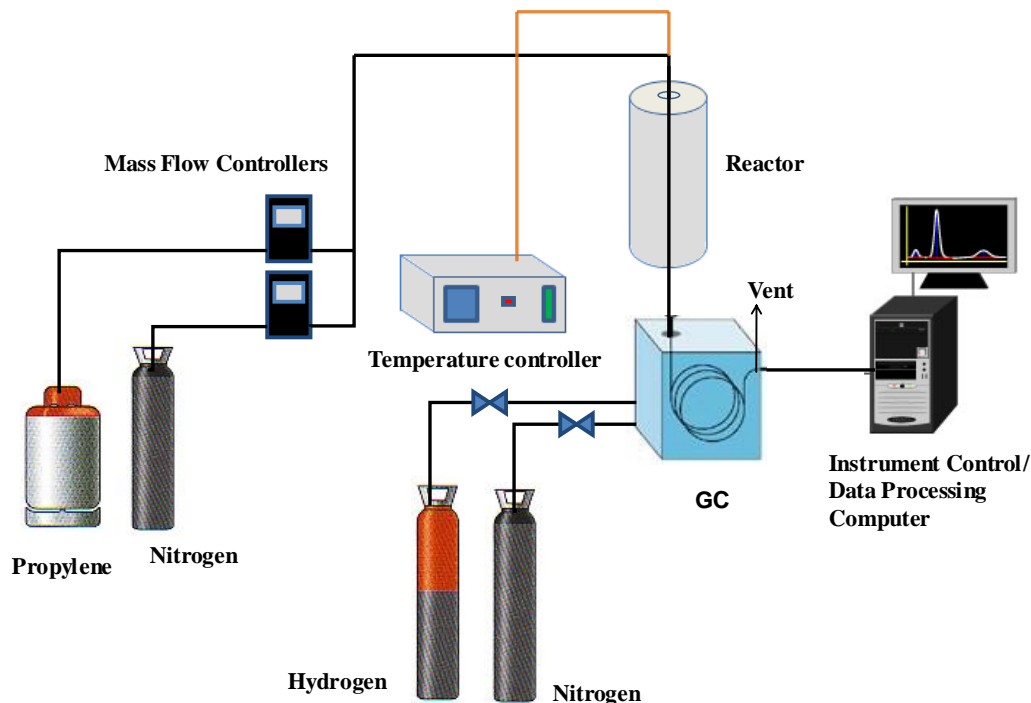
Figure 1. Schematic diagram of the propylene aromatization setup

A fixed bed of catalyst was prepared by loading an appropriate amount of activated catalyst on quartz wool in the reactor. The amount of quartz wool was kept constant for all the experimental runs. A type K thermocouple measured the temperature at the center of the catalyst bed and a Eurotherm 2116 controller provided feedback to a tube furnace. Separate Aalborg GFC17 mass flow controllers controlled the flow rates of propylene and nitrogen.

An in-line gas chromatograph (SRI 8610C), fitted with a flame ionization detector (GC-FID) and Alltech Hayesep Q 80/100 column, measured product concentrations in the reactor effluent. Separation of peaks was obtained by temperature programming on the GC. The temperature program initiated at 35 °C for 3 min, then ramped at 40 °C / min to 120 °C and maintained at this temperature for 45 min. For GC sampling analysis, an automatic gas sampling valve injected 1.00 mL of sample into a GC column. The sampling frequency was 50 min and each activity run continued for 400 min.

For every experimental run, steady state was achieved when the aromatics' concentration in the product stream became constant. Once steady state was achieved, four GC sampling analyses were averaged to determine product yields and propylene conversion. Propylene aromatization over zeolites is a reaction that occurs under severe catalyst deactivation. To avoid loss of activity due to catalyst deactivation and coke formation, fresh catalyst was loaded in the reactor for each experimental run.

Design of Experiments

A two-level, four-factor full-factorial design was set up to determine which factors influence the aromatization of propylene. The four factors were the Si:Al ratio, amount of catalyst, propylene feed concentration, and reaction temperature. The responses measured were the propylene conversion as well as the yields of benzene, toluene, *p*-xylene, *o*-xylene, and total BTX. Yields were determined on a carbon basis by dividing the mass of carbon obtained for each product by the total mass of carbon fed to the reactor as propylene. The design was unreplicated and the order of experiments was randomized. Experimental noise was quantified using the method developed by Lenth.[42] This method assumes that three-way interactions are not significant and uses

14

these to estimate the standard error. Hence, only individual factors and their two-way interactions were considered for analysis.

The original experimental factors (uncoded units) were transformed into coded units and designated as −1 (low) and +1 (high). The low and high values of these factors, shown in Table 1, were determined using previously published studies as a guide [21, 33-40, 43, 44].

Table 1. Experimental factors and their uncoded set point values.

Factors	(-) Low values	(+) High values
Si:Al ratio of HZSM-5	50	80
Catalyst amount (g)	0.2	1
Propylene concentration (mol%)	8.9	12.5
Reaction Temperature (°C)	400	500

The effect of each factor was obtained by using the difference between the average responses at the high and low levels of each factor.[45] A larger absolute value for an effect indicates that it has a greater impact on the response. To evaluate the statistical significance of effects of various factors, a two-sample t-test using the means at the high and low settings was performed and a probability value (p-value) was calculated. For the effect to be statistically significant at a 95% confidence level, the p-value should be less than or equal to 0.05.

An important part of this work was the study of interactions between the four factors. The ability to determine interactions is the major benefit of using a factorial DOE approach. An interaction occurs when the effect of one factor depends on the value of one of the other factors. The magnitude of an interaction is defined as one-half of the difference between the effect of a factor at the high value of a second factor and the effect of the first factor at the low value of the second factor. For this analysis, the statistical software package, MINITAB^{TM} 15, was used as an analysis tool to obtain main effects and interactions and to create Pareto, interaction, and other charts for interpretation.[45]

Results and Discussion

All experimental runs were carried out according to the full factorial design (Table 2). The responses are also shown in Table 2.

Table 2. Factors and response table showing yields of benzene, toluene, *p*-xylene, *o*-xylene, total BTX, and propylene conversion.

Standard Order	Run Order	Si:Al Ratio	Temperature (°C)	Propylene concentration (%)	Catalyst amount (g)	Benzene Yield (%)	Toluene Yield (%)	*p*-xylene Yield (%)	*o*-xylene Yield (%)	Total BTX Yield (%)	Propylene conversion (%)
1	4	50	400	8.9	0.2	1	5.6	6.2	1.4	14	75
2	2	80	400	8.9	0.2	0.27	1.6	2.3	0.48	4.7	66
3	8	50	500	8.9	0.2	2.1	8.1	5.9	1.7	18	64
4	14	80	500	8.9	0.2	0.64	2.5	2.6	0.68	6.4	39
5	10	50	400	12.5	0.2	1.4	7.2	6.2	1.3	16	76
6	3	80	400	12.5	0.2	0.47	2.5	2.8	0.59	6.4	71
7	12	50	500	12.5	0.2	3	8.8	5.6	1.5	19	67
8	15	80	500	12.5	0.2	0.87	3.5	3.3	0.81	8.5	48
9	9	50	400	8.9	1	3.1	11	7.7	1.9	24	74
10	5	80	400	8.9	1	0.75	3.9	4.1	0.89	9.6	78
11	6	50	500	8.9	1	3.4	12	7.9	2.2	25	67
12	13	80	500	8.9	1	2	6.7	4.8	1.3	15	63
13	16	50	400	12.5	1	3.8	12	7.2	1.7	25	71
14	11	80	400	12.5	1	2.5	9.9	7.3	1.4	21	79
15	7	50	500	12.5	1	7.9	15	6.3	1.6	31	67
16	1	80	500	12.5	1	4.7	13	7.4	2	27	66

The determination of significant factors and their interactions
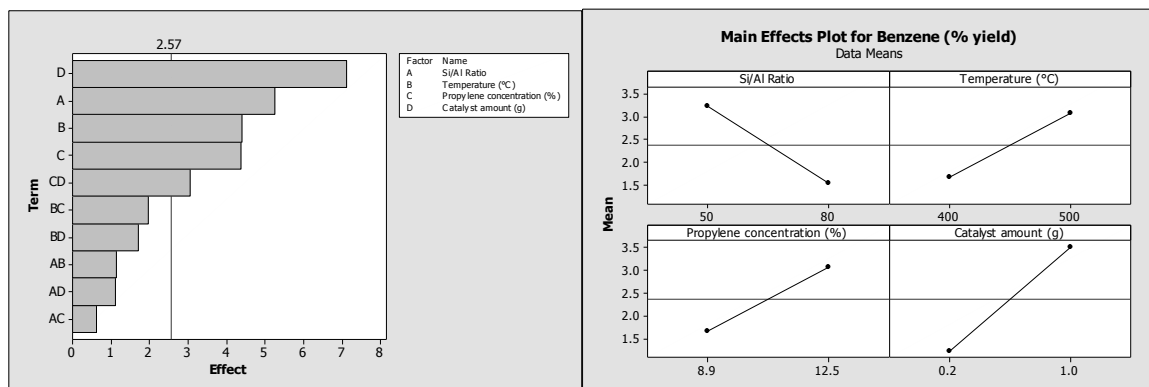
Figure 2. (a) Pareto chart of effects for yield of benzene, (b) main effects plot for yield of benzene - each point in main effects plot represents the mean value of four experimental data points, either at low or high level.

Figures 2 through 6 include Pareto charts (Panel a in each figure) of the effects of each factor and the interaction for all responses as well as main effects plots (Panel b). For example, 'CD' in Fig. 2a represents the effect of the interaction between factors C (propylene concentration) and D (catalyst amount). The vertical line in each Pareto chart represents the line of significance, which is based on 95% confidence. Any bar (representing the effect) in a Pareto chart extending beyond this line is considered a significant term. For example, Fig. 2a shows that the Si:Al ratio and catalyst amount had the greatest effects on aromatization. Reaction temperature is also significant for the yield of all individual aromatics except *p*-xylene. A detailed discussion of the influence of these factors on BTX yields is provided in the next two sections.
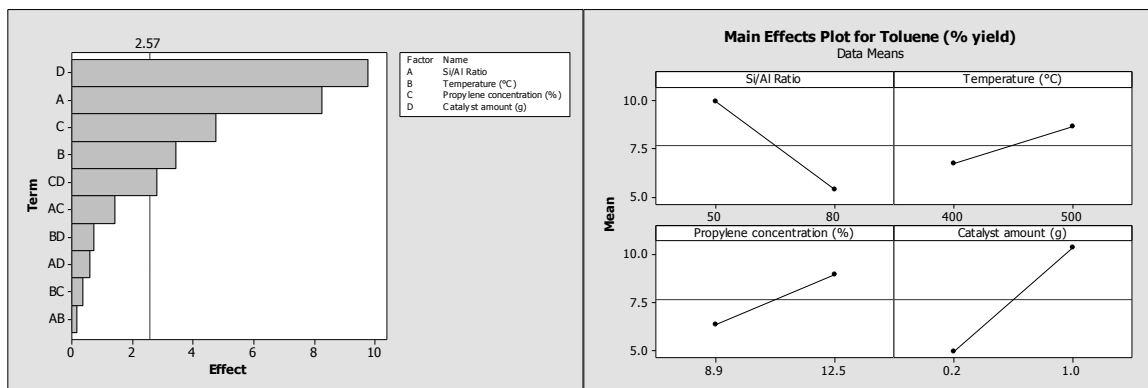
Figure 3. (a) Pareto chart for effects for yield of toluene, (b) main effects plot for yield of toluene

Figures 2a and 3a show that the interaction between propylene concentration and catalyst amount is significant for benzene and toluene production. By contrast, the yields of *p*- and *o*-xylenes are significantly influenced by a different interaction, namely that between the Si:Al ratio and the propylene feed concentration.
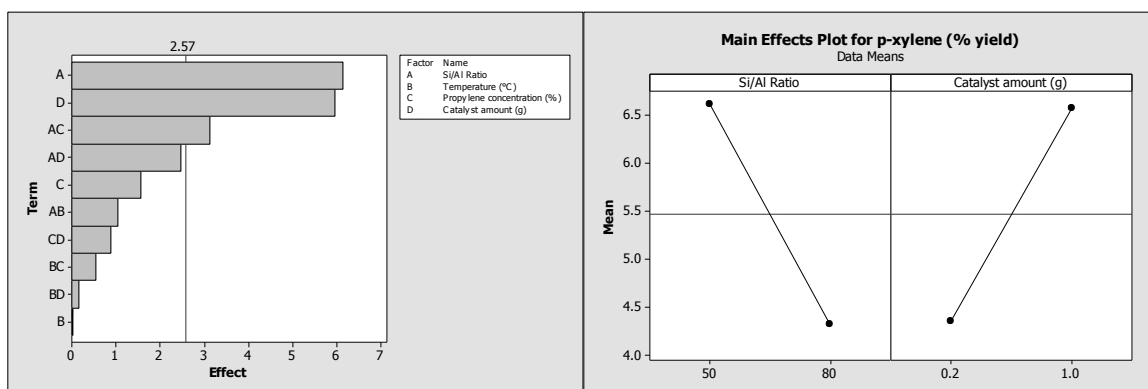
Figure 4. (a) Pareto chart for effects for yield of *p*-xylene, (b) main effects plot for yield of *p*-xylene
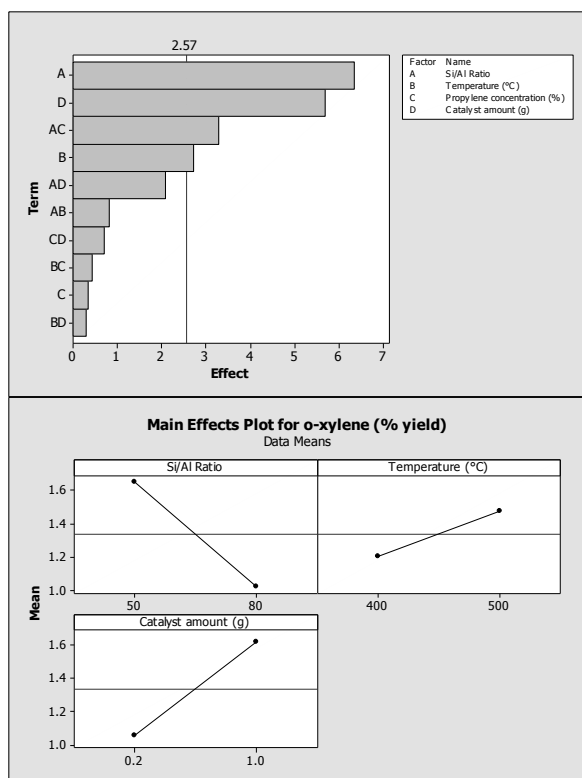
Figure 5. (a) Pareto chart for effects for yield of *o*-xylene, (b) main effects plot for yield of *o*-xylene

Moreover, the interaction between Si:Al ratio and catalyst amount is close to being significant for the yields of *p*-xylene (Figure 4a) and *o*-xylene (Figure 5a). Figure 7 shows detailed information of how each significant interaction impacts product yields. Since the yields of benzene and toluene account for more than 60% of the total aromatics yield for all of the experiments conducted in this study, the results for total BTX and for individual yields of benzene and toluene are similar.

The Effect of The Si:Al Ratio in The HZSM-5 Catalyst on BTX Yield

Panel b of Figures 2-6 indicates how changing each factor impacted the various product yields. Increasing the Si:Al ratio decreased the yield of aromatics. This is

because the catalytic activity of HZSM-5 is mainly due to the Brönsted acid sites present in the bridging hydroxyl groups in the Si-O-Al triad, in which it is the aluminum that exhibits significant acidity.[46] Apparently, the Si:Al stoichiometry of active sites may be higher than 1:1 and the additional alumina (Al-O-) fragments may boost their catalytic activity. The active tetrahedral site (T-site) is occupied by tetrahedrally coordinated silicon and aluminum atoms.

Several theoretical studies have been conducted on locating the active T-site occupied by Al.[46] According to this study, the adsorbed propylene forms surface intermediates, e.g., alkoxides responsible for β-scission and hydride transfer reactions. The activation energy is required to form a protonated molecule when a feed propylene molecule comes in contact with a Brønsted acid proton. The value of this activation energy also depends on the interaction between the zeolite wall and the protonated molecule.[47-49] The alkoxide formation energies were shown to depend on zeolite structures. The Al sites greatly increase the heat of propylene adsorption on ZSM-5.[47-49] The location and number of Al sites are known to affect catalytic activity. The proton affinity, acid strength, and binding energies are greatly influenced by the composition of ZSM-5 and its structure.[50, 51] For a Si:Al ratio of 50, the available Al sites are more dense than for a ratio of 80.

This published information corroborates the results obtained in the current study. The activity effects of Si:Al ratio appear to be due to the differences in total acidity. Acid strength increases with a decrease in Si:Al ratio, which may demonstrate a higher catalytic activity towards the BTX production for ZSM-5 having a lower Si:Al ratio, as observed in this study.

The Effect of Reaction Temperature on Aromatization
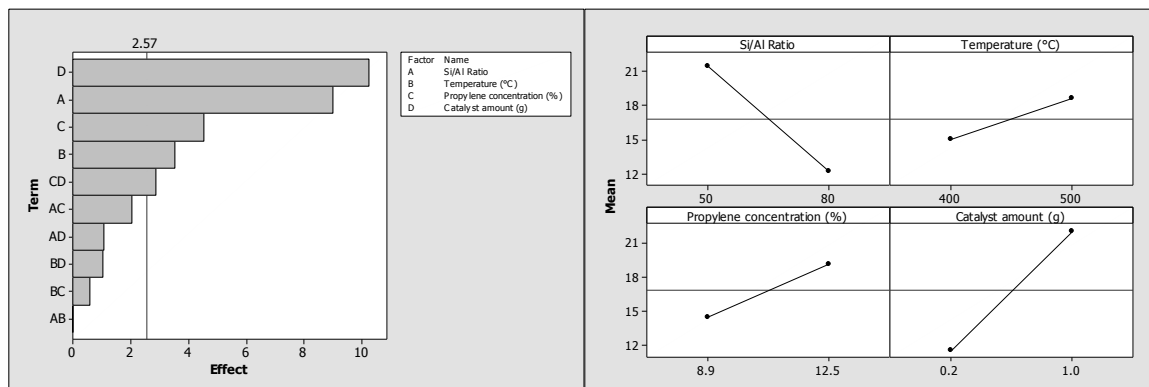
Figure 6. (a) Pareto chart for effects for yield of total BTX, (b) main effects plot for yield of total BTX

The yields of all BTX but *p*-xylene increased significantly with temperature, as shown in Figs. 2-6. An explanation of this trend can be offered based on previous mechanistic studies. At lower and moderate temperatures, the bridging hydroxyl groups in HZSM-5 were reported to form hydrogen bonds with the neighboring oxygen atoms. With an increase in temperature, this hydrogen bond breaks, the availability of free bridging hydroxyl groups increases, and thus the acidity and catalytic activity increases. Therefore at higher temperatures, protons possess the necessary energy to overcome the activation energy barrier.[52, 53] Moreover, at higher temperatures, the tendency of a propylene molecule to crack into C_2 intermediates increases, which is important for promoting aromatics formation because the major pathway for aromatization is believed to be through the combination of C_2 fragments (Scheme 1). Based on the experimental results obtained in this study, the temperature essential for this critical step is within the range considered, i.e., between 400 and 500 $^{\circ}$C.

The lack of a strong temperature effect on *p*-xylene yield is unusual and may be the result of two competing temperature effects. It may indicate that not only are the catalytic sites responsible for the synthesis of this product different from those specific for toluene and benzene, but also that the specificity of these sites is reduced as temperature increases. More specifically, at higher temperature, it would be expected that increased catalytic activity increases the amount of xylenes produced, along with all other BTX compounds. But at the same time, less thermodynamically stable *p*-xylene (or its intermediates, Scheme 1) may, at high temperature and in the presence of hydrogen, readily undergo hydrodealkylation to form toluene and benzene. Thus, the net increase in yield of *p*-xylene may be offset, leading to a near-zero net temperature influence.[36] Thus, the xylene/toluene ratio may be varied by adjusting the process operational parameters.

The Effect of Propylene Feed Concentration and Catalyst Loading on Aromatization

Increasing the feed propylene concentration increases the overall aromatics yield (Fig. 6b). This effect cannot be explained by simple first-order kinetics. Not just the process *rate* but the *yield* increases, i.e., a higher fraction of propylene in the feed is converted into aromatics when more propylene is present. For a first order reaction, conversion is independent of feed concentration. By contrast, a second order reaction would show increasing conversion with feed concentration, as seen here. This implies that the reactions to form aromatics may be bimolecular, i.e., more than one propylene molecule is involved at the rate limiting step.
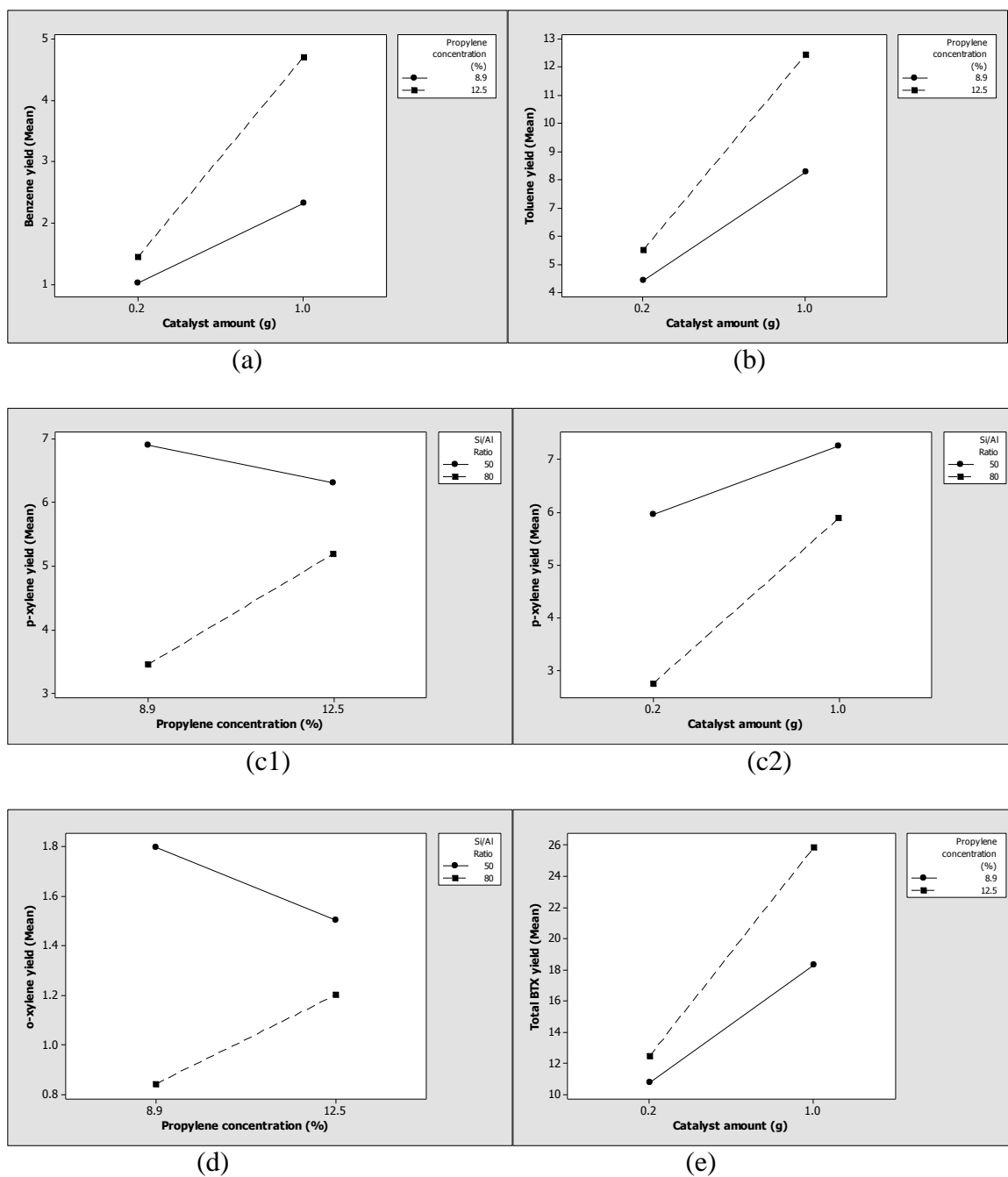
Figure 7. Significant interaction effects plots for yields of (a) benzene, (b) toluene, (c1 & c2) *p*-xylene, (d) *o*-xylene and (e) total BTX.

Increasing the catalyst amount leads to higher conversion, as expected. With an increased catalyst amount, the number of available active sites also increases and this eventually yields more aromatics. The results presented in sections 3.3 and 3.4 indicate

that increasing temperature and catalyst amounts increase the aromatics yields. However, this is complicated by the fact that increased temperature also decreases propylene conversion (Fig. 8).

(a)
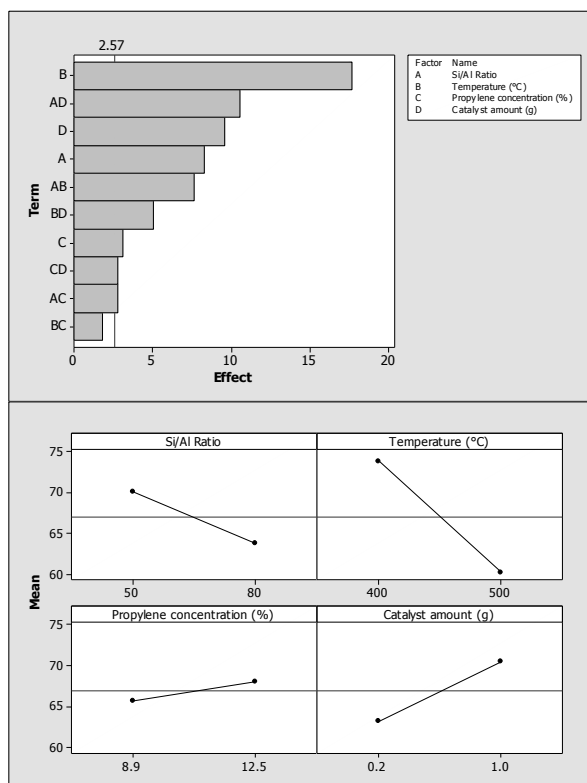
(b)
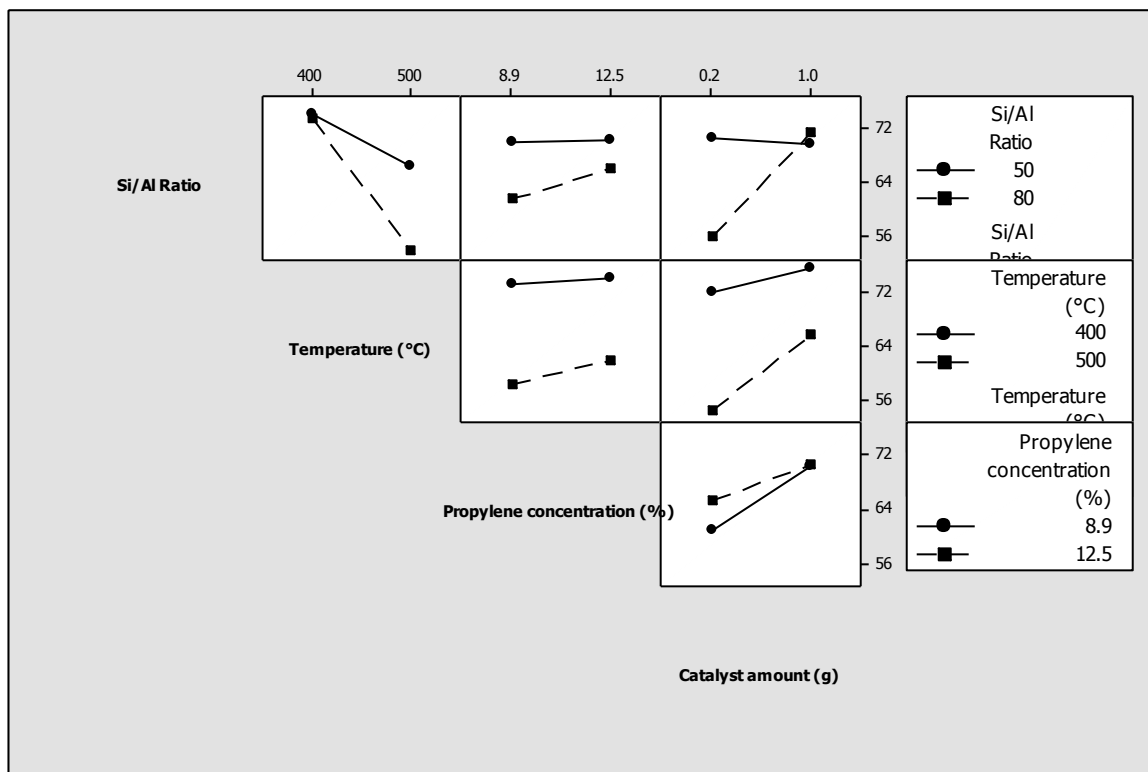
(c)

Figure 8. (a) Pareto chart, (b) main effects plot and (c) interaction plots for conversion of propylene

One potential explanation of this effect is based on kinetics. Higher temperatures, along with the formation of BTX, may also cause coke formation and the deactivation of catalyst that make side products (listed in section 3.5), e.g., aliphatic hydrocarbons. No significant deactivation of the catalyst was observed, however, over the time of each experimental run.

As an alternative explanation, not only kinetic but also thermodynamic factors may cause this behavior. Thermodynamically, higher temperatures favor decomposition reactions. Thus, while some propylene is converted into aromatics and other products,

26

additional propylene may be formed due to either side decomposition reactions or reverse reactions catalyzed by zeolites. Supporting this statement, the concentration of intermediate-size aliphatic side products, C_6-C_8, was low when the process was conducted at 500 °C as compared to 400 °C, yet the concentration of low-MW aliphatics -- propane, ethane and ethylene -- were much greater at the higher temperature (not shown). Unfortunately, the obtained C_6-C_8 aliphatic hydrocarbon homology and isomer profiles did not provide sufficient mechanistic information due to their low amounts.

Effects from Significant Interactions

Figure 7 shows that the interaction between hydrocarbon feed concentration and catalyst amount was significant. The propylene concentration-catalyst amount interaction plots for benzene, toluene, and total BTX yields are given in Fig. 7 (a), 7 (b), and 7 (e), respectively. When the catalyst amount was increased from 0.2 g to 1.0 g, the effect of changing propylene feed concentration on benzene yield increased.

Figures 7b and 7e show the same trend for the yields of toluene and total BTX, respectively. At low catalyst amounts, only a small effect of propylene concentration was observed as perhaps all propylene adsorption sites that produce benzene and toluene were occupied. At greater catalyst amounts, these sites were not saturated at the low propylene feed concentration. As a result, a simultaneous increase in propylene concentration and catalyst amount significantly increased the yield of benzene and toluene (and hence total BTX). Thus, the proper balance between the levels of these factors is important to control the yields of benzene and toluene for process optimization.

In contrast to the yields of benzene and toluene, a significant interaction effect was observed for xylenes between the Si:Al ratio and the propylene feed concentration, Fig. 7 (c1) and (d). For a Si:Al ratio of 80, there was an increase in xylene yield when the feed concentration was increased, but for a Si:Al ratio of 50, the effect was reversed and more xylenes were produced at the lower propylene concentration. Thus, an increase in the Al content in the catalyst increased xylene yields, even at lower feed concentrations.

The interaction of Si:Al ratio with the catalyst amount also had a closer significant effect on the *p*-xylene yield , Fig. 7 (c2). When the catalyst amount was kept constant at 0.20 g, the difference in the yields of *p*-xylene at Si:Al ratios of 50 and 80 was almost double that at a 1.0 g catalyst loading. Apparently, specific xylene-producing catalytic sites became saturated when the propylene concentration increased. The observed positive interaction between the Si:Al ratio (i.e., density of active alumina sites) and propylene concentration, which is specific only for xylene production, can be explained by a greater than 1:1 catalyst : propylene stoichiometry of these specific xylene-producing sites. Perhaps, xylene-producing sites would be more likely to form with a greater aluminum content of the catalyst.

Major path

Cracking –C_2

+C_2 olefin

C_3 olefin — Cracking -C_1 → **C_2 olefins** ← **C_4 intermediates** ← **C_4 olefin**

Major path →

+C_3 olefin

+C_2 olefin   *Proposed major path*   +C_3 olefin

Proposed path

C_5 intermediates — *Proposed major path* → **C_7 intermediates**

Major path

+C_3 olefin

dehydrocyclization

toluene

Proposed minor path →   **C_8 intermediates**

+C_2 olefin

Minor path

C_6 linear

dehydrocyclization

dehydrocyclization

xylenes

Hydrodealkylation at high temperature

benzene ←

Figure 9. Scheme (1) for Propylene aromatization reaction pathways

Stoichiometrically two molecules of propylene adsorbed on a catalyst may yield benzene as a major product after their dimerization, cyclization, and dehydrogenation (a minor path in Scheme 1). Similarly, 3-carbon units directly derived from propylene could enter the process at various steps (other minor paths in Scheme 1). Prior theoretical research indicates that aromatics are predominantly produced by the combination of C_2 units (major paths in Scheme 1). This information has been confirmed by our analysis of aliphatic products. Ethylene was, by far, the most abundant aliphatic by-product formed, with its concentration being about 1/10 of the initial propylene feed (not shown). The subsequent oligomerization of the resulting C_2 fragments would yield xylenes. However,

the results of the experimental studies reported here suggest that HZSM-5 is rather selective towards the production of C_7 aromatics, irrespective of the reaction conditions and Si:Al ratio.

Furthermore, considering only the major paths of Scheme 1 contradicts evidence obtained in this study that xylenes are produced on different catalytic sites than benzene and toluene. Thus, xylenes cannot be viewed as essential intermediates of toluene synthesis, via subsequent methyl transfer, Scheme 1.

An alternative explanation, shown as hypothetical pathways in Scheme 1, suggests that a C_4 fragment would react with propylene to form toluene directly. By contrast, xylenes would involve the combination of C_2 units only. Then, toluene would be expected to have the highest yield based on propylene's specific chemical features as a C_3 alkene. Namely, to form ethylene or other reactive C_2 intermediates, propylene has to be cracked into C_1 and C_2 hydrocarbons. However, this process would require high amounts of energy to break either a double bond or a single bond at the vinyl position to the double bond.

This hypothesis, stating the participation of some C_3 fragments in the process mechanism, would explain why an increase in propylene feed concentration significantly increases toluene yield but does not affect those of xylenes. This hypothetical route should not overshadow the role of methyl transfer reactions, which appear to be significant. Significant methane amounts were observed among the reaction products in the current work. The effective C_3 unit essential for toluene formation could actually be a combination of a C_2 and C_1 fragments. These two routes would be kinetically indistinguishable.

The ratios of the yields of benzene/toluene as well as that of benzene/xylene increase with increasing temperature, keeping all other reaction factors constant (Table II). These trends can be explained by possible hydrodealkylation of toluene and xylenes or intermediates of their synthesis at high temperatures as shown in Scheme 1.

Statistical Model for Total BTX Yield

In fitting a statistical model, three assumptions must be verified: (1) residuals are randomly and normally distributed, (2) residuals are not correlated with the predicted Y, and (3) residuals do not exhibit any trends over time.[45] For this work, all of these assumptions were verified by examining the appropriate residual plots.

The use of a statistical design of experiments methodology is an effective way to determine and study the interactions between the reaction conditions and is an important step in process optimization. The coefficients of estimated effects and interaction are shown in Table 3. Note that these coefficients should be used with the coded values of the four factors and their interactions. The impacts of each factor on the toluene yield are greater than on the yield of any other individual aromatic compound because toluene is the predominant BTX product. From the coefficients listed in Table 3, models for each response can be constructed. For example, the statistical model for total BTX, *in coded units*, is as follows:

Total BTX (% yield) = 17 − 4.6 (Si:Al ratio) + 1.8 (temperature) + 2.3 (propylene concentration) + 5.2 (catalyst amount) + 1.5 (propylene concentration*catalyst amount).

Table 3. Summary of the effect of each significant variable and 2-way interaction on every response

Coefficient		Factors				2-way interactions					
		Si/Al Ratio	Temperature (°C)	Propylene concentration (mol%)	Catalyst amount (g)	AB	AC	AD	BC	BD	CD
Response	Mean	[A]	[B]	[C]	[D]						
% yield of benzene	2.4	-0.85	0.71	0.70	1.1	-	-	-	-	-	0.49
% yield of toluene	7.7	-2.3	0.95	1.3	2.7	-	-	-	-	-	0.77
% yield of p-xylene	5.5	-1.1	-	0.29	1.1	-	1.2	0.46	-	-	-
% yield of o-xylene	1.3	-0.31	0.14	0.017	0.28	-	0.16	-	-	-	-
% yield of total BTX	17	-4.6	1.8	2.3	5.2	-	-	-	-	-	1.5
Propylene conversion (%)	67	-3.2	-6.8	1.2	3.7	-2.9	1.1	4.1	-	1.9	-1.1

Conclusions

A statistical design of experiments (DOE) methodology identified the significant reaction parameters and their interactions that influence propylene aromatization. Of the factor-ranges studied, the HZSM-5 Si:Al ratio and catalyst amount had the greatest impact on BTX yield. The reaction temperature significantly increased the yields of benzene, toluene, o-xylene and total BTX, while the effect of feed concentration is significant only for benzene, toluene and total BTX yields. The interaction between initial propylene feed concentration and amount of catalyst was statistically significant for benzene, toluene, and total BTX yields. By contrast, the Si:Al ratio-feed concentration interaction only impacts the yields of xylenes, which follow different trends from benzene and toluene. Thus, benzene and toluene appear to be produced on the same catalyst sites whereas xylenes are produced on different sites. A consequence of this insight is that it is possible to manipulate the toluene (plus benzene) to xylene yield ratio in propylene aromatization. The present work demonstrates that the catalyst Si to Al ratio is one such adjustable parameter. Others include zeolite size/structural conditions and the presence or absence of dopants in the catalyst.

A statistical model was proposed for the prediction of each response. To maximize overall aromatic yields, the Si:Al ratio of catalyst should be at a lower level, and all the other reaction conditions should be at higher levels, based on the range of factors included in this study. Since the interaction effects can be determined only by using a design of experiments strategy, it can be concluded that this statistical DOE approach is a useful tool in optimizing the reaction conditions for the catalytic reforming process to produce aromatics using zeolite catalysts.

CHAPTER III
AROMATIZATION OF PROPYLENE OVER NANOSCALE HZSM-5

Introduction and Background

Propylene is one of the major short chain hydrocarbon byproducts in petroleum refining. A high concentration of propylene and other light alkenes are also produced from TAG oil cracking. TAG cracking generates relatively high concentrations of propylene and as will be shown in later chapters, additional propylene is generated during the reforming of middle volatility alkenes. The reforming of propylene is one of the most common ways to generate chemical grade BTEX, especially toluene. The technology to do this reforming is mature and thus traditional propene reforming is not of interest in this research. However, recently it has been proposed that nano-sized zeolites may have advantages over traditional micro-sized zeolites in certain applications. To our knowledge, no one has studied the use of nano-sized zeolites for propene reforming. Aromatization is a catalytic reforming process which converts light aliphatic hydrocarbons into more valuable aromatic products.

Zeolites are widely used as catalysts for aromatization reactions. Available literature shows that HZSM-5, either plain or doped with metals, efficiently converts propylene to aromatic compounds with a high selectivity. It has been suggested, that additional improvements may be possible using recently developed nanoscale zeolites.

Nanoscale zeolites have been synthesized at the laboratory scale [54-57]. Currently, the synthesis, application and comparison of nanoscale zeolites with microscale zeolites is getting considerable attention in the academic and industrial research communities [58]. Several researchers have reported the effectiveness of nanocrystalline zeolites for the catalytic conversion of mid-chain hydrocarbons [59]. For example, a nano-sized HZSM-5 catalyst was studied for the aromatization of olefins in petroleum feedstock [55]. Successful attempts were also made to reduce the olefin content in FCC gasoline [60] and nanoscale ZSM-5 was found to be a good catalyst for the minimization of coke yield. Most of these aforementioned studies were focused on the feasibility of using nanoscale ZSM-5 for mixtures of hydrocarbons.

However to our best knowledge, there is no existing published work on using a nanoscale HZSM-5 for aromatization of propylene. In this study, nanoscale HZSM-5 catalyst is synthesized and used for aromatization of propylene with the application of DOE-based parameterization, in comparison with the results obtained earlier for microscale HZSM-5.

Experimental

Nanoscale Catalyst Synthesis and Characterization

Nanoscale HZSM-5 catalyst was synthesized by using a laboratory procedure described elsewhere [61]. The detailed procedure for catalyst synthesis is listed in Appendix A1. Activation of ZSM-5 was achieved by calcination at 500 °C for 5 hours in air to convert the ammonium form into HZSM-5. X-ray diffraction (XRD) patterns of the catalyst powder were obtained by using a Phillips X'Pert PRO X-ray Diffractometer.

Transmission electron micrographs (TEM) of HZSM-5 were obtained by using a JEOL JEM-2100 microscope.

Nanoscale Catalyst Testing

A two-level, three-factor (temperature, propylene concentration and catalyst loading), full-factorial design of experiments (DOE) was used. Catalyst activity tests were performed and the results were analyzed as detailed in prior chapter 2. A fixed bed of catalyst was prepared by loading an appropriate amount of activated catalyst on quartz wool in the reactor. The amount of quartz wool was kept constant for all the experimental runs. A type K thermocouple measured the temperature at the center of the catalyst bed and a Eurotherm 2116 controller provided feedback to a tube furnace. Separate Aalborg GFC17 mass flow controllers controlled the flow rates of propylene and nitrogen.

For every experimental run, steady state was achieved when the aromatics' concentration in the product stream became constant. Once steady state was achieved, four GC sampling analyses were averaged to determine product yields and propylene conversion. To avoid the loss of activity due to the catalyst deactivation and coke formation, fresh catalyst was loaded in the reactor for each experimental run. The analytical methods and equipment are discussed in chapter 2 and in Appendix A4.

Results and Discussion

Characterization of Nanoscale HZSM-5

Fig.10a presents the XRD pattern of the nanoscale catalyst powder. These patterns feature two distinct peaks between 2 Theta positions at 5-10 and well defined peaks between positions 22-25. In XRD, Theta is an angle of incoming EM wave, as well as the

angle of diffracted EM in regard to Bragg's planes. So the total change in angle of the EM wave equals 2 THETA. Small patterns are also observed around 2 Theta positions at 13-17, 30, and 45-47. These patterns match the positions corresponding to the HZSM-5 framework structure [57, 61], which confirms that the prepared catalyst is a HZSM-5 type zeolite.
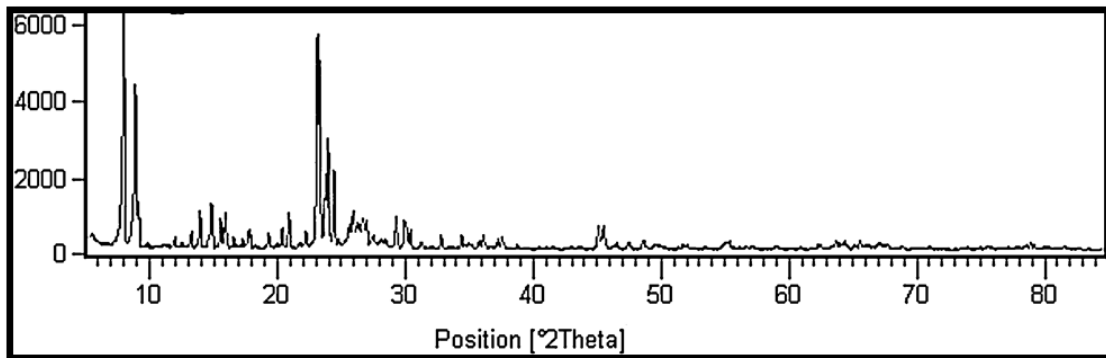
(a)   (b)
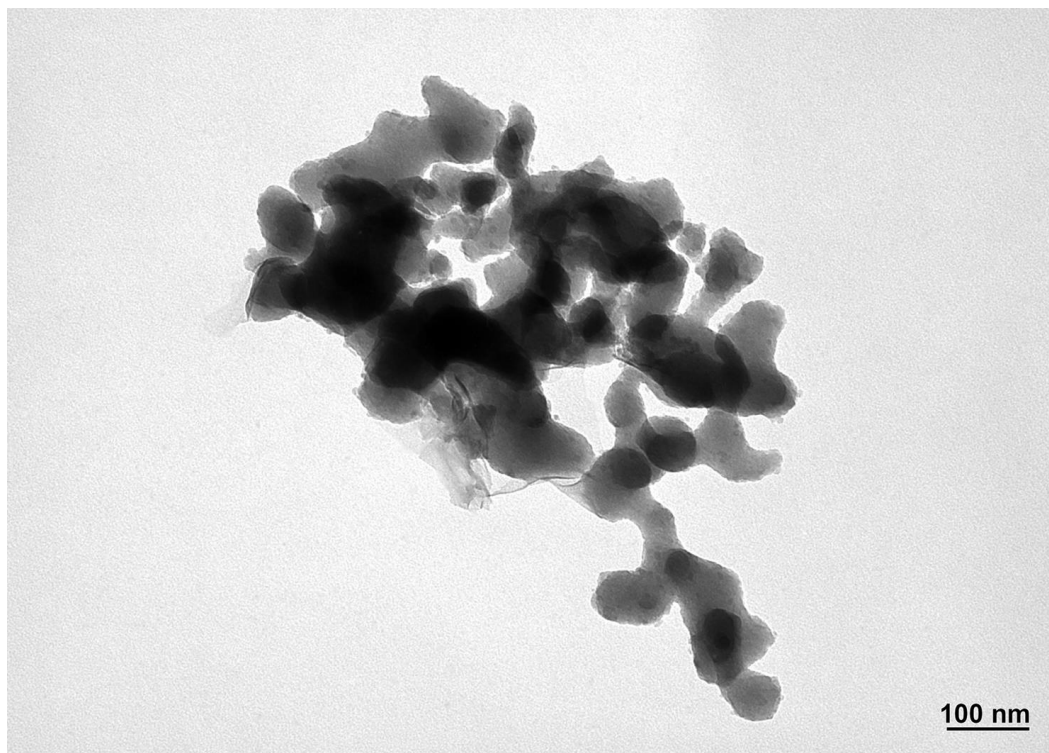
Figure. 10. (a) XRD) pattern (b) TEM image of nanoscale HZSM-5

The transmission electron micrograph shown in figure 10b suggests that the particle size of synthesized ZSM-5 is in a range of 20-50 nm which is consistent with the literature [61]. The agglomeration of nanoparticles observed may be inevitable due to the attractive van der Waals forces and the presence of moisture in the air at room temperature. However, the agglomeration would be less likely at elevated reaction temperatures such as 400-500 °C, thus being of little concern for propylene aromatization.

Effects of Factors, Interactions and Particle Size of HZSM-5 on BTX Yield

The experimental reaction conditions and their results are listed in table 4.

Table 4. Factors and response table showing BTX yield and individual aromatic compound fractions

Runs	Temperature (°C)	Propylene concentration (%)	Catalyst loading (g)	Total BTX (% yield)	Benzene (% fraction)	Toluene (% fraction)	Xylenes (% fraction)
1	500	12.5	1	29	31	48	21
2	500	12.5	0.5	21	13	44	43
3	400	12.5	0.5	17	8	43	49
4	500	12.5	0.5	22	12	43	43
5	400	8.9	1	17	11	44	45
6	500	8.9	1	23	24	47	29
7	400	8.9	0.5	15	7	41	52
8	500	8.9	1	23	24	47	29
9	400	12.5	1	19	13	47	40
10	400	12.5	0.5	17	8	43	49
11	400	8.9	1	17	10	44	46
12	400	12.5	1	20	13	48	39
13	500	12.5	1	29	32	49	19
14	500	8.9	0.5	14	12	43	45
15	500	8.9	0.5	15	11	42	47
16	400	8.9	0.5	14	6	40	54

The BTX yields obtained were lower for a nonoscale HZSM-5 than for a commercial microscale HZSM-5 catalyst (Fig. 11).
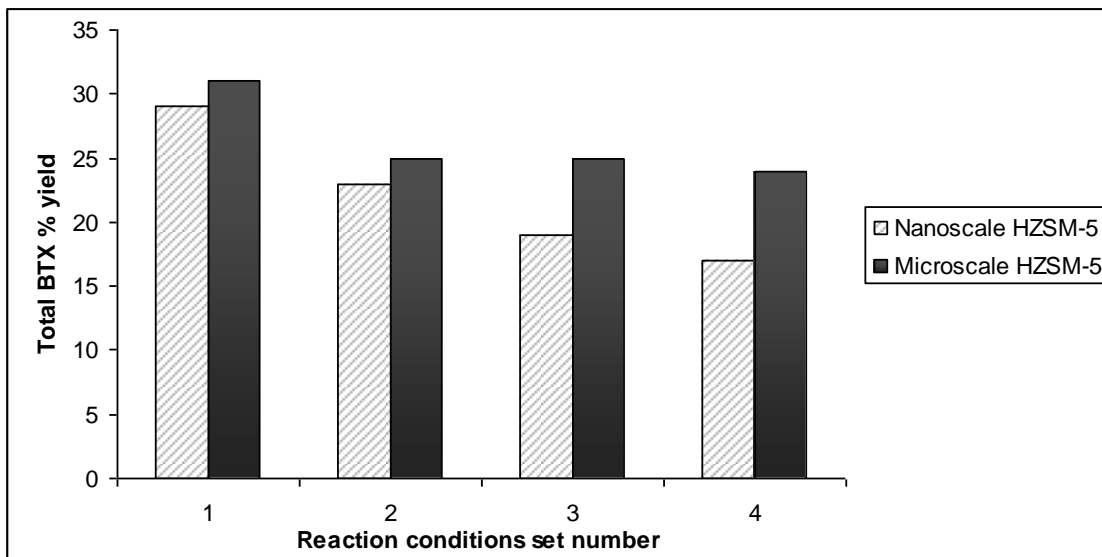
Figure 11. Comparison between performance of nanoscale and microscale HZSM-5 on aromatics yield at 4 different reaction conditions.

Aromatization of propylene is highly dependent on the diffusion of feed molecules into HZSM-5 pores. For the formation of aromatics, shape selectivity of HZSM-5 is an important factor. Since the number of active sites inside pores is lower in nanoscale ZSM-5 and since the overall diffusion path is also smaller in the nanoscale ZSM-5, it causes lower yields of aromatics in comparison with the commercial HZSM-5 catalyst. All three factors (temperature, propylene concentration and catalyst amount) had a significant effect on the fraction of the propylene that converted to aromatics, expressed as % yield of total BTX.
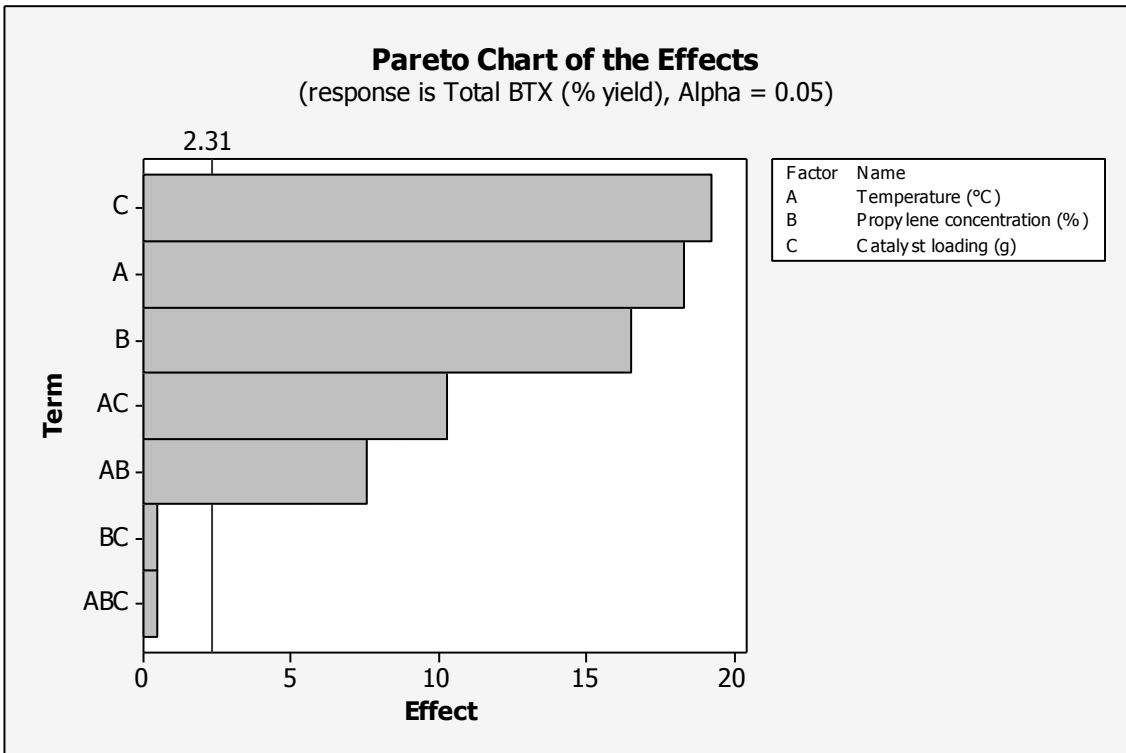
(a)
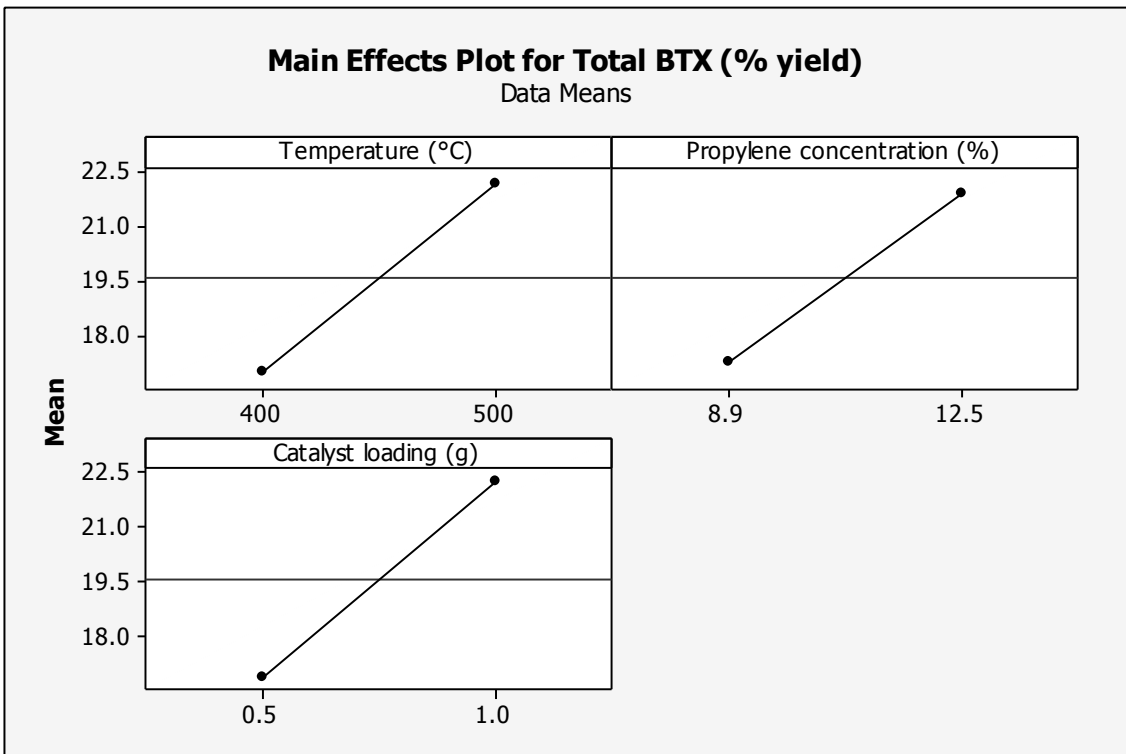
(b)
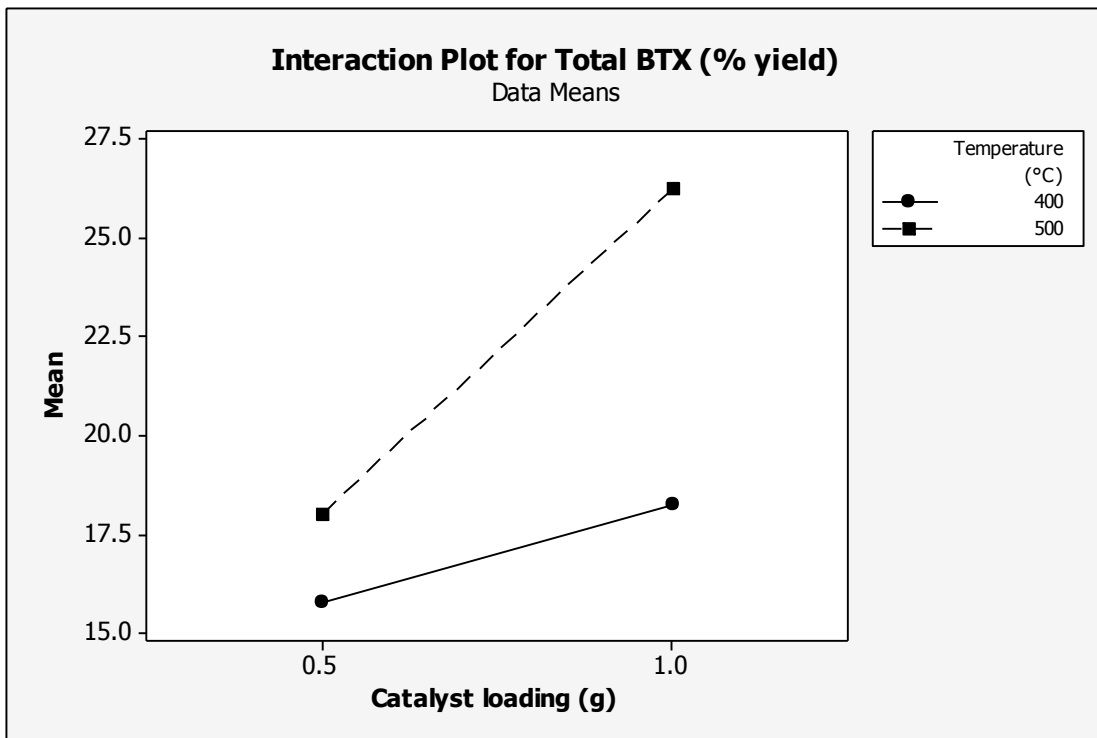
(c1)   (c2)
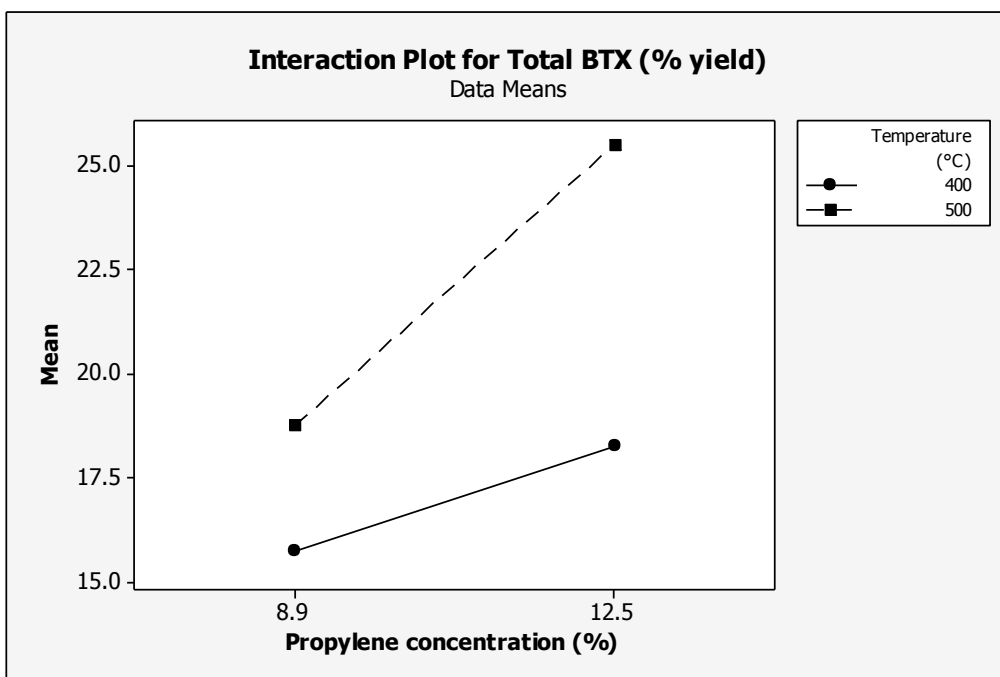
Figure 12. (a) Pareto chart, (b) main effects plot, and (c1 & c2) interaction plots for % total BTX yield.

The Pareto chart (Fig. 12a) shows that the interactions of temperature with propylene concentration (AB) as well as with catalyst amount (AC) had a significant effect on the BTX yield because their effects exceed the vertical line of significance at 2.31 (Fig. 12a). Fig. 12b shows the main effects plots of reaction temperature, propylene concentration and catalyst amount on the total BTX yield. The interaction plots of AB and AC are shown in Figures 12c1 and 12c2. An increase in all three factors resulted in a significant increase in BTX yield. Similar effects were observed and explained for the microscale HZSM-5 in a prior chapter. Thus, the effects of factors on BTX yields are irrespective the particle size. According to literature [54, 62, 63] a reduction in zeolite catalyst particle size makes that catalyst efficient because of increased surface area. However, this was not explicitly observed in this work.

A possible explanation may involve the active site concentration at the zeolite surface. The postulate is that nanoscale increases the overall active site concentration outside the catalyst pores. For most catalysts, this will result in a more efficient conversion and may help to inhibit secondary, undesirable reactions. However, the zeolite doesn't just facilitate the reactions by surface sites, it appears to also induce ring formation by the size/structure of the pores. As zeolite particle size is reduced, the outer surface area available for the reaction increases. Thus, the total number of acid sites on the outer surface area increases and the number of active sites inside pores decrease. Similarly, the effective pore channel length is also small for the nanoscale zeolite. When a propylene molecule comes in contact with the outer surface of HZSM-5, it undergoes decomposition into C_1 and C_2 fragments over Lewis acid sites. By contrast, only Brønsted acid sites distinctly small inner zeolite pores are responsible for cyclization.

Thus, the formation of cyclic intermediates on the outer surface of HZSM-5 is less likely due to the absence of small specific porous shape which causes cyclization. Hence the overall activity of nanoscale HZSM-5 to produce aromatics decreases.
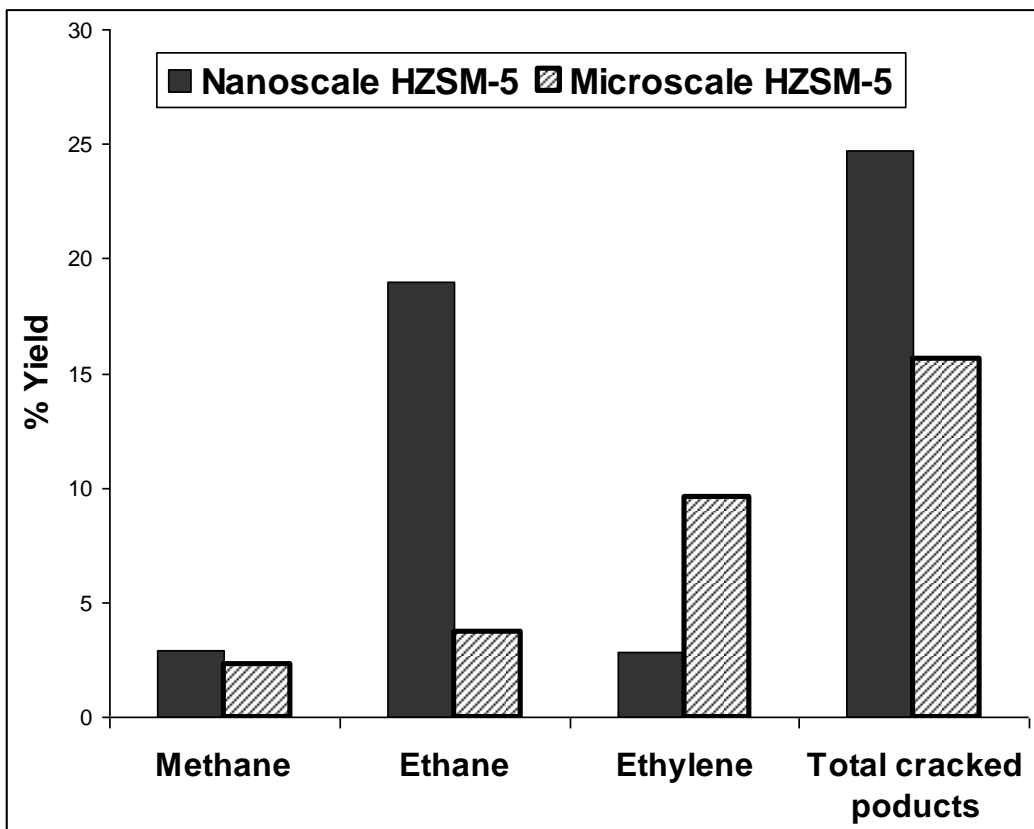
Figure 13. Propylene cracking activities over nanoscale and microscale HZSM-5 catalysts at the same reaction conditions

Fig. 13 confirms the formation of methane, ethane and ethylene as the presumed byproducts of propylene cracking. Amounts of these cracking products are greater than those formed by using microscale HZSM-5. This difference confirms that the cracking reactions are dominant over aromatization reactions when the nanoscale HZSM-5 was used. The significant interactions of temperature with propylene concentration and catalyst loading (AB and AC) (Fig 12a) have a common factor, reaction temperature.

43

When the propylene feed concentration was increased, the simultaneous increase of reaction temperature significantly increased the aromatics yield (Fig. 12c2). This is an indication that aromatization of propylene is a multimolecular reaction.

Interaction AC (Fig. 12c1) indicates that, within the bounds of the DOE, at higher catalyst loading and a higher reaction temperature the yield of aromatics increases. As explained previously, cracking of propylene molecules at higher temperature yields more C_1 and C_2 which readily diffuse through zeolite pores to form cyclic aromatic compounds. When the catalyst loading is increased, acid sites on the outer surface or zeolite enhance propylene cracking and, at the same time, more pores become available for cyclization which increases the overall yield of aromatics.

Effects of Factors and Their Interactions on Xylene Yields

Xylene yield rises significantly with increased catalyst loading when commercially available micro sized HZSM-5 is used [Chapter 2]. However, in this study the yield (or concentration, whichever is more accurate) of xylene decreased (Fig. 14b) with increased catalyst loading.

(a)

44

(b)

(c1)

Interaction Plot for xylenes (% distribution)
Data Means
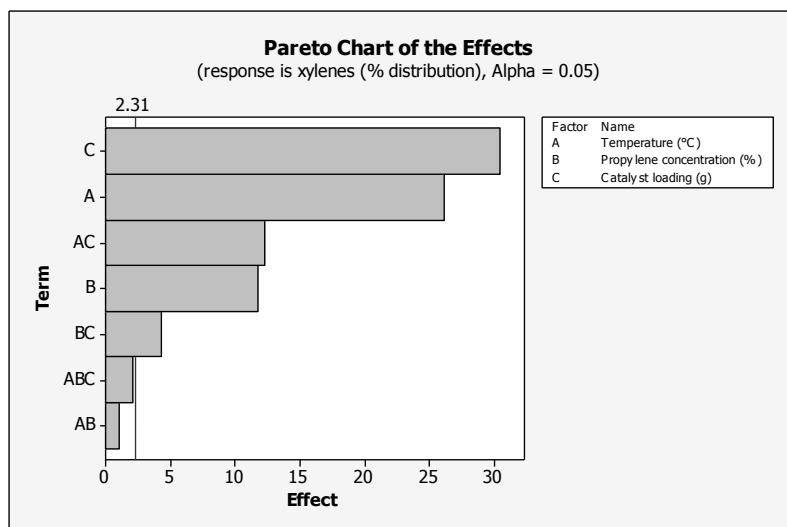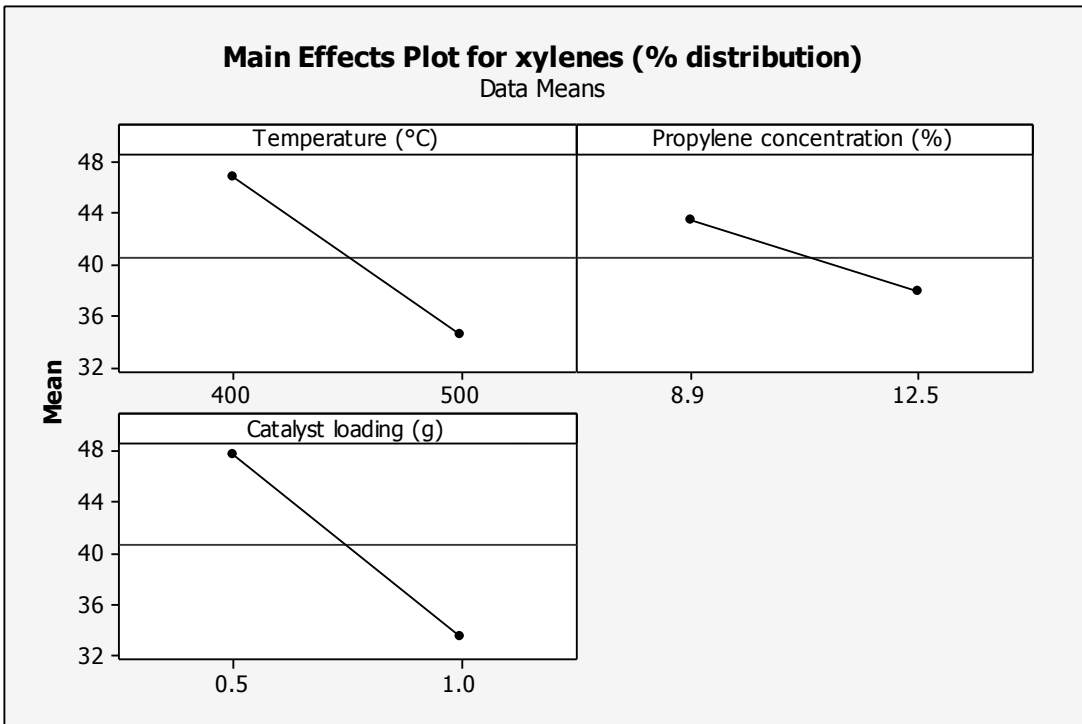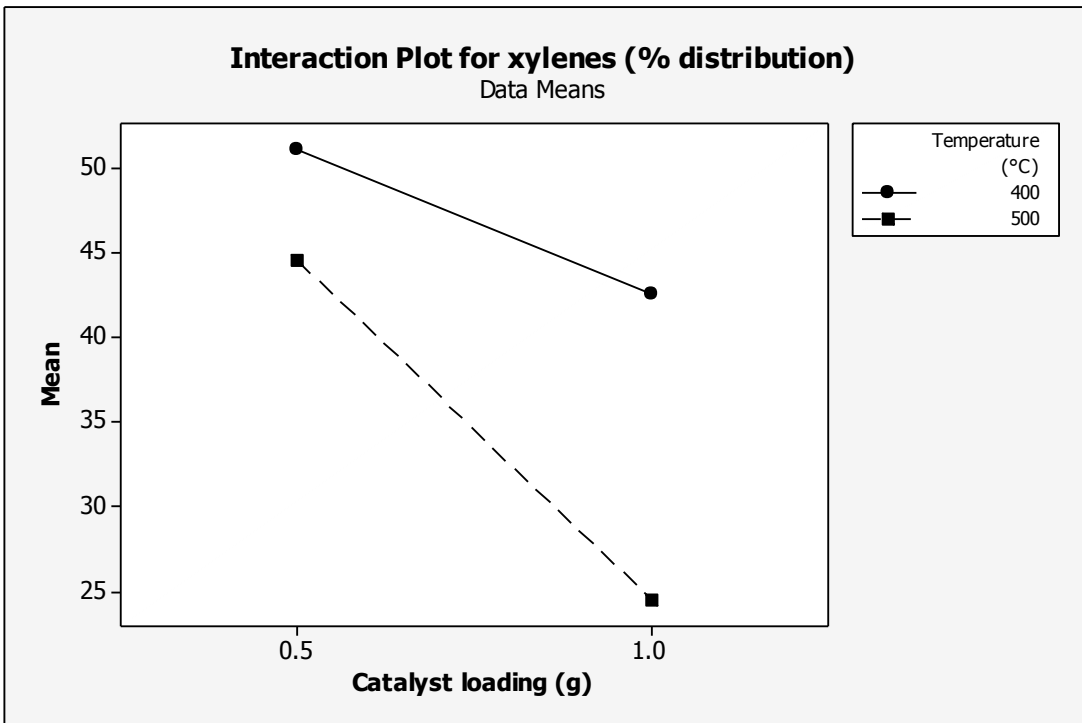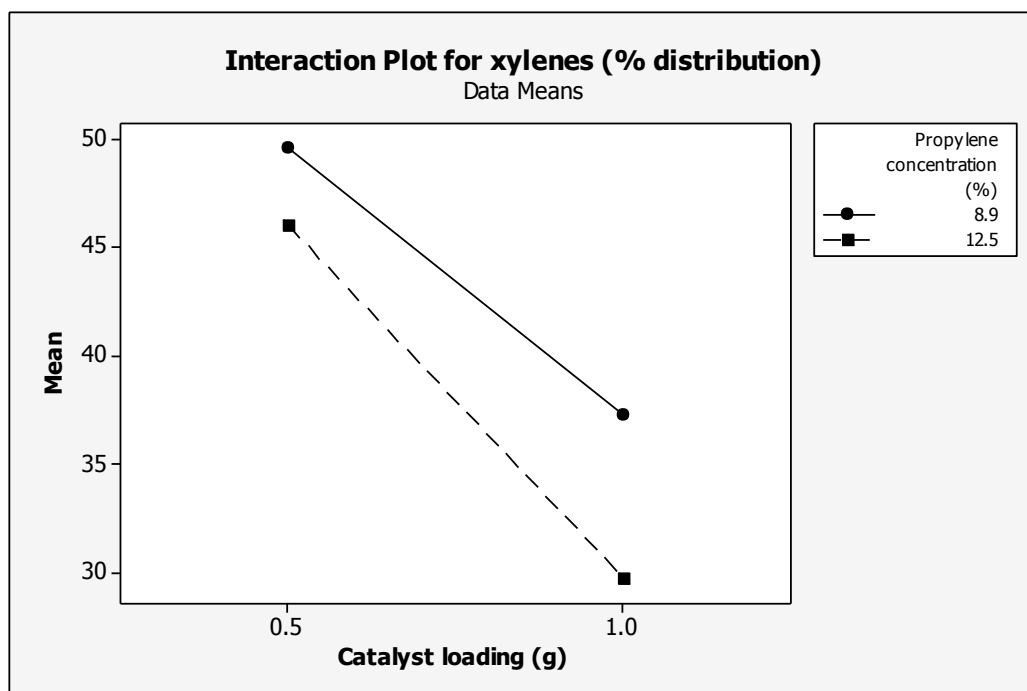
(c2)

Figure 14. (a) Pareto chart, (b) main effects plot, and (c1 & c2) interaction plots for % fraction of xylenes.

At the same time, benzene and toluene yields significantly increased. This is possibly due to a greater impact of the (hydro)dealkylation of xylenes. Large particles contain layers of pore channels attached to each other. So, once the xylene molecule is formed inside the pore, it travels from one pore to another pore of another layer inside one single large catalyst particle (crystal). Thus, more xylene molecules are trapped inside large particles and hence hydrodealkylation of xylene occurring on the outer surface is limited. However, in a small nano sized zeolite particle, a xylene molecule stays within the pores only for a short time due to the lack of adjacent crystal layer pores. Since the amounts of xylene molecules outside zeolite pore are greater; they eventually become hydrodealkylated into more benzene and toluene.

The interaction plot for xylenes (Fig. 14c1) shows that the effect of temperature on xylene yield depends on the catalyst loading. Higher amounts of catalyst at higher temperature are responsible for lowering the xylene yields because of a possible dealkylation of xylenes. This confirms the assumption that nanoscale HZSM-5 favors cracking, including hydrodealkylation. Similarly, an interaction plot for xylenes (Fig. 14c2) also confirms lower xylene yields when the catalyst amount is increased. Thus, even though the reaction temperature and propylene feed concentrations are at higher levels, they promote cracking of C8 intermediates and xylenes. As a result, nanoscale HZSM-5 appears to be a great cracking/dealkylation catalyst rather than an aromatization catalyst.

As the size of HZSM-5 catalyst decreases, its surface area increases which causes an increase in external active acid sites and a significant reduction in acid sites inside the pores. Acid sites on an external surface area cause cracking of feed and intermediate molecules. On the other hand, cyclization of linear molecules is hindered due to a loss in available acid sites inside pores.

Benzene/Toluene Yields and Mechanistic Considerations

Figs. 14 and 15 show that benzene and toluene are formed at the expense of xylenes.

(a)

(b)

Interaction Plot for Benzene (% distribution)
Data Means
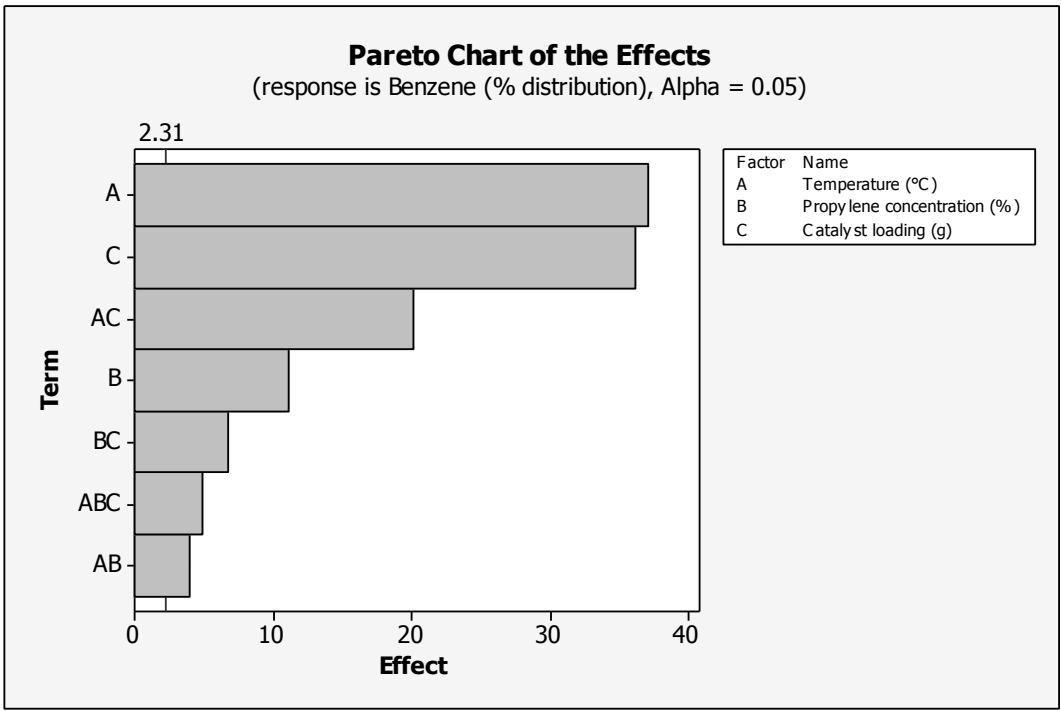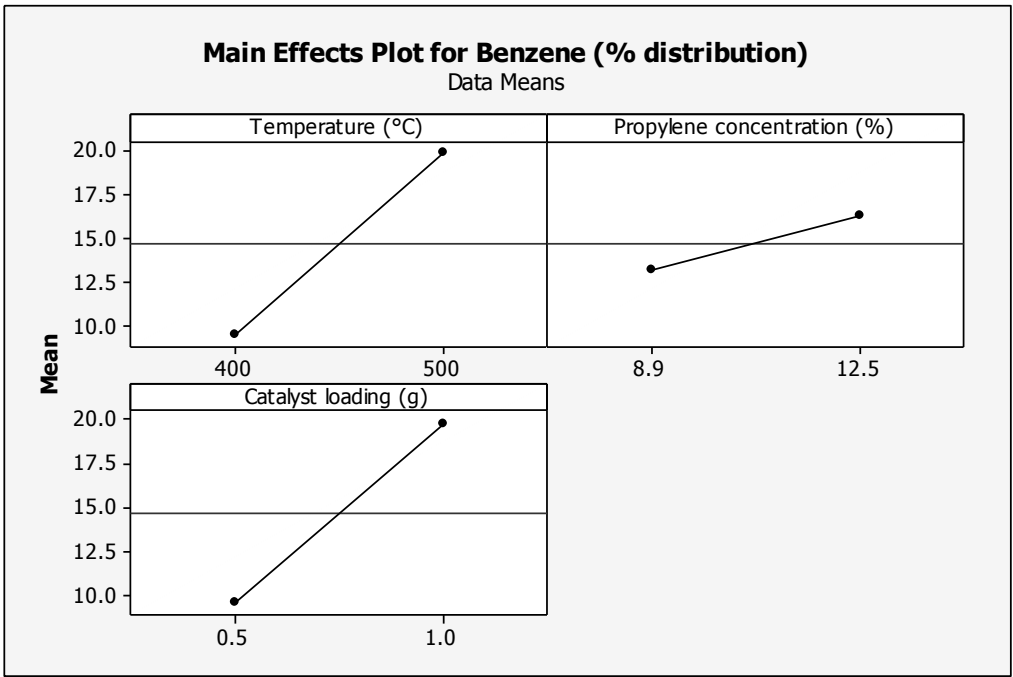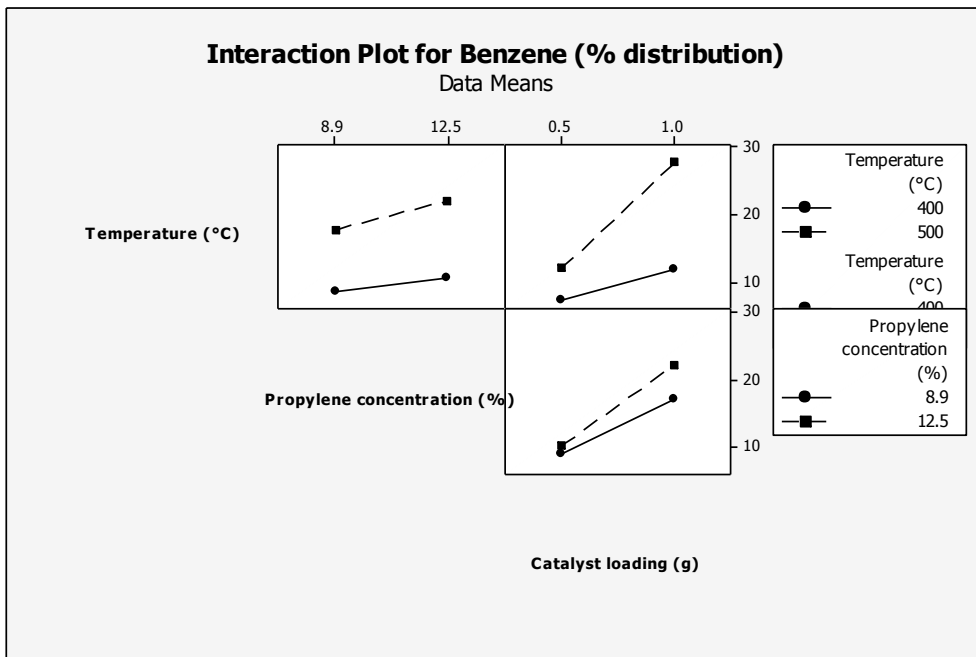
(c)

Figure 15. (a) Pareto chart, (b) main effects plot, and (c) interaction plots for % fraction of benzene.

The interaction plot for the relative yield of toluene (Fig. 16c) shows that the effect of reaction temperature depends on propylene feed concentration.

Pareto Chart of the Effects
(response is Toluene (% distribution), Alpha = 0.05)
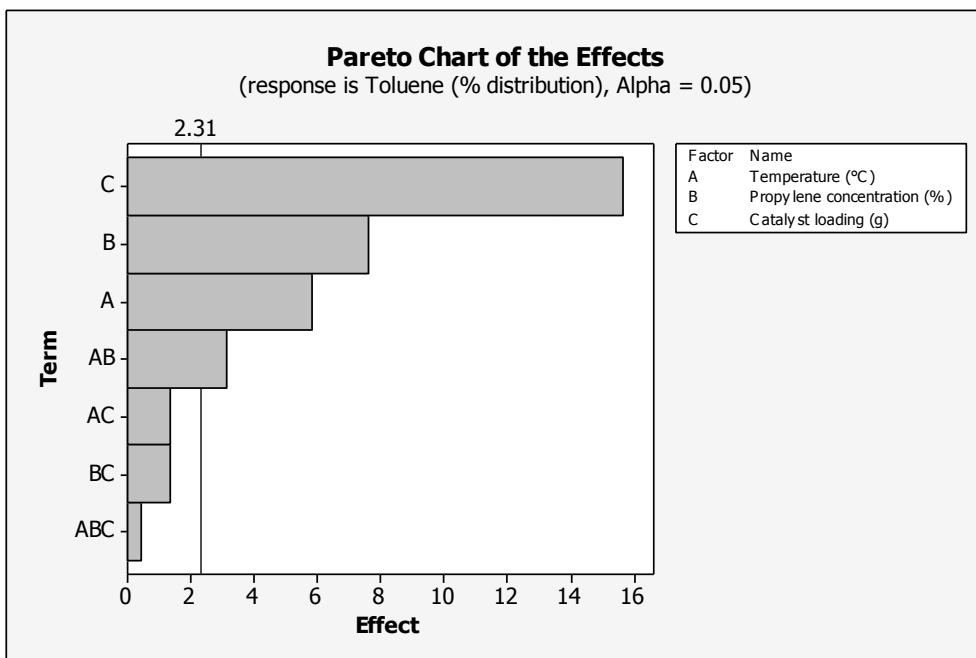
(a)
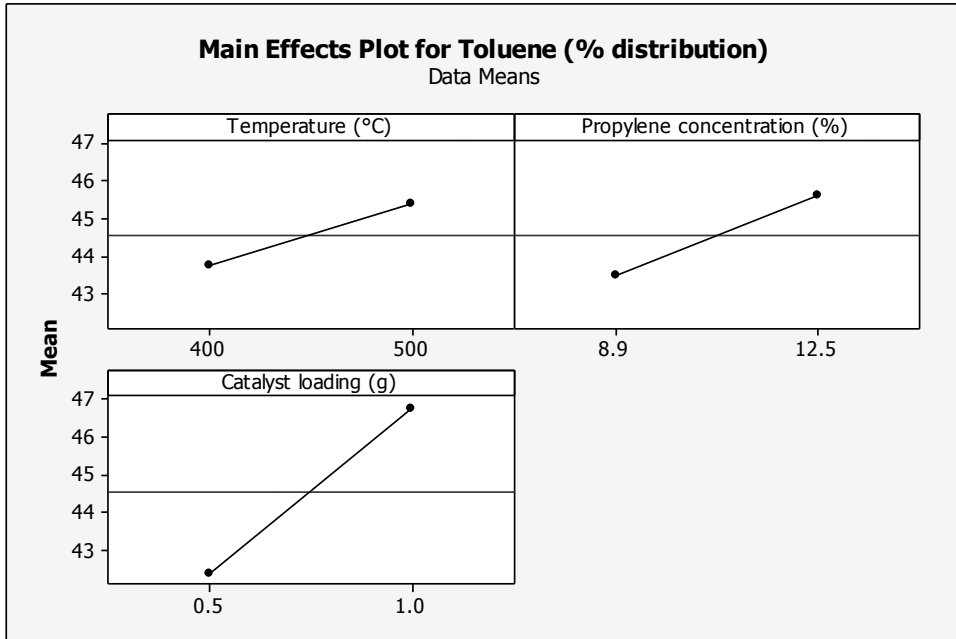
(b)
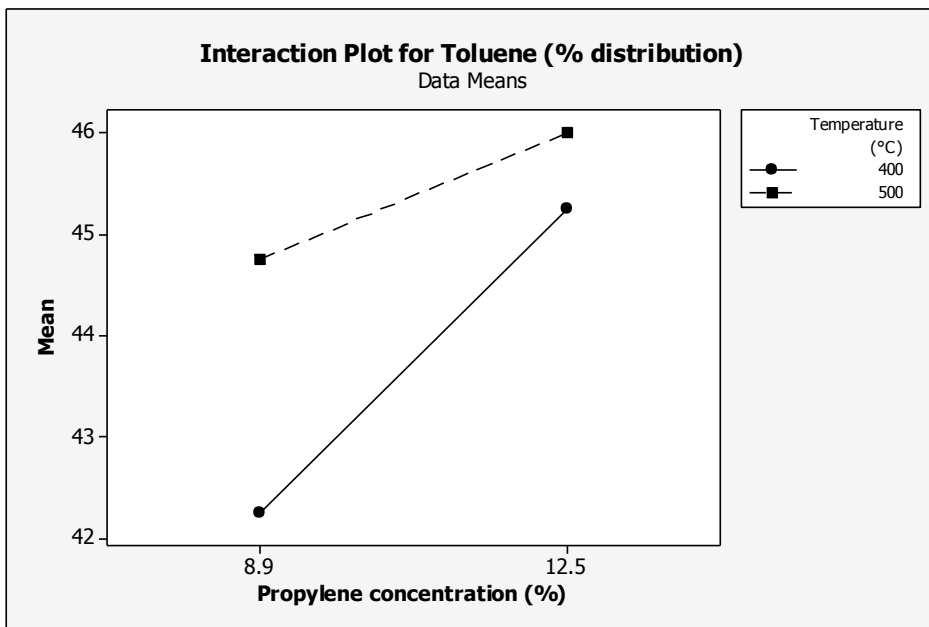
(c)

Figure 16. (a) Pareto chart, (b) main effects plot, and (c) interaction plots for % fraction of toluene.

At the higher level of propylene concentration, toluene yields are almost the same, regardless of the reaction temperatures. In other words, the effect of reaction temperature diminishes at higher feed concentration. So, it can be inferred that toluene formation over nanoscale HZSM-5 catalyst is diffusion controlled. The Pareto chart for toluene (Fig. 16a) also confirms the dominance of diffusion (catalyst loading shows a greater effect than temperature).

From the observed trends in BTX and xylene production, two pathways for toluene formation may be proposed

1) $C_2 + C_2 + C_3$ (diffusion inside HZSM-5 pore/dehydrocyclization) = Toluene + H_2

2) Xylene (dealkylation/hydrodealkylation) = Toluene + methane

This may be a possible reason for the formation of significant quantities of methane during aromatization of propylene over nanoscale HZSM-5 catalyst.

Conclusions

Nanoscale zeolites are not suitable for aromatization of propene to BTX as they appear to facilitate other reactions, such as propene cleavage to ethylene and methane. A statistical design of experiments (DOE) approach determined that all the three reaction factors (temperature, propylene concentration and catalyst loading) significantly influenced the aromatization. In addition to benzene, toluene and xylenes, other hydrocarbons such as methane, ethane, ethylene and butane were also formed over nano-sized HZSM-5. Since shape selectivity is important for HZSM-5 zeolites, the performance of nanoscale zeolite is highly dependent on the overall molecular diffusion length and availability of active sites inside zeolite pores for dehydrocyclization to aromatics. The nanoscale HZSM-5 catalyst was proven to be a hydrocarbon cracking

catalyst and less suitable for aromatization of propylene than microscale HZSM-5. This work can potentially be beneficial for petroleum catalytic cracking and dealkylation process

CHAPTER IV

CONVERSION OF 1-TETRADECENE TO AROMATIC COMPOUNDS

Introduction

Aromatic compounds, particularly BTEX (benzenes, toluene, ethylbenzene and xylenes) are commercially used as starting materials for manufacturing polymers, resins, industrial fibers and elastomers. The most common use of BTEX are as solvents. They are also present in gasoline to increase its octane rating. The most promising method for the production of aromatic compounds (BTEX) is catalytic conversion [23, 64].

Presently, the sources for the production of aromatics are petroleum and coal. Various processes have been commercialized for converting light alkanes, olefins and petroleum naphtha into aromatic compounds via catalytic cracking and reforming routes. Current academic as well as industrial research is focused on the production of aromatic compounds from light alkanes and alkenes [24-26, 28-32, 34-41, 44, 47, 64-70]. Fatty acids[71, 72] and olefins such as ethylene, propylene, butene, hexene and octene have also been aromatized by using zeolite catalysts[73-75]. ZSM-5 catalysts in hydrogen form or in the metal (Ga, Zn) doped forms showed the best results for conversion of olefins into aromatic compounds.

1-hexene was successfully converted into aromatics in a plug flow reactor by using Ga doped HZSM-5 catalysts by R. J. Nash et. al. [76] and it was observed that C_8

aromatics are major aromatic products at lower temperatures. At higher temperatures, dealkylation of C_8 aromatics yield more benzene and toluene.

Most notably, at lower residence time, Nash observed that cracking dominates, resulting in the formation of light alkenes, such as propylene, as primary products. However, significant amounts of bulkier molecules and aromatics were produced when the residence time was increased. This suggests that for C_6 and greater carbon chain lengths, aromatics formation is a multi-step process where cracking of the feedstock to lighter alkenes occurs in the first step with cyclization and dehydrogenation occurring in subsequent steps. Similar trends were observed for 1-octene aromatization in the same study. Yuning Li and coauthors also reported [69, 77] the conversion of 1-hexene to aromatic compounds in a continuous fixed bed reactor by using ZSM-5 type zeolites. This conversion of α-olefins to aromatics was achieved between temperature ranges of 350 °C - 480 °C.

Aromatization of *n*-octene over nanoscale HZSM-5 catalysts were also carried out in a continuous flow fixed bed reactor [70]. Toluene and xylenes were the major aromatics and individual aromatic formation was greatly influenced by the levels of strong acid sites within the catalyst. In another study of *n*-octene aromatization over nanoscale HZSM-5 catalysts[59], it was observed that lower temperatures produced greater concentrations of xylenes, and that selectivity towards benzene and toluene formation increases with an increase in temperature.

Processes for the aromatization of C3-C6 olefins have been commercialized [see chapter 1] while middle chain length (C_6, C_8) olefins have also been studied, as described

above. However, to our best knowledge, no work has been conducted to date to study the aromatization of α-olefins having a chain length greater than 10 carbon atoms. Distinguished by the chemical formula C_nH_{2n}, 1-tetradecene is a commercially important α-olefin for the manufacture of detergents, surfactants, linear alkylbenzenes [78-81]. \Previous studies associated with 1-tetradecene have concentrated on its use as a comonomer in copolymerization reactions [82-84]. 1-tetradecene is also used in functional drilling fluids, lubricants, automotive additives, and metal working agents.

For the present study, 1-tetradecene was selected as one of a series of model compounds to assist in developing a process to improve the ability to produce renewable aromatics from triacyl glyceride (TAG) oils, such as crop oils (soy, corn, canola, etc.), algal oil and microbial oils, and from fatty acids such as restaurant wastes and animal fats. The primary objective was to determine if C10-C16 alpha olefins, which are present in the organic liquid product generated during non-catalytic cracking, could be effectively converted into aromatics. A secondary objective was to explore the reaction conditions using DOE methodologies in order to gain insight into the significant effects of reaction conditions and their interactions on aromatization

Experimental

Materials

The ZSM-5 catalyst (CBV 2314 – $SiO_2/Al2O_3$ ratio = 23) was purchased from Zeolyst International, Conshohocken, PA, USA. 1-Tetradecene (97% purity), GC grade standards, benzene, toluene, ethylbenzene, xylenes, naphthalene and 2-chlorotoluene were purchased from Sigma-Aldrich, Saint Louis, Missouri, USA. The commercial ZSM-

5 catalyst was supplied in its ammonium form. The ammonium form was converted into its hydrogen form by calcination at 550 °C for 5 hours in an air circulated oven, generating activated HZSM-5 catalyst.

Experimental Setup

A Parr series 4575 fixed head, bench top, high temperature, high pressure autoclave type reactor was used. This reactor (500 mL) was equipped with a cooling channel to control the reaction temperature and a stirrer that agitated the catalyst and reaction mixture. The reaction temperature was controlled and monitored by a K-type thermocouple connected to Parr 4843 controller, which also monitored and controlled the impeller speed. The reactor was equipped with a gas inlet connected to a nitrogen cylinder to maintain initial reaction pressures.

Experimental Procedures

The required catalyst amounts (4-15 g) and 1-tetradecene (100 g) were charged to the catalytic reactor. The reactor was purged with nitrogen gas to remove air prior to heating. The reactor was heated to a desired temperature for the allotted time with its contents being stirred at 300 rpm. Once the reaction was completed, reactor contents were cooled down to room temperature and then the gaseous products were collected in a gas bag by slowly opening the reactor vent. The entire reactor contents were weighed and then filtered to separate coke/solid particles from liquid reformates. The collected samples were dissolved in methanol to ensure miscibility and submitted to analysis.

The amount of coke formed was determined by subtracting the weight of the catalyst fed to the reactor from that of the catalyst obtained after reaction, thus accounting

for the coke deposit developed on its surface. The yield of gases was determined by the difference between the masses of the tetradecene fed and the combined mass of the reformate and coke produced.

Chemical Characterization of Reformate

The reformate characterization was based on the adopted GC-FID/MS method [85] but targeting quantification of aromatic standards using GC-FID-MS (Agilent 5890 Series II with 5973 MS). For detailed characterization of the reformate aromatic products, a faster screening analytical protocol was adopted using GC-MS (Agilent 5890 Series II with 5973 MS). The temperatures of the GC injector and transfer line to MS were set at 250 ℃ and 280 ℃, respectively. The oven temperature program was started at 40 °C for 5 min and then ramped at 15 ℃/min to 310 °C and held at this temperature for 5 min. The sample injections of 1 µL were performed in the split mode (1:20) at a helium constant flowrate of 1.5 mL/min. The GC-MS analysis was performed with electron ionization, the solvent delay was of 4 min in a mass range of 50-500 amu.

The aromatics were identified based on their GC retention time and pattern of homolog and isomer elution as detailed elsewhere (Kubátová et al., 2011) . The retention times for thus identified aromatic hydrocarbons are listed in Table 5. The aromatics' quantification was based on BTEX (benzene, toluene, ethylbenzene and xylenes) standards using a full calibration between 0.01 to 5.0 wt.%, with the addition of an internal standard (chlorotoluene) to the sample. The BTEX were directly quantified based on the major ions (Table 5).

Table 5. List of compound name, calibration standard and quantification ion

Compound name	Formula	Molecular weight	Retention time (min.)	Quantification Ion
Benzene	C_6H_6	78	4.6	78
Toluene	C_7H_8	92	7.1	91
Ethylbenzene	C_8H_{10}	106	9.1	91
p-Xylene	C_8H_{10}	106	9.3	91
o-Xylene	C_8H_{10}	106	9.7	91
o-Xylene 105	C_8H_{10}	106	9.7	105
Naphthalene	$C_{10}H_8$	128	13.7	128
Benzene C_{3z}	C_9H_{12}	120	10.2	105
Benzene, C_{3a}	C_9H_{12}	120	10.8	105
Benzene, C_{3b}	C_9H_{12}	120	10.9	105
Benzene, C_{3x}	C_9H_{12}	120	11.1	105
Benzene, C_{3y}	C_9H_{12}	120	11.3	105
Benzene, C_{4a}	$C_{10}H_{14}$	134	11.5	105
Benzene, C_{4b}	$C_{10}H_{14}$	134	11.6	119
Benzene, C_{4c}	$C_{10}H_{14}$	134	11.7	119
Indane	C_9H_{10}	118	11.9	105
Benzene, C_{4y}	$C_{10}H_{14}$	134	12.0	105
Benzene, butyl-	$C_{10}H_{14}$	134	12.1	91
Benzene, C_{4d}	$C_{10}H_{14}$	134	12.2	105
Benzene, C_{4x}	$C_{10}H_{14}$	134	12.28	105
Benzene C_{4e}	$C_{10}H_{14}$	134	12.37	105
Benzene C_{4f}	$C_{10}H_{14}$	134	12.4	105
Benzene, C_{4z}	$C_{10}H_{14}$	134	12.47	105
Indane, C_{1a}	$C_{10}H_{12}$	132	12.52	105
Benzene C_{5y}	$C_{11}H_{16}$	148	13.06	105
Indane, C_1	$C_{11}H_{14}$	132	13.13	105
Benzene, C_{5a}	$C_{11}H_{14}$	148	13.17	105
Indane, C_{1x}	$C_{11}H_{14}$	132	13.27	105
Benzene, C_{5b}	$C_{11}H_{16}$	148	13.48	105
Benzene, C_{5z}	$C_{11}H_{16}$	148	13.61	105
Benzene, pentyl-	$C_{11}H_{16}$	148	13.31	91
Benzene, C_{5x}	$C_{11}H_{16}$	148	13.41	105
Indane, C_2	$C_{11}H_{14}$	146	13.73	105
Benzene, C_{6a}	$C_{12}H_{18}$	162	14.19	105
Benzene, C_{6y}	$C_{12}H_{18}$	162	14.27	105
Benzene, hexyl-	$C_{12}H_{18}$	162	14.36	91
Benzene, C_{6x}	$C_{12}H_{18}$	162	14.44	105
Naphthalene, C_{1y}	$C_{11}H_{10}$	142	14.83	128
Naphthalene, C_{1x}	$C_{11}H_{10}$	142	15.01	128
Benzene, heptyl-	$C_{13}H_{20}$	176	15.34	91
Benzene, C_{7x}	$C_{13}H_{20}$	176	15.41	105
Naphthalene, ethyl	$C_{12}H_{12}$	156	15.75	128
Naphthalene, C_{2x}	$C_{12}H_{12}$	156	15.85	128

Table 5 continued

Naphthalene, C_{2y}	$C_{12}H_{12}$	156	16	128
Benzene, octyl-	$C_{14}H_{22}$	190	16.25	91
Benzene, C_{8x}	$C_{14}H_{22}$	190	16.30	105
Naphthalene, C_{3x}	$C_{13}H_{14}$	170	16.71	128
Naphthalene, C_{3y}	$C_{13}H_{14}$	170	16.82	128
Benzene, nonyl-	$C_{15}H_{24}$	204	17.10	91
Benzene, C_{9x}	$C_{15}H_{24}$	204	17.16	105
Benzene, decyl	$C_{16}H_{26}$	218	17.91	91
Benzene, C_{10x}	$C_{16}H_{26}$	218	17.96	105
Benzene, C_{11a}	$C_{17}H_{28}$	232	18.11	105
Benzene, C_{11b}	$C_{17}H_{28}$	232	18.18	105
Benzene, undecenyl	$C_{17}H_{28}$	232	18.67	91
Benzene, C_{11x}	$C_{17}H_{28}$	232	18.73	105

For quantitation of other alkyl aromatics, signals of representative ions were used employing a calibration slope obtained ion of m/z 105 for *o*-xylene. In rare cases when the *m/z* 105 signal was of low intensity, other characteristic ions were used listed in Table 5. The mass balance closure for two selected samples was estimated based on the percent response obtained from the total ion current chromatograms and its proportionality to the aromatic compounds. A 2 level, 3 factor, full factorial experimental design was used to study the catalytic conversion of 1-tetradecene over an HZSM-5 zeolite having a SiO_2/Al_2O_3 (Si/Al) ratio of 23. The reaction temperature (^oC), olefin (tetradecene) to catalyst ratio (OCR), and reaction time (minutes) were chosen as the factors to be studied. All the aromatization experiments were performed in a random order.

The amount of feed 1-tetradecene used was kept constant for all experiments. After each aromatization run, the mass of liquids and coke/solids formed were determined and the organic liquid products were further analyzed to –quantify the individual and total aromatics produced.

Results and Discussion

Aromatic Hydrocarbon Product Yields

A typical chromatogram of the reaction product mixture is shown in Fig. 17.
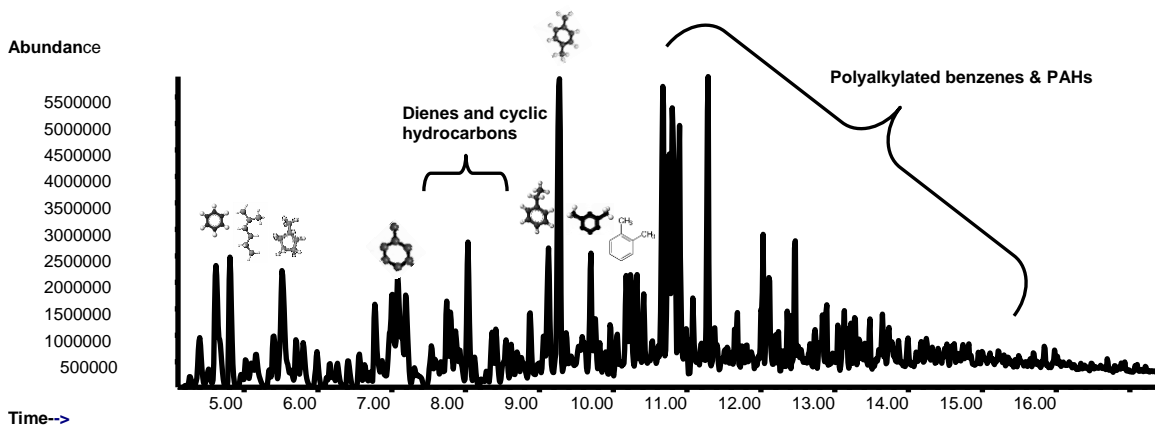
Figure 17. Chromatogram of liquid products obtained by using HZSM-5. Operational conditions were 375 ºC, OCR = 10 and reaction time of 30 minutes.

The trends in monoaromatic hydrocarbon yields shown in Fig. 18 were similar for BTEX and its higher-MW homologs: Lower OCR and higher temperature promoted the formation of all aromatics, thus indicating the catalytic nature of their formation and necessity of prior feedstock cracking, respectively.

60
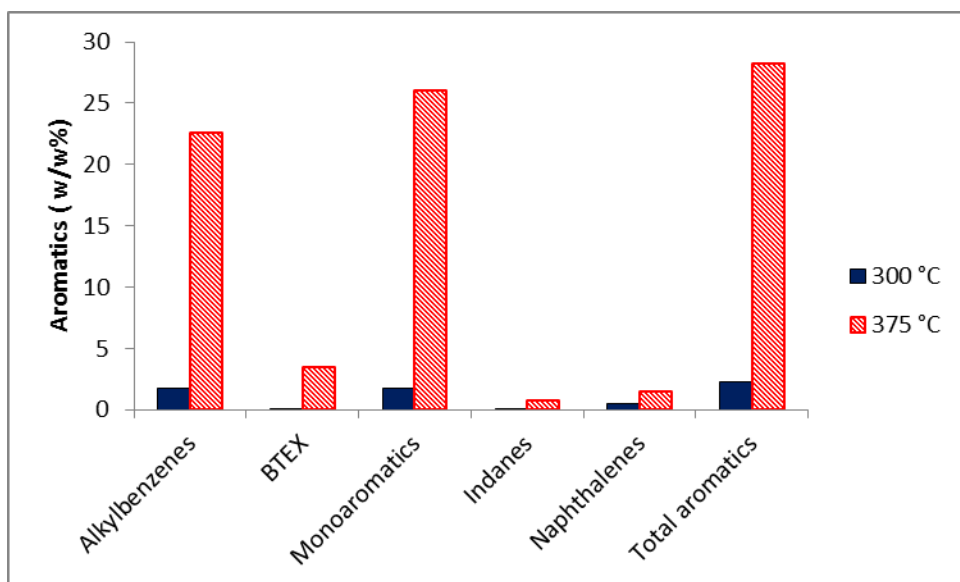
b)
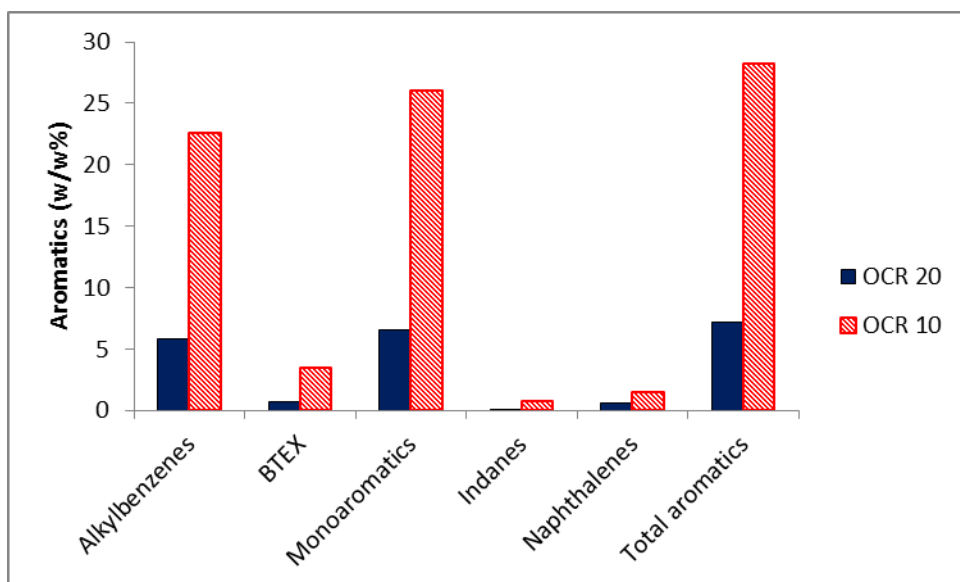
Figure 18. Comparison of aromatic hydrocarbon yields obtained by 1-tetradecene aromatization varying a) reaction temperatures (where OCR* was 10 and time was 30 minutes), b) OCR (where temperature was 375 °C and time was 30 minutes). The Y axis represents the concentration (wt%) of aromatic hydrocarbons in the product.
* OCR = Olefin to catalyst ratio

A more detailed analysis distinguishing monoaromatics from diaromatics (Table 6) corroborated this conclusion with one exception: Low temperature promoted the formation of diaromatics at the expense of monoaromatics. This observation may explain the preferred formation of coke at a lower temperature as discussed in the next section.

Table 6. Detailed composition of the aromatic hydrocarbon product fraction formed under the maximum yield conditions in runs #3 (Tables 7 and 8) and its replicate. The reforming reaction conditions were as follows: 375 ºC, OCR = 10 and reaction time of 30 minutes. The isomers are listed in the order of their chromatographic elution.

Aromatic hydrocarbon	Sample 1	Sample 2	Average	StDev (+/-)
Benzene C3z	0.15	0.17	0.16	0.012
Benzene, C3a	5.6	6.0	5.8	0.25
Benzene, C3b	0.89	0.99	0.94	0.07
Benzene, C3x	0.61	0.67	0.64	0.045
Benzene, C3y	3.5	3.8	3.7	0.24
Benzene, C4a	0.057	0.068	0.062	0.01
Benzene, C4b	0.38	0.44	0.41	0.04
Benzene, C4c	0.33	0.37	0.35	0.03
Benzene, C4y	1.8	2.0	1.9	0.11
Benzene, C4x	0.20	0.22	0.21	0.01
Benzene C4e	0.55	1.4	0.99	0.63
Benzene C4f	0.49	1.4	0.96	0.67
Benzene, C4z	1.8	1.4	1.6	0.23
Benzene C5y	0.34	0.38	0.36	0.027
Benzene, C5a	0.94	1.0	0.99	0.08
Benzene, C5b	0.73	0.81	0.77	0.06
Benzene, C5x	0.13	0.13	0.13	0.00
Benzene, C6a	0.16	0.20	0.18	0.03
Benzene, C6y	0.11	0.12	0.12	0.01
Benzene, C6x	0.06	0.08	0.07	0.01
Benzene	0.06	0.06	0.06	0.01
Toluene	0.77	0.85	0.81	0.06
Ethylbenzene	0.26	0.29	0.28	0.02
p-Xylene	1.7	1.8	1.7	0.09
o-Xylene	0.41	0.46	0.43	0.04
Indane	0.03	0.03	0.03	0.005
Indane, C1a	0.11	0.30	0.21	0.13
Indane, C1	0.25	0.04	0.15	0.15
Indane, C1x	0.15	0.17	0.16	0.01
Indane, C2	0.12	0.16	0.14	0.03
Benzene, butyl-	0.47	0.52	0.49	0.03
Benzene, pentyl-	0.12	0.15	0.13	0.02

Table 6 continued

Benzene, hexyl-	0.04	0.05	0.05	0.01
Benzene, heptyl-	0.02	0.02	0.02	0.00
Naphthalene	0.09	0.09	0.09	0.00
Naphthalene, decahydro-C2	0.08	0.08	0.08	0.00
Naphthalene, C1y	0.35	0.39	0.37	0.03
Naphthalene, C1x	0.11	0.12	0.12	0.01
Naphthalene, ethyl	0.07	0.07	0.07	0.00
Naphthalene, C2x	0.30	0.33	0.32	0.02
Naphthalene, C2y	0.15	0.16	0.15	0.01
Naphthalene, C3x	0.16	0.18	0.17	0.01
Naphthalene, C3y	0.052	0.052	0.052	0.00

Liquid, Gas and Coke Product Yields

Table 7 shows the yields of gas, coke and liquid products from 1-tetradecene obtained in the same runs as those discussed above.

Table 7. Gases, liquids and coke yields obtained from 1-tetradecene conversion

Expt.	Reaction Temp. (°C)	Time (Min.)	OCR	Gases produced, %	Liquid products produced, %	Coke produced, %
1	300	30	10	13	73	12
2	300	60	10	18	68	13
3	375	30	10	46	43	9.0
4	375	60	10	47	47	6.0
5	375	60	20	29	53	16
6	300	60	20	9.5	83	6.7
7	375	30	20	38	58	3.2
8	300	30	20	5.5	87	6.7

The yield of coke was maximized at low temperature. In combination with the low yield of aromatics obtained under these conditions, low temperature appears to be unsuitable for the reforming process. By contrast, gas phase yields were maximized at high temperature. Furthermore, those runs that produced most aromatics were also characterized by higher yields of gases, with the corresponding reduction of the OLP yields. The available literature on zeolite catalysis corroborates this trend; it is often explained by the formation of small C_2-C_3 size intermediates of aromatization [2, 3, 15].

Table 8. Aromatic product yields (wt%) obtained in experiments on 1-tetradecene conversion.

Expt. No.	Temp. (°C)	Time (min)	OCR	Alkyl benzenes	BTEX	mono- aromatics	Indanes	Naphthalenes diaromatics	Total aromatics
1	300	30	10	1.7	0.05	1.7	0.00	0.50	2.2
2	300	60	10	3.0	0.20	3.2	0.030	0.50	3.7
3	375	30	10	22	3.5	25	0.70	1.5	28
4	375	60	10	15	2.2	17	0.40	1.1	19
5	375	60	20	8.0	1.1	9.2	0.10	0.70	10
6	300	60	20	1.4	0.30	1.7	0.00	0.50	2.2
7	375	30	20	5.7	0.70	6.4	0.020	0.60	7.0
8	300	30	20	0.30	0.00	0.30	0.00	0.40	0.70

Thus, the general main reactions postulated in literature on zeolite catalysis appear to be similar for low-MW and high-MW alkenes as feedstocks. However, the data shown in Table 7 and Fig. 18 showed one significant difference in the product composition compared to zeolite-catalyzed reforming of lower-MW alkenes, for which BTEX were the main aromatic products. The reformate obtained upon 1-tetradecene

conversion was dominated by predominantly branched alkylbenzenes of a larger size than

BTEX. prompted an even more detailed analysis of the reaction products, i. e., on the

level of individual chemical species, which is discussed in the next section.

Yields of Individual Compounds and Homology Profiles

The detailed composition of aromatics in the reformate for run #3 that yielded the

greatest amount of aromatic products, is shown in Table 8. As one can see, many if not

all of the possible isomers were formed, although their relative amounts vary. For C_3-

substituted benzenes, isomers were observed in reasonable abundance. By contrast, only

seven C_4- and C_5-substituted aromatic products were observed, despite the increase of the

theoretical number of isomers in this homological series. Apparently, some isomers of

higher MW were formed in lower amounts, below their limit of quantification or even

identification.

To assess the products' homology profile, the amounts of isomers were combined

to yield the plot shown in Fig. 19.
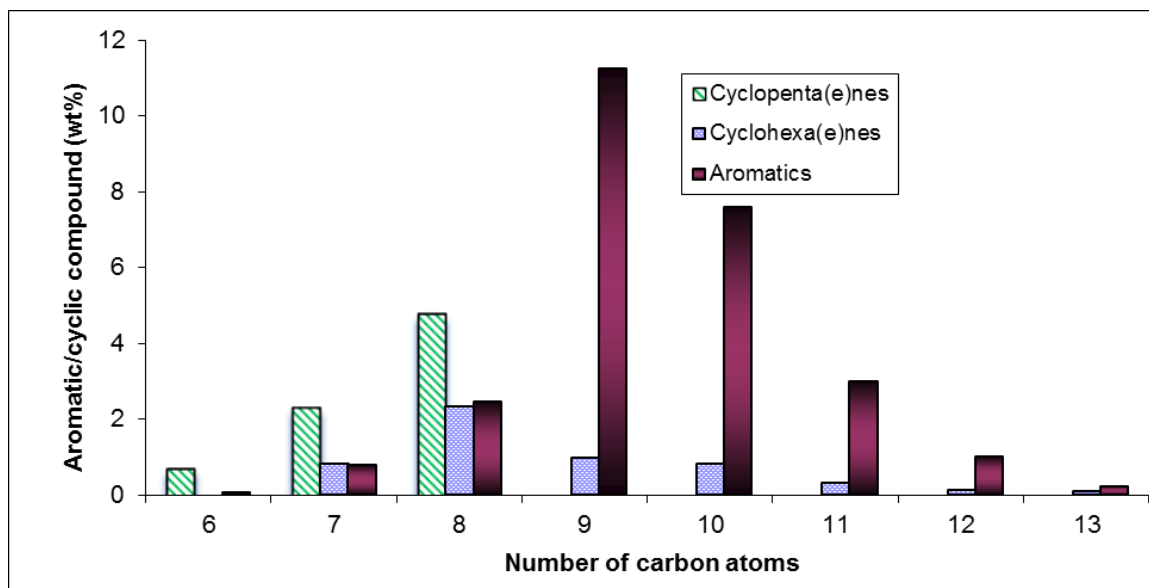
Figure 19. Homology profiles of the alicyclic and aromatic hydrocarbon products. The reforming reaction conditions were 375 ºC, OCR = 10 and reaction time of 30 minutes.

The observed profile corroborated the hypothesis stated in the previous paragraph that higher that C_3-substituted products were formed in lower abundance. Furthermore, C_9 aromatics turned out to be the most abundant in contrast to the previous studies in which BTEX were the most abundant products of zeolite action.

Mechanistic Implications

The obtained information on cyclic product homology profiles may lead to the following mechanistic considerations. Perhaps, the main intermediates formed as a result of 1-tetradecene cracking are larger in size than the C_2 (adsorbed ethylene) intermediates, which were earlier postulated for lower-MW feedstocks [39, 86]. This conclusion might, at the first glance, contradict the well-known match of the sizes of BTEX molecules and zeolite pores [87]. However, larger alkylbenzene molecules may be formed from larger intermediates within the near-surface pores.

This suggestion corroborates the following observation. As one can see from Fig. 19, significant amounts of cyclohexanes/cyclohexanes were formed in addition to aromatics. Furthermore, the product homology profiles for aromatics and the corresponding alicyclic hydrocarbons do not match, the latter peaking at a lower size, i.e., C_8. These observations suggest that the primary cyclization and subsequent aromatization occur on different zeolite sites, with the aromatization sites being closer to the surface. As a result, smaller C_6-C_8 cyclic intermediates matching the pore size move into the depth of the zeolite network where they "survive" till the product recovery.

By contrast, larger-size intermediates are forced to undergo aromatization, which stabilizes them as products. Perhaps, with larger-size substrates the zeolite surface sites responsible for cracking/dealkylation turn out to be saturated. This may explain the shift of the aromatics' homology profile from C_7-C_8 for smaller-size alkene feedstocks to C_9 for 1-tetradecene. Corroborating this hypothesis, C_9 aromatics were found to be predominant when carboxylic acids of triglycerides, other large molecules, were treated with zeolites under similar conditions [88].

The obtained homology profile of cyclopenta(e)nes (Fig. 19) offers additional support to this hypothesis, as only $>C_9$ homologs of these products were recovered, even though the C_8 homologs were most abundant. Since these compounds cannot be stabilized by aromatization, unlike cyclohexa(e)nes, it appears that they may "survive" cracking/reforming only if they diffuse into the zeolite pore network, which is restricted to the BTEX size.

Conclusions

In the presence of HZSM-5, 1-tetradecene is converted to aromatic hydrocarbons of a predominantly larger size than BTEX ($>C_8$). Higher reaction temperature (375 ^{o}C) and lower olefin to catalyst ratio (OCR) increase the aromatics yield, although gas phase products are also formed in abundance under such conditions. Besides aromatics, significant amounts of cyclohexanes, cyclohexenes and cyclopenta(e)nes are recovered, with the size of these products peaking at C_8. Given the size of the zeolite pores matching that of BTEX molecules, larger-size aromatic hydrocarbons may be formed at the pore opening, near the zeolite surface; this factor may be characteristic and specific for large substrates, such as 1-tetradecene. Also, cyclization and aromatization of the primary intermediates appear to be uncoupled, with larger-size substrates promoting the formation of slightly larger-size aromatic but not alicyclic products.

CHAPTER V
A NOVEL TWO STEP PROCESS FOR THE PRODUCTION OF RENEWABLE
AROMATIC HYDROCARBONS

Introduction

Crude oil is the major current source for production of aromatics, which are used for gasoline octane enhancement. Aromatics from coal are produced commercially in small amounts and most end up in the form of a pitch or asphalt products. Considering the dwindling supply of petroleum, there is a growing interest in developing renewable resources for producing aromatics and organic chemicals. These include several attempts to produce phenolics by pyrolysis of lignin including zeolite catalysis [89].

Several studies [90-96] were conducted to convert biomass and pyrolytic bio-oils into hydrocarbons by using porous catalysts such as H-Y zeolites, HZSM-5, H-modernite. The reaction temperature was varied from 290 °C – 410 °C. For silica-alumina catalysts, the yields of aromatics were only between 4-7 wt% even at higher temperatures whereas the coke yields were as high as 30 wt%. By contrast, HZSM-5 produced only about 15 wt% coke. Although aromatics accounted for as much as 86 wt% of the organic liquid product (OLP) formed, the OLP yield with HZSM-5 was merely 22 wt%. Thus, low OLP yields brought the total aromatics yield down to 19 wt% with respect to the feedstock [97-99].

Triglyceride (TG) oils, such as palm, soybean, canola and other cooking oils, is the third promising feedstock for the production of valuable organic chemicals; it is

particularly well-suited for production of aromatic hydrocarbons as opposed to phenolics [100-105]. Thermal as well as catalytic cracking [106, 107] of TGs yield aromatic and other hydrocarbon products [108-111] along with simple molecules, i.e., water, CO and CO_2. Catalytic conversion may occur at lower temperatures [5, 106-109, 112, 113] .

Various catalysts were explored for production of fuels and chemicals from crop oil [111]. Among these catalysts, zeolite HZSM-5 showed a high selectivity towards the production of specific-size (C_6-C_8) aromatics, i.e., benzene, toluene, ethylbenzenes and xylenes (BTEX). Such a specificity of HZSM-5 is due to its defined pore size and specific geometry of the active acid sites. Just as with lignin conversion, one significant problem of using zeolite catalysts including HZSM-5 was high yield of coke and, particularly, low-MW gas phase hydrocarbons.

Our previous studies demonstrated that thermal cracking of triacylglyceride oils becomes significant only at temperatures above 400 °C [5]. Detailed protocols using gas chromatography with mass spectrometry and flame ionization detection (GC-MS/FID) enabled identification and quantification of more than 200 compounds [85].

The OLP of such thermally cracked triacylglyceride oils contained significant amounts of C_2-C_{12} fatty acids, fuel-incompatible products, which were nearly absent when any catalysts were used [112, 114]. These fatty acids were successfully separated from OLP produced during a scalable continuous process [115]. In the other studies of soybean oil TG cracking at 400 °C, short chain fatty acids, alkanes, alkenes and about 5 % of aromatic hydrocarbons were produced [5, 109]. In an attempt to produce kerosene type fuel from canola oil, the 2% yield of aromatic hydrocarbons was reported [6] whereas experiments on soybean oil cracking at 430 °C showed a lower (1.1 wt%) yield

of aromatics, along with a high (34 wt%) yield of fatty acids. In a study of oleic acid cracking at 400 °C [114], paraffins, aromatics and olefins were produced by the use of HZSM-5 catalyst. The reaction pathways included decarboxylation, decarbonylation, cracking, oligomerization, cyclization and aromatization, along with alkyl group rearrangement. C_7-C_{11} aromatics were produced in larger quantities than the other homologs. However, a significant portion of the feedstock remained unreacted even at 400 °C.

This paper describes a novel two-step process for an efficient production of aromatic hydrocarbons from a renewable source, soybean oil. Conducting the process in two steps, i.e., thermal followed by HZSM-5 catalyzed TG cracking, addressed the main problems of both processes when they were conducted in one step, i.e., high yield of unwanted acid and gas products, respectively. A novel application of detailed GC-MS analysis protocols revealed a significant yield of aromatics and other cyclic hydrocarbons and demonstrated somewhat unexpected features of the product composition.

Experimental

Materials

Refined soybean oil was provided by Ag Processing Inc, a cooperative located in the state of Minnesota, USA. The ammonium forms of two different ZSM-5 catalysts having different SiO_2/Al_2O_3 ratios (CBV5524G and CBV 2314) were purchased from Zeolyst International, Conshohocken, PA, USA. These were converted into their hydrogen forms by calcination at 550 °C for 5 hours in an air circulated oven, generating HZSM-5 catalysts. Gas chromatographic (GC) grade standards for benzene, toluene,

ethylbenzene, xylenes, naphthalene and 2-chlorotoluene were purchased from Sigma-Aldrich, Saint Louis, Missouri, USA.

Non-catalytic cracking experiments

The non-catalytic cracking of soybean oil was conducted in a small pilot-scale (seven L/hr) continuous reactor [109] as shown in Fig. 20.
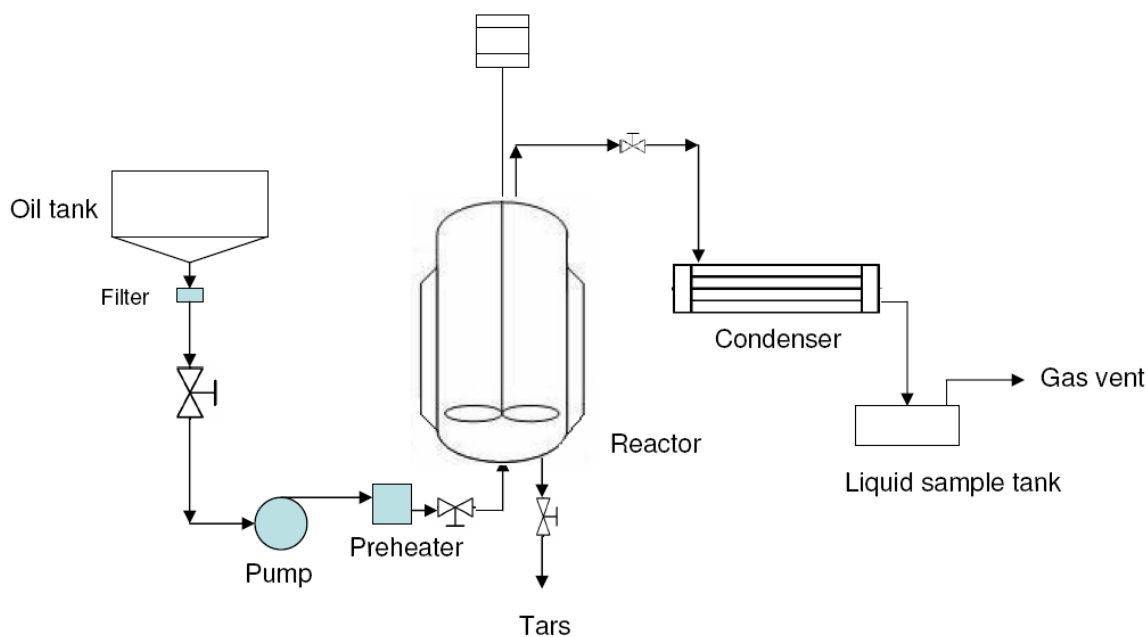
Figure 20. Reactor setup for thermal cracking of soybean oil

The feed oil was pumped (with a Neptune Chemical Pump Company proportioning diaphragm pump model 515-A-N3, Lansdale, PA, USA) from a 68 L tank through a filter to remove solids and other particles, then through a preheater where it was heated to about 150 °C and into the cracking reactor. The cracking reactor was 9.7L 304SS surrounded by three independently controlled external ceramic band heaters used

to maintain the temperature within the reactor at the desired operating temperature (435 ℃). A mechanical agitator shaft, installed off-center to minimize vortexing, was operated at rotation speeds of approximately 400 RPM. The two impellers were directionally reversed (i.e., one 'up-mixing' and the other 'down-mixing') in order to promote desirable mixing. The cracked products leaving the reactor passed through a condenser cooled with tap water to room temperature. The liquid crackate was collected into a storage tank and the gases were taken out through a gas vent.

The liquid crackate was further purified by distillation at 300 °C in a batch lab-scale distillation apparatus to remove heavy polymeric compounds similar to tar.

Catalytic reforming experiments

A schematic of the experimental reactor setup is shown in Figure 21
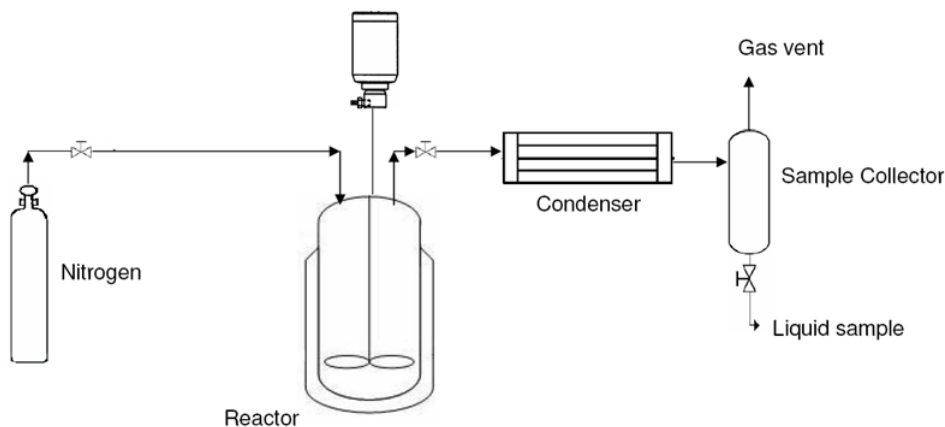
Figure 21. Reactor setup for the aromatization of thermally cracked soybean oil

A Parr series 4575 fixed head, bench top, high temperature, high pressure autoclave type reactor was used as the reforming reactor. This reactor (500 mL) was equipped with a cooling channel to control the reaction temperature and a stirrer that

agitated the catalyst and reaction mixture. The reaction temperature was controlled and monitored by a K-type thermocouple connected to Parr 4843 controller, which also monitored and controlled the impeller speed. The reactor was equipped with a gas inlet connected to a nitrogen cylinder to maintain initial reaction pressures.

Operating parameters for the various experiments are provided in Table 9.

Table 9. Experimental conditions for the catalytic (SiO_2/Al_2O_3=23) conversion of OLP and the corresponding main product yields.

Run	Reaction conditions			Yield (w/w%)			Concentration in the reformate (w/w%)					
	Temp (°C)	OCR*	Time (min.)**	Liquids	Coke	Gases	Alkyl benzenes	BTEX	Mono Aromatics	Indane	Naphthalenes	Total aromatics
1	300	7	5	84	9	7	15	1.8	16	2.1	1.6	20
2	300	7	20	88	7.9	4.1	15	1.9	17	2.3	1.7	21
3	300	15	5	90	2.6	7.4	12	1.5	14	1.7	1.3	17
4	300	15	20	87	3	10	15	1.7	17	2.1	1.7	21
5	350	11	12.5	87	7	6	15	1.9	17	2.0	1.6	20
6	350	7	12.5	88	6.4	5.6	15	2.0	17	2.1	1.6	21
7	400	7	5	78	9.5	12.5	13	2.5	16	1.5	1.7	19
8	400	7	20	76	9.8	14.2	21	3.8	25	3.0	2.4	30
9	400	15	5	86	6	8	19	2.2	21	2.9	2.0	26
10	400	15	20	84	5	11	12	2.0	14	2.0	1.5	18
11	432	4.5	12.5	80	5	15	38	8.7	47	4.3	7.1	58
12	432	4.5	12.5	81	5	14	37	8.7	46	5.2	6.9	58

* OCR = OLP to catalyst ratio
** This reaction time is defined as the duration during which the reaction was held at the target temperature excluding reactor warmup and cool down time.

The required quantities of catalyst and OLP were charged to the reactor. The reactor was purged with nitrogen to remove air prior to heating. The reactor was then heated to the desired temperature and maintained at this temperature for an allotted time with its contents being stirred at 300 rpm. Once the reaction was completed, the reactor contents were cooled down to room temperature and then the gaseous products were collected in a gas bag by slowly opening the reactor vent. The entire reactor contents were weighed and then filtered to separate coke/solid particles from liquid reformates. The collected samples were dissolved in methanol to ensure miscibility and submitted to analysis.

The amount of coke formed was determined by subtracting the weight of the catalyst fed to the reactor from that of the catalyst obtained after reaction, thus accounting for the coke deposition on the catalyst surface. The yield of gases was determined by the difference between the masses of the OLP fed to the reactor and the combined mass of the reformate and coke produced.

Chemical characterization

For characterization of the OLP and reformate aromatic products, an analytical protocol using GC-MS (Agilent 5890 Series II with 5973 MS) was based on a GC-FID/MS method developed by Štávová et al. (2012) allowing for accurate identification and tentative quantification of aromatics. The temperatures of the GC injector and the transfer line to the MS were set at 250 ºC and 280 ºC, respectively. The oven temperature program was started at 40 °C for 5 min and then ramped at 15 ºC/min to 310 °C and held

at this temperature for 5 min. The sample injections of 1 μL were performed in split mode (1:20) at a helium constant flowrate of 1.5 mL/min. The GC-MS analysis was performed with electron ionization using a solvent delay of 4 min in a mass range of 50-500 amu.

The aromatic hydrocarbons were identified based on their GC retention time and pattern of homologue and isomer elution as detailed elsewhere (Kubátová et al., 2011). The retention times for the identified aromatic hydrocarbons are listed in Supplementary Table 9.

The aromatics' quantification was based on BTEX (benzene, toluene, ethylbenzene and xylenes) standards using a full calibration between 0.01 to 5.0 wt.%, with the addition of an internal standard (chlorotoluene) to the sample. The BTEX were directly quantified based on the major ions (Table 10).

Table 10. Details of GC-MS analysis used for reformate identification

Compound name	Formula	Molecular weight	Retention time (min.)	Quantification Ion
Benzene	C_6H_6	78	4.6	78
Toluene	C_7H_8	92	7.1	91
Ethylbenzene	C_8H_{10}	106	9.1	91
p-Xylene	C_8H_{10}	106	9.3	91
o-Xylene	C_8H_{10}	106	9.7	91
o-Xylene 105	C_8H_{10}	106	9.7	105
Naphthalene	$C_{10}H_8$	128	13.7	128
Benzene C_{3z}	C_9H_{12}	120	10.2	105
Benzene, C_{3a}	C_9H_{12}	120	10.8	105
Benzene, C_{3b}	C_9H_{12}	120	10.9	105
Benzene, C_{3x}	C_9H_{12}	120	11.1	105
Benzene, C_{3y}	C_9H_{12}	120	11.3	105
Benzene, C_{4a}	$C_{10}H_{14}$	134	11.5	105
Benzene, C_{4b}	$C_{10}H_{14}$	134	11.6	119
Benzene, C_{4c}	$C_{10}H_{14}$	134	11.7	119
Indane	C_9H_{10}	118	11.9	105
Benzene, C_{4y}	$C_{10}H_{14}$	134	12.0	105
Benzene, butyl-	$C_{10}H_{14}$	134	12.1	91
Benzene, C_{4d}	$C_{10}H_{14}$	134	12.2	105
Benzene, C_{4x}	$C_{10}H_{14}$	134	12.28	105
Benzene C_{4e}	$C_{10}H_{14}$	134	12.37	105

Table 10 continued

Benzene C$_{4f}$	C$_{10}$H$_{14}$	134	12.4	105
Benzene, C$_{4z}$	C$_{10}$H$_{14}$	134	12.47	105
Indane, C$_{1a}$	C$_{10}$H$_{12}$	132	12.52	105
Benzene C$_{5y}$	C$_{11}$H$_{16}$	148	13.06	105
Indane, C$_1$	C$_{11}$H$_{14}$	132	13.13	105
Benzene, C$_{5a}$	C$_{11}$H$_{14}$	148	13.17	105
Indane, C$_{1x}$	C$_{11}$H$_{14}$	132	13.27	105
Benzene, C$_{5b}$	C$_{11}$H$_{16}$	148	13.48	105
Benzene, C$_{5z}$	C$_{11}$H$_{16}$	148	13.61	105
Benzene, pentyl-	C$_{11}$H$_{16}$	148	13.31	91
Benzene, C$_{5x}$	C$_{11}$H$_{16}$	148	13.41	105
Indane, C$_2$	C$_{11}$H$_{14}$	146	13.73	105
Benzene, C$_{6a}$	C$_{12}$H$_{18}$	162	14.19	105
Benzene, C$_{6y}$	C$_{12}$H$_{18}$	162	14.27	105
Benzene, hexyl-	C$_{12}$H$_{18}$	162	14.36	91
Benzene, C$_{6x}$	C$_{12}$H$_{18}$	162	14.44	105
Naphthalene, C$_{1y}$	C$_{11}$H$_{10}$	142	14.83	128
Naphthalene, C$_{1x}$	C$_{11}$H$_{10}$	142	15.01	128
Benzene, heptyl-	C$_{13}$H$_{20}$	176	15.34	91
Benzene, C$_{7x}$	C$_{13}$H$_{20}$	176	15.41	105
Naphthalene, ethyl	C$_{12}$H$_{12}$	156	15.75	128
Naphthalene, C$_{2x}$	C$_{12}$H$_{12}$	156	15.85	128
Naphthalene, C$_{2y}$	C$_{12}$H$_{12}$	156	16	128
Benzene, octyl-	C$_{14}$H$_{22}$	190	16.25	91
Benzene, C$_{8x}$	C$_{14}$H$_{22}$	190	16.30	105
Naphthalene, C$_{3x}$	C$_{13}$H$_{14}$	170	16.71	128
Naphthalene, C$_{3y}$	C$_{13}$H$_{14}$	170	16.82	128
Benzene, nonyl-	C$_{15}$H$_{24}$	204	17.10	91
Benzene, C$_{9x}$	C$_{15}$H$_{24}$	204	17.16	105
Benzene, decyl	C$_{16}$H$_{26}$	218	17.91	91
Benzene, C$_{10x}$	C$_{16}$H$_{26}$	218	17.96	105
Benzene, C$_{11a}$	C$_{17}$H$_{28}$	232	18.11	105
Benzene, C$_{11b}$	C$_{17}$H$_{28}$	232	18.18	105
Benzene, undecenyl	C$_{17}$H$_{28}$	232	18.67	91
Benzene, C$_{11x}$	C$_{17}$H$_{28}$	232	18.73	105

For quantitation of other alkyl aromatics, signals of representative ions were used employing a calibration slope obtained ion of *m/z* 105 for *o*-xylene. In rare cases when the *m/z* 105 signal was of low intensity, other characteristic ions were used as listed in Table 10. The other groups of products, i.e., cyclohexa(e)nes, cyclopenta(e)nes, monocarboxylic acids, etc., were analyzed in a similar way, using for quantification the characteristic ions listed in Table 10. The reformate compositions for two selected

samples were estimated based on the percent response obtained from the total ion current

chromatograms and proportionality to the aromatic compounds.

Results and Discussion

Analysis of the OLP obtained by non-catalytic cracking of soybean oil

The OLP yields and composition determined using GC-FID/MS are provided in

Table 11

Table 11. Summary composition of OLP obtained from non-catalytically cracked crop oil.

Reaction conditions					
Temperature (^{o}C)	435	435	435		
Pressure (psig)	30	20	40		
				Mean	StDev
Concentrations, (w/w%)					
Linear alkanes	9.3	10.3	9.5	9.7	0.53
Branched alkanes	0.1	0.1	0.1	0.1	0.0
Bicycloalkanes	0.1	0.1	0.1	0.1	0.0
Cycloalkanes	1.6	1.5	1.7	1.6	0.10
Alkenes with C=C bonds at the terminal position	4.5	4.5	4.4	4.5	0.058
Alkenes with a C=C bond at a non-terminal position	7.1	6.5	7	6.9	0.32
Alkadienes	0.2	0.1	0.2	0.17	0.058
Cycloalkenes	1.7	1.6	1.7	1.7	0.058
Ketones	0.8	1	0.8	0.87	0.12
BTEX	0.5	0.5	0.6	0.53	0.058
Monoaromatics (non-BTEX)	3.5	3.3	3.1	3.3	0.2
Indanes	0.35	0.46	0.36	0.39	0.050
Naphthalenes	0.51	0.46	0.39	0.45	0.049
Phenol	0.1	0.1	0.1	0.1	0.0
Saturated linear carboxylic acids	18	14	18	17	2.3
Saturated linear dicarboxylic acids	2	6.1	5.2	4.4	2.2
Identified compounds	53	54	57	55	2.1
Unidentified compounds, estimated by peak integration	8.2	9.9	12	10	1.9
Unresolved peaks, estimated by integration of a "hump"	21	39	44	35	12
Total	85	105	117	97	16

for the non-catalytic cracking step. This composition is consistent with earlier published results [12, 116].

The operational conditions for the non-catalytic cracking reaction, particularly the use of a higher temperature (435 °C) compared to the prior published work (Kozliak et al. 2013; Luo et al., 2010), were selected to generate a higher abundance of alkenes for reforming into aromatics. The resulting OLP, purified from the crackate liquid after the first reaction step (i.e. non-catalytic cracking) also contained high concentrations of alkanes and linear saturated carboxylic acids. Since the resulting OLP compositions obtained in all three experimental runs were similar, the first sample of those shown in Table 11 was selected as the feedstock for the second reaction step.

Analysis of reformate and other products obtained from the catalytic conversion of soybean cracking-derived OLP

For the second reaction step, the catalytic reforming, a series of cursory parameterization experiments were performed following a Design of Experiments strategy, i.e., conducting the minimum experiments to cover the pertinent ranges of several parameters. These parameters, i.e., operational conditions (temperature, OLP to catalyst ratio, OCR and time) along with the resulting yields of the most significant groups of products are listed in Table 9.

An increase of the reaction temperature from 300 ºC to 400 ºC resulted in a significant increase in the yield of all types of aromatics (Fig. 22A). This trend is consistent with the literature [10] and can be explained by the facilitation of adsorption and diffusion of feed molecules into zeolite pores, where the formation of aromatic rings takes place [73].
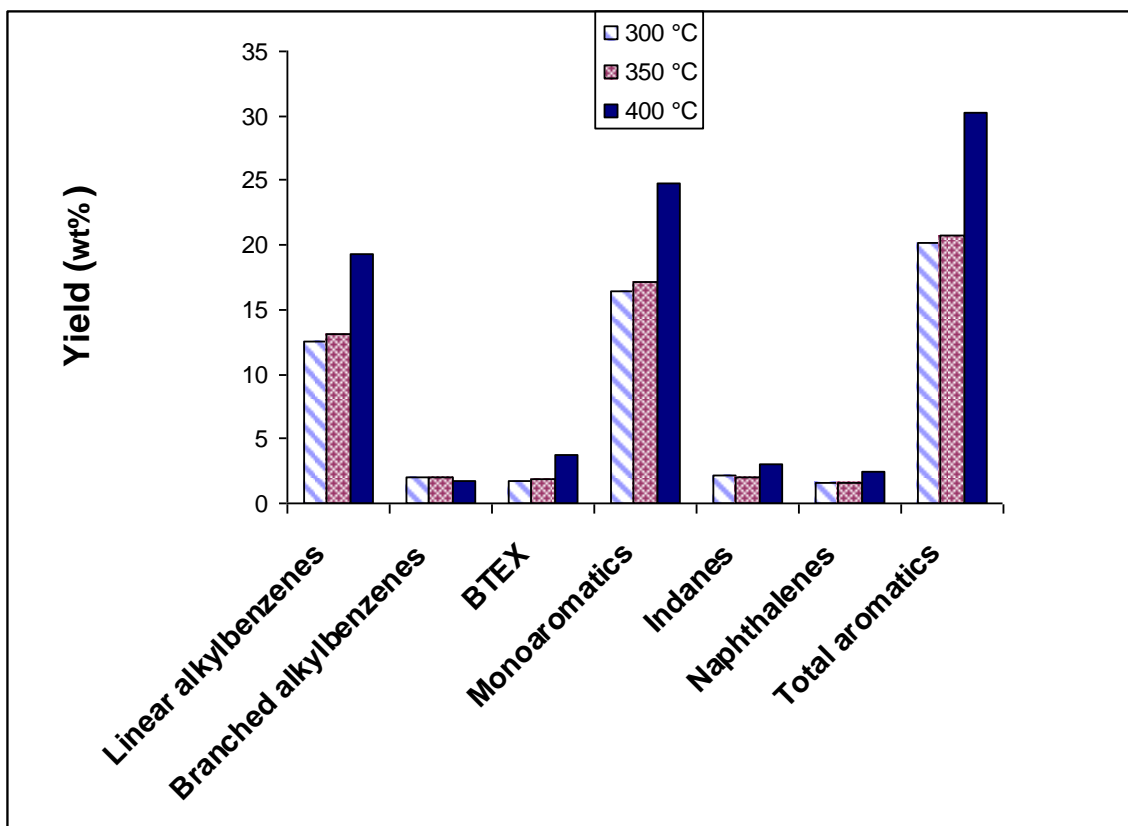
A
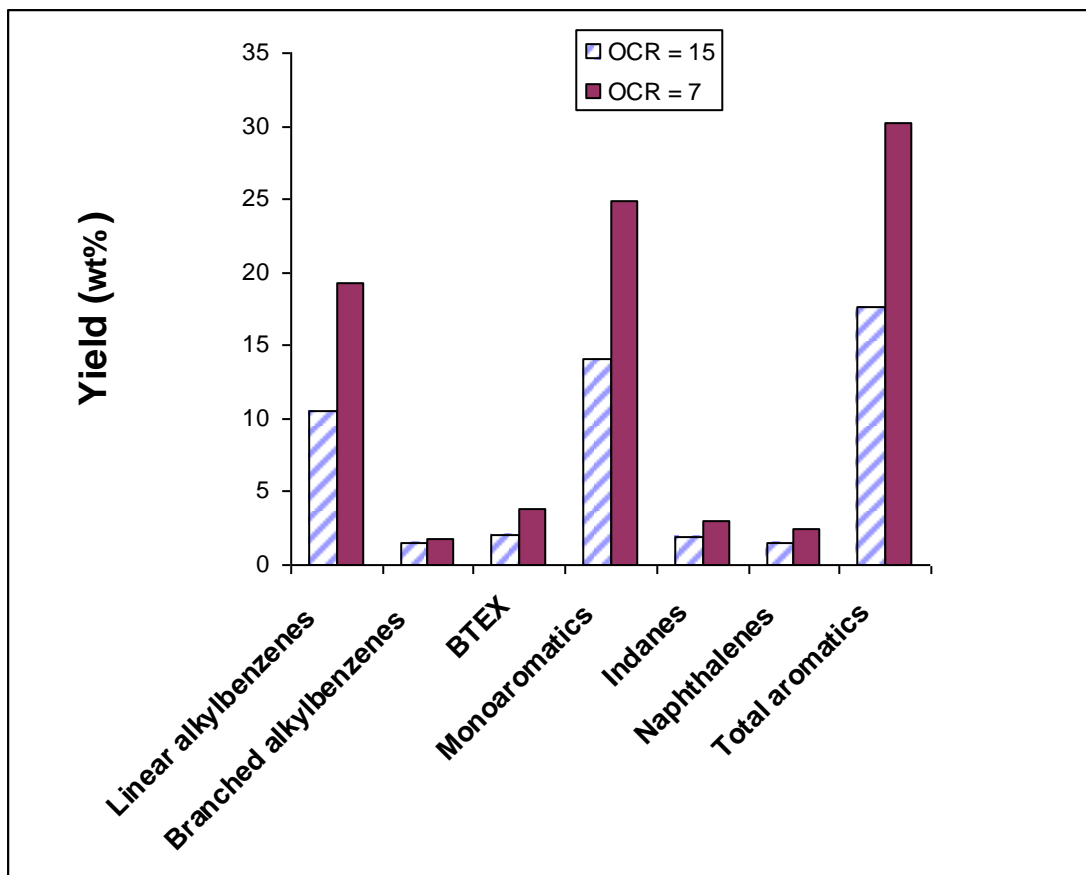
B
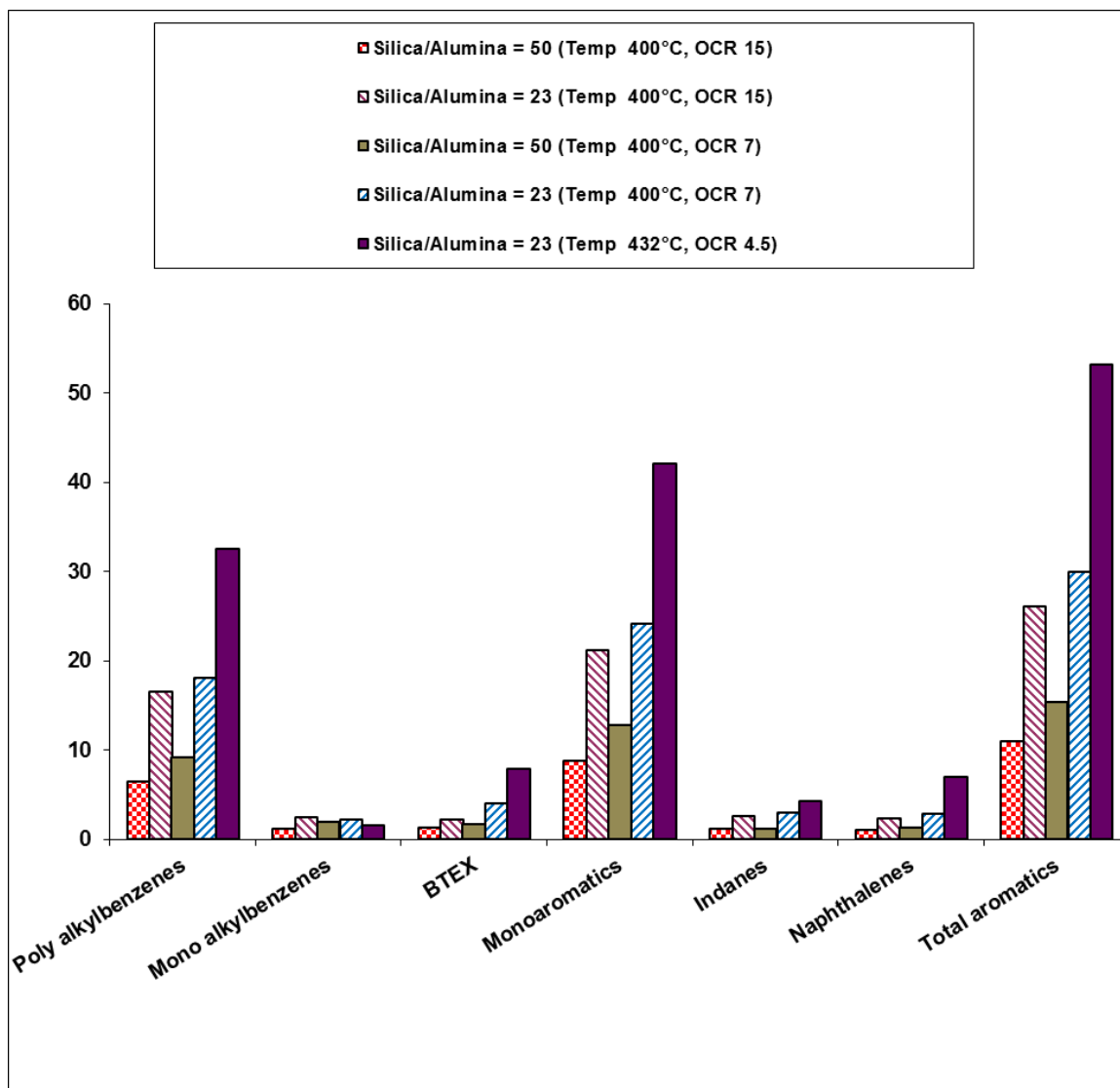
C

Figure 22. The effect of A) reaction temperature, B) OLP-to-catalyst ratio and C) silica/alumina ratio on aromatics' yields. Monoaromatics include all benzene derivatives; total aromatics also include diaromatics, i.e., naphthalenes and indanes. Polyaromatics were detected only in trace amounts.

Higher temperatures may also encourage the cracking of long chain molecules, which may be particularly significant for OLP reforming. Once this additional cracking occurs, the additional smaller molecules produced may easily enter the HZSM-5 pore

channel network to yield more aromatics. Finally, thermal scission of hydrogen bonds within the zeolite structure may lead to greater catalytic activity [52, 53].

The total aromatic hydrocarbon yields declined with an increase in the oil-to-catalyst ratio (OCR), as expected (Fig. 22B). This relation confirms that the observed significant reforming is truly catalytic and apparently taking place on the Brønsted acid sites within the HZSM-5 pores.

Figure 22C depicts the yields of each type of aromatic hydrocarbon as a function of the silica/alumina (SiO_2/Al_2O_3) ratio at two different OCRs. The first two columns (from the left) in each cluster in Fig. 22C present the results obtained with an OCR of 15 while the third and fourth columns present the results obtained for an OCR of 7. The first and third columns in each cluster represent the yields over HZSM-5 with a SiO_2/Al_2O_3 ratio of 50 whereas the second and fourth columns represent the yields when this ratio was set at 23.

With both OCR ratios, the yields of all types of aromatic hydrocarbons almost tripled when the SiO_2/Al_2O_3 ratio was decreased from 50 to 23. The yields further increased when the OCR was lowered to 4.5 and the temperature increased to 432 ºC at a SiO_2/Al_2O_3 ratio of 23 (the rightmost column in Fig. 22C). The detailed composition of samples obtained in the runs under such conditions, which showed the maximum concentration of aromatics with minimum coke formation, will be discussed henceforth. The observation of a higher yield of aromatics at a lower Si/Al ratio corroborates the well-known paradigm that the catalytic activity of HZSM-5 is mainly due to the Brönsted acid sites present in the forms of bridging hydroxyl groups in the Si-O-Al triad, in which it is the aluminum that exhibits significant acidity [46, 51]. The effects of the SiO_2/Al_2O_3

ratio on HZSM-5 catalytic activity appear to be due to the differences in total acidity as the acid strength increases with a decrease in this ratio. This difference may explain a higher catalytic activity of such catalysts towards the production of aromatics as observed in this study.

The gas and solid (coke) fractions of the product

Coke formation is an unavoidable step in acid catalyzed reactions over HZSM-5 catalysts [117-120]. However, our results showed that high yields of aromatics may be combined with a low yield of coke (Table 9). Furthermore, it was observed that the lower the silica/alumina ratio, the lower the coke yield. A similar trend was observed in previously published work on hydrocarbon conversion [117, 121].

The yield of gaseous products was 15-28 w/w% of the OLP feed. Given that the gas phase product yield for the first step (non-catalytic cracking of soybean oil) was 6 w/w%, the overall yield of gases was rather low, 21-34 w/w%. When soybean oil conversion with HZSM-5 was attempted in one step (400-420 °C) in our lab (Kadrmas et al., 2015), the gas phase yield was in a range of 31-57 w/w%, consistent with literature data [112, 114].

The results from a detailed analysis of the gaseous products formed during the OLP reforming with HZSM-5 under optimized conditions are listed in Table 12.

Table 12. Composition of the gas fraction obtained by catalytic OLP*
reforming**

	Sample 1 Concentration	Sample 2 Concentration
Coke yield (w/w%)	5	5
Liquid yield (w/w%)	80	81
Gas yield (w/w%)	15	14
Gas concentration	(vol %)	(vol %)
CO	3.0	2.8
Methane	6.3	6.4
CO2	1.3	1.5
Ethane	0.39	0.28
Ethylene	12	13
Propylene	55	54
Butane	16	16
Butane	2.4	2.1
Pentane	0.62	0.57
Hexane	0.53	0.58
Hydrogen	3.1	2.8

* OLP = Organic Liquid Products
** The reforming reaction conditions were: reaction temperature = 432 ºC, OLP to catalyst ratio = 4.5, reaction time = 12.5 minutes, silica:alumina ratio = 23.

The observed significant production of CO and CO_2 is consistent with decarboxylation of oxygenated compounds as discussed in the next section. As a less expected observation, propylene accounted for 54 vol % of gaseous products whereas the concentrations of C_2 hydrocarbons, ethylene and ethane, were low.

This selectivity towards propylene was not expected since the current paradigm is that ethylene-like zeolite-bound intermediates are essential for reforming, so ethylene was observed as the predominant gas phase product in earlier studies [112, 114]. This unexpected result, combined with the low fraction of BTEX among the aromatic products (as opposed to earlier studies with different feedstocks [112, 122] prompted the detailed study of the reaction product speciation and homology provided in the next section.

Detailed chemical speciation analysis of a sample obtained at optimized reforming reaction conditions

Table 13 shows the speciation of chemicals comprising both the feedstock and reformate product associated with the second step reaction.

Table 13. Detailed chemical composition (concentration) of both the original OLP[*] and liquid reformate (average of two replicates)[**].

Products	Feedstock (w/w%)	Reformate Sample 1 (w/w%)	Reformate Sample 2 (w/w%)	Reformate Average (w/w%)
Alkanes	9.8	20	22	21
Alkenes	11.4	0.58	0.61	0.6
Dienes	0.17	1.2	1.4	1.3
Cyclic compounds	3.4	13	14	13
Ketones	0.87	ND[***]	ND	ND
BTEX	0.53	8.7	9.2	8.9
Monoaromatics (non-BTEX)	3.3	37	41	39
Indanes	0.39	5.2	4.6	4.9
Naphthalenes	0.45	6.9	7.7	7.3
Carboxylic (fatty) acids	21.4	ND	ND	ND
Unidentified & unresolved	45	6.1	6.9	6.5
Total	97	98	107	102.5

* OLP = Organic Liquid Products
** The reforming reaction conditions were 432 ºC, OLP to Catalyst Ratio = 4.5 and reaction time of 12.5 minutes under the silica:alumina ratio = 23
*** ND = not detected, i.e., below the limit of detection

As one can see, several drastic differences occur between the feedstock OLP and product reformate compositions. The concentrations of aromatics, cyclic hydrocarbons and alkanes increased in the product at the expense of alkenes, carboxylic acids and unidentified compounds. Basically, just about anything in the feedstock including unidentified and unresolved species was converted into either cyclic compounds or *n*-alkanes or aromatics. The chemistry of this process will now be analyzed considering one group of compounds at a time while trying to decipher its fate.
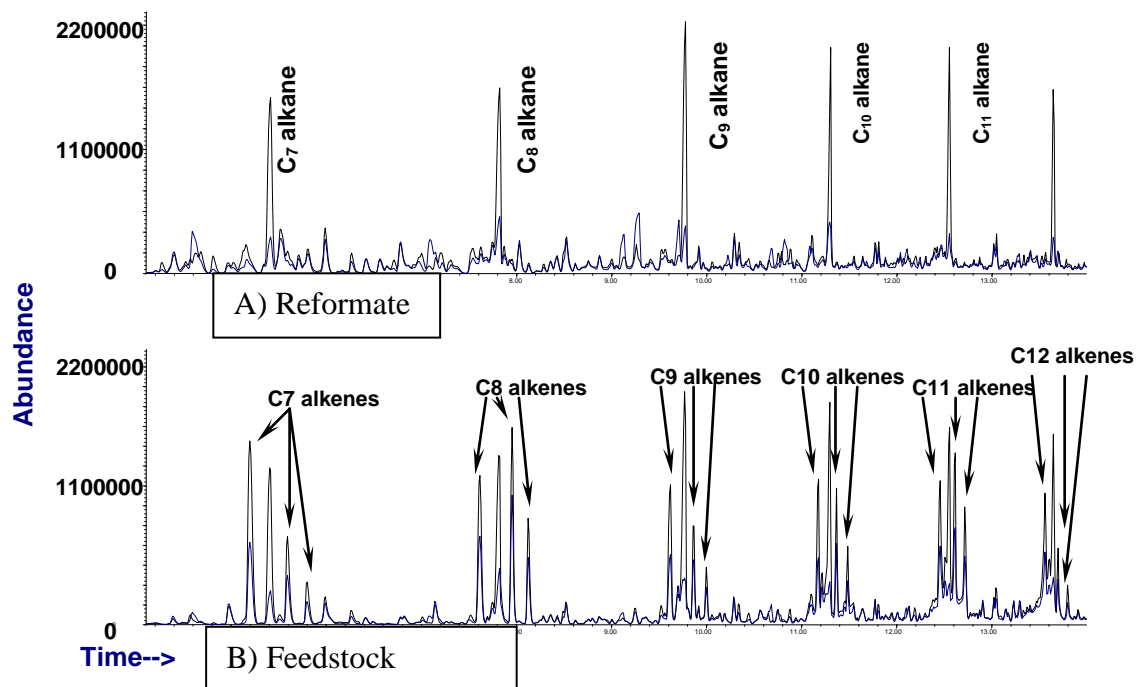
Figure 23. Selected ion chromatograms showing the alkane and alkene peaks (common ions 57 and 59) in A) the reformate and B) the feedstock (Organic Liquid Product)

Figure 23a shows that the distinct peaks of alkenes were identified only in the feedstock (OLP obtained after the first, non-catalytic cracking step). By contrast, a similar selected ion chromatogram of the reformate showed only negligible concentrations of alkenes (Fig. 23b). The reformate featured higher concentrations of alkanes compared to the feedstock (Fig. 23b). To determine the origin of these alkanes, the carboxylic acid profile was analyzed.

Carboxylic acids and alkanes

Figure 24 shows distinct carboxylic acid peaks identified only in the feedstock OLP analysis (Fig. 24A).
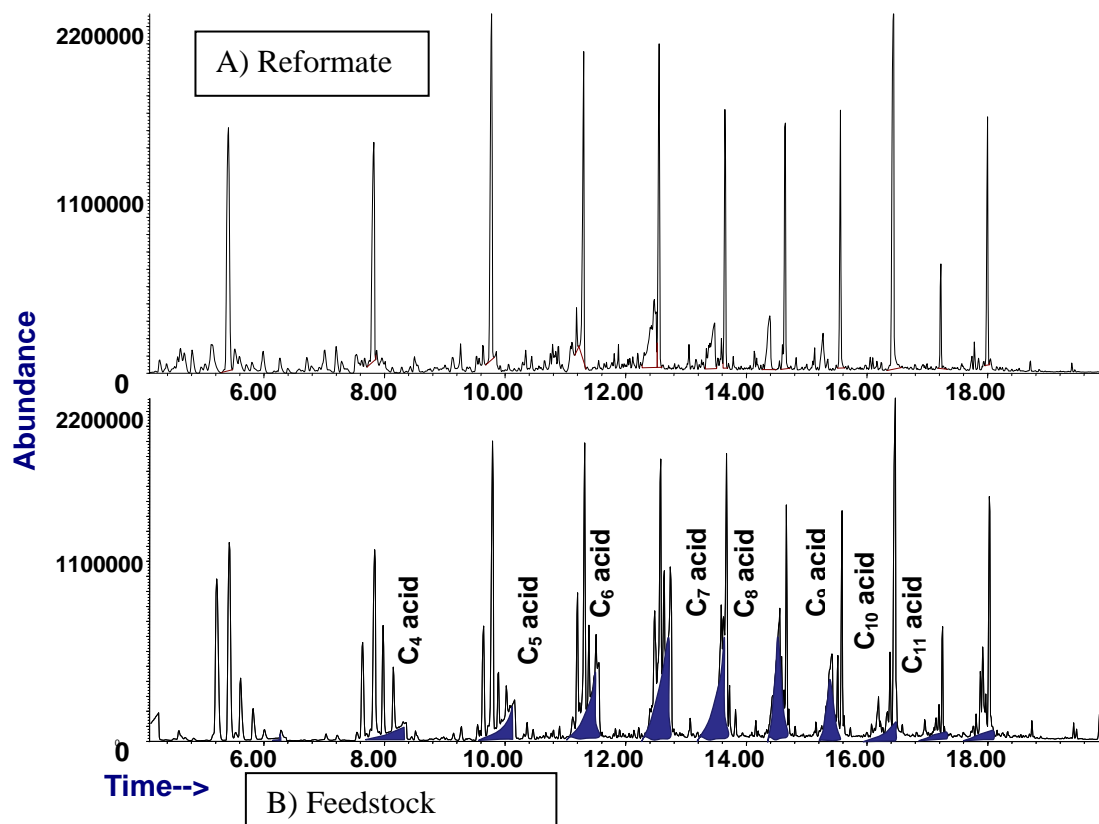
Figure 24. Selected ion chromatograms showing the carboxylic acid peaks (common ion 60) in
A) the reformate and B) the feedstock (Organic Liquid Product)

Carboxylic acids exhibit broad specific front-tailing peaks due to their polar
nature. By contrast, a similar selected ion chromatogram of the reformate shows only
negligible concentrations of carboxylic acids (Fig. 24B). Combined with the observation
of higher concentrations of *n*-alkanes in the reformate (Table 13), it can be concluded that
carboxylic acids of OLP are most likely being converted into alkanes by
decarboxylation/decarbonylation.
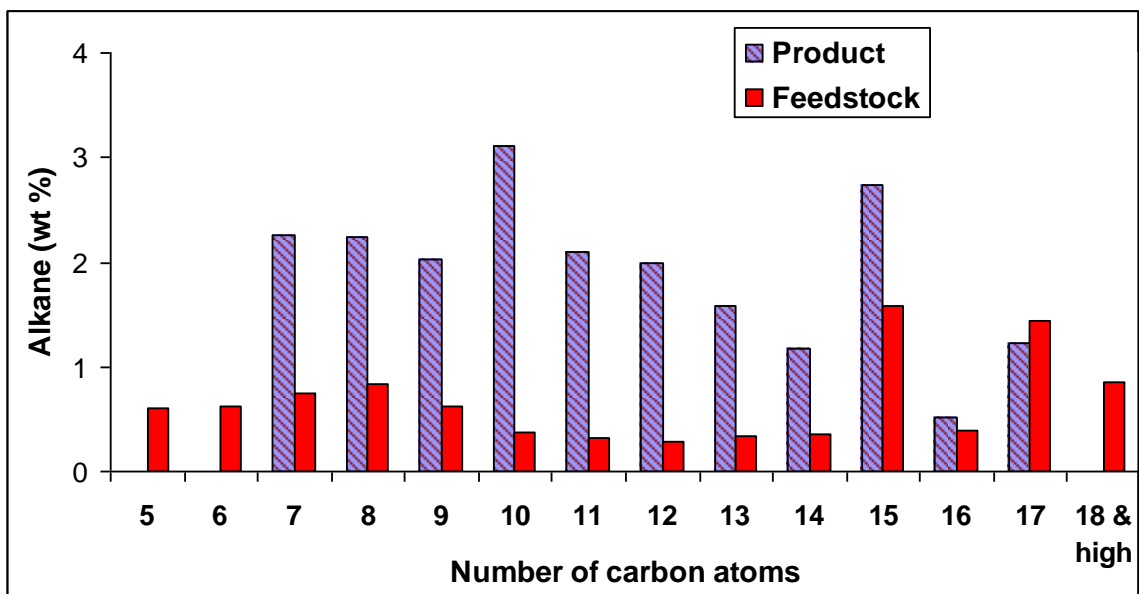
Figure 25. A comparison of alkane homology profiles in the reformate (product) and in the feedstock (Organic Liquid Product). The average values are provided for the two samples in the product.

Figure 25 depicts the homology profile of alkanes and shows the different fates of various sized alkanes. The short-chain C_5-C_6 alkanes are absent from the reformate. Apparently, they are essentially all reformed into aromatics. Similarly, the large-size C_{17}^+ alkanes missing from the reformate were most likely cracked into smaller alkanes, some of which were then reformed into aromatics by the zeolite. It should be noted that alkanes of this size do not typically crack under the reaction conditions employed (particularly, at such a relatively low temperature), suggesting that these reactions were facilitated by the HZSM-5 catalyst.

By contrast, the mid-size alkanes are more abundant in the reformate than in the OLP feedstock. Yet, the homology profile of the carboxylic acids in the feedstock does not match that of the alkanes in the product (Fig. 25). Thus, carboxylic acid decarboxylation by itself does not account for the observed alkane homology profile, reinforcing the postulate that C_{17}^+ alkanes are cracking in the reactor. Additionally, the

decarboxylation of carboxylic acids may be accompanied both by subsequent alkane reforming (for smaller products) and cracking (for larger products), thus further skewing the resulting alkane homology profile.

Aromatic and Other Cyclic Hydrocarbons

Figure 26 presents the homology profiles of aromatics and cyclohexenes/cyclohexanes which comprise the bulk of the other cyclic compounds present in both the OLP feedstock and reformate associated with the second reaction step.
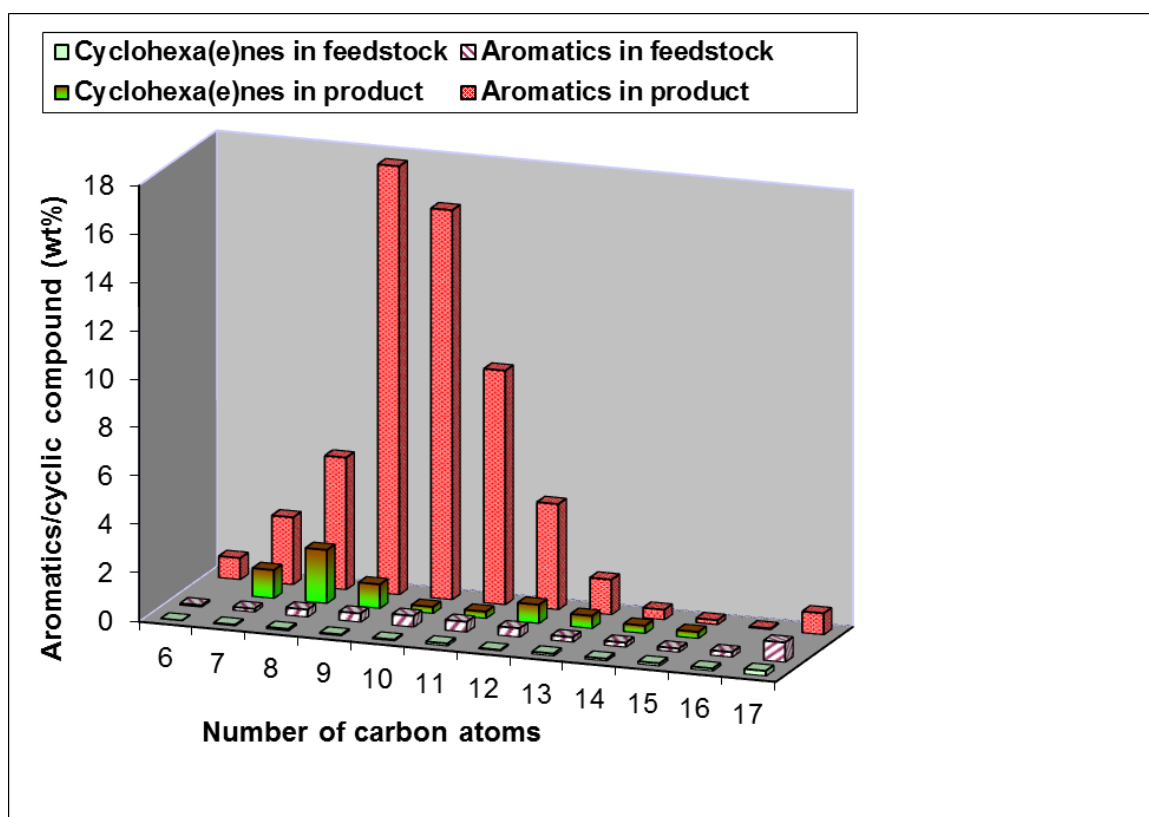
Figure 26. Aromatic hydrocarbons and cyclohexa(e)nes in the feedstock (Organic Liquid Product) and reformate

Aromatics having carbon numbers 15-17 are present in nearly the same amounts in both the feedstock and product (Fig. 26). Thus, they were not produced during the second reaction and appear to be generated during the initial non-catalytic cracking step.

To enhance the observed homology profiles, Table 14 lists all of the identified aromatic hydrocarbon compounds in the reformate.

Table 14. The concentrations of aromatic hydrocarbons in replicate liquid reformate samples

Aromatic hydrocarbon	Formula	Sample1[*] (w/w%)	Sample2[*] (w/w%)	Average (w/w%)	StDev (+/-, w/w%)
Benzene, C3a	C_9H_{12}	9.00	9.69	9.34	0.49
Benzene, C3b	C_9H_{12}	0.67	0.76	0.72	0.06
Benzene, C3x	C_9H_{12}	2.51	2.76	2.64	0.18
Benzene, C3y	C_9H_{12}	3.90	4.23	4.06	0.23
Benzene C3z[**]	C_9H_{12}	0.88	0.95	0.92	0.06
Benzene, C4a	$C_{10}H_{14}$	0.33	0.38	0.36	0.04
Benzene, C4b	$C_{10}H_{14}$	0.52	0.55	0.53	0.03
Benzene, C4c	$C_{10}H_{14}$	0.53	0.59	0.56	0.04
Benzene, C4d	$C_{10}H_{14}$	0.22	0.25	0.23	0.02
Benzene C4e	$C_{10}H_{14}$	0.67	0.66	0.66	0.01
Benzene C4f	$C_{10}H_{14}$	0.68	0.66	0.67	0.02
Benzene C4x	$C_{10}H_{14}$	1.56	1.71	1.64	0.11
Benzene C4y	$C_{10}H_{14}$	3.02	3.33	3.17	0.22
Benzene, C4z	$C_{10}H_{14}$	2.34	2.60	2.47	0.19
Benzene, C5a	$C_{11}H_{16}$	0.80	1.43	1.12	0.44
Benzene, C5b	$C_{11}H_{16}$	0.78	0.86	0.82	0.06
Benzene, C5x	$C_{11}H_{16}$	2.51	2.80	2.66	0.21
Benzene C5y	$C_{11}H_{16}$	0.61	0.68	0.64	0.05
Benzene C5z	$C_{11}H_{16}$	0.08	0.10	0.09	0.01
Benzene, C6a	$C_{12}H_{18}$	0.55	0.63	0.59	0.06
Benzene, C6x	$C_{12}H_{18}$	1.47	1.66	1.56	0.13
Benzene C6y	$C_{12}H_{18}$	0.38	0.41	0.40	0.03
Benzene, C7x	$C_{13}H_{20}$	0.61	0.67	0.64	0.04
Benzene, C8x	$C_{14}H_{22}$	0.34	0.33	0.33	0.00
Benzene, C9x	$C_{15}H_{24}$	0.16	0.19	0.17	0.02
Benzene, C10x	$C_{16}H_{26}$	0.05	0.06	0.06	0.01
Benzene, C11a	$C_{17}H_{28}$	0.40	0.43	0.41	0.03
Benzene, C11b	$C_{17}H_{28}$	0.37	0.42	0.39	0.04
Benzene, C11x	$C_{17}H_{28}$	0.07	0.09	0.08	0.01
Benzene	C_6H_6	0.86	0.93	0.89	0.05
Toluene	C_7H_8	2.68	2.88	2.78	0.14
Ethylbenzene	C_8H_{10}	1.34	1.49	1.42	0.10
p-Xylene	C_8H_{10}	2.66	2.85	2.76	0.13
o-Xylene	C_8H_{10}	1.21	1.34	1.28	0.09
Indane	C_9H_{10}	1.20	1.32	1.26	0.09
Indane, C1a	$C_{10}H_{12}$	1.41	1.53	1.47	0.09

Table 14 continued

Indane, C1	$C_{10}H_{12}$	1.04	0.06	0.55	0.69
Indane, C1x	$C_{10}H_{12}$	1.18	1.32	1.25	0.10
Indane, C2	$C_{11}H_{14}$	0.42	0.44	0.43	0.02
Benzene, butyl-[***]	$C_{10}H_{14}$	0.68	0.74	0.71	0.04
Benzene, pentyl-[***]	$C_{11}H_{16}$	0.53	0.61	0.57	0.05
Benzene, hexyl-[***]	$C_{12}H_{18}$	0.21	0.25	0.23	0.03
Benzene, heptyl-[***]	$C_{13}H_{20}$	0.23	0.26	0.24	0.02
Benzene, octyl-[***]	$C_{14}H_{22}$	0.07	0.09	0.08	0.01
Benzene, nonyl-[***]	$C_{15}H_{24}$	0.01	0.02	0.02	0.00
Naphthalene	$C_{10}H_8$	1.69	1.88	1.79	0.13
Naphthalene, C1x	$C_{11}H_{10}$	1.04	1.13	1.09	0.06
Naphthalene, C1y	$C_{11}H_{10}$	2.14	2.34	2.24	0.10
Naphthalene, ethyl	$C_{12}H_{12}$	0.44	0.49	0.47	0.04
Naphthalene, C2x	$C_{12}H_{12}$	0.66	0.71	0.68	0.04
Naphthalene, C2y	$C_{12}H_{12}$	0.41	0.46	0.43	0.04
Naphthalene, C3x	$C_{13}H_{14}$	0.42	0.49	0.45	0.05
Naphthalene, C3y	$C_{13}H_{14}$	0.14	0.09	0.11	0.04

*   Samples 1 and 2 represent the reformate samples obtained from the replicates of experiments with conditions of 432 ºC, OCR = 4.5 and reaction time of 12.5 minutes under the silica:alumina ratio = 23.

**   The number/character (e.g. C4a, C4b, C4x, C4y) represent the isomer profiles for the given number of carbon atoms in the alkyl groups attached to the aromatic ring.

*** These *n*-alkylbenzenes are listed separately and not included in the isomer profiles.

Almost 3/4 of them by weight are the isomers of C_3-, C_4- and C_5-substituted benzenes. By contrast, the BTEX fraction, i.e., benzene along with the C_1- and C_2-substituted benzenes (C_6-C_8 in Fig. 26 for aromatics), is rather small. This observation was unexpected as BTEX were the main products of the zeolite-facilitated reactions in most of the earlier studies regardless of the feedstock [112-114, 122, 123]. The only exception was a study by Benson et al., 2009 in which the symmetric trimethylbenzene also showed a large abundance. Perhaps in order for larger-size substrates to be reformed, such as the alkenes, alkanes and carboxylic acids present in the OLP, the mechanism of aromatics' formation has to be re-visited.

This conclusion is echoed by the unexpectedly high concentration of non-aromatized cyclic compounds recovered in the reformate. The concentration of alicyclic compounds in the reformate (14 w/w%) was almost 5 times higher than in the OLP feedstock (3 w/w%). This is an unexpected feature not observed earlier. The majority of these cyclic compounds were cyclohexanes which, according to the current paradigm, were expected to be immediately dehydrogenated resulting in benzene ring formation. Cyclopentanes were also produced in sizable amounts. This feature has not been observed before for zeolite catalysis. The unusual speciation and homology profiles of cyclic products warranted further re-visiting of the mechanism of HZSM-5 catalysis.

The literature discusses the mechanisms for HZSM-5 facilitated reactions based on its pore size of 5.4–5.6 Å [124]. The kinetic diameters [125] of benzene, toluene and xylenes are of the size between 5.85 Å – 6.8 Å [126]. Thus the current generally accepted explanation is that after BTEX are produced inside the porous HZSM-5 channels, they desorb out of the zeolite pores and then undergo alkylation on the zeolite

surface. This mechanism explains the prevalence of BTEX among the products in earlier studies conducted with HZSM-5. However, the current study puts this hypothesis into question. Not only are monoaromatics larger than BTEX in size prevalent in the reformate, but even diaromatics (indane and naphthalenes) along with alicyclic hydrocarbons are produced. Perhaps larger-size aromatics are formed at the pore openings rather than in their depths. If the process is transport limited, this may create the situation where the near-surface sites at such openings produce the bulk of the cyclic products.

The formation of larger than BTEX aromatics is consistent with propylene rather than ethylene being the main gas phase product. This finding indicates that C_3 – size intermediates rather than the earlier postulated C_2 are predominant. The observed zeolite specificity was still size-specific, as the yield of bicyclic aromatic (indanes and naphthalenes) yield was lower than that of monoaromatics, and the polycyclic aromatics were virtually absent. The low rate of polycyclics' formation may be a reason for the low coke yield observed in this study.

Notably, the predominant cyclohexane size produced was smaller than the predominant size of aromatics produced. This finding indicates that cyclization and aromatic hydrocarbon formation may occur on different sites. Just as with larger-size aromatics, alicyclic hydrocarbons may be formed near the zeolite surface and then desorb before cyclohexa(e)nes could be reformed to aromatic hydrocarbons.

The overall reformate composition

A comparison between the OLP feedstock components and the product reformate compounds (Table 13) shows the success of the proposed two-step process. The reformed product is devoid of the chemicals incompatible with fuel as alkenes and carboxylic acids are virtually removed. Aromatic and alicyclic hydrocarbons comprise the bulk of the reformate, along with the higher concentration of *n*-alkanes. This reformate may be used as a high-octane-number fuel or as a source of valuable cyclic compounds to replace petrochemicals. Additional aromatics may be formed by converting the main gas-phase product, propylene, into BTEX [86].

Conclusions

Non-catalytically cracked and purified soybean oil was successfully converted into a mixture containing high concentrations of aromatic and cyclic hydrocarbons by using HZSM-5 as a catalyst. A low OCR, high silica:alumina ratio and high temperature in the reformation reaction step were shown to increase the efficiency of aromatics production during reforming as well as increased cyclization resulting in the highest concentration of aromatic and alicyclic hydrocarbons (58 and 13 w/w%, respectively) along with the lowest yields of coke/solids and non-condensible gases. Alkenes and carboxylic acids were virtually completely converted in the second reaction step. The speciation and homology profiles of cyclic products obtained bring into question the current understanding of aromatics' formation within the depth of zeolite pores. It appears that cyclic and aromatic compounds are formed near the zeolite surface but on different sites, with the varied-size intermediate precursors of cyclic compounds.

CHAPTER VI

CONCLUSIONS AND RECOMMENDATIONS

The results of this work showed that lower Silica/Alumina ratio of HZSM-5 yields more aromatics and lower coke. The minimum Silica/Alumina ratio used in this study was 23. It would be interesting to try synthesizing HZSM-5 with a Silica/Alumina ratio lower than 23 (preferably lower than 15) and use it for the catalytic conversion step.

In this work, a batch slurry process was used for the second step. Further experiments in a continuous reactor might show some interesting results. Optimization experiments in a continuous reactor may alter the coke formation, especially when atmospheric pressure is used.

The results of this work are promising for the production of bio-based aromatic compounds from cracked crop oils. This work was mostly focused on the conversion of OLP. However, the results of an experimental run on tars/heavier liquid compounds indicate the possibility of future research work on the catalytic conversion of heavies into aromatic compounds. Response surface methodology could potentially lead to optimum reaction conditions for catalytic cracking and reforming reactions of heavies and tars.

This work was focused on unused virgin soybean oil conversion. Currently, a significant portion of used oil is being used in small scale industries for the production of biodiesel. Most of this used oil comes from food courts, restaurants edible oil and food industries. It would be worth trying this used oil as a feedstock for the proposed future research work.

APPENDICES

APPENDIX A: PROCEDURES

A1: Procedure for synthesis of nanoscale HZSM-5 catalyst

Table 15. Chemicals and quantities required for nanoscale HZSM-5 synthesis

Total Volume	mL	239.3	80	160	240	320
NaOH	g	4	1.34	2.67	4.01	5.35
NaAlO$_2$	g	1.64	0.55	1.10	1.64	2.19
Water	mL	135	45.13	90.26	135.39	180.53
25wt% silica sol (0.00499mol/mL)	mL	104.3	34.87	69.74	104.61	139.47
25wt% silica sol is equivalent to:						
30wt% silica sol (0.00599mol/mL)	mL	86.89	29.05	58.09	87.14	116.19
Water	mL	17.41	5.82	11.64	17.46	23.28
Total Water	mL	152.41	50.95	101.91	152.86	203.81

1. Weigh out NaOH according to table

2. Weigh out NaAlO$_2$ according to table

3. Measure deionized water according to table

4. Add the NaOH and the NaAlO$_2$ to the de-ionized (DI) water

5. Stir this solution at 300rpm

6. Measure 30wt% silica sol according to table

7. Slowly add the silica sol to the solution while it is spinning

8. Allow this solution to be mixed until homogeneous

9. Divide this solution into 1-4 separate autoclaves

10. Stir the mixture in each autoclave at 300rpm for 5 hours

11. Following the stirring period allow the solution to age in the autoclave for 24 hours

12. The autoclave is then closed and place in an oven for 24 hours at 180°C

Washing

13. The contents of each autoclave are then placed in separate centrifuge bottles

14. De-ionized water is then added to fill the bottle ¾ full

15. The bottle is then placed in the centrifuge for 10 minutes

16. The water is then decanted from the solids

17. Steps 14-16 are repeated 3 times.

Ion Exchange

18. Weigh out 5.4 grams of $(NH_4^+)_2SO_4^{2-}$

19. Measure 40mL DI water

20. Add the solid, DI water, and $(NH_4^+)_2SO_4^{2-}$ to a beaker and stir at 300rpm for 1 hour

Washing

21. The contents of each autoclave are then placed in filtered using vacuum filtration

22. The zeolite is rinsed with DI water until the filtrate is free of sulfate anions as indicated by adding $BaCl_2$ dropwise and looking for a $BaSO_4$ precipitate

Drying

23. Remove the zeolite from the filter and allow it to air dry

24. Place the zeolite solid in an oven and heat at 500°C for 4 hours.

A2: Procedure to operate the autoclave/reactor for catalytic experiments

Catalytic conversion experimental runs were performed by using the procedure using the following steps.

Steps

1) Measure the required amount / quantity of the catalyst and starting materials.

2) Make sure that the autoclave is cleaned properly by wiping it with clean paper.

3) Add the starting materials into the autoclave reactor.

4) Use the sand paper to clean the upper part / surfaces of the reactor.

5) Apply grease / gel to the surface of reactor before closing it.

6) Close the reactor and tighten the screws. Apply the torques 5 lbs, 15 lbs, and 25 lbs.

7) Cover the autoclave reactor with the heating jacket.

8) Turn the water supply on.

9) Switch on the reactor controller unit. If the red light in 'on', then press the black button inside (at the back of the controller)

10) Make sure that the controller displays temperature (^{0}C), speed (R.P.M) and pressure (psig)

11) Make sure that all the vent, lines, valves are open except the one on the reactor.

12) Make sure that all the knobs on the reactor are closed.

13) Purging with Nitrogen –

   ▪ Start the Nitrogen flow by opening the valves on the N_2 gas cylinder.

- Open the knob on the reactor to supply Nitrogen into the reactor. The pressure on the display will now increase.

- When the pressure increases to about 150 psig, close Nitrogen inlet knob.

- Now open the vent slowly and vent off the Nitrogen to make the pressure to 0 psig.

- Repeat this purging twice to make sure that all of the air has been removed from the reactor.

14) Set the temperature (on the controller) to a desired value. Switch on the heating button.

15) Switch on the stirrer and increase the stirring speed (RPM) to a desired value.

16) As the temperature increases, the pressure also increases. So monitor the pressure continuously to keep it below 3500 psig. If the pressure increases to / beyond 3500 psig, immediately shut down the process and vent off the products to reduce the pressure and to avoid the damage.

17) Note down the reaction start time when the temperature on the controller first hits the set value of temperature.

Mass Balance

1) Weigh the catalyst and mark this value as A.

2) Weigh the OLP and mark this value as B.

3) Feed the reactor with catalyst and OLP.

4) Close the reactor and apply the required torques on it.

5) Open the nitrogen valve and allow it to flow through the reactor to remove air

6) Once the purging is over, close nitrogen valve

7) Close all the inlet and outlet valves of the reactor.

8) Start the water flow for reactor cooling channel and for the condenser.

9) Set the desired temperature and impeller speed values on controller.

10) Start the heating and the stirring of the reaction mixture.

11) Ensure that there is no reactor leak by spraying soapy water on reactor parts.

12) During the experiment, ensure that the reaction pressure doesn't exceed the limit.

13) Once the reaction is over, cool down the contents inside the reactor to 20 ^{0}C without opening it.

14) Slowly open the vent and collect gaseous products in gas bag (plastic)

15) Weigh empty bottle with top (OR empty beaker).

16) Open the reactor and transfer all of its contents into the above bottle (or a beaker) and close it

17) Weight the bottle or the beaker having the reactor contents

18) Weight of the contents is the difference in weights of full and empty bottle/beaker. This is total weight of liquid products, solid products, coke and catalyst. Mark this value as C

To separate liquids and solids (products, coke, catalyst):

1) Weigh a dry filter paper.

2) Filter the products.

3) Once filtration is over, immediately weigh filter paper with coke on it.

4) The difference in 1 and 3 is weight of catalyst+coke+solids+trapped volatile materials.

5) Weigh the liquid (weight of full vial – weight of empty vial).

6) Dry the filter paper and contents and weigh again.

7) Now 3 – 6 gives weight of volatiles those were trapped in paper, and coke.

8) Now 6 – 1 gives weight of catalyst+coke+solids. Mark this value as D

 ➢ D - A = weight of coke+solid products. Mark this value as E

 ➢ C – D = weight of liquid products. Mark this value as F

 ➢ B – E – F = weight of gaseous products. Mark this value as G

Final calculations:

· Coke and solid products yield = 100*E/B (%W/W)

· Liquid products yield = 100*F/B (%W/W)

· Gaseous products yield = 100*G/B (%W/W).

A3: Procedure for GC sample preparation and analysis

A3.1 Instructions for HP 5890 series II gas chromatograph

How to set the flow rates for the GC:

- Use soap bubble flow meter

- Attach the flow meter to split, purge, column or detector vent.

- Make a proper soap bubble and measure the flow rate by using the electronic display.

This can be done by measuring the time required for the bubble to cover certain volume

range.

- It takes a while to get hold on this, so practice measuring the flow rates several times.

- Adjust split vent He gas flow to about 30 mL/min.

- Adjust purge vent (septum) He gas flow to about 3 mL/min.

- Adjust column He gas flow to about 1 mL/min.

- Adjust FID air flow to about 400 mL/min.

- Adjust FID H_2 flow to about 30 mL/min.

- Adjust FID He flow to about 35 mL/min

A3.2 Pocedure to start the GC:

1. Start the flows of He (UHP grade), H2, air, and N2 by turning on the main valves of the gas cylinders. If the main pressure for any tank is less than 100 psi, it should be replaced.

2. OPEN the He, H2, & air manifold valves (toggle on/off) to the GC (#1, 2, or 3) you will be using.

3. Note which injector/detector ports have the column installed (A-front or B-back) and confirm the pressures and flow rates as shown in table on 1st page. Use the manual bubble meter to verify the flow rates (a stop watch on the instrument for determination is a convenient tool for the determination). Set flow rates from lowest to highest.

The flow rates are determined by connecting the flow meter to the outlets of detector (when detector is off and cold), split line, and septum purge.

If the flow rates need to be reset, open completely the total flow control, set the column head pressure to achieve sufficient flow rate on the column; setup of the flow rate on the septum purge; Open the makeup gas on the detector; and decrease the flow rate on split line by the total flow control.

4. Turn on the GC main power and set the heated zones to nominal initial temperatures (oven 35 °C, injector 250 °C, and detector 300 °C).

5. Configure the injector for split operation (set Purge A (or B) ON) and ignite the FID:

a. Through the GC keypad, set DET A (or B) ON, set SIG1 to A (or B), and press SIG1 (twice). This displays the FID signal (in pA), which should be less than 1 pA before ignition.

b. Use a long-tip butane lighter to ignite flame. When the temperature of the detector reaches 150 °C, the detector can be ignited. To ignite the FID, turn the HYGROGEN fully ON, after 2-4 seconds proceed with AIR. Lower the butane flame to the collector opening, observe the FID signal to see response. Although the ignitor button is disabled, sometimes pushing it at the moment of igniting with butane lighter helps).

c. If the FID ignites, an audible pop may be heard. The signal will jump above 100 pA then quickly drop back to between $10 - 20$ pA and remain stable to with $\pm$ 0.1 pA (you can use a glossy surface like mirror or spatula to verify there is a flame). Turn the AUX GAS fully ON, make sure that flame stays lit.

6. Turn ON the integrator. Consult the instruction manual for operational commands.

A3.3 *Important notes:*

- Hydrogen, aux gas and air knobs must be completely on or off.

- To light FID, only long tip butane lighter must be used.

- Carrier gas flow must always be there while heating the column, otherwise the column will be damaged.

- The pressure in the tanks of hydrogen, air and helium must be above 100 psi.

A3.4 *Procedure to make standards for GC analysis (HP 5890 series II)*

Make a mixture of benzene, toluene, ethylbenzene, ortho-xylene and paraxylene (BTEX).

Each 200 μL was added in a single vial and the vial was capped. This was 20 % mixture

of BTEX. Then 0.4 % mixture is prepared from this 20 % mixture by dilution. The

detailed procedure is written as follows:

To make 0.4 % solution:

Methylene chloride (CH_2Cl_2) is used as solvent. 20 μL of above (20 % BTEX) mixture is

added into 980 μL methylene chloride (CH_2Cl_2). The syringes of 10 μL, 100 μL and 1000

μL (1 ml) were used for the perfect measurement of the volume. This mixture was

prepared in a vial and once both solutions were added into a vial, the vial was capped

immediately. This capped vial was then shaken well using the vortex.

Thus 0.4 % solution was prepared.

To make 0.04 % solution:

In a vial 100 μL of above mixture (0.4 %) was taken and it was diluted with 900 μL of

methylene chloride (CH_2Cl_2) _ diluted 10 times. The vial was capped and shaken with the

vortex.

To make 0.004 % solution:

In a vial 100 μL of above mixture (0.4 %) was taken and it was diluted with 900 μL of

methylene chloride (CH_2Cl_2) _ diluted 10 times. The vial was capped and shaken with the

vortex. Similarly 0.0004 % and 0.00004 % solution were prepared using 10 times dilution each time.

Internal Standards

2 – chlorotoluene was chosen as the internal standards.

2 – chlorotoluene was diluted to make 0.5 % solution with methylene chloride (CH2Cl2). To make this solution, 20 μL of 2 – chlorotoluene was mixed with 3.980 ml (3980 μL) of methylene chloride (CH_2Cl_2) in a vial. This was capped and mixed on vortex. Then 100 μL of this 0.5 % of 2 – chlorotoluene (Internal standards = IS) was added into each of the diluted BTEX mixture solutions. The final vials were labeled and stored in the fridge.

A3.5 Protocol for standards and samples preparation for GC-MS

Preparing internal standards :

provide weights below

concentration of IS

1- take a 22 mL vial   g   mg/mL

2- weight the empty vial

3- add 200 μL of CT= 2-chlorotoluene

4- weight the vial

5- add 20 mL of MeOH

6- weight the vial

The IS is ready to use now

-          Preparing the Standards for calibration Curve

To make 5% solution of B, T, E, O-X, P-X and dilute it 10 times:

Standard # 1:		mg	µL	density g/mL	mg/mL
1	weight the empty vial				
2	add naphthalene	10			5
3	weight the vial				
4	add anthracene	10			5
5	weight the vial				
6	add p-xylene		90		
7	weight the vial				
8	add o-xylene		90		
9	weight the vial				
10	add ethyl benzene		90		
11	weight the vial				
12	add toluene		90		
13	weight the vial				
14	add benzene		90		
15	weight the vial				
16	add MeOH		1550	0.7916	
	total volume		2000		

The above mentioned standard is further diluted 10x.

Standard # 2:   in empty autosampler vial 900 µL above + 900 µL MeOH

Standard # 2:   in empty autosampler vial 900 µL St#1 + 900 µL MeOH

Standard # 3:   in empty autosampler vial 900 µL St#2+ 900 µL MeOH

Standard # 4:   in empty autosampler vial 900 µL St#3+ 900 µL MeOH and so on

Preparing samples :

1-   Weight a vial

2-   Add 800 micro Liters of MeOH

3-   Weight the vial

4-   Add 100 micro liters of IS

5-   Weight the vial

6-   Add 100 micro liters of sample

7-   Weight the vial

8-   Cap the vial

A 4: Procedure for aromatization of propylene

1. Weigh 0.1g of "quartz support" by using a digital balance.

2. Weigh 1g or 0.2g of catalyst (β-zeolite or HZSM5) by using a digital balance.

3. Put a half of the quartz support in the reactor, put the catalyst and the rest of the quartz support on it, making a fixed bed of catalyst

4. Assemble the reactor, turn on the thermo couple and adjust temperature of 400℃ or 500℃.

5. Open the valve of Nitrogen gas tank as carrier gas and adjust the mass flow controller of the carrier gas to over 100 for purging the reactor.

6. Open the valves of Hydrogen and Nitrogen gas tank, turn on the GC and check if

   the actual values of the gases are same as the set points on GC.

   (set point: Carrier gas 1 = 12 or 13; Hydrogen 1= 25; Air = 4)

7. Push the "Flame Ignite" button on the GC and check the steam from the GC to

   confirm that the flame is ignited. (Note: If no peak is detected, it means that you

   need to ignite the flame.)

8. Adjust the detector to Medium or High or High (Filtered) as required.

9. Turn on the computer and open the software named "Peaksimple 378".

10. Click [Edit] →[Channel]→[Postrun], then rename the file name and tick the

    Auto-increment check box.

    (e.g. SLF19May(2010).CHR)
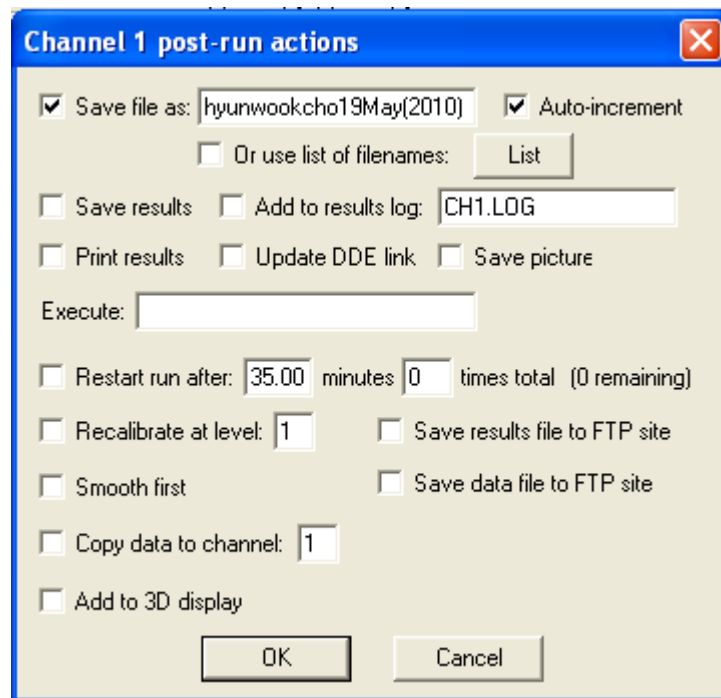
11. Click [Edit] →[Channel]→[Event]. Load the file named "C:/peak372-

    1/peak372/Ch1.evt".

Channel 1 events

C:\peak372-1\peak372\Ch1.evt

Time	Event
0.000	ZERO
0.030	SOUND
0.050	G ON (ValveRotate)
3.000	G OFF (ValveRotate)

Add...   Change...   Remove   Describe...

Load...   Save...   Clear   Print

OK   Shift...
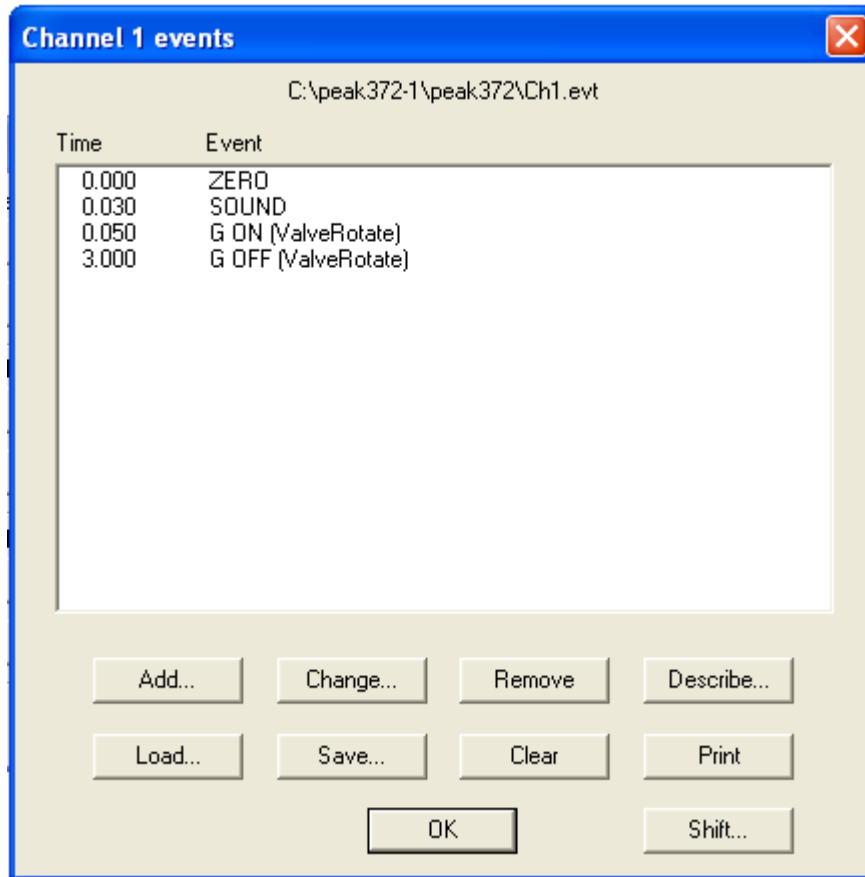
12. Press the spacebar or click [Acquisition]→[Run] for the "blank run" to check if there is the propylene peak detected or not.

13. Open Microsoft Excel and input the data in the form as shown below.
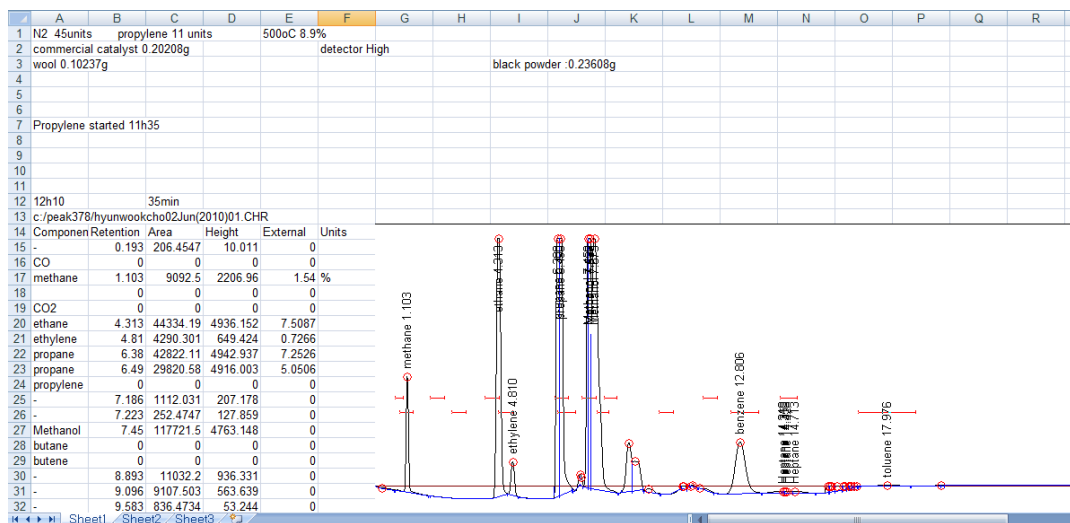
14. When the temperature of the thermocouple reaches 400 °C or 500 °C, open the valve of propylene gas tank and record the time. (e.g. Propylene started 11h35)

15. 1) Adjust the mass flows of Propylene (Process gas) and Nitrogen (Carrier gas) to the value of 11 and 45 respectively on the mass flow controller if the Concentration of the Propylene is 8.9%.

    2) Adjust the mass flows of Propylene (Process gas) and Nitrogen (Carrier gas) to the value of 11 and 31 respectively on the mass flow controller if the Concentration of the Propylene is 12.5%.

16. Stop the "blank run" by clicking [Acquisition]→[Stop]. (Note: If you click [Stop+Postrun], the file is saved on your computer. However, if you click [Stop], the file is not saved.)

17. In order to start the first run, wait at least for 30 minutes since after starting propylene flow because the whole system reaches steady-state after 30 minutes from the opening the valve of propylene gas tank.)

18. When the temperature of the GC is at the room temperature (33 °C), start the run. Every run takes about 33minutes and after that, click [Acquisition]→[Stop+Postrun]. During the run the temperature reaches 219°C, then it takes about 15 minutes to cool down from 219°C. Totally, it takes about 50 minutes for one run.

19. Click [Edit]→[Manual Integration], to adjust the baseline of the peaks.
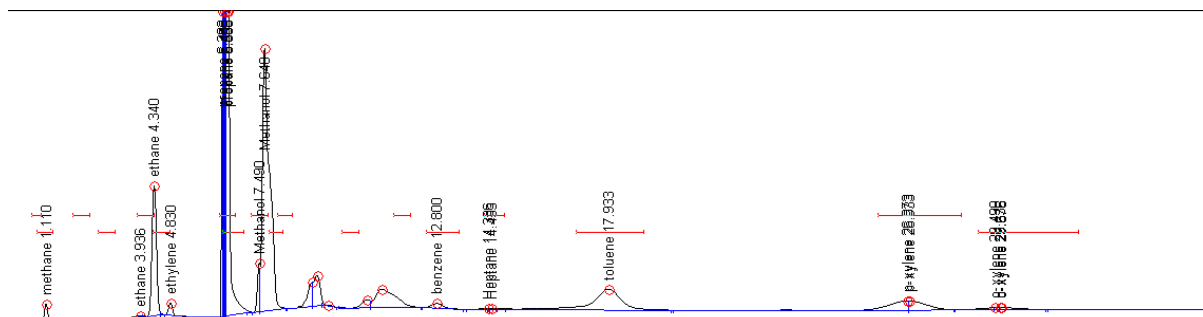
20. Run the GC until 400 minutes of the reaction time is completed. It is necessary to run the aromatization at least for 200 minutes in each and every set of the runs.

	A	B	C	D	E	F	G	H	I
1	N2 31units	propylene 11 units			400oC 12.5%				
2	commercial catalyst 0.20589g					detector High			weight of coke 0.02592g
3	wool 0.10425g								
7		50	95	140	200	250	300	350	400
8	propylene	14.3248	12.4795	12.2801	10.999	10.3499	11.4888	11.7097	11.7838
9	benzene	0.7196	0.165	0.1754	0.1827	0.1171	0.1101	0.0561	0.055
10	toluene	5.5347	2.2974	2.0464	1.4418	1.3281	1.0916	0.9656	0.8707
11	p-xylene	18.1885	6.4114	6.4382	4.6679	4.1959	3.8502	3.4288	3.1947
12	o-xylene	6.0828	0.6202	1.4721	0.8764	0.9031	0.7023	0.6084	0.5556
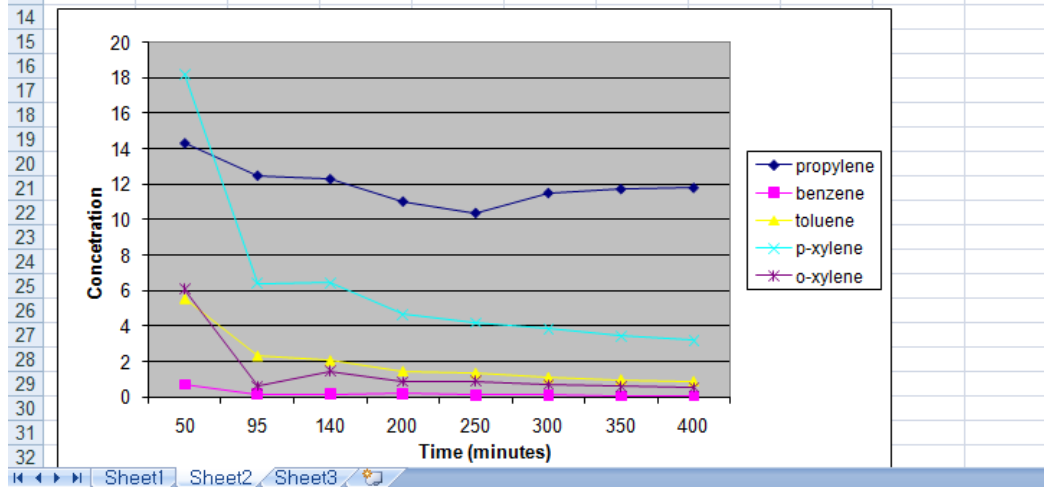
21. Prepare the chart as shown above.

22. After 3 minutes since you start the last run, you can hear the beep sound. Then, turn off the thermocouple, close the valve of Propylene gas tank and adjust the

value of Nitrogen (Carrier gas) on mass flow controller to over 100 for cleaning the whole system.

23. When the temperature of the GC is at 33℃, close the valve of Nitrogen gas tank, then also, close the valves of Hydrogen and Nitrogen gas tanks.

24. Turn off the computer and GC.

25. On the paper, collect the previous catalyst and 0.1g of quartz support inside the reactor.

26. By using about 0.005g of quartz support, get rid of the catalyst inside the reactor and put it on the paper.

27. Weigh all the things you collect. (Catalyst, 0.1g of quartz support, 0.05g of quartz support, and one paper)

28. Calculate the mass of coke on the catalyst.

Events ([Edit] →[Channel]→[Event])

c:/peak372-1/peak372/Ch1.evt
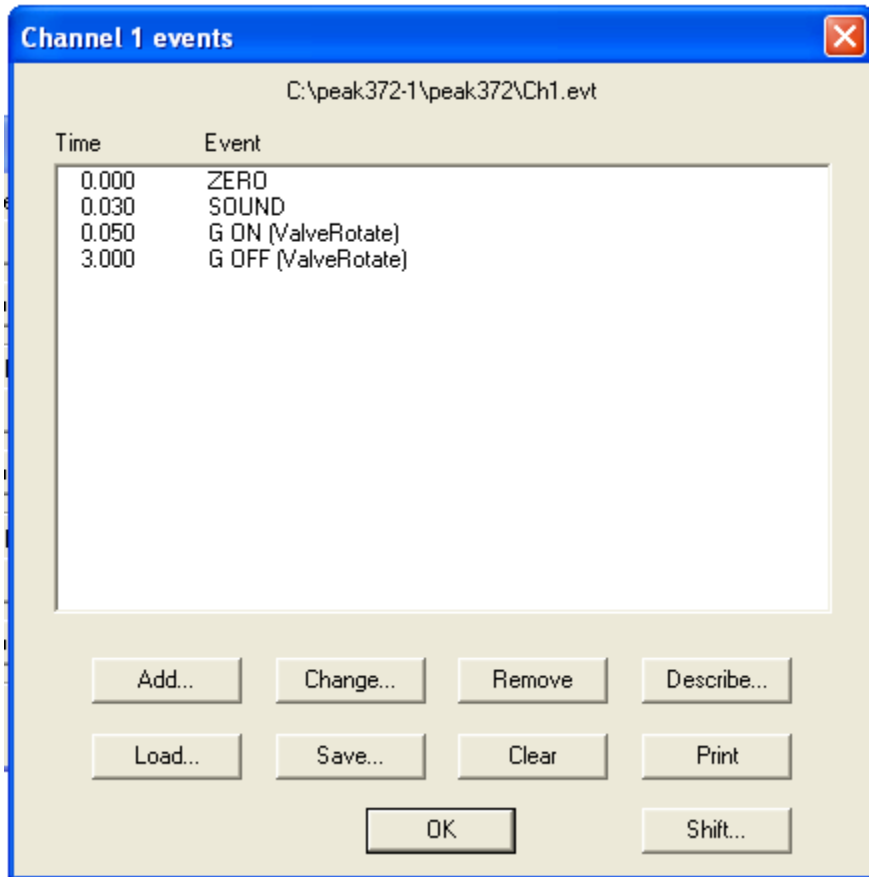
Components ([Edit] →[Channel]→[Components])

c:/peak378/btex.cpt
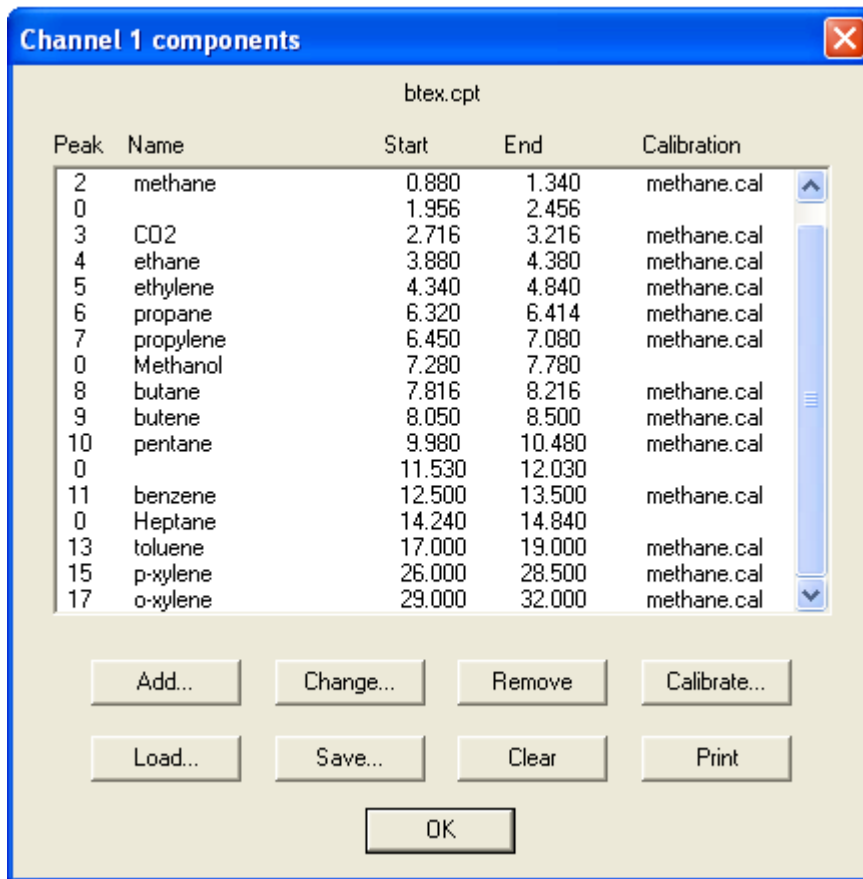
Table 16. GC Calibration components and the residence times

Peak	Name	Start	End	Calibration
1	CO	0.720	1.000	methane.cal
2	Methane	0.880	1.340	methane.cal
3	CO2	2.716	3.216	methane.cal
4	Ethane	3.880	4.380	methane.cal
5	Ethylene	4.340	4.840	methane.cal
6	Propane	6.320	6.414	methane.cal
7	Propylene	6.450	7.080	methane.cal
0	Methanol	7.280	7.780	

8	Butane	7.816	8.216	methane.cal
9	Butane	8.050	8.500	methane.cal
10	Pentane	9.980	10.480	methane.cal
11	Benzene	12.500	13.500	methane.cal
0	Heptane	14.240	14.840	
13	Toluene	17.000	19.000	methane.cal
15	p-xylene	26.000	28.500	methane.cal
17	o-xylene	29.000	32.000	methane.cal

Temperature ([Edit] →[Channel]→[Temperature])

c:/peak372-1/peak372/gasbtexhaeysep.tem
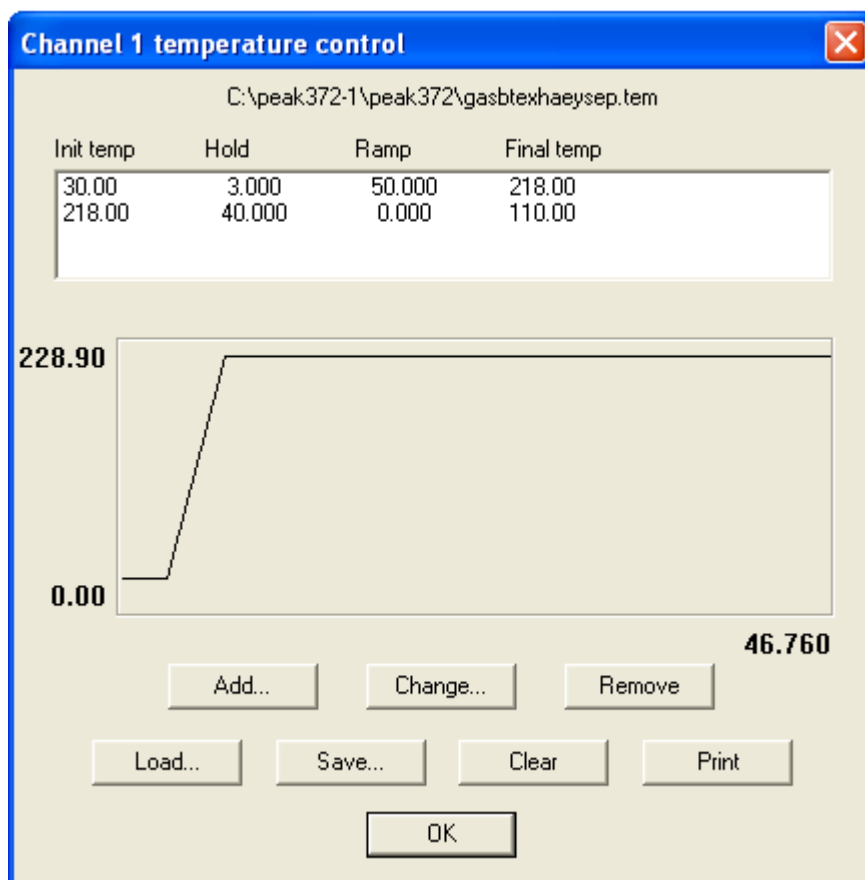
A 5: Procedure for non-catalytic cracking of crop oil

The non-catalytic cracking of soybean oil was conducted in a continuous reactor applying the following steps.

1) Soybean oil was stored in the oil tank.

2) The reactor was preheated to the desired temperature by using the heating jackets attached to all zones of the reactor (upper, middle, bottom).

3) The feed oil was passed through a filter to remove solids and other particles from the feed oil.

4) The oil was pumped through the preheater to heat the oil to about 150 ^{0}C.

5) The preheated oil was continuously pumped into the reactor from its bottom and stirred continuously and heated to about 420 ^{0}C where it was cracked into smaller molecules.

6) The level of oil was maintained in the reactor throughout the experimental run, in such a way that only cracked molecules present in vapor form come out of the upper part of the reactor.

7) Thus the crackate, boiling only below 420 ^{0}C, was continuously passed through the condenser and the condensed liquid products were stored into a storage tank.

8) This liquid crackate was again distilled at 300 ^{0}C and used for further aromatization experiments.

9) The reaction pressure of 50 psig was kept constant throughout the experiment. Once the non-catalytic cracking reaction was over, the reactor was cooled down to the room temperature.

10) The tars were taken out from the bottom of the reactor.

11) The coke deposited on the reactor walls and stirrer, was scraped off by using an iron scraper and the reactor was cleaned properly with acetone, if needed.

12) The gases were taken out through a gas vent.

A 6: Procedure of obtaining SEM images of zeolite catalyst samples

The instrument details of Hitachi SU 8010 SEM (scanning electron microscope) are shown in the following figure 27.
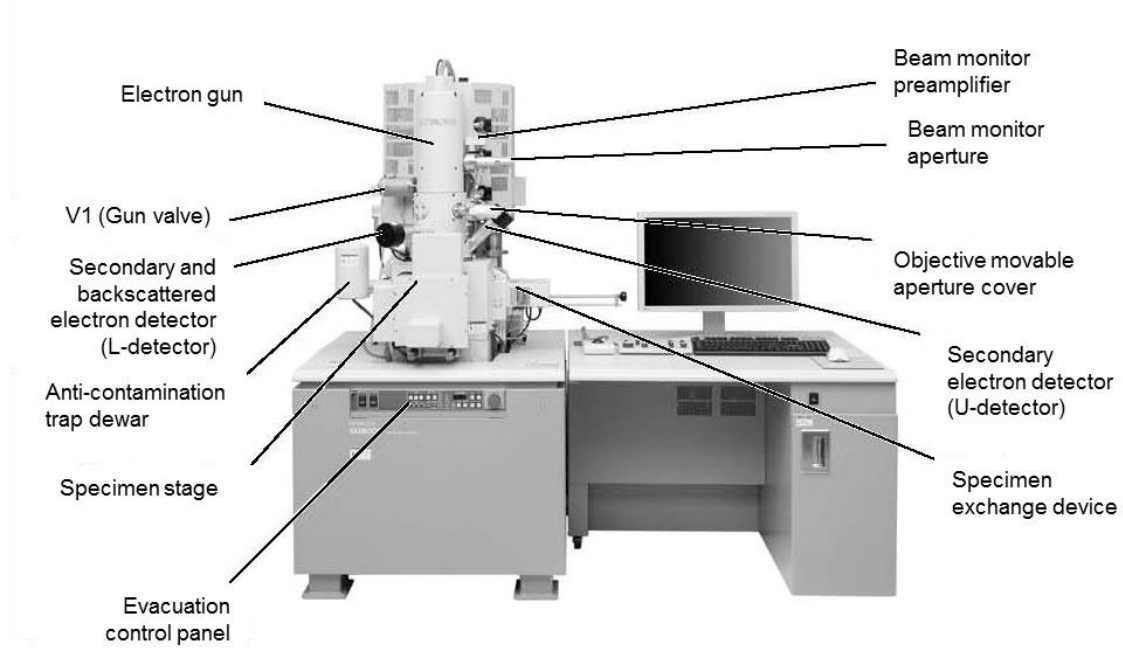
Figure 27. SEM instrument diagram and important components.

1) To obtain proper separation of zeolite particles, add a small quantity of zeolite in methanol and use ultrasonic instrument until the aggregation of particles disappears.

2) Add the dispersed particles in solution as a drop on a sample holder and let it dry for about 5 minutes.

3) Load the sample into the sample chamber.

4) Turn on the electron gun and choose an initial voltage, for example 10 kV, and try to get a clear image of the sample under low magnification by manipulating the coarse and fine focus knobs.

5) If a clear image can not be obtained, then change the voltage and continue to adjust the focus until the sample will be clearly visible.

6) First, observe the sample under low magnification, and then switch it to the high magnification. Observe the focusing process.

7) Take the desired number of images of the samples at the desired voltage and at the required magnification.

The section view of SU801O SEM column is as follows:
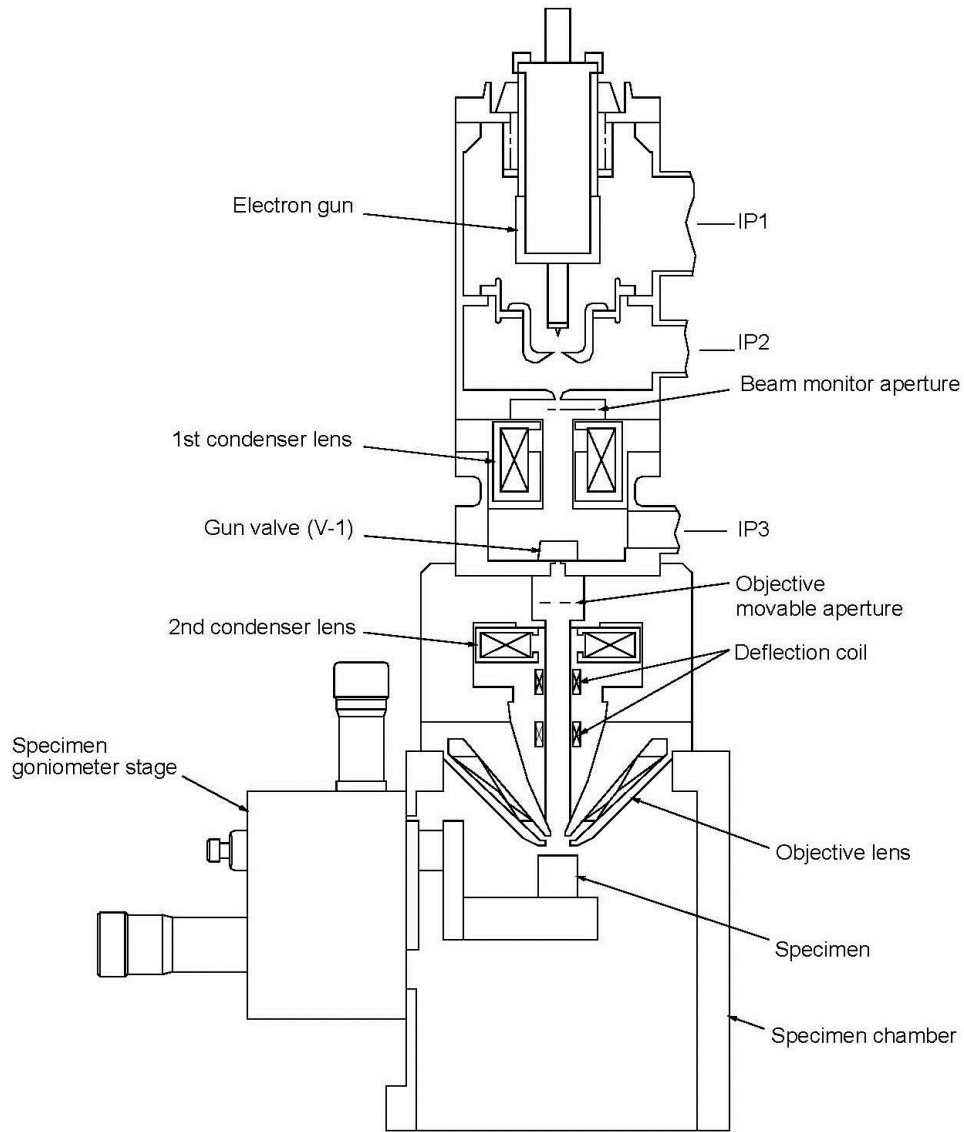
Figure 28. SEM column diagram

NOTE: Basic working parameters such as signal mode (secondary electron or

backscattered electron), accelerating voltage, working distance, and magnification times,

should be adjusted as needed.

APPENDIX B: RAW DATA OF STATISTICAL ANALYSIS

B1: Raw DOE Minitab data for OLP aromatization

Response Surface Regression: BTEX yield versus Block, Temperature , OCR, ...

The analysis was done using coded units.

Estimated Regression Coefficients for BTEX yield

Term	Coef	SE Coef	T	P
Constant	1.98627	0.11762	16.888	0.000
Block	-0.06006	0.06559	-0.916	0.384
Temperature (°C)	0.50123	0.07871	6.368	0.000
OCR	-0.23073	0.07871	-2.931	0.017
Time (min.)	0.11545	0.07871	1.467	0.177
Temperature (°C)*Temperature (°C)	0.26372	0.07909	3.335	0.009
OCR*OCR	0.03093	0.07909	0.391	0.705
Time (min.)*Time (min.)	-0.03419	0.07909	-0.432	0.676
Temperature (°C)*OCR	-0.19895	0.10161	-1.958	0.082
Temperature (°C)*Time (min.)	0.08970	0.10161	0.883	0.400
OCR*Time (min.)	-0.17686	0.10161	-1.741	0.116

S = 0.287408   PRESS = 8.11649

R-Sq = 88.80% R-Sq(pred) = 0.00% R-Sq(adj) = 76.36%

Analysis of Variance for BTEX yield

Source	DF	Seq SS	Adj SS	Adj MS	F
Blocks	1	0.06925	0.06925	0.06925	0.84
Regression	9	5.82759	5.82759	0.64751	7.84
Linear	3	4.23727	4.23727	1.41242	17.10
Temperature (°C)	1	3.34976	3.34976	3.34976	40.55
OCR	1	0.70981	0.70981	0.70981	8.59

Source	DF	Seq SS	Adj SS	Adj MS	F
Time (min.)	1	0.17770	0.17770	0.17770	2.15
Square	3	0.95908	0.95908	0.31969	3.87
Temperature (°C)*Temperature (°C)	1	0.92886	0.91850	0.91850	11.12
OCR*OCR	1	0.01478	0.01263	0.01263	0.15
Time (min.)*Time (min.)	1	0.01543	0.01543	0.01543	0.19
Interaction	3	0.63123	0.63123	0.21041	2.55
Temperature (°C)*OCR	1	0.31663	0.31663	0.31663	3.83
Temperature (°C)*Time (min.)	1	0.06436	0.06436	0.06436	0.78
OCR*Time (min.)	1	0.25024	0.25024	0.25024	3.03
Residual Error	9	0.74343	0.74343	0.08260	
Lack-of-Fit	5	0.73628	0.73628	0.14726	82.35
Pure Error	4	0.00715	0.00715	0.00179	
Total	19	6.64027			

Source	P
Blocks	0.384
Regression	0.003
Linear	0.000
Temperature (°C)	0.000
OCR	0.017
Time (min.)	0.177
Square	0.050
Temperature (°C)*Temperature (°C)	0.009
OCR*OCR	0.705
Time (min.)*Time (min.)	0.676
Interaction	0.121
Temperature (°C)*OCR	0.082
Temperature (°C)*Time (min.)	0.400
OCR*Time (min.)	0.116
Residual Error	
Lack-of-Fit	0.000

Pure Error

Total

BTEX

Obs	StdOrder	yield	Fit	SE Fit	Residual	St Resid
1	10	1.925	1.926	0.128	-0.002	-0.01
2	6	3.793	3.500	0.243	0.294	1.90
3	5	1.933	1.920	0.243	0.013	0.09
4	7	1.749	1.503	0.243	0.247	1.60
5	12	1.980	1.926	0.128	0.054	0.21
6	8	1.986	2.287	0.243	-0.301	-1.95
7	2	2.458	2.736	0.243	-0.277	-1.80
8	1	1.785	1.515	0.243	0.270	1.75
9	11	1.994	1.926	0.128	0.067	0.26
10	3	1.481	1.805	0.243	-0.324	-2.10 R
11	4	2.186	2.230	0.243	-0.044	-0.29
12	9	1.929	1.926	0.128	0.003	0.01
13	18	1.974	2.144	0.235	-0.170	-1.03
14	15	2.307	2.506	0.235	-0.198	-1.20
15	20	2.019	2.046	0.141	-0.027	-0.11
16	13	1.791	1.931	0.235	-0.141	-0.85
17	16	1.996	1.752	0.235	0.244	1.48
18	14	3.755	3.568	0.235	0.187	1.13
19	19	1.936	2.046	0.141	-0.111	-0.44
20	17	1.982	1.767	0.235	0.215	1.31

R denotes an observation with a large standardized residual.

Estimated Regression Coefficients for BTEX yield using data in uncoded units

Term	Coef
Constant	8.38721

Block   -0.0600577

Temperature (°C)   -0.0558654

OCR   0.321635

Time (min.)   0.0117202

Temperature (°C)*Temperature (°C)   0.000105489

OCR*OCR   0.00193314

Time (min.)*Time (min.)   -6.07754E-04

Temperature (°C)*OCR   -9.94727E-04

Temperature (°C)*Time (min.)   0.000239187

OCR*Time (min.)   -0.00589537

Response Surface Regression: BTEX yield versus Temperature , OCR, Time (min.)

The analysis was done using coded units.

Estimated Regression Coefficients for BTEX yield

Term	Coef	SE Coef	T	P
Constant	1.94821	0.09561	20.376	0.000
Temperature (°C)	0.50123	0.07514	6.670	0.000
OCR	-0.23073	0.07514	-3.071	0.011
Time (min.)	0.11545	0.07514	1.536	0.153
Temperature (°C)*Temperature (°C)	0.26616	0.07531	3.534	0.005
OCR*OCR	0.03337	0.07531	0.443	0.666
Temperature (°C)*OCR	-0.19895	0.09701	-2.051	0.065
Temperature (°C)*Time (min.)	0.08970	0.09701	0.925	0.375
OCR*Time (min.)	-0.17686	0.09701	-1.823	0.096

S = 0.274378   PRESS = 6.17448

R-Sq = 87.53% R-Sq(pred) = 7.01% R-Sq(adj) = 78.46%

Analysis of Variance for BTEX yield

Source	DF	Seq SS	Adj SS	Adj MS	F
Regression	8	5.81216	5.81216	0.72652	9.65
Linear	3	4.23727	4.23727	1.41242	18.76
Temperature (°C)	1	3.34976	3.34976	3.34976	44.50
OCR	1	0.70981	0.70981	0.70981	9.43
Time (min.)	1	0.17770	0.17770	0.17770	2.36
Square	2	0.94365	0.94365	0.47182	6.27
Temperature (°C)*Temperature (°C)	1	0.92886	0.94039	0.94039	12.49
OCR*OCR	1	0.01478	0.01478	0.01478	0.20
Interaction	3	0.63123	0.63123	0.21041	2.79
Temperature (°C)*OCR	1	0.31663	0.31663	0.31663	4.21
Temperature (°C)*Time (min.)	1	0.06436	0.06436	0.06436	0.85
OCR*Time (min.)	1	0.25024	0.25024	0.25024	3.32
Residual Error	11	0.82811	0.82811	0.07528	
Lack-of-Fit	6	0.82040	0.82040	0.13673	88.59
Pure Error	5	0.00772	0.00772	0.00154	
Total	19	6.64027			

Source	P
Regression	0.001
Linear	0.000
Temperature (°C)	0.000
OCR	0.011
Time (min.)	0.153
Square	0.015
Temperature (°C)*Temperature (°C)	0.005
OCR*OCR	0.666
Interaction	0.090
Temperature (°C)*OCR	0.065
Temperature (°C)*Time (min.)	0.375
OCR*Time (min.)	0.096

Residual Error

  Lack-of-Fit   0.000

  Pure Error

Total

BTEX

Obs	StdOrder	yield	Fit	SE Fit	Residual	St Resid
1	10	1.925	1.948	0.096	-0.024	-0.09
2	6	3.793	3.561	0.224	0.233	1.47
3	5	1.933	1.981	0.224	-0.048	-0.30
4	7	1.749	1.564	0.224	0.186	1.17
5	12	1.980	1.948	0.096	0.032	0.12
6	8	1.986	2.348	0.224	-0.362	-2.29 R
7	2	2.458	2.797	0.224	-0.338	-2.14 R
8	1	1.785	1.576	0.224	0.209	1.32
9	11	1.994	1.948	0.096	0.045	0.18
10	3	1.481	1.866	0.224	-0.385	-2.44 R
11	4	2.186	2.291	0.224	-0.105	-0.66
12	9	1.929	1.948	0.096	-0.019	-0.07
13	18	1.974	2.137	0.156	-0.163	-0.72
14	15	2.307	2.414	0.207	-0.107	-0.59
15	20	2.019	1.948	0.096	0.071	0.28
16	13	1.791	1.839	0.207	-0.049	-0.27
17	16	1.996	1.660	0.207	0.336	1.87
18	14	3.755	3.476	0.207	0.278	1.55
19	19	1.936	1.948	0.096	-0.012	-0.05
20	17	1.982	1.760	0.156	0.222	0.98

R denotes an observation with a large standardized residual.

Estimated Regression Coefficients for BTEX yield using data in uncoded units

Term	Coef
Constant	8.58226
Temperature (°C)	-0.0565492
OCR	0.318277
Time (min.)	-0.00347368
Temperature (°C)*Temperature (°C)	0.000106466
OCR*OCR	0.00208578
Temperature (°C)*OCR	-9.94727E-04
Temperature (°C)*Time (min.)	0.000239187
OCR*Time (min.)	-0.00589537

Response Surface Regression: BTEX yield versus Temperature , OCR, Time (min.)

Estimated Regression Coefficients for BTEX yield

Term	Coef	SE Coef	T	P
Constant	1.97195	0.07651	25.774	0.000
Temperature (°C)	0.50123	0.07258	6.906	0.000
OCR	-0.23073	0.07258	-3.179	0.008
Time (min.)	0.11545	0.07258	1.591	0.138
Temperature (°C)*Temperature (°C)	0.26394	0.07258	3.636	0.003
Temperature (°C)*OCR	-0.19895	0.09370	-2.123	0.055
Temperature (°C)*Time (min.)	0.08970	0.09370	0.957	0.357
OCR*Time (min.)	-0.17686	0.09370	-1.887	0.084

$S = 0.265031$ $PRESS = 5.33200$

$R\text{-Sq} = 87.31\%$ $R\text{-Sq(pred)} = 19.70\%$ $R\text{-Sq(adj)} = 79.90\%$

Analysis of Variance for BTEX yield

Source	DF	Seq SS	Adj SS	Adj MS	F

Source	DF	Seq SS	Adj SS	Adj MS	F
Regression	7	5.79737	5.79737	0.82820	11.79
Linear	3	4.23727	4.23727	1.41242	20.11
Temperature (°C)	1	3.34976	3.34976	3.34976	47.69
OCR	1	0.70981	0.70981	0.70981	10.11
Time (min.)	1	0.17770	0.17770	0.17770	2.53
Square	1	0.92886	0.92886	0.92886	13.22
Temperature (°C)*Temperature (°C)	1	0.92886	0.92886	0.92886	13.22
Interaction	3	0.63123	0.63123	0.21041	3.00
Temperature (°C)*OCR	1	0.31663	0.31663	0.31663	4.51
Temperature (°C)*Time (min.)	1	0.06436	0.06436	0.06436	0.92
OCR*Time (min.)	1	0.25024	0.25024	0.25024	3.56
Residual Error	12	0.84290	0.84290	0.07024	
Lack-of-Fit	7	0.83518	0.83518	0.11931	77.30
Pure Error	5	0.00772	0.00772	0.00154	
Total	19	6.64027			

Source	P
Regression	0.000
Linear	0.000
Temperature (°C)	0.000
OCR	0.008
Time (min.)	0.138
Square	0.003
Temperature (°C)*Temperature (°C)	0.003
Interaction	0.073
Temperature (°C)*OCR	0.055
Temperature (°C)*Time (min.)	0.357
OCR*Time (min.)	0.084
Residual Error	
Lack-of-Fit	0.000
Pure Error	

Total

BTEX

Obs	StdOrder	yield	Fit	SE Fit	Residual	St Resid
1	10	1.925	1.972	0.077	-0.047	-0.19
2	6	3.793	3.549	0.215	0.244	1.58
3	5	1.933	1.969	0.215	-0.036	-0.23
4	7	1.749	1.552	0.215	0.197	1.27
5	12	1.980	1.972	0.077	0.008	0.03
6	8	1.986	2.336	0.215	-0.350	-2.26 R
7	2	2.458	2.785	0.215	-0.326	-2.11 R
8	1	1.785	1.564	0.215	0.221	1.43
9	11	1.994	1.972	0.077	0.022	0.09
10	3	1.481	1.854	0.215	-0.373	-2.41 R
11	4	2.186	2.279	0.215	-0.093	-0.60
12	9	1.929	1.972	0.077	-0.043	-0.17
13	18	1.974	2.160	0.141	-0.186	-0.83
14	15	2.307	2.349	0.141	-0.041	-0.18
15	20	2.019	1.972	0.077	0.047	0.19
16	13	1.791	1.857	0.197	-0.067	-0.38
17	16	1.996	1.595	0.141	0.401	1.79
18	14	3.755	3.494	0.197	0.260	1.46
19	19	1.936	1.972	0.077	-0.036	-0.14
20	17	1.982	1.783	0.141	0.199	0.89

R denotes an observation with a large standardized residual.

Estimated Regression Coefficients for BTEX yield using data in uncoded units

Term	Coef
Constant	8.24459
Temperature (°C)	-0.0559262
OCR	0.364164
Time (min.)	-0.00347368
Temperature (°C)*Temperature (°C)	0.000105576
Temperature (°C)*OCR	-9.94727E-04
Temperature (°C)*Time (min.)	0.000239187
OCR*Time (min.)	-0.00589537

Response Surface Regression: BTEX yield versus Temperature , OCR, Time (min.)

The analysis was done using coded units.

Estimated Regression Coefficients for BTEX yield

Term	Coef	SE Coef	T	P
Constant	1.9719	0.07626	25.858	0.000
Temperature (°C)	0.5012	0.07235	6.928	0.000
OCR	-0.2307	0.07235	-3.189	0.007
Time (min.)	0.1154	0.07235	1.596	0.135
Temperature (°C)*Temperature (°C)	0.2639	0.07235	3.648	0.003
Temperature (°C)*OCR	-0.1989	0.09340	-2.130	0.053
OCR*Time (min.)	-0.1769	0.09340	-1.894	0.081

S = 0.264177   PRESS = 3.53742

R-Sq = 86.34%   R-Sq(pred) = 46.73%   R-Sq(adj) = 80.03%

Analysis of Variance for BTEX yield

Source	DF	Seq SS	Adj SS	Adj MS	F
Regression	6	5.73301	5.73301	0.95550	13.69

Source	DF	Seq SS	Adj SS	Adj MS	F
Linear	3	4.23727	4.23727	1.41242	20.24
Temperature (°C)	1	3.34976	3.34976	3.34976	48.00
OCR	1	0.70981	0.70981	0.70981	10.17
Time (min.)	1	0.17770	0.17770	0.17770	2.55
Square	1	0.92886	0.92886	0.92886	13.31
Temperature (°C)*Temperature (°C)	1	0.92886	0.92886	0.92886	13.31
Interaction	2	0.56687	0.56687	0.28344	4.06
Temperature (°C)*OCR	1	0.31663	0.31663	0.31663	4.54
OCR*Time (min.)	1	0.25024	0.25024	0.25024	3.59
Residual Error	13	0.90726	0.90726	0.06979	
Lack-of-Fit	8	0.89954	0.89954	0.11244	72.85
Pure Error	5	0.00772	0.00772	0.00154	
Total	19	6.64027			

Source	P
Regression	0.000
Linear	0.000
Temperature (°C)	0.000
OCR	0.007
Time (min.)	0.135
Square	0.003
Temperature (°C)*Temperature (°C)	0.003
Interaction	0.043
Temperature (°C)*OCR	0.053
OCR*Time (min.)	0.081
Residual Error	
Lack-of-Fit	0.000
Pure Error	
Total	

BTEX

Obs	StdOrder	yield	Fit	SE Fit	Residual	St Resid
1	10	1.925	1.972	0.076	-0.047	-0.19
2	6	3.793	3.459	0.193	0.334	1.85
3	5	1.933	2.059	0.193	-0.125	-0.70
4	7	1.749	1.641	0.193	0.108	0.60
5	12	1.980	1.972	0.076	0.008	0.03
6	8	1.986	2.246	0.193	-0.260	-1.44
7	2	2.458	2.874	0.193	-0.416	-2.31 R
8	1	1.785	1.474	0.193	0.311	1.72
9	11	1.994	1.972	0.076	0.022	0.09
10	3	1.481	1.764	0.193	-0.284	-1.57
11	4	2.186	2.369	0.193	-0.183	-1.01
12	9	1.929	1.972	0.076	-0.043	-0.17
13	18	1.974	2.160	0.141	-0.186	-0.83
14	15	2.307	2.349	0.141	-0.041	-0.18
15	20	2.019	1.972	0.076	0.047	0.19
16	13	1.791	1.857	0.196	-0.067	-0.38
17	16	1.996	1.595	0.141	0.401	1.79
18	14	3.755	3.494	0.196	0.260	1.47
19	19	1.936	1.972	0.076	-0.036	-0.14
20	17	1.982	1.783	0.141	0.199	0.89

R denotes an observation with a large standardized residual.

Estimated Regression Coefficients for BTEX yield using data in uncoded units

Term	Coef
Constant	7.19814
Temperature (°C)	-0.0529364
OCR	0.364164

Time (min.)   0.0802418

Temperature (°C)*Temperature (°C)   0.000105576

Temperature (°C)*OCR   -9.94727E-04

OCR*Time (min.)   -0.00589537

Response Surface Regression: BTEX yield versus Temperature , OCR, Time (min.)

Estimated Regression Coefficients for BTEX yield

Term	Coef	SE Coef	T	P
Constant	1.9719	0.08301	23.757	0.000
Temperature (°C)	0.5012	0.07875	6.365	0.000
OCR	-0.2307	0.07875	-2.930	0.011
Time (min.)	0.1154	0.07875	1.466	0.165
Temperature (°C)*Temperature (°C)	0.2639	0.07875	3.352	0.005
Temperature (°C)*OCR	-0.1989	0.10166	-1.957	0.071

S = 0.287539   PRESS = 3.22801

R-Sq = 82.57% R-Sq(pred) = 51.39% R-Sq(adj) = 76.34%

Analysis of Variance for BTEX yield

Source	DF	Seq SS	Adj SS	Adj MS	F
Regression	5	5.48277	5.48277	1.09655	13.26
Linear	3	4.23727	4.23727	1.41242	17.08
Temperature (°C)	1	3.34976	3.34976	3.34976	40.52
OCR	1	0.70981	0.70981	0.70981	8.59
Time (min.)	1	0.17770	0.17770	0.17770	2.15
Square	1	0.92886	0.92886	0.92886	11.23
Temperature (°C)*Temperature (°C)	1	0.92886	0.92886	0.92886	11.23
Interaction	1	0.31663	0.31663	0.31663	3.83
Temperature (°C)*OCR	1	0.31663	0.31663	0.31663	3.83

Residual Error	14 1.15750	1.15750	0.08268	
Lack-of-Fit	9 1.14978	1.14978	0.12775	82.77
Pure Error	5 0.00772	0.00772	0.00154	
Total	19 6.64027			

Source	P
Regression	0.000
Linear	0.000
Temperature (°C)	0.000
OCR	0.011
Time (min.)	0.165
Square	0.005
Temperature (°C)*Temperature (°C)	0.005
Interaction	0.071
Temperature (°C)*OCR	0.071
Residual Error	
Lack-of-Fit	0.000
Pure Error	
Total	

BTEX

Obs	StdOrder	yield	Fit	SE Fit	Residual	St Resid
1	10	1.925	1.972	0.083	-0.047	-0.17
2	6	3.793	3.282	0.184	0.511	2.31 R
3	5	1.933	1.882	0.184	0.051	0.23
4	7	1.749	1.818	0.184	-0.069	-0.31
5	12	1.980	1.972	0.083	0.008	0.03
6	8	1.986	2.423	0.184	-0.437	-1.98
7	2	2.458	3.051	0.184	-0.593	-2.68 R
8	1	1.785	1.651	0.184	0.134	0.60

9	11	1.994	1.972	0.083	0.022	0.08
10	3	1.481	1.587	0.184	-0.107	-0.48
11	4	2.186	2.192	0.184	-0.006	-0.03
12	9	1.929	1.972	0.083	-0.043	-0.15
13	18	1.974	2.160	0.153	-0.186	-0.77
14	15	2.307	2.349	0.153	-0.041	-0.17
15	20	2.019	1.972	0.083	0.047	0.17
16	13	1.791	1.857	0.213	-0.067	-0.35
17	16	1.996	1.595	0.153	0.401	1.65
18	14	3.755	3.494	0.213	0.260	1.35
19	19	1.936	1.972	0.083	-0.036	-0.13
20	17	1.982	1.783	0.153	0.199	0.82

R denotes an observation with a large standardized residual.

Estimated Regression Coefficients for BTEX yield using data in uncoded units

Term	Coef
Constant	8.00876
Temperature (°C)	-0.0529364
OCR	0.290472
Time (min.)	0.0153927
Temperature (°C)*Temperature (°C)	0.000105576
Temperature (°C)*OCR	-9.94727E-04

Response Surface Regression: BTEX yield versus Temperature (°C), OCR

Estimated Regression Coefficients for BTEX yield

Term	Coef	SE Coef	T	P
Constant	1.9719	0.08613	22.896	0.000
Temperature (°C)	0.5012	0.08171	6.134	0.000

OCR   -0.2307 0.08171 -2.824 0.013

Temperature (°C)*Temperature (°C) 0.2639 0.08171 3.230 0.006

Temperature (°C)*OCR   -0.1989 0.10548 -1.886 0.079

S = 0.298351   PRESS = 3.14039

R-Sq = 79.89% R-Sq(pred) = 52.71% R-Sq(adj) = 74.53%

Analysis of Variance for BTEX yield

Source	DF	Seq SS	Adj SS	Adj MS	F
Regression	4	5.3051	5.3051	1.32627	14.90
Linear	2	4.0596	4.0596	2.02978	22.80
Temperature (°C)	1	3.3498	3.3498	3.34976	37.63
OCR	1	0.7098	0.7098	0.70981	7.97
Square	1	0.9289	0.9289	0.92886	10.44
Temperature (°C)*Temperature (°C)	1	0.9289	0.9289	0.92886	10.44
Interaction	1	0.3166	0.3166	0.31663	3.56
Temperature (°C)*OCR	1	0.3166	0.3166	0.31663	3.56
Residual Error	15	1.3352	1.3352	0.08901	
Lack-of-Fit	4	0.3691	0.3691	0.09226	1.05
Pure Error	11	0.9661	0.9661	0.08783	
Total	19	6.6403			

Source	P
Regression	0.000
Linear	0.000
Temperature (°C)	0.000
OCR	0.013
Square	0.006
Temperature (°C)*Temperature (°C)	0.006
Interaction	0.079

Temperature (°C)*OCR   0.079

Residual Error

  Lack-of-Fit   0.425

  Pure Error

Total

      BTEX

Obs	StdOrder	yield	Fit	SE Fit	Residual	St Resid
1	10	1.925	1.972	0.086	-0.047	-0.17
2	6	3.793	3.167	0.172	0.626	2.57 R
3	5	1.933	1.766	0.172	0.167	0.68
4	7	1.749	1.703	0.172	0.046	0.19
5	12	1.980	1.972	0.086	0.008	0.03
6	8	1.986	2.307	0.172	-0.322	-1.32
7	2	2.458	3.167	0.172	-0.708	-2.91 R
8	1	1.785	1.766	0.172	0.018	0.07
9	11	1.994	1.972	0.086	0.022	0.08
10	3	1.481	1.703	0.172	-0.222	-0.91
11	4	2.186	2.307	0.172	-0.122	-0.50
12	9	1.929	1.972	0.086	-0.043	-0.15
13	18	1.974	1.972	0.086	0.002	0.01
14	15	2.307	2.349	0.159	-0.041	-0.16
15	20	2.019	1.972	0.086	0.047	0.17
16	13	1.791	1.857	0.221	-0.067	-0.33
17	16	1.996	1.595	0.159	0.401	1.59
18	14	3.755	3.494	0.221	0.260	1.30
19	19	1.936	1.972	0.086	-0.036	-0.13
20	17	1.982	1.972	0.086	0.010	0.04

R denotes an observation with a large standardized residual.

Estimated Regression Coefficients for BTEX yield using data in uncoded units

Term	Coef
Constant	8.20117
Temperature (°C)	-0.0529364
OCR	0.290472
Temperature (°C)*Temperature (°C)	0.000105576
Temperature (°C)*OCR	-9.94727E-04

Response Surface Regression: BTEX yield versus Temperature (°C), OCR

The analysis was done using coded units.

Estimated Regression Coefficients for BTEX yield

Term	Coef	SE Coef	T	P
Constant	1.9719	0.09275	21.260	0.000
Temperature (°C)	0.5012	0.08799	5.696	0.000
OCR	-0.2307	0.08799	-2.622	0.018
Temperature (°C)*Temperature (°C)	0.2639	0.08799	3.000	0.008

S = 0.321309   PRESS = 2.93079

R-Sq = 75.12%   R-Sq(pred) = 55.86%   R-Sq(adj) = 70.46%

Analysis of Variance for BTEX yield

Source	DF	Seq SS	Adj SS	Adj MS	F
Regression	3	4.9884	4.9884	1.66281	16.11
Linear	2	4.0596	4.0596	2.02978	19.66
Temperature (°C)	1	3.3498	3.3498	3.34976	32.45
OCR	1	0.7098	0.7098	0.70981	6.88
Square	1	0.9289	0.9289	0.92886	9.00
Temperature (°C)*Temperature (°C)	1	0.9289	0.9289	0.92886	9.00
Residual Error	16	1.6518	1.6518	0.10324	
Lack-of-Fit	5	0.6857	0.6857	0.13714	1.56
Pure Error	11	0.9661	0.9661	0.08783	
Total	19	6.6403			

Source	P
Regression	0.000
Linear	0.000
Temperature (°C)	0.000
OCR	0.018
Square	0.008
Temperature (°C)*Temperature (°C)	0.008
Residual Error	
Lack-of-Fit	0.250
Pure Error	
Total	

BTEX

Obs	StdOrder	yield	Fit	SE Fit	Residual	St Resid
1	10	1.925	1.972	0.093	-0.047	-0.15
2	6	3.793	2.968	0.147	0.825	2.89 R
3	5	1.933	1.965	0.147	-0.032	-0.11
4	7	1.749	1.504	0.147	0.245	0.86
5	12	1.980	1.972	0.093	0.008	0.03
6	8	1.986	2.506	0.147	-0.521	-1.82
7	2	2.458	2.968	0.147	-0.509	-1.78
8	1	1.785	1.965	0.147	-0.181	-0.63
9	11	1.994	1.972	0.093	0.022	0.07
10	3	1.481	1.504	0.147	-0.023	-0.08
11	4	2.186	2.506	0.147	-0.321	-1.12
12	9	1.929	1.972	0.093	-0.043	-0.14
13	18	1.974	1.972	0.093	0.002	0.01
14	15	2.307	2.349	0.171	-0.041	-0.15
15	20	2.019	1.972	0.093	0.047	0.15
16	13	1.791	1.857	0.238	-0.067	-0.31
17	16	1.996	1.595	0.171	0.401	1.47

18   14 3.755 3.494 0.238   0.260   1.21

19   19 1.936 1.972 0.093   -0.036   -0.12

20   17 1.982 1.972 0.093   0.010   0.03

R denotes an observation with a large standardized residual.

Estimated Regression Coefficients for BTEX yield using data in uncoded units

Term	Coef
Constant	12.0309
Temperature (°C)	-0.0638784
OCR	-0.0576821
Temperature (°C)*Temperature (°C)	0.000105576

B2: Raw DOE Minitab data for propylene aromatization

BENZENE:

Results for: NEW SI AL PROPYLENE REGRESSION.MTW

Factorial Fit: Benzene (% y versus Si/Al Ratio, Temperature , ...

Estimated Effects and Coefficients for Benzene (% yield) (coded units)

Term	Effect	Coef	SE Coef	T	P
Constant		2.3704	0.1605	14.77	0.000
Si/Al Ratio	-1.6924	-0.8462	0.1605	-5.27	0.003
Temperature (°C)	1.4179	0.7089	0.1605	4.42	0.007
Propylene concentration (%)	1.4080	0.7040	0.1605	4.39	0.007
Catalyst amount (g)	2.2892	1.1446	0.1605	7.13	0.001
Si/Al Ratio*Temperature (°C)	-0.3650	-0.1825	0.1605	-1.14	0.307
Si/Al Ratio* Propylene concentration (%)	-0.2015	-0.1007	0.1605	-0.63	0.558
Si/Al Ratio*Catalyst amount (g)	-0.3608	-0.1804	0.1605	-1.12	0.312
Temperature (°C)* Propylene concentration (%)	0.6331	0.3166	0.1605	1.97	0.106

Temperature (°C)*Catalyst amount (g)   0.5531   0.2766   0.1605   1.72 0.145

Propylene concentration (%)*   0.9847   0.4923   0.1605   3.07 0.028

  Catalyst amount (g)

S = 0.641884   PRESS = 21.0952

R-Sq = 96.47%   R-Sq(pred) = 63.86%   R-Sq(adj) = 89.41%

Analysis of Variance for Benzene (% yield) (coded units)

Source	DF	Seq SS	Adj SS	Adj MS	F	P
Main Effects	4	48.389	48.389	12.0974	29.36	0.001
2-Way Interactions	6	7.921	7.921	1.3202	3.20	0.111
Residual Error	5	2.060	2.060	0.4120		
Total	15	58.371				

Estimated Coefficients for Benzene (% yield) using data in uncoded units

Term	Coef
Constant	7.9287
Si/Al Ratio	0.111055
Temperature (°C)	-0.0159355
Propylene concentration (%)	-1.35940
Catalyst amount (g)	-8.72320
Si/Al Ratio*Temperature (°C)	-2.43346E-04
Si/Al Ratio*	-0.00373129
Propylene concentration (%)	
Si/Al Ratio*Catalyst amount (g)	-0.0300658
Temperature (°C)*	0.00351729
Propylene concentration (%)	
Temperature (°C)*Catalyst amount (g)	0.0138276
Propylene concentration (%)*	0.683785
Catalyst amount (g)	

Effects Pareto for Benzene (% yield)

Alias Structure

I

Si/Al Ratio

Temperature (°C)

Propylene concentration (%)

Catalyst amount (g)

Si/Al Ratio*Temperature (°C)

Si/Al Ratio*Propylene concentration (%)

Si/Al Ratio*Catalyst amount (g)

Temperature (°C)*Propylene concentration (%)

Temperature (°C)*Catalyst amount (g)

Propylene concentration (%)*Catalyst amount (g)

Factorial Fit: Benzene (% y versus Si/Al Ratio, Temperature , ...

Estimated Effects and Coefficients for Benzene (% yield) (coded units)

Term	Effect	Coef	SE Coef	T	P
Constant		2.3704	0.1953	12.14	0.000
Si/Al Ratio	-1.6924	-0.8462	0.1953	-4.33	0.001
Temperature (°C)	1.4179	0.7089	0.1953	3.63	0.005
Propylene concentration (%)	1.4080	0.7040	0.1953	3.60	0.005
Catalyst amount (g)	2.2892	1.1446	0.1953	5.86	0.000
Propylene concentration (%)*	0.9847	0.4923	0.1953	2.52	0.030
Catalyst amount (g)					

S = 0.781225   PRESS = 15.6240

R-Sq = 89.54%   R-Sq(pred) = 73.23%   R-Sq(adj) = 84.32%

Analysis of Variance for Benzene (% yield) (coded units)

Source	DF	Seq SS	Adj SS	Adj MS	F	P
Main Effects	4	48.389	48.389	12.0974	19.82	0.000
2-Way Interactions	1	3.878	3.878	3.8781	6.35	0.030
Residual Error	10	6.103	6.103	0.6103		
Total	15	58.371				

Unusual Observations for Benzene (% yield)

Benzene

Obs	StdOrder	(% yield)	Fit	SE Fit	Residual	St Resid
7	15	7.85981	6.26642	0.47840	1.59339	2.58R

R denotes an observation with a large standardized residual.

Estimated Coefficients for Benzene (% yield) using data in uncoded units

Term	Coef
Constant	-1.85493
Si/Al Ratio	-0.0564144
Temperature (°C)	0.0141786
Propylene concentration (%)	-0.019159
Catalyst amount (g)	-4.45505
Propylene concentration (%)*	0.683785
Catalyst amount (g)	

Effects Pareto for Benzene (% yield)

Alias Structure

I

Si/Al Ratio

Temperature (°C)

Propylene concentration (%)

Catalyst amount (g)

Propylene concentration (%)*Catalyst amount (g)

-----x-----

TOLUENE:

Results for: NEW SI AL PROPYLENE REGRESSION.MTW

Factorial Fit: Toluene (% y versus Si/Al Ratio, Temperature , ...

Estimated Effects and Coefficients for Toluene (% yield) (coded units)

Term	Effect	Coef	SE Coef	T	P
Constant		7.668	0.2760	27.78	0.000
Si/Al Ratio	-4.567	-2.283	0.2760	-8.27	0.000
Temperature (°C)	1.902	0.951	0.2760	3.45	0.018
Propylene concentration (%)	2.616	1.308	0.2760	4.74	0.005
Catalyst amount (g)	5.401	2.700	0.2760	9.78	0.000
Si/Al Ratio*Temperature (°C)	-0.094	-0.047	0.2760	-0.17	0.871
Si/Al Ratio*	0.790	0.395	0.2760	1.43	0.212
Propylene concentration (%)					
Si/Al Ratio*Catalyst amount (g)	0.320	0.160	0.2760	0.58	0.587
Temperature (°C)*	0.202	0.101	0.2760	0.37	0.729
Propylene concentration (%)					
Temperature (°C)*Catalyst amount (g)	0.407	0.204	0.2760	0.74	0.494
Propylene concentration (%)*	1.546	0.773	0.2760	2.80	0.038
Catalyst amount (g)					

S = 1.10395   PRESS = 62.3977

R-Sq = 97.67%   R-Sq(pred) = 76.13%   R-Sq(adj) = 93.01%

Analysis of Variance for Toluene (% yield) (coded units)

Source	DF	Seq SS	Adj SS	Adj MS	F	P
Main Effects	4	241.962	241.962	60.491	49.64	0.000
2-Way Interactions	6	13.337	13.337	2.223	1.82	0.263
Residual Error	5	6.094	6.094	1.219		
Total	15	261.393				

Unusual Observations for Toluene (% yield)

Toluene

Obs	StdOrder	(% yield)	Fit	SE Fit	Residual	St Resid
9	9	10.9614	9.7049	0.9153	1.2566	2.04R

R denotes an observation with a large standardized residual.

Estimated Coefficients for Toluene (% yield) using data in uncoded units

Term	Coef
Constant	21.6156
Si/Al Ratio	-0.296636
Temperature (°C)	0.0049693
Propylene concentration (%)	-1.37465
Catalyst amount (g)	-11.0552
Si/Al Ratio*Temperature (°C)	-6.27597E-05
Si/Al Ratio*	0.0146376
Propylene concentration (%)	
Si/Al Ratio*Catalyst amount (g)	0.0267077
Temperature (°C)*	0.00112372
Propylene concentration (%)	
Temperature (°C)*Catalyst amount (g)	0.0101773
Propylene concentration (%)*	1.07388
Catalyst amount (g)	

Effects Pareto for Toluene (% yield)

Alias Structure

I

Si/Al Ratio

Temperature (°C)

Propylene concentration (%)

Catalyst amount (g)

Si/Al Ratio*Temperature (°C)

Si/Al Ratio*Propylene concentration (%)

Si/Al Ratio*Catalyst amount (g)

Temperature (°C)*Propylene concentration (%)

Temperature (°C)*Catalyst amount (g)

Propylene concentration (%)*Catalyst amount (g)

Factorial Fit: Toluene (% y versus Si/Al Ratio, Temperature , ...

Estimated Effects and Coefficients for Toluene (% yield) (coded units)

Term	Effect	Coef	SE Coef	T	P
Constant		7.668	0.2483	30.88	0.000
Si/Al Ratio	-4.567	-2.283	0.2483	-9.20	0.000
Temperature (°C)	1.902	0.951	0.2483	3.83	0.003
Propylene concentration (%)	2.616	1.308	0.2483	5.27	0.000
Catalyst amount (g)	5.401	2.700	0.2483	10.88	0.000
Propylene concentration (%)*	1.546	0.773	0.2483	3.11	0.011
Catalyst amount (g)					

S = 0.993253   PRESS = 25.2557

R-Sq = 96.23%   R-Sq(pred) = 90.34%   R-Sq(adj) = 94.34%

Analysis of Variance for Toluene (% yield) (coded units)

Source	DF	Seq SS	Adj SS	Adj MS	F	P
Main Effects	4	241.962	241.962	60.4905	61.32	0.000
2-Way Interactions	1	9.565	9.565	9.5653	9.70	0.011
Residual Error	10	9.866	9.866	0.9866		
Total	15	261.393				

Unusual Observations for Toluene (% yield)

Toluene

Obs	StdOrder	(% yield)	Fit	SE Fit	Residual	St Resid
16	13	12.0925	13.7822	0.6082	-1.6897	-2.15R

R denotes an observation with a large standardized residual.

Estimated Coefficients for Toluene (% yield) using data in uncoded units

Term	Coef
Constant	4.07075
Si/Al Ratio	-0.152231
Temperature (°C)	0.0190200
Propylene concentration (%)	0.082470
Catalyst amount (g)	-4.73936
Propylene concentration (%)*	1.07388
Catalyst amount (g)	

Effects Pareto for Toluene (% yield)

Alias Structure

I

Si/Al Ratio

Temperature (°C)

Propylene concentration (%)

Catalyst amount (g)

Propylene concentration (%)*Catalyst amount (g)

-------X----------------

P-XYLENE

Results for: NEW SI AL PROPYLENE REGRESSION.MTW

Factorial Fit: p-xylene (% versus Si/Al Ratio, Temperature , ...

Estimated Effects and Coefficients for p-xylene (% yield) (coded units)

Term	Effect	Coef	SE Coef	T	P
Constant		5.466	0.1858	29.42	0.000
Si/Al Ratio	-2.286	-1.143	0.1858	-6.15	0.002
Temperature (°C)	0.012	0.006	0.1858	0.03	0.975
Propylene concentration (%)	0.578	0.289	0.1858	1.56	0.181
Catalyst amount (g)	2.212	1.106	0.1858	5.95	0.002
Si/Al Ratio*Temperature (°C)	0.384	0.192	0.1858	1.03	0.349
Si/Al Ratio*	1.165	0.582	0.1858	3.13	0.026
Propylene concentration (%)					
Si/Al Ratio*Catalyst amount (g)	0.923	0.461	0.1858	2.48	0.056
Temperature (°C)*	-0.206	-0.103	0.1858	-0.55	0.604
Propylene concentration (%)					
Temperature (°C)*Catalyst amount (g)	0.056	0.028	0.1858	0.15	0.885
Propylene concentration (%)*	0.333	0.166	0.1858	0.90	0.412
Catalyst amount (g)					

S = 0.743012   PRESS = 28.2658

R-Sq = 94.95%   R-Sq(pred) = 48.24%   R-Sq(adj) = 84.84%

Analysis of Variance for p-xylene (% yield) (coded units)

Source	DF	Seq SS	Adj SS	Adj MS	F	P
Main Effects	4	41.808	41.808	10.4521	18.93	0.003
2-Way Interactions	6	10.043	10.043	1.6738	3.03	0.122
Residual Error	5	2.760	2.760	0.5521		
Total	15	54.612				

Estimated Coefficients for p-xylene (% yield) using data in uncoded units

Term	Coef
Constant	28.8270
Si/Al Ratio	-0.468206
Temperature (°C)	-0.0051229
Propylene concentration (%)	-0.86557
Catalyst amount (g)	-5.33854
Si/Al Ratio*Temperature (°C)	0.000255862
Si/Al Ratio* Propylene concentration (%)	0.0215660
Si/Al Ratio*Catalyst amount (g)	0.0768755
Temperature (°C)* Propylene concentration (%)	-0.00114297
Temperature (°C)*Catalyst amount (g)	0.00141048
Propylene concentration (%)* Catalyst amount (g)	0.231050

Effects Pareto for p-xylene (% yield)

Alias Structure

I

Si/Al Ratio

Temperature (°C)

Propylene concentration (%)

Catalyst amount (g)

Si/Al Ratio*Temperature (°C)

Si/Al Ratio*Propylene concentration (%)

Si/Al Ratio*Catalyst amount (g)

Temperature (°C)*Propylene concentration (%)

Temperature (°C)*Catalyst amount (g)

Propylene concentration (%)*Catalyst amount (g)

Factorial Fit: p-xylene (% versus Si/Al Ratio, Propylene co, ...

Estimated Effects and Coefficients for p-xylene (% yield) (coded units)

Term	Effect	Coef	SE Coef	T	P
Constant		5.466	0.2048	26.69	0.000
Si/Al Ratio	-2.286	-1.143	0.2048	-5.58	0.000
Propylene concentration (%)	0.578	0.289	0.2048	1.41	0.186
Catalyst amount (g)	2.212	1.106	0.2048	5.40	0.000
Si/Al Ratio*	1.165	0.582	0.2048	2.84	0.016

 Propylene concentration (%)

S = 0.819037   PRESS = 15.6119

R-Sq = 86.49%   R-Sq(pred) = 71.41%   R-Sq(adj) = 81.57%

Analysis of Variance for p-xylene (% yield) (coded units)

Source	DF	Seq SS	Adj SS	Adj MS	F	P
Main Effects	3	41.808	41.808	13.9359	20.77	0.000
2-Way Interactions	1	5.425	5.425	5.4248	8.09	0.016
Residual Error	11	7.379	7.379	0.6708		
Lack of Fit	3	6.361	6.361	2.1202	16.65	0.001
Pure Error	8	1.018	1.018	0.1273		
Total	15	54.612				

Estimated Coefficients for p-xylene (% yield) using data in uncoded units

Term	Coef
Constant	22.0402

Si/Al Ratio   -0.306943

Propylene concentration (%)   -1.24127

Catalyst amount (g)   2.76532

Si/Al Ratio*   0.0215660

  Propylene concentration (%)

Effects Pareto for p-xylene (% yield)

Alias Structure

I

Si/Al Ratio

Propylene concentration (%)

Catalyst amount (g)

Si/Al Ratio*Propylene concentration (%)

------X------

O-XYLENE

Results for: NEW SI AL PROPYLENE REGRESSION.MTW

Factorial Fit: o-xylene (% versus Si/Al Ratio, Temperature , ...

Estimated Effects and Coefficients for o-xylene (% yield) (coded units)

Term	Effect	Coef	SE Coef	T	P
Constant		1.3362	0.04934	27.08	0.000
Si/Al Ratio	-0.6280	-0.3140	0.04934	-6.36	0.001
Temperature (°C)	0.2690	0.1345	0.04934	2.73	0.041
Propylene concentration (%)	0.0337	0.0168	0.04934	0.34	0.747
Catalyst amount (g)	0.5618	0.2809	0.04934	5.69	0.002
Si/Al Ratio*Temperature (°C)	0.0817	0.0409	0.04934	0.83	0.445
Si/Al Ratio*	0.3258	0.1629	0.04934	3.30	0.021
Propylene concentration (%)					
Si/Al Ratio*Catalyst amount (g)	0.2070	0.1035	0.04934	2.10	0.090
Temperature (°C)*	-0.0434	-0.0217	0.04934	-0.44	0.679

Propylene concentration (%)

Temperature (°C)*Catalyst amount (g)   0.0299   0.0150   0.04934   0.30   0.774

Propylene concentration (%)*   0.0700   0.0350   0.04934   0.71   0.510

 Catalyst amount (g)

S = 0.197354   PRESS = 1.99418

R-Sq = 95.11%   R-Sq(pred) = 49.92%   R-Sq(adj) = 85.33%

Analysis of Variance for o-xylene (% yield) (coded units)

Source	DF	Seq SS	Adj SS	Adj MS	F	P
Main Effects	4	3.1341	3.1341	0.78353	20.12	0.003
2-Way Interactions	6	0.6535	0.6535	0.10892	2.80	0.139
Residual Error	5	0.1947	0.1947	0.03895		
Total	15	3.9823				

Estimated Coefficients for o-xylene (% yield) using data in uncoded units

Term	Coef
Constant	6.78236
Si/Al Ratio	-0.120369
Temperature (°C)	0.00127680
Propylene concentration (%)	-0.303618
Catalyst amount (g)	-1.27603
Si/Al Ratio*Temperature (°C)	5.44948E-05
Si/Al Ratio*	0.00603392
Propylene concentration (%)	
Si/Al Ratio*Catalyst amount (g)	0.0172492
Temperature (°C)*	-2.40911E-04
Propylene concentration (%)	
Temperature (°C)*Catalyst amount (g)	0.00074829
Propylene concentration (%)*	0.0486306
Catalyst amount (g)	

Effects Pareto for o-xylene (% yield)

Alias Structure

I

Si/Al Ratio

Temperature (°C)

Propylene concentration (%)

Catalyst amount (g)

Si/Al Ratio*Temperature (°C)

Si/Al Ratio*Propylene concentration (%)

Si/Al Ratio*Catalyst amount (g)

Temperature (°C)*Propylene concentration (%)

Temperature (°C)*Catalyst amount (g)

Propylene concentration (%)*Catalyst amount (g)

Factorial Fit: o-xylene (% versus Si/Al Ratio, Temperature , ...

Estimated Effects and Coefficients for o-xylene (% yield) (coded units)

Term	Effect	Coef	SE Coef	T	P
Constant		1.3362	0.05145	25.97	0.000
Si/Al Ratio	-0.6280	-0.3140	0.05145	-6.10	0.000
Temperature (°C)	0.2690	0.1345	0.05145	2.61	0.026
Propylene concentration (%)	0.0337	0.0168	0.05145	0.33	0.750
Catalyst amount (g)	0.5618	0.2809	0.05145	5.46	0.000
Si/Al Ratio*	0.3258	0.1629	0.05145	3.17	0.010

 Propylene concentration (%)

S = 0.205808   PRESS = 1.08434

R-Sq = 89.36%   R-Sq(pred) = 72.77%   R-Sq(adj) = 84.05%

Analysis of Variance for o-xylene (% yield) (coded units)

Source	DF	Seq SS	Adj SS	Adj MS	F	P

Main Effects   4 3.1341 3.1341 0.78353 18.50 0.000

2-Way Interactions   1 0.4247 0.4247 0.42467 10.03 0.010

Residual Error   10 0.4236 0.4236 0.04236

Total   15 3.9823

Unusual Observations for o-xylene (% yield)

         o-xylene

Obs StdOrder (% yield)   Fit   SE Fit Residual St Resid

  1   16   1.98147 1.61731 0.12603 0.36416   2.24R

R denotes an observation with a large standardized residual.

Estimated Coefficients for o-xylene (% yield) using data in uncoded units

Term	Coef
Constant	5.16141
Si/Al Ratio	-0.0854968
Temperature (°C)	0.00269019
Propylene concentration (%)	-0.382850
Catalyst amount (g)	0.702248
Si/Al Ratio*	0.00603392
Propylene concentration (%)	

Effects Pareto for o-xylene (% yield)

Alias Structure

I

Si/Al Ratio

Temperature (°C)

Propylene concentration (%)

Catalyst amount (g)

Si/Al Ratio*Propylene concentration (%)

-----X-----

TOTAL BTX:

Results for: NEW SI AL PROPYLENE REGRESSION.MTW

Factorial Fit: Total BTX (% versus Si/Al Ratio, Temperature , ...

Estimated Effects and Coefficients for Total BTX (% yield) (coded units)

Term	Effect	Coef	SE Coef	T	P
Constant		16.840	0.5104	33.00	0.000
Si/Al Ratio	-9.173	-4.586	0.5104	-8.99	0.000
Temperature (°C)	3.601	1.801	0.5104	3.53	0.017
Propylene concentration (%)	4.636	2.318	0.5104	4.54	0.006
Catalyst amount (g)	10.464	5.232	0.5104	10.25	0.000
Si/Al Ratio*Temperature (°C)	0.006	0.003	0.5104	0.01	0.995
Si/Al Ratio*	2.079	1.040	0.5104	2.04	0.097
Propylene concentration (%)					
Si/Al Ratio*Catalyst amount (g)	1.089	0.545	0.5104	1.07	0.335
Temperature (°C)*	0.586	0.293	0.5104	0.57	0.591
Propylene concentration (%)					
Temperature (°C)*Catalyst amount (g)	1.047	0.523	0.5104	1.03	0.352
Propylene concentration (%)*	2.934	1.467	0.5104	2.87	0.035
Catalyst amount (g)					

S = 2.04142   PRESS = 213.370

R-Sq = 97.91%   R-Sq(pred) = 78.57%   R-Sq(adj) = 93.72%

Analysis of Variance for Total BTX (% yield) (coded units)

Source	DF	Seq SS	Adj SS	Adj MS	F	P
Main Effects	4	912.42	912.42	228.104	54.74	0.000
2-Way Interactions	6	62.22	62.22	10.371	2.49	0.168
Residual Error	5	20.84	20.84	4.167		
Total	15	995.48				

Estimated Coefficients for Total BTX (% yield) using data in uncoded units

Term	Coef
Constant	65.1537
Si/Al Ratio	-0.774156

155

Temperature (°C)   -0.0148123

Propylene concentration (%)   -3.90324

Catalyst amount (g)   -26.3929

Si/Al Ratio*Temperature (°C)   0.000004252

Si/Al Ratio*   0.0385062

  Propylene concentration (%)

Si/Al Ratio*Catalyst amount (g)   0.0907665

Temperature (°C)*   0.00325713

  Propylene concentration (%)

Temperature (°C)*Catalyst amount (g)   0.0261637

Propylene concentration (%)*   2.03735

  Catalyst amount (g)

Effects Pareto for Total BTX (% yield)

Alias Structure

I

Si/Al Ratio

Temperature (°C)

Propylene concentration (%)

Catalyst amount (g)

Si/Al Ratio*Temperature (°C)

Si/Al Ratio*Propylene concentration (%)

Si/Al Ratio*Catalyst amount (g)

Temperature (°C)*Propylene concentration (%)

Temperature (°C)*Catalyst amount (g)

Propylene concentration (%)*Catalyst amount (g)

Factorial Fit: Total BTX (% versus Si/Al Ratio, Temperature , ...

Estimated Effects and Coefficients for Total BTX (% yield) (coded units)

Term	Effect	Coef	SE Coef	T	P
Constant		16.840	0.5513	30.54	0.000
Si/Al Ratio	-9.173	-4.586	0.5513	-8.32	0.000
Temperature (°C)	3.601	1.801	0.5513	3.27	0.008
Propylene concentration (%)	4.636	2.318	0.5513	4.20	0.002
Catalyst amount (g)	10.464	5.232	0.5513	9.49	0.000
Propylene concentration (%)*	2.934	1.467	0.5513	2.66	0.024
Catalyst amount (g)					

S = 2.20529   PRESS = 124.500

R-Sq = 95.11%   R-Sq(pred) = 87.49%   R-Sq(adj) = 92.67%

Analysis of Variance for Total BTX (% yield) (coded units)

Source	DF	Seq SS	Adj SS	Adj MS	F	P
Main Effects	4	912.42	912.42	228.104	46.90	0.000
2-Way Interactions	1	34.43	34.43	34.428	7.08	0.024
Residual Error	10	48.63	48.63	4.863		
Total	15	995.48				

Unusual Observations for Total BTX (% yield)

Total BTX

Obs	StdOrder	(% yield)	Fit	SE Fit	Residual	St Resid
16	13	24.7287	28.6429	1.3505	-3.9142	-2.25R

R denotes an observation with a large standardized residual.

Estimated Coefficients for Total BTX (% yield) using data in uncoded units

Term	Coef
Constant	11.9611
Si/Al Ratio	-0.305766
Temperature (°C)	0.0360136
Propylene concentration (%)	0.065377

Catalyst amount (g)   -8.71944

Propylene concentration (%)*   2.03735

 Catalyst amount (g)

Effects Pareto for Total BTX (% yield)

Alias Structure

I

Si/Al Ratio

Temperature (°C)

Propylene concentration (%)

Catalyst amount (g)

Propylene concentration (%)*Catalyst amount (g)

Results for: SI AL PROPYLENE REGRESSION CONVERSION PROPYLENE

DATA.MTW

Factorial Fit: Propylene co versus Si/Al Ratio, Temperature , ...

Estimated Effects and Coefficients for Propylene conversion (%) (coded units)

Term	Effect	Coef
Constant		66.938
Si/Al Ratio	-6.375	-3.188
Temperature (°C)	-13.625	-6.813
Propylene concentration (%)	2.375	1.187
Catalyst amount (g)	7.375	3.687
Si/Al Ratio*Temperature (°C)	-5.875	-2.938
Si/Al Ratio*	2.125	1.062

 Propylene concentration (%)

Si/Al Ratio*Catalyst amount (g)   8.125   4.063

Temperature (°C)*   1.375   0.688

  Propylene concentration (%)

Temperature (°C)*Catalyst amount (g)   3.875   1.937

Propylene concentration (%)*   -2.125 -1.063

  Catalyst amount (g)

Si/Al Ratio*Temperature (°C)*   0.125   0.062

  Propylene concentration (%)

Si/Al Ratio*Temperature (°C)*   1.625   0.812

  Catalyst amount (g)

Si/Al Ratio*   -0.375 -0.187

  Propylene concentration (%)*

  Catalyst amount (g)

Temperature (°C)*   -0.125 -0.063

  Propylene concentration (%)*

  Catalyst amount (g)

Si/Al Ratio*Temperature (°C)*   -0.375 -0.188

  Propylene concentration (%)*

  Catalyst amount (g)

S = *   PRESS = *

Analysis of Variance for Propylene conversion (%) (coded units)

Source	DF	Seq SS	Adj SS	Adj MS	F	P
Main Effects	4	1145.25	1145.25	286.312	*	*
2-Way Interactions	6	505.88	505.88	84.313	*	*
3-Way Interactions	4	11.25	11.25	2.812	*	*
4-Way Interactions	1	0.56	0.56	0.563	*	*
Residual Error	0	*	*	*		
Total	15	1662.94				

Estimated Coefficients for Propylene conversion (%) using data in uncoded units

Term	Coef
Constant	7.18519
Si/Al Ratio	2.56852
Temperature (°C)	0.250046
Propylene concentration (%)	1.85185
Catalyst amount (g)	104.861
Si/Al Ratio*Temperature (°C)	-0.00826620
Si/Al Ratio* Propylene concentration (%)	-0.0648148
Si/Al Ratio*Catalyst amount (g)	-2.02778
Temperature (°C)* Propylene concentration (%)	-0.00787037
Temperature (°C)*Catalyst amount (g)	-0.302083
Propylene concentration (%)* Catalyst amount (g)	-9.72222
Si/Al Ratio*Temperature (°C)* Propylene concentration (%)	0.000254630
Si/Al Ratio*Temperature (°C)* Catalyst amount (g)	0.00642361
Si/Al Ratio* Propylene concentration (%)* Catalyst amount (g)	0.138889
Temperature (°C)* Propylene concentration (%)* Catalyst amount (g)	0.0208333
Si/Al Ratio*Temperature (°C)* Propylene concentration (%)* Catalyst amount (g)	-3.47222E-04

Effects Pareto for Propylene conversion (%)

Alias Structure

I

Si/Al Ratio

Temperature (°C)

Propylene concentration (%)

Catalyst amount (g)

Si/Al Ratio*Temperature (°C)

Si/Al Ratio*Propylene concentration (%)

Si/Al Ratio*Catalyst amount (g)

Temperature (°C)*Propylene concentration (%)

Temperature (°C)*Catalyst amount (g)

Propylene concentration (%)*Catalyst amount (g)

Si/Al Ratio*Temperature (°C)*Propylene concentration (%)

Si/Al Ratio*Temperature (°C)*Catalyst amount (g)

Si/Al Ratio*Propylene concentration (%)*Catalyst amount (g)

Temperature (°C)*Propylene concentration (%)*Catalyst amount (g)

Si/Al Ratio*Temperature (°C)*Propylene concentration (%)*Catalyst amount (g)

* NOTE * Could not graph the specified residual type because MSE = 0 or the

  degrees of freedom for error = 0.

Factorial Fit: Propylene co versus Si/Al Ratio, Temperature , ...

Estimated Effects and Coefficients for Propylene conversion (%) (coded units)

Term	Effect	Coef	SE Coef	T	P
Constant		66.938	0.3843	174.20	0.000
Si/Al Ratio	-6.375	-3.188	0.3843	-8.30	0.000
Temperature (°C)	-13.625	-6.813	0.3843	-17.73	0.000
Propylene concentration (%)	2.375	1.187	0.3843	3.09	0.027

Catalyst amount (g)   7.375 3.687 0.3843 9.60 0.000

Si/Al Ratio*Temperature (°C)   -5.875 -2.938 0.3843 -7.64 0.001

Si/Al Ratio*   2.125 1.062 0.3843 2.77 0.040

  Propylene concentration (%)

Si/Al Ratio*Catalyst amount (g)   8.125 4.063 0.3843 10.57 0.000

Temperature (°C)*   1.375 0.688 0.3843 1.79 0.134

  Propylene concentration (%)

Temperature (°C)*Catalyst amount (g)   3.875 1.937 0.3843 5.04 0.004

Propylene concentration (%)*   -2.125 -1.063 0.3843 -2.77 0.040

  Catalyst amount (g)

S = 1.53704   PRESS = 120.96

R-Sq = 99.29%   R-Sq(pred) = 92.73%   R-Sq(adj) = 97.87%

Analysis of Variance for Propylene conversion (%) (coded units)

Source	DF	Seq SS	Adj SS	Adj MS	F	P
Main Effects	4	1145.25	1145.25	286.312	121.19	0.000
2-Way Interactions	6	505.88	505.88	84.313	35.69	0.001
Residual Error	5	11.81	11.81	2.362		
Total	15	1662.94				

Estimated Coefficients for Propylene conversion (%) using data in uncoded units

Term	Coef
Constant	122.149
Si/Al Ratio	0.722685
Temperature (°C)	-0.0215278
Propylene concentration (%)	-4.45023
Catalyst amount (g)	-62.5955
Si/Al Ratio*Temperature (°C)	-0.00391667
Si/Al Ratio*	0.0393519
Propylene concentration (%)	
Si/Al Ratio*Catalyst amount (g)	0.677083
Temperature (°C)*	0.00763889

Propylene concentration (%)

Temperature (°C)*Catalyst amount (g)   0.0968750

Propylene concentration (%)*   -1.47569

  Catalyst amount (g)

Effects Pareto for Propylene conversion (%)

Alias Structure

I

Si/Al Ratio

Temperature (°C)

Propylene concentration (%)

Catalyst amount (g)

Si/Al Ratio*Temperature (°C)

Si/Al Ratio*Propylene concentration (%)

Si/Al Ratio*Catalyst amount (g)

Temperature (°C)*Propylene concentration (%)

Temperature (°C)*Catalyst amount (g)

Propylene concentration (%)*Catalyst amount (g)

Factorial Fit: Propylene co versus Si/Al Ratio, Temperature , ...

Estimated Effects and Coefficients for Propylene conversion (%) (coded units)

Term	Effect	Coef	SE Coef	T	P
Constant		66.938	0.4492	149.00	0.000
Si/Al Ratio	-6.375	-3.188	0.4492	-7.10	0.000
Temperature (°C)	-13.625	-6.813	0.4492	-15.16	0.000
Propylene concentration (%)	2.375	1.187	0.4492	2.64	0.038
Catalyst amount (g)	7.375	3.687	0.4492	8.21	0.000
Si/Al Ratio*Temperature (°C)	-5.875	-2.938	0.4492	-6.54	0.001

163

Si/Al Ratio*   2.125   1.062   0.4492   2.37 0.056

  Propylene concentration (%)

Si/Al Ratio*Catalyst amount (g)   8.125   4.063   0.4492   9.04 0.000

Temperature (°C)*Catalyst amount (g)   3.875   1.938   0.4492   4.31 0.005

Propylene concentration (%)*   -2.125 -1.063   0.4492 -2.37 0.056

  Catalyst amount (g)

S = 1.79699   PRESS = 137.778

R-Sq = 98.83%   R-Sq(pred) = 91.71%   R-Sq(adj) = 97.09%

Analysis of Variance for Propylene conversion (%) (coded units)

Source	DF	Seq SS	Adj SS	Adj MS	F	P
Main Effects	4	1145.25	1145.25	286.312	88.66	0.000
2-Way Interactions	5	498.31	498.31	99.663	30.86	0.000
Residual Error	6	19.37	19.37	3.229		
Total	15	1662.94				

Estimated Coefficients for Propylene conversion (%) using data in uncoded units

Term	Coef
Constant	85.3675
Si/Al Ratio	0.722685
Temperature (°C)	0.0602083
Propylene concentration (%)	-1.01273
Catalyst amount (g)	-62.5955
Si/Al Ratio*Temperature (°C)	-0.00391667
Si/Al Ratio*	0.0393519
Propylene concentration (%)	
Si/Al Ratio*Catalyst amount (g)	0.677083
Temperature (°C)*Catalyst amount (g)	0.0968750
Propylene concentration (%)*	-1.47569
Catalyst amount (g)	

Effects Pareto for Propylene conversion (%)

Alias Structure

I

Si/Al Ratio

Temperature (°C)

Propylene concentration (%)

Catalyst amount (g)

Si/Al Ratio*Temperature (°C)

Si/Al Ratio*Propylene concentration (%)

Si/Al Ratio*Catalyst amount (g)

Temperature (°C)*Catalyst amount (g)

Propylene concentration (%)*Catalyst amount (g)

APPENDIX C: ADDITIONAL EXPERIMENTAL RUNS AND DATA

C1: Aromatization of α-olefins

A set of preliminary experiments were performed to study the feasibility of catalytic reforming of α-olefins. Four model compounds, 1-hexene, 1-octene, 1-decene and 1-tetradecene were chosen and experiments were conducted by using zeolite catalysts, as shown in Table 17. For all the experiments, the amount of feed olefin was kept constant at 200 mL and the effects of three factors, reaction temperature, reaction time and catalyst amount, was studied.

It was observed that significant amounts of aromatic compounds were produced in each experiment. These include light aromatics like benzene, toluene, ethylbenzene, p-xylene and o-xylene. P-xylene is the major individual aromatic compound among all the aromatics produced. When the levels of the reaction conditions were changed, the product distribution also changed. This suggests that the amount of a particular individual aromatic compound could be controlled by changing the reaction conditions. From the results of preliminary reforming reactions of model compounds, it can be concluded that C6 - C14 α-olefins can be aromatized by zeolite catalysts and HZSM-5 catalyst yields more aromatics than zeolite beta.

Apart from liquid reformates, certain larger amounts of gaseous products, coke and solids were also produced during the α-olefin catalytic reforming reactions, hence there was a need to quantify them. 1-hexene, alone was easily converted into light aromatics (BTEX) and 1-tetradecene was found to be difficult to aromatize and hence further aromatization experiments were conducted to convert it into BTEX by using HZSM-5 as a catalyst.

Table 17. Preliminary catalytic reforming experimental conditions for α-olefins study

Experiment Numbers	Olefins	Temperature (°C)	Time (min.)	Catalyst amount (g) and type
1	Octene	400	60	7 (HZSM-5)
2	1-Octene	300	30	5 (Zeolite beta)
3	1-Decene	400	15	5 (HZSM-5)
4	1-Decene	350	5	7 (HZSM-5)
5	1-Decene	400	5	5 (HZSM-5)
6	1-Tetradecene	400	5	5 (HZSM-5)
7	1-Hexene	400	30	5 (HZSM-5)
8	1-Hexene+1-tetradecene	400	30	5 (HZSM-5)
9	1-Hexene+1-Octene	350	15	5 (Zeolite beta)
10	1-Hexene+1-Decene	425	15	5 (HZSM-5)
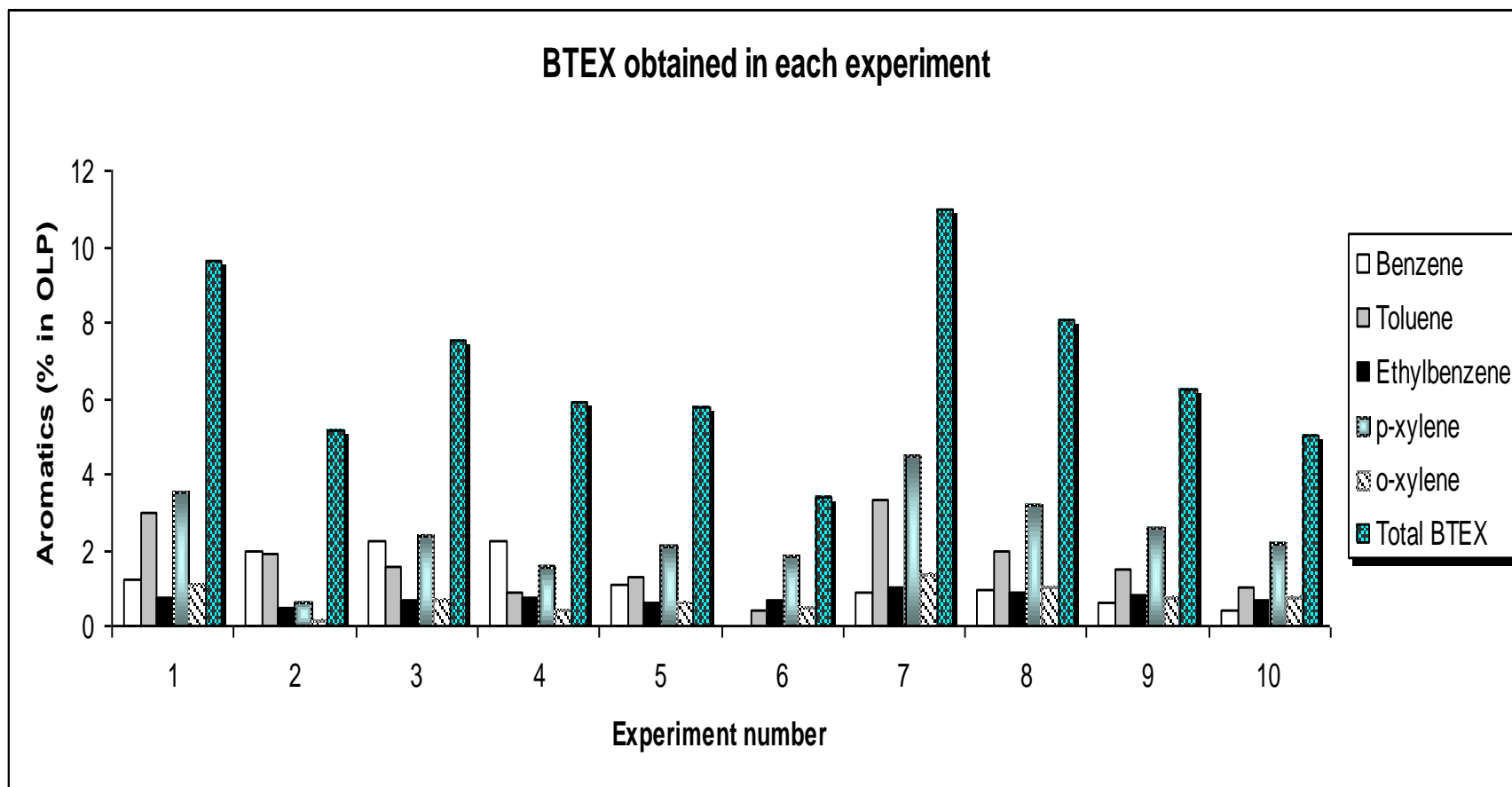
Figure 29. Results of preliminary catalytic reforming experiments performed on α-olefins.

C2: Catalytic conversion of thermally cracked crop (soybean) oil

Optimization of the reaction conditions for liquid, coke and gas yields during the catalytic conversion of cracked crop oil over zeolite catalyst

Design of experiments (DOE) techniques were used for the optimization of reaction conditions for the zeolite catalysis of cracked crop oil. A full factorial design analysis allows one to obtain a basic knowledge of the effects of reaction conditions and their statistical significance.

A two-level, three-factor full-factorial design was set up to determine which factors influence each response. The three factors were the reaction temperature (A) in ºC, OLP to catalyst ratio (OCR) designated as B, Reaction time (C) in minutes. The responses measured were the % yields of liquids, coke/solids and gases. Yields were determined by dividing the final weights of product responses by the mass of OLP fed to the reactor. The design was unreplicated and the order of experiments was randomized. Experimental noise was quantified using the method developed by Lenth [127]. This method assumes that three-way interactions are not significant and uses these to estimate the standard error. Hence, only individual factors and their two-way interactions were considered for analysis.

Response Surface Methodology (RSM) consisting of a Central Composite Design (CCD) was used for obtaining and processing the statistical experimental data.

Low and high levels were selected and coded into -1 and +1 whereas center points of the factors were calculated by using a formula: [(high level-low level)/2] and coded as 0. Results of experiments conducted at the center point levels were used for testing the

presence or absence of curvature in the statistical model. If there was a presence of a significant curvature, then a quadratic model was proposed instead of a linear one. The number of reaction factors in the factorial part of a CCD determined the alpha values correspond to the star points [128].

A larger absolute value for an effect indicates that it has a greater impact on the response. To evaluate the statistical significance of effects of various factors, a two-sample t-test using the means at the high and low settings was performed and a probability value (p-value) was calculated. For the effect to be statistically significant at a 95% confidence level, the p-value should be less than or equal to 0.05.

The ability to determine interactions is the major benefit of using a factorial DOE approach. An interaction occurs when the effect of one factor depends on the value of one of the other factors. The magnitude of an interaction is defined as one-half of the difference between the effect of a factor at the high value of a second factor and the effect of the first factor at the low value of the second factor. For this analysis, the statistical software package, MINITAB^{TM} 15, was used as an analysis tool to obtain main effects and interactions and to create Pareto, interaction, and other charts for interpretation.

Aromatization of OLP over HZSM-5 with a Silica:Alumina ratio of 50

A 2-level, 3-factor, full factorial experimental design was used to study the feasibility of aromatizing soybean oil OLP. The low and high values of the factors are shown in Table 18.

Table 18. Factors used to study OLP aromatization with their low and high values

Factors	Low	High
Temperature (ºC)	300	325
OLP to catalyst ratio (OCR)	5	10
Time (Min.)	20	60

All the OLP aromatization experiments were randomized and conducted using the full factorial experimental design. It was observed that the liquid reformates contained viscous (high molecular weight) compounds. The gluey (sticky) nature of these liquid products might possibly be because of polymeric tar formation during the reforming step. Liquids of high viscosity were non-elutable in GC. Hence, the liquid reformates were distilled up to 300 ºC and these distilled samples were analyzed by GC-FID. The concentrations of aromatic compounds were measured in the volume % of liquid reformates. The results obtained are shown in Table 19.

Table 19. List of preliminary experiments consisting of the reaction conditions and BTEX concentrations in the liquid products

Run	Temp. (ºC)	OCR	Time (Min.)	Benzene (%)	Toluene (%)	Ethylbenzene (%)	p-xylene (%)	o-xylene (%)	Total BTEX (%)
1	300	10	60	0.2492	1.271	0.9424	0.9852	0.8451	4.293
2	325	10	20	0.3368	1.614	1.127	1.554	0.9927	5.626
3	300	5	60	0.7668	4.182	2.101	6.451	2.005	15.50
4	300	5	20	0.2989	1.544	1.096	1.559	0.9750	5.474
5	325	5	20	0.6822	3.005	1.694	4.360	1.466	11.20
6	325	10	60	0.3605	1.732	1.176	1.988	1.028	6.285
7	300	10	20	0.2504	1.234	0.9095	0.8749	0.8252	4.094
8	325	5	60	0.9609	5.746	2.415	8.256	2.584	19.96

Changing the levels of a few reaction factors helped in generating higher amounts of aromatics even at a lower temperature. The results for gaseous products (% yield), liquid reformate (% yield) and coke/solids (% yield) are shown in Table 20.

Table 20. Gases, liquids and coke and solid product yields after OLP conversion

Run	Temperature (°C)	OLP to catalyst ratio	Time (min.)	Gases (% yield)	Liquid reformate (% yield)	Coke/solids (% yield)
1	300	10	60	5.572	87.33	7.097
2	300	5	20	25.60	64.49	9.902
3	300	5	60	29.24	63.91	6.840
4	300	10	20	5.080	87.82	7.097
5	325	5	60	51.70	39.80	8.500
6	325	10	20	6.550	86.95	6.500
7	325	10	60	10.49	81.53	7.980
8	325	5	20	38.10	53.28	8.620

Table 20 shows that the yields of coke/solids and gaseous products were fairly high at the reaction conditions at which higher aromatics concentration was observed. This leads to the total aromatics yield to be smaller than 5 wt %. In other words, low liquid yield was observed (Table 20) for any set of reaction conditions showing (Table 19) high concentration of BTEX. Simply, as the liquid yield decreases, its BTEX concentration increases. This trend indicated that there should be a trade off between liquid yields and their BTEX concentrations.

As the reaction temperature increases from 300 ºC to 325 ºC, the concentration of all the individual aromatics as well as total BTX increased (Table 19). A decrease in OCR was responsible for an increase in aromatics contents in OLP. However, the amounts of undesired gases products increased when OCR was low.
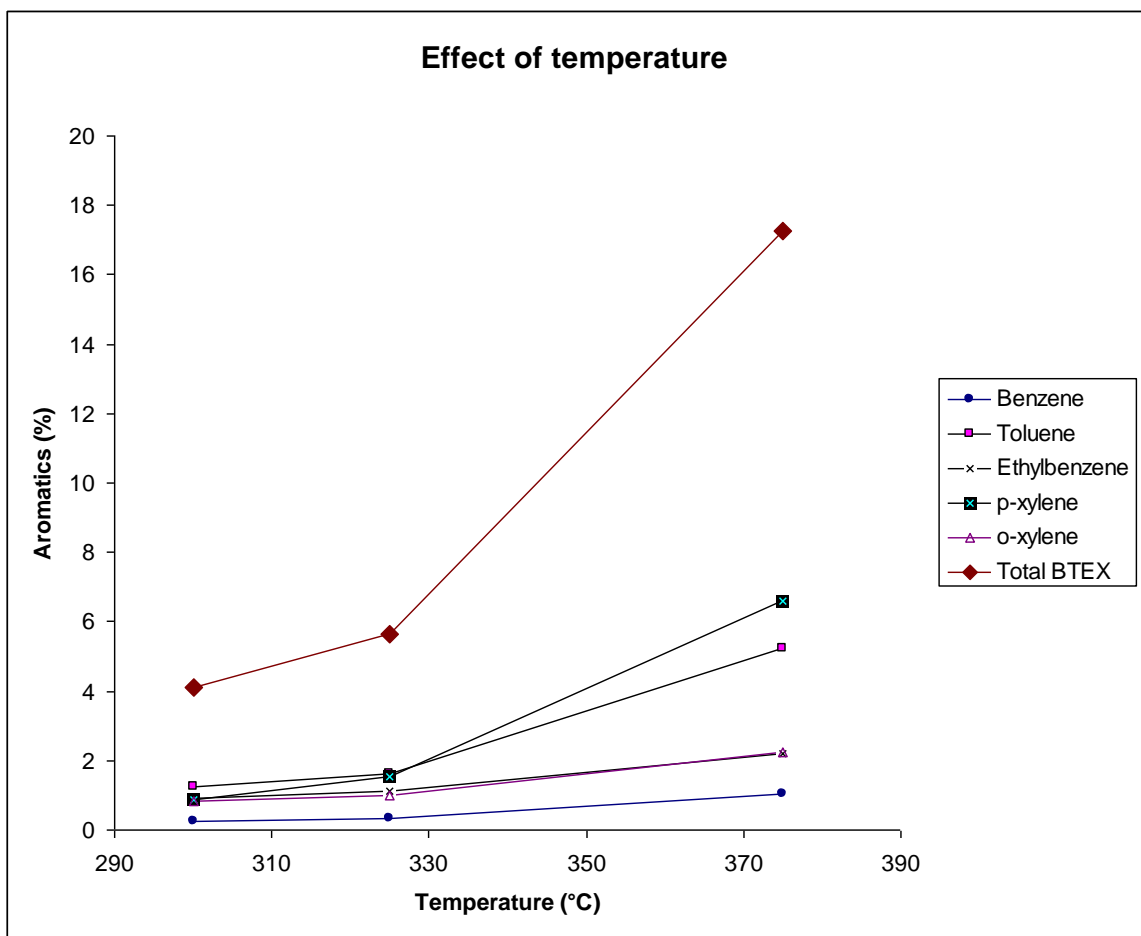
Figure 30. The effect of temperature on aromatization (BTEX concentration) at a constant reaction time of 20 min. and OCR of 10.
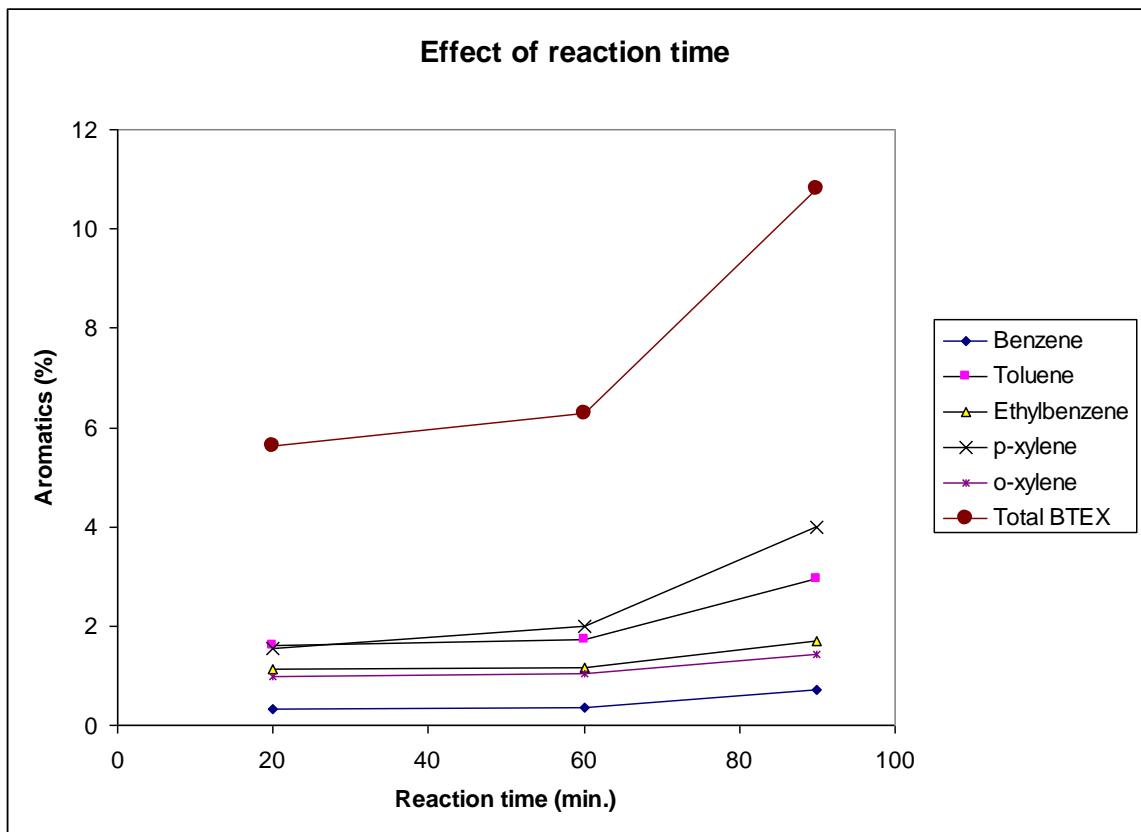
Figure 31. The effect of reaction time on aromatization (BTEX concentration) at a reaction temperature of 325 ºC and at a OCR of 10.

An increase in the reaction temperature from 325 ºC to 375 ºC and similar increase in the reaction time from 60 minutes to 90 minutes, there was an abrupt rise in the aromatics concentration in the reformates. It means that these two factors did not have significant effects on aromatization up to 325 ºC and 60 minutes, but a significant rise in aromatic concentration was observed beyond these limits. There was not much change observed in the amount of gases formed. So, further optimization experiments will help to study the effects of these factors on OLP aromatization optimum levels of factors.

New experimental design

With an increase in reaction temperature, the amount of liquid products obtained was significantly lower. It was difficult to collect and separate liquids from coke/solids at higher reaction temperature. (e.g. when the reaction conditions were reaction temperature = 400 °C, OCR = 10 and reaction time = 90 minutes, yield of coke was about more than 20% by weight. Liquid product yield was low. Coke was deposited on the catalyst particles and liquids were trapped in it. This caused difficulties in separating liquids). Correspondingly, the yield of gaseous products also increased. Due to this effect, the reaction pressure was difficult to control. When gas yield was higher, the reactor was shut down to avoid explosion. It was concluded from the above facts that the present catalyst produced very higher amounts of coke and gaseous products.

A new hypothesis was proposed and tested to control the yields of gases and coke. According to this hypothesis, the silica:alumina (SiO_2:Al_2O_3) ratio of HZSM-5 catalyst was adjusted and activity tests were conducted (CBV 5524G vs CBV 2314). Our previous studies [73] on propylene aromatization over HZSM-5 concluded that the SiO_2:Al_2O_3 ratio should be lowered for the greater yields of aromatic compounds. A new HZSM-5 catalyst with a SiO_2:Al_2O_3 ratio of 23 was used and a few exploratory experiments were conducted. When the reaction conditions were reaction temperature = 400 °C, OCR = 10 and reaction time = 90 minutes, the yield of coke was less than 10%. Thus coke formation was reduced to less than half. The reaction with a new catalyst was easy to control and reaction pressure was significantly lowered within the range of reactor's safe operating limits.

Aromatization of OLP over HZSM-5 with a Silica:Alumina ratio of 23

Based on the above mentioned results, levels of experimental design were changed, (Table 21).

Table 21. Experimental factors and their uncoded levels for OLP aromatization.

Factors	Notation	(-1)	(0)	(+1)
		Low values	Center	High values
Reaction Temperature (^{o}C)	A	300	350	400
OLP to catalyst ratio (OCR)	B	7	11	15
Reaction time (minutes)	C	5	12.5	20

Catalytic reforming experiments were conducted on the newly selected HZSM-5 catalyst having a SiO_2:Al_2O_3 ratio of 23. Table 22 shows the reaction conditions chosen and the yields of liquids, coke/solids as well as gaseous products.

Table 22. A full factorial experimental design consisting of the reaction conditions and the responses

Expt No.	Temperature (^{o}C)	OCR	Time (min.)	% Liquids yield	% coke/solids yield	% gases yield
1	400	7	5	78	10	12
2	300	15	20	91	2.1	6.9
3	350	11	12.5	87	7	6
4	400	15	5	86	6	8
5	300	15	5	92	0.6	7.4
6	350	11	12.5	88	6.4	5.6
7	400	7	20	76	10	14
8	350	11	12.5	88	7	5
9	350	11	12.5	88	6.5	5.5
10	300	7	20	88	7.9	4.1
11	400	15	20	84	5	11
12	350	11	12.5	88	7	5
13	350	11	12.5	87	6.5	6.5
14	300	7	5	84	9	7

In the above listed full factorial design, six center point experiments were included to test if any curvature is significant while preparing the statistical models. The experimental design analysis was conducted by using Minitab 15 software. The main effects plots are shown in the figure 32.
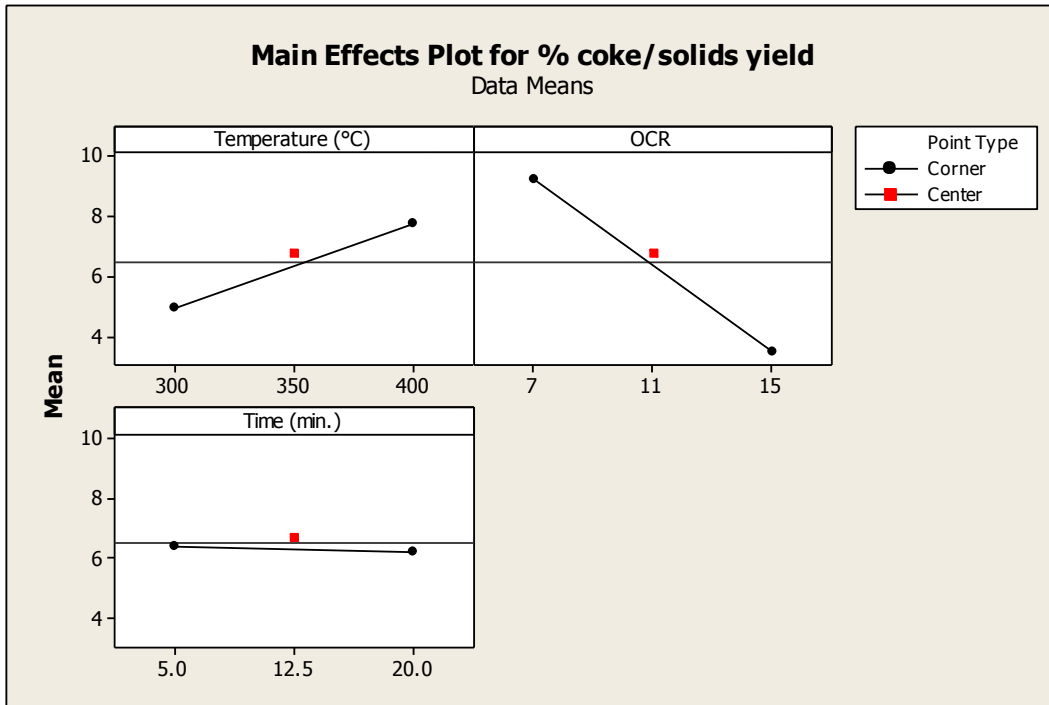
Figure 32. Main effect plots of coke/solids yields after OLP reforming

The main effects plots for coke / solid products yield (Fig. 32) indicate, the outliers which represent the center point experiments (shown as red dots in all the plots). The center points are not very far away from the main effects line. This usually happens when there is an interaction effect which significantly affects the response. It also suggests that the statistical model may be a linear model.
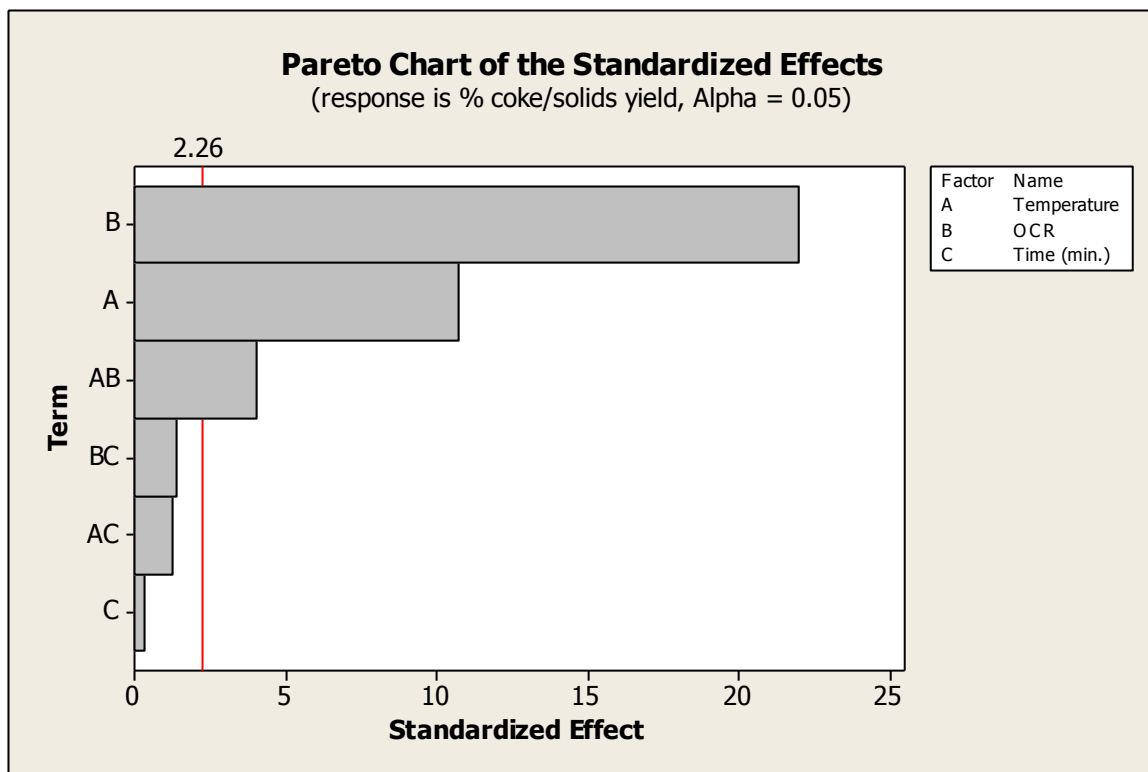
Figure 33. Pareto chart of coke/solids yields after OLP reforming

Figure 33 shows Pareto chart of the effects of each factor and the interaction for the response (coke/solids yield). For example, 'AB' represents the effect of the interaction between factors A (reaction temperature) and B (OCR). The vertical line in this Pareto chart represents the line of significance, which is based on 95% confidence. Any bar (representing the effect) in a Pareto chart extending beyond this line is considered a significant term.

As per the method followed by Length [127], the three way interaction were assumed to be insignificant and only two-way interactions were considered while analyzing this full experimental factorial design. Two factors, namely reaction temperature and OCR, were found to have significant effects on the yields of coke / solid products. The reaction time did not affect coke yield at all.
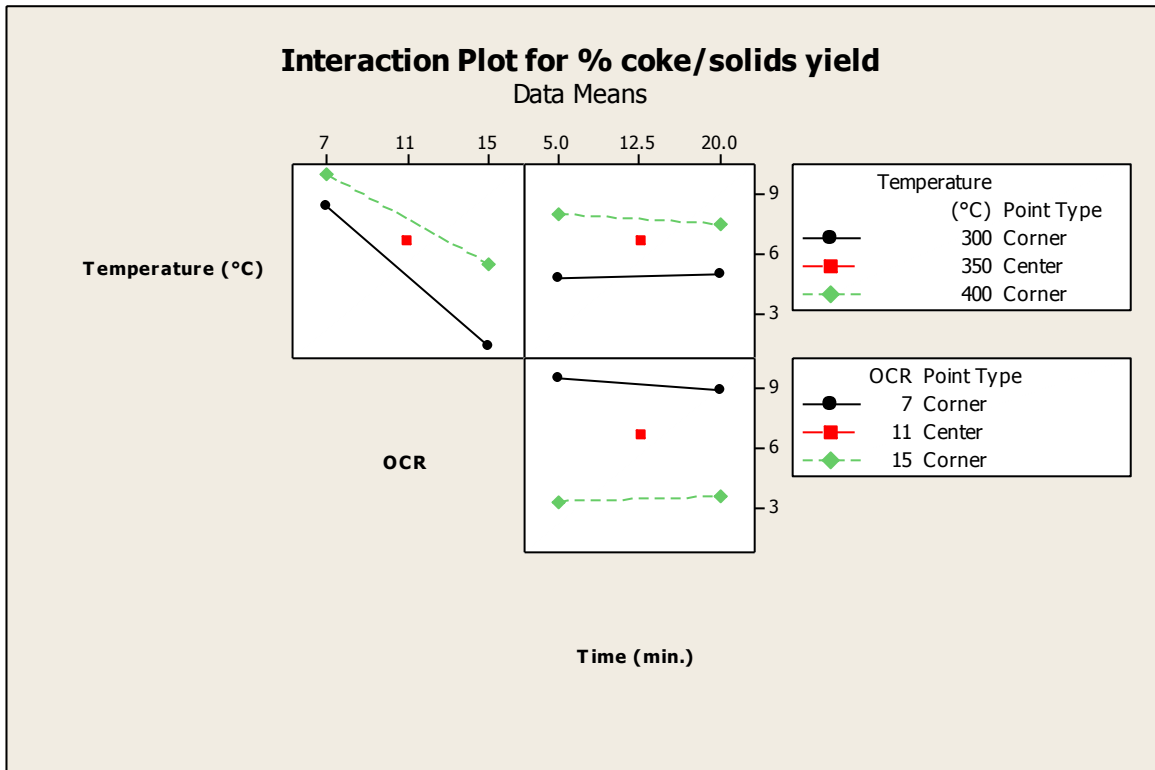
Figure 34. Interaction plots for coke/solids yield after OLP reforming

One major advantage of using the DOE methodology is its ability to identify significant interaction effects. The interaction between reaction temperature and OCR was determined to have the largest significant effect on coke yield. The reaction time did not show a significant effect on coke/solids yield. Hence, while proposing a statistical model, reaction time factor was discarded and only the remaining two factors were taken into account along with their interaction. Based on this information, the statistical model for % coke/solids yield was proposed as follows:

Coke/solids yield=6.206+1.419*Temperature-2.906*OCR+0.531*Temperature*OCR

This can be represented as follows:

Y2=6.206+1.419*A-2.906*B+0.531*A*B

The contour plot appears as the following chart
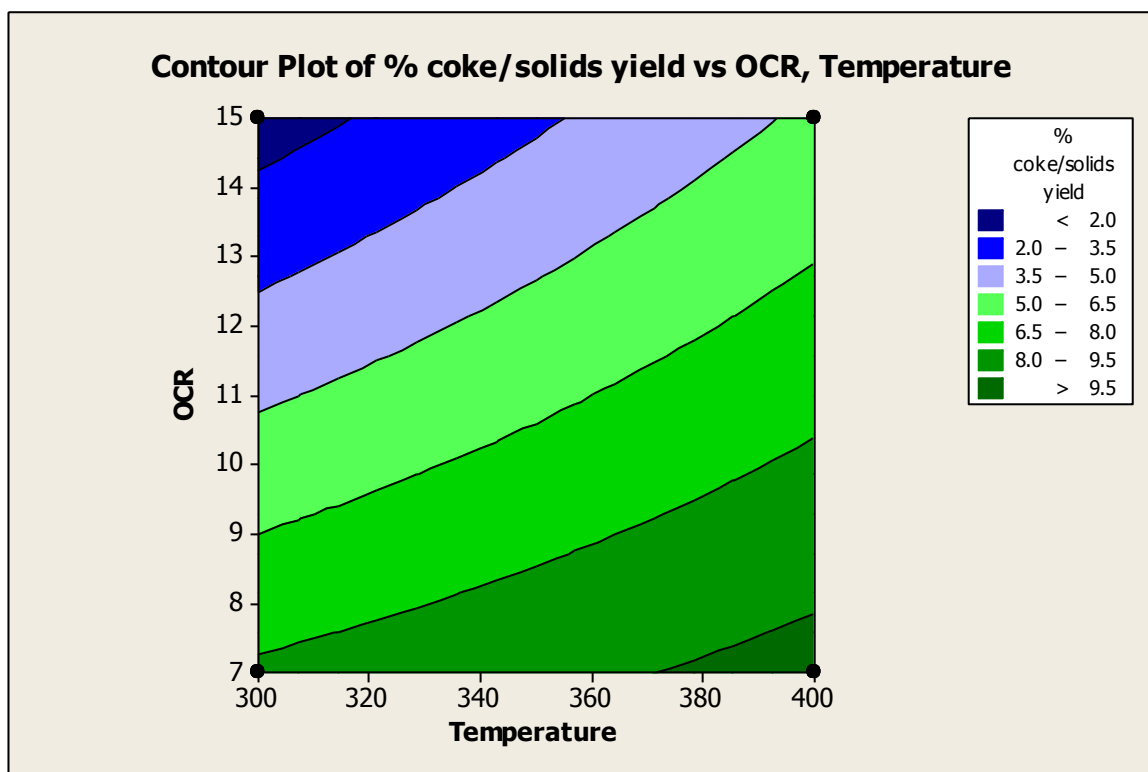
Figure 35. Contour plot of coke/solids yield after OLP reforming

The optimum for the lowest coke/solids yield appeared to be in the region when OCR was kept at its highest level and the reaction temperature was kept at its lowest level (Fig. 35). However, it may not be possible to get the highest optimum level of aromatics yield at these levels because an increase in temperature increases the aromatics formation activity of HZSM-5 catalyst. This contour plot can be used to determine the optimum temperature for increased aromatics yield still keeping the coke yield in the range of 2-8% by weight.
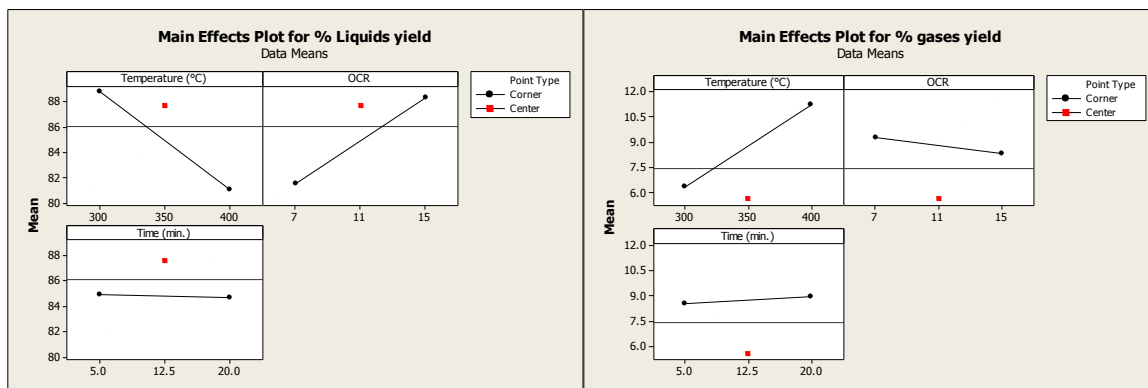
(a)   (b)

Figure 36. Main effects plots for a) Liquid yield, b) gases yield obtained after OLP

conversion

Fig. 36 shows main effects plots for liquids and gases yields. For the yields of liquids and

gases the center points have P values less than 0.05. Since the center point P-values were

less than 0.05, center points are significant. Significant center point means there is a

significant curvature. So we do not have linear models for all these responses [128]. So, a

simple linear model cannot explain which variable contributes how much in the response.

Hence, star points were added in the experimental design and further experiments were

conducted. Table 23 shows a new design for the Response Surface Methodology (RSM)

Table 23. A Central Composite Design (CCD) design consisting of the experimental

reaction conditions and the responses

Expt. No.	Temperature (°C)	OCR	Time (min.)	% Liquids yield	% coke/solids yield	% gases yield
1	350	11	12.5	87	7	6
2	400	7	20	76	9.8	14.2
3	300	7	20	88	7.9	4.1
4	300	15	20	91	2.1	6.9
5	350	11	12.5	88	6.4	5.6
6	400	15	20	84	5	11
7	400	7	5	78	9.5	12.5
8	300	7	5	84	9	7
9	350	11	12.5	88	7	5
10	300	15	5	92	0.6	7.4
11	400	15	5	86	6	8
12	350	11	12.5	88	6.5	5.5
13	350	11	24.7475	87	7	6
14	350	4.468	12.5	78	14	8
15	350	11	12.5	88	7	5
16	268.35	11	12.5	87	7	6
17	350	17.532	12.5	92	3.3	4.7
18	431.65	11	12.5	82	5	13
19	350	11	12.5	87	6.5	6.5
20	350	11	0.2525	88	7	5

These star points represent the square points [e.g. $(OCR)^2$] which contribute to the

curvature. The square points contain the value of alpha (1.633). The exponent terms

result in the curvature and this model could contain the exponents up to 2nd power.

RSM application for liquids and gases yields

An initial analysis of RSM Central Composite Design analysis showed neither the

factor, reaction time (C), nor its interactions and square terms had a significant effect on

both responses (liquids and gases yields). This was confirmed by checking their P-values

which were higher than 0.05.

A statistical model for % liquids yield was proposed as follows:

Liquids yield=87.59-2.937*Temperature+3.710*OCR-1.299*(Temperature)^2 -

1.112*(OCR)^2

This can be represented as follows:

Y1=87.59-2.937*A+3.710*B-1.299*A*A-1.112*B*B
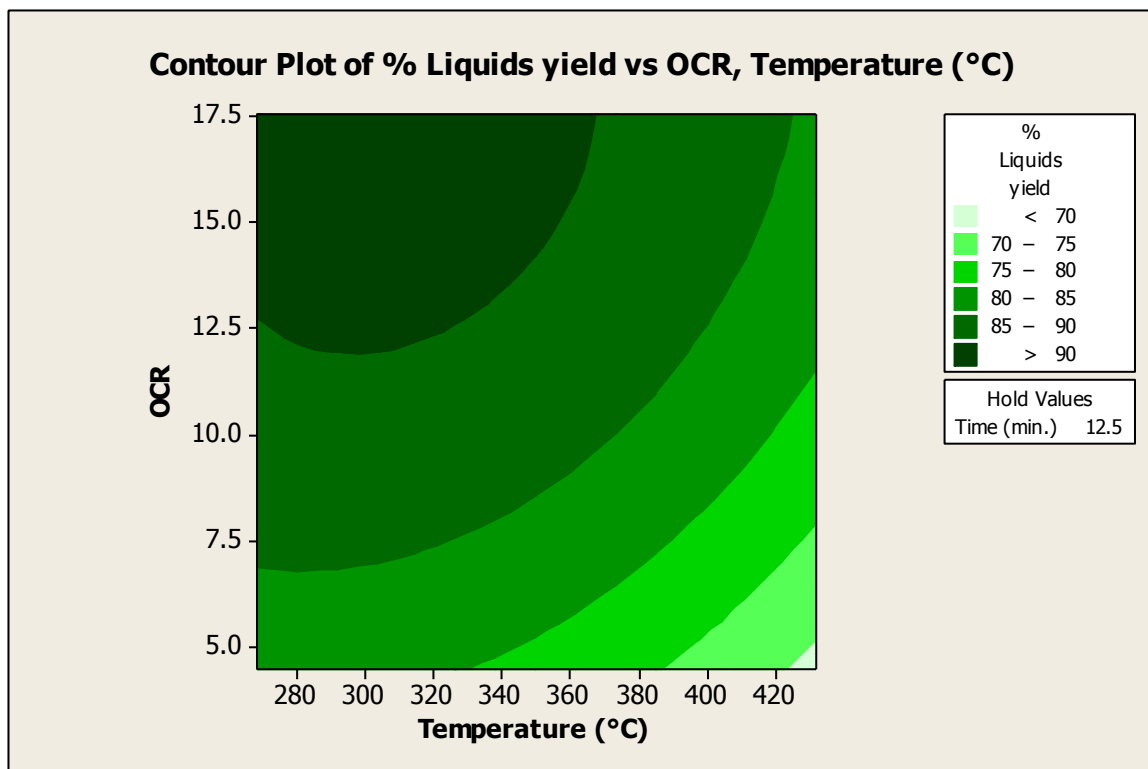
Figure 37. Contour plot of liquid yield obtained after OLP conversion

The contour plot of liquid yield is shown in Fig.37. The optimum for the highest liquids yield appeared to be in the region when OCR was kept at its highest level and the reaction temperature was kept at its lowest level. Similar to coke/solids yields, this contour plot can be used to determine the optimum conditions for increased aromatics yield because higher temperatures will be required to produce large amounts of aromatics for HZSM-5 catalyst.

The statistical model for % gas yield was proposed as follows:

Gases yield=5.653+2.38*Temperature-0.7417*OCR+1.804*Temperature* Temperature
+0.6228*OCR*OCR-1.363*Time*Time

This can be represented as follows:

Y1=5.653+2.38*A-0.7417*B+1.804*A* A +0.6228*B*B-1.363*A*B
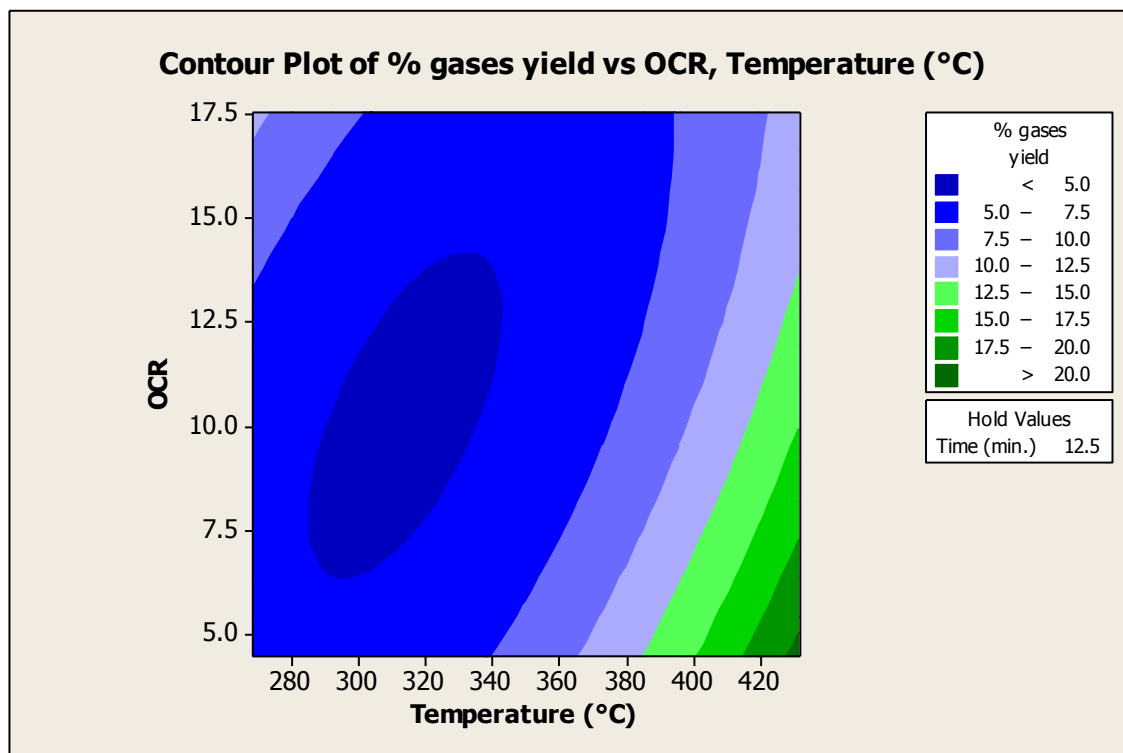
Figure 38. Contour plot of gases yield obtained after OLP conversion

The contour plot of gas yield is shown in Fig.38. The optimum for the lowest gas fraction yield appeared to be in the region when OCR was kept near midpoint (center) level and the reaction temperature was kept slightly below the center point. Similar to coke/solids yields, this contour plot can be used to determine the optimum conditions for increased aromatics yield because higher temperatures will be required to produce large amounts of aromatics for HZSM-5 catalyst.

Highest aromatics yield was observed at the reaction conditions 432 C, OCR of 4.47 and reaction time of 12.5 minutes. Total yield of gaseous products was 15 % (wt/wt) of OLP feed. A detailed analysis of these gaseous products was performed and the results are listed as follows:

Table 24. Gaseous components of OLP reforming reaction

Gas component	Concentration (wt %)
CO	2.8
methane	6.4
CO2	1.5
ethane	0.28
ethylene	13
propylene	54
butane	16
butene	2.1
pentane	0.57
hexane	0.58
Hydrogen	2.8

The production of CO and CO_2 confirms that the HZSM-5 catalyst is capable of decarboxylation of oxygenated compounds of the feedstocks. Mechanistic considerations of decarboxylation reactions over HZSM-5 are discussed in the forthcoming section of liquid product analysis. 54 % of gaseous products constitute propylene alone. This shows that the HZSM-5 catalyst is highly selective towards of propylene as a cracked gaseous product.

Optimization of the reaction conditions for maximizing aromatics yield

A full factorial design with center points was prepared and experiments were conducted. The results are listed in Table 25.

185

Table 25. A full factorial experimental design consisting of the reaction conditions and the response for initial OLP aromatization runs

Experiment No.	Temperature (°C)	OCR	Time (min.)	BTEX yield (wt %)
1	400	15	5	2.2
2	300	7	5	1.8
3	300	15	20	1.7
4	400	7	20	3.8
5	400	15	20	2.0
6	400	7	5	2.5
7	350	11	12.5	2.0
8	350	11	12.5	2.0
9	300	15	5	1.5
10	300	7	20	1.9

The DOE analysis shows that the reaction time did not significantly affect the BTEX yield. An increase in the aromatization reaction temperature significantly increases the BTEX yield. In contrast, a decrease in OCR was responsible for a significant increase in the BTEX yield. The center point does not fit linearly because it deviate from the linear plots of reaction temperature, time as well as OCR. This leads to a conclusion that a curvature exists and the final model is nonlinear (quadratic). This was also confirmed by verifying the p-values of center point/curvature in the regression analysis.

The Central composite design with the star points was then used for the optimization of reaction conditions through a proposal of a quadratic model. The results are listed in Table 26.

Table 26. A Central Composite Design consisting of the experimental reaction conditions and the responses

Expt. No.	Temperature (°C)	OCR	Time (min.)	Alkyl benzene yield	n-alkyl benzene yield	BTEX yield	Mono aromatics yield	Indanes sum	Naphthalenes yield	Total aromatics yield
1	350	11	12.5	13	2.0	1.9	17	2.0	1.6	20
2	400	7	20	19	1.8	3.8	25	3.0	2.4	30
3	300	7	20	13	2.2	1.9	17	2.3	1.7	21
4	300	15	20	13	2.1	1.7	17	2.1	1.7	21
5	350	11	12.5	13	2.1	2.0	17	2.1	1.6	21
6	400	15	20	11	1.5	2.0	14	2.0	1.5	18
7	400	7	5	12	1.3	2.5	16	1.5	1.7	19
8	300	7	5	13	2.0	1.8	16	2.1	1.6	20
9	350	11	12.5	13	2.1	2.0	17	2.1	1.6	21
10	300	15	5	10	1.7	1.5	14	1.7	1.3	17
11	400	15	5	16	2.4	2.2	21	2.9	2.0	26
12	350	11	12.5	13	2.0	1.9	17	2.2	1.7	21
13	350	11	24.7	13	2.1	2.0	17	1.8	1.8	21
14	350	4.5	12.5	14	1.9	2.3	18	1.6	1.6	21
15	350	11	12.5	13	1.8	2.0	16	2.0	1.6	20
16	268	11	12.5	13	2.1	1.8	16	1.9	1.5	19
17	350	17.5	12.5	13	2.1	2.0	17	2.1	1.7	21
18	432	11	12.5	17	2.0	3.8	22	3.1	2.3	28
19	350	11	12.5	14	2.1	1.9	18	2.2	1.8	22
20	350	11	0.253	13	2.1	2.0	17	2.1	1.6	20

Table 26 summarizes the yields of aromatic compounds for the respective sets of experimental conditions. The statistical model was trimmed to only the significant factors and the interactions as per the CCD methodology [128]. The residual vs. fits, residual vs. order and the Normal Probability plots indicate the verification and satisfaction of the three assumptions:

(1) Residuals are randomly and normally distributed, (2) residuals are not correlated with the predicted Y, and (3) residuals do not exhibit any trends over time [128].

This means that the model statistically fits well.
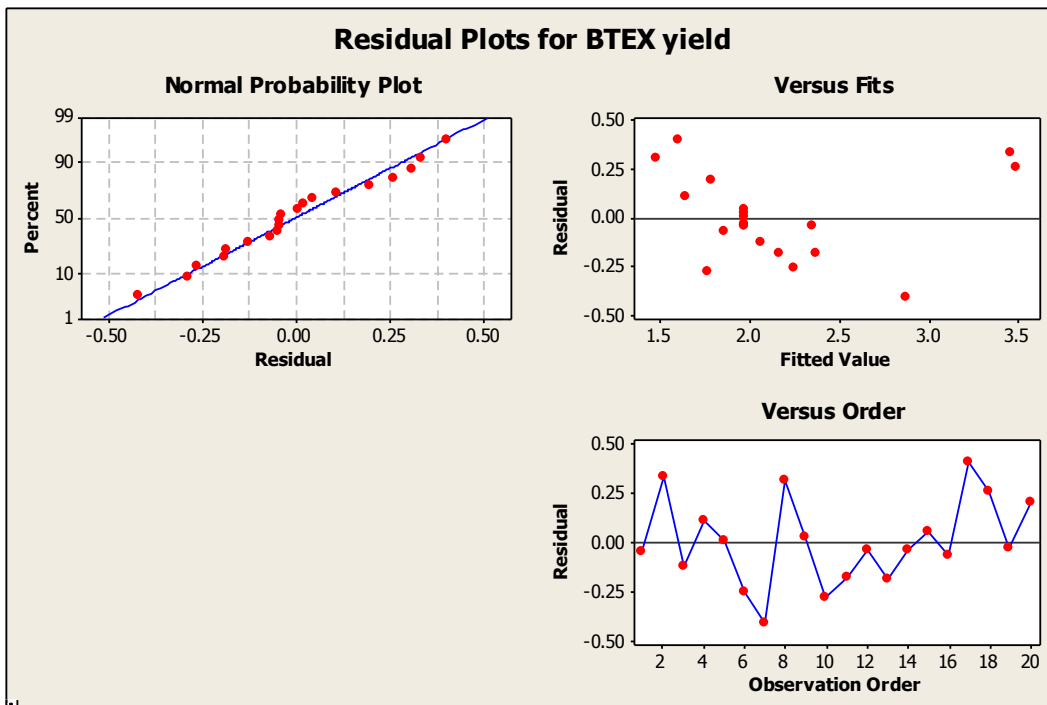
Figure 39. Residual plots for BTEX yield obtained after OLP conversion

The contour and surface plots were obtained by the Response Surface Methodology technique (shown in the following Figs. 40 and 41). The areas of greater aromatics yields are distinctly visible in these plots.
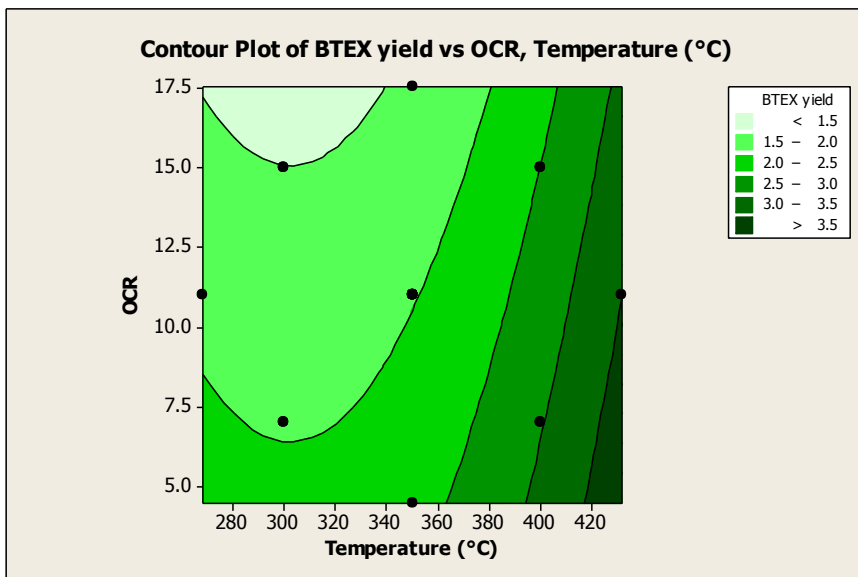
Figure 40. Contour plot of BTEX yield obtained after OLP conversion
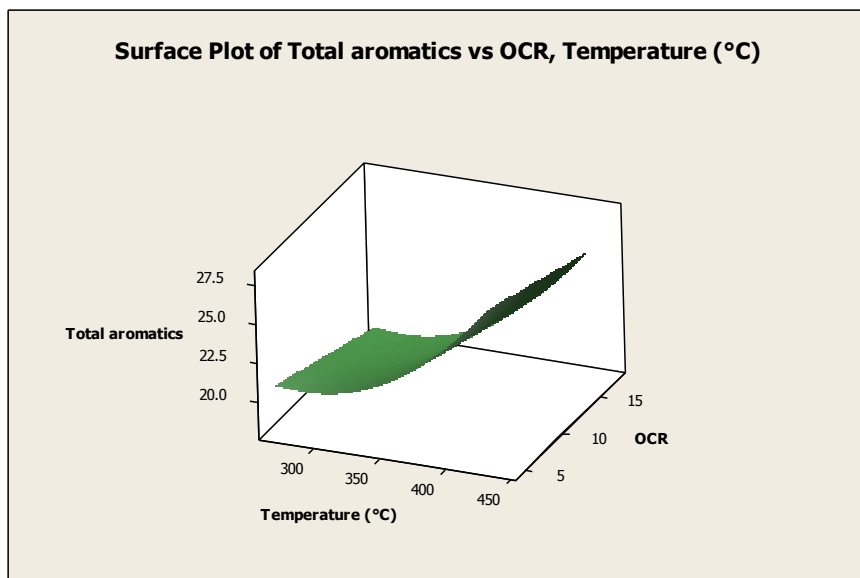
Figure 41. Surface plot of aromatics yield obtained after OLP conversion

A statistical model was proposed as follows:

Model: $1.97 + 0.501*\text{Temperature} - 0.231*\text{OCR} + 0.264*(\text{Temperature})^2$

By the use of Response Optimizer tool, the predicted optimized conditions were found as the reaction temperature of 432 ºC and the OCR of 4.47. Aromatization experiments were performed in duplicate at these reaction conditions and the results were as follows:

Coke yield = 5 % (5 % for the replicate)

Liquid products yield = 80% (81% for the replicate)

Gaseous products yield = 15 % (14 %or the replicate)

The detailed identification of non-BTEX aromatics was performed. Surprisingly, this sample contained significant amounts of alkyl benzenes totaling to about 60 % aromatics in the liquid reformate products.

Conclusions

Non-catalytically cracked soybean oil can be aromatized by using HZSM-5 catalysts. Initial feasibility experiments suggested that the OLP to the catalyst ratio was the only factor having a significant detrimental effect on aromatization. Reaction time and temperature tend to have a positive incremental effect on aromatization. Further experiments were conducted in search of optimum reaction conditions for highest yields of aromatics and liquids products as well as the lowest possible yields of coke/solids and gases. Response Surface Methodology (RSM) was used for optimization and the contour plots clearly showed the regions of optimum levels of liquids, coke and gases yields. The reaction temperature and OCR were found to have significant effects on the responses whereas reaction time was not significant. A statistical linear model was proposed for coke/solids yield. However the resulting data did not fit in linear models and hence quadratic models were proposed for liquids and gases yields. It was found that the highest yield of total aromatics (47 wt%) was obtained at optimum reaction temperature 432 °C and OCR 4.47. Alkanes and cyclic compounds were also produced in significant quantities. The negligible yields of alkenes and carboxylic acids in the catalytic reforming step lead to the conclusion that the smaller silica:alumina ratio of HZSM-5 is preferred for aromatization reactions in which decarboxylation is desired.

APPENDIX D: PUBLISHED PREPRINTS

This section represents the published part of this research work. The papers are listed as they are published by American Chemical Society. The figure numbers, table numbers of these preprints are not changed into the dissertation format to distinguish them as published material (as is).

TRIGLYCERIDES AS AN ALTERNATIVE FEEDSTOCK FOR AROMATIC COMPOUNDS

Swapnil L. Fegade[1], Brian Tande[1], Wayne Seames[1], Alena Kubátová[2], Evguenii Kozliak[2]

[1]Department of Chemical Engineering, University of North Dakota, 241 Centennial Drive, Grand Forks, ND 58202-7101, USA

[2]Department of Chemistry, University of North Dakota, P.O. Box 9024, Grand Forks, ND 58202, USA

ABSTRACT

A successful attempt was made to convert cracked soybean oil into aromatic compounds by using HZSM-5 catalyst. The reaction temperature tends to have lower effect on aromatization below 325 °C. A significant increase in aromatics concentration was observed when the reaction temperature was increased to 375 °C. Similarly, an increase in reaction time also resulted in an increase in aromatics concentration in the liquid products. Individual products distribution was greatly influenced by the ratio of organic liquid product (OLP) to catalyst ratio. Soybean oil could be an effective alternative feedstock for the production of aromatic compounds.

Introduction

Currently, the primary source of BTEX, other aromatics, and industrial organic chemicals is petroleum. Considering the limited availability of petroleum, there is a growing interest in developing renewable resources for aromatics and other organic chemicals. For example, because lignins are polymeric materials made of complex aromatic rings, many attempts have been made to produce aromatics from lignin. These include several successful attempts to prepare phenolics by the pyrolysis of lignin present the wood[129]. In the oxidative environment, the pyrolysis and depolymerization of lignin based polymeric materials produce aromatic aldehydes; while reductive environment was responsible for producing alkyl phenols[130].

Low temperature catalytic pyrolysis and hydropyrolysis of woody biomass showed a product distribution of a wide range of aromatic hydrocarbons. The first step is the decomposition of this woody biomass. The decomposed mass then undergoes secondary reactions to produce light hydrocarbon molecules. It was also observed that the catalyst selection is very important in aromatization of biomass. This product distribution could be controlled by controlling the reaction conditions[131].

Triglyceride oils, such as palm oil, canola oil and other crop oils, are also a promising feedstock for the production of valuable organic chemicals, including aromatics. The non-catalytic as well as catalytic cracking of these molecules under FCC conditions yields aromatic hydrocarbon molecules. The catalytic cracking of triglyceride oils also produces water, CO, CO_2 and other hydrocarbons by removing oxygen carbon and hydrogen from the molecule[132].

Katikaneni et. al., studied the catalytic cracking of canola oil to convert it into fuels

and chemicals[133] and found that the organic liquid products (OLP) obtained by canola oil cracking consisted of aliphatic as well as aromatic hydrocarbons. They also found that the amount of aromatics formed was more when the reaction temperature and catalyst acidity were increased. The comparative studies of the catalysts showed that HZSM-5 yields more aromatic compounds. The objective of this work is to determine the feasibility of converting cracked soybean oil into more valuable aromatic compounds such as benzene, toluene, ethylbenzene, p-xylene, o-xylene (BTEX).

Experimental

Materials. The catalyst ZSM-5 (CBV5524G) was purchased from Zeolyst International. GC grade standards, benzene, toluene, ethylbenzene, p-xylene, o-xylene and 2-chlorotoluene were also purchased from Sigma-Aldrich. Organic liquid products (OLP) were obtained from cracked soybean oil[134].

   Catalytic conversion of OLP. The required amounts of catalyst and soybean oil OLP were charged to the autoclave reactor. This reactor was closed, and then was purged with nitrogen gas to remove air. Once the purging was over, the nitrogen valve was closed. All the inlet and outlet valves of the reactor were also closed. The water flows were started for the reactor cooling channels and for a condenser connected to reactor. The reactor was heated while the reactor contents were stirred at set values. Once the reaction was over, the reactor contents were allowed to cool down to room temperature and then the gaseous products were collected in a gas bag by slowly opening reactor vent. The coke/solid particles were separated from liquid products. The reaction temperature (°C), OLP to catalyst ratio (OCR), and reaction time (minutes) were chosen as the reaction conditions to be studied. After each aromatization run, the amounts of gases,

liquids and coke/solids formed were determined and the liquid products were further analyzed to find out % total BTEX (benzene, toluene, ethylbenzene and xylenes) in liquid products.

The liquid products obtained from the above experimental runs, were analyzed on HP 5890 series II gas chromatograph by using 2-cholrotoluene as an internal standard. The injector and detector temperatures of GC were set at 250 °C and 300 °C respectively. A proper separation of peaks was obtained by temperature programming on GC. The temperature program was started at 30 °C for 1 minute and then ramped at 10 °C / minute to 250 °C and maintained at this temperature for 15 minutes.

Results and Discussion

After the products analysis on GC, it was observed that the liquid products obtained after catalytic conversion contained benzene, toluene, ethylbenzene and xylenes. A decrease in the feed OLP to catalyst ratio significantly increased the % of all individual aromatics as well as total BTEX present in the liquid products. From fig. 1, it can be clearly seen that this increase in all individual aromatics is not directly proportional to a

decrease in the OLP to catalyst ratio. The products distribution is greatly influenced by
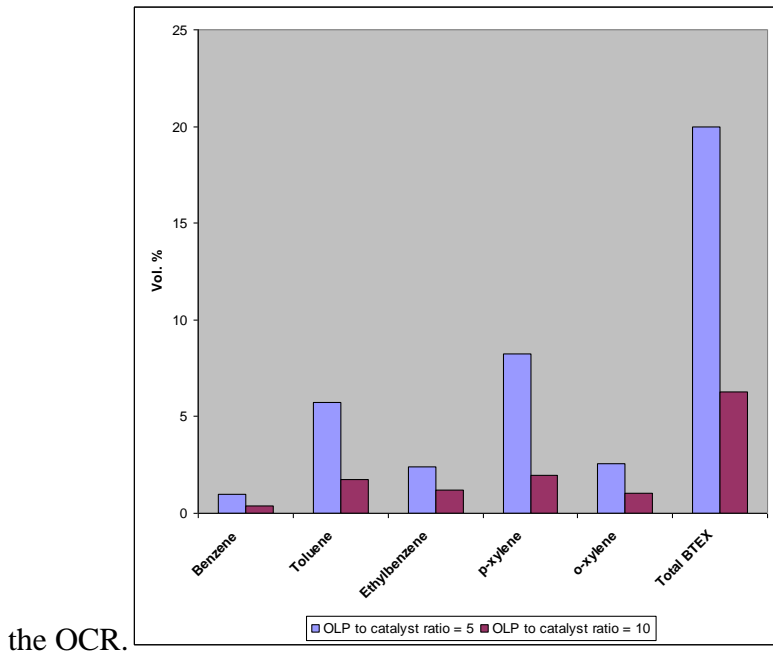
the OCR.

Figure 1. The Individual aromatics volume % along with total BTEX present in the

liquid products obtained by using two different OLP to catalyst ratios.

Table 1. The % yields of gases, liquids and coke/solids obtained along with the

reaction conditions

Temperature (^{o}C)	OLP to catalyst ratio	Time (min.)	Gases (% yield)	Liquid reformate (% yield)	Coke/solids (% yield)
300	10	60	5.6	87	7.1
300	5	20	26	66	9.9
300	5	60	29	64	6.8
300	10	20	5.1	88	7.1
325	5	60	52	40	8.5
325	10	20	6.6	87	6.5

325	10	60	11	82	8.0
325	5	20	38	53	8.6

Table 1 shows the % yields of gases, liquids as well as solids/coke produced in each experiment. The OLP to catalyst ratio is the only factor which had a significant effect on the yields of gases and liquid products. When organic chemicals come in contact with HZSM-5, they also undergo catalytic cracking and produce many small gaseous molecules. If OCR is at a lower level, an amount of catalyst available for cracking activity increases, therefore amount of gases formed also increases. None of these factors showed a significant effect on the % yield of coke and solid products.
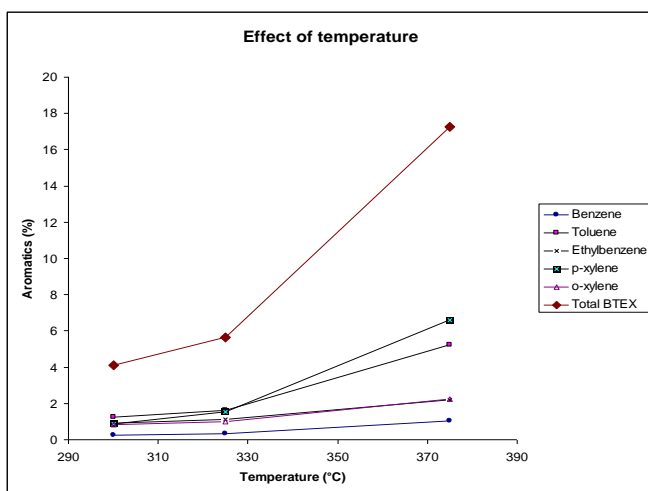
Figure 2. The effect of temperature on aromatization of OLP keeping reaction time of 20 min. and OCR of 10 as constants.
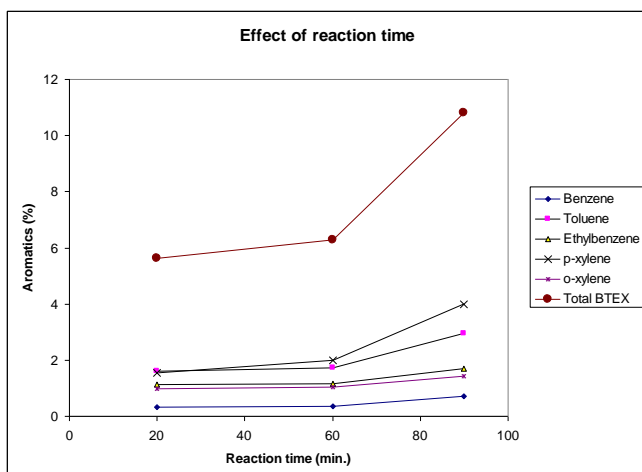
Figure 3. The effect of reaction time on aromatization keeping reaction temperature of 325 °C and OCR of 10 as constants.

Figures 2 and 3 as shown above, clearly indicate that with an increase in the reaction temperature from 325 °C to 375 °C and similar increase in the reaction time from 60 minutes to 90 minutes, there was an abrupt rise in the aromatics contents of the liquid products. This indicates that the catalyst is more active for aromatization above 325 °C. These two factors did not have significant effects on aromatization up to 325 °C and 60 minutes, but significant rise in aromatics contents was observed beyond these limits. There was not much change observed in the amount of gases formed at these conditions. So, further optimization experiments will help to study the effects of these factors on OLP aromatization at optimum levels of reaction conditions.

Conclusions

Soybean oil OLP can be successfully aromatized by using HZSM-5 catalysts. OLP to the catalyst ratio was found to have a greater detrimental effect on aromatization. Reaction time and temperature tend to have a positive incremental effect on

197

aromatization. The yields of gaseous products as well as liquid reformates are significantly affected by OLP to catalyst ratio. Yield of gases are lowered and yields of liquid reformates are increased with the increase in this ratio. Further experiments at optimum levels of reaction temperatures and time will be beneficial to increase the yield of OLP, amount of BTEX and to decrease the yield of gases.

CATALYTIC CONVERSION OF 1-TETRADECENE TO AROMATIC COMPOUNDS OVER ZEOLITES UNDER MILD CONDITIONS

Swapnil L. Fegade[1], Brian Tande[1], Wayne Seames[1], Alena Kubátová[2], Evguenii Kozliak[2]

[1]Department of Chemical Engineering, University of North Dakota, 241 Centennial Drive, Grand Forks, ND 58202-7101, USA

[2]Department of Chemistry, University of North Dakota, P.O. Box 9024, Grand Forks, ND 58202, USA

ABSTRACT

Catalytic cracking of1-tetradecene was performed by using HZSM-5 catalyst to determine the feasibility of producing value-added aromatic compounds such as benzene, toluene, ethylbenzene and xylenes (BTEX). A two level, full factorial design of experiments was applied to determine which factors significantly influence the catalytic cracking process. Three factors, temperature ($300-375^0$C), olefin to catalyst ratio (10-20) and reaction time (30-60 Min.) were chosen for this study. An increase in the reaction temperature increases the % total BTEX in liquid products and an increase in olefin to catalyst ratio decreases the amount of total BTEX in liquid products. However, these trends were exactly opposite for the % yield of liquid products. The results of this study may be used to recycle waste 1-tetradecene from functional drilling fluids, and may likely be applicable to other alpha olefins.

Introduction

Presently, the sources for the production of aromatic compounds are petroleum, fossil fuels and coal. Various processes were commercialized for converting light alkanes, olefins and petroleum naphtha into aromatic compounds via catalytic cracking and reforming routes. Current academic as well as industrial research is focused on the production of aromatic compounds from light alkanes and alkenes[28, 34, 38, 41, 41, 44, 47, 65, 67]. Although there is work done on aromatization of lower olefins and mid chain (C6, C8) olefins, there is a lack of work on aromatization of α-olefins having more than 10 carbon atoms[59, 76]. The α-olefin 1-tetradecene is commercially important for the manufacture of detergents, surfactants, linear alkylbenzenes and most of the academic and industrial research studies about 1-tetradecene have been presently concentrated on using it as comonomer in copolymerization reactions[83]. 1-tetradecene is also used in functional drilling fluids, lubricants, automotive additives, metal working agents. Apart from these, the applications of 1-tetradecene are limited and hence there is a need to explore new applications for this α-olefin. In the present study, our preliminary objective is to study the feasibility of using 1-tetradecene as a source for producing aromatics rich liquids and to determine what factors significantly influence this aromatization process.

Experimental

Materials. The catalysts ZSM-5 (CBV5524G) was purchased from Zeolyst International. 1-tetradecene was purchased from Sigma-Aldrich. GC grade standards, benzene, toluene, ethylbenzene, p-xylene, o-xylene and 2-chlorotoluene were also purchased from Sigma-Aldrich.

Catalyst preparation. The catalyst calcination was first performed at 500 °C for 5 hours in an air circulated oven. This commercial catalyst was present in ammonium form. During calcination, the catalyst was converted into the hydrogen form and this catalyst was then identified as HZSM-5. This HZSM-5 catalyst was then used for catalytic conversion of 1-tetradecene.

Catalytic conversion of 1-tetradecene. The required amounts of catalyst and 1-tetradecene were charged to the autoclave reactor. This reactor was closed, and then was purged with nitrogen gas to remove air. Once the purging was over, the nitrogen valve was closed. All of the inlet and outlet valves of reactor were also closed. The water flows were started for the reactor cooling channel and for a condenser connected to reactor. The reactor was heated and the reactor contents were stirred at set values. Once the reaction was over, the reactor contents were allowed to cool down to room temperature and then the gaseous products were collected in a gas bag by slowly opening the reactor vent. The coke/solid particles were then separated from the liquid products.

The liquid products obtained from the experimental runs, were analyzed on an HP 5890 series II gas chromatograph by using 2-cholrotoluene as an internal standard. The injector and detector temperatures of GC were set at 250 °C and 300 °C, respectively. A proper separation of peaks was obtained by temperature programming on GC. The temperature program was started at 50 °C for 1 minute and then ramped at 10 °C / minute to 250 °C and maintained at this temperature for 15 minutes.

Statistical design of experiments (DOE). A 2 level, 3 factor, full factorial experimental design was used to find out which factors significantly affected the catalytic conversion of 1-tetradecene. The reaction temperature (°C), olefin (1-tetradecene) to

catalyst ratio (OCR), and reaction time (minutes) were chosen as the factors. After each aromatization run, the amounts of gases, liquids and coke/solids formed were determined and the organic liquid products were further analyzed to determine the total composition of BTEX (benzene, toluene, ethylbenzene and xylenes). The low and high values of the factors are shown in Table 1.

Factors	Low	High
(A) Temperature (°C)	300	375
(B) Olefin to catalyst ratio (OCR)	10	20
(C) Time (Min.)	30	60

Results and Discussion

It was found that temperature has a significant effect on % total BTEX present in liquid products, as shown by the Pareto charts of the standardized effects (Fig. 1). Fig. 2 shows the main effects plots and it is clearly seen that as the reaction temperature increases from 300 °C to 375 °C, the % of the total BTX in liquid products increases. The olefin to catalyst ratio showed a positive incremental effect on aromatization. On the other hand, the third factor, reaction time, was not significant for BTEX production. From Fig. 2, it was observed that the aromatic content in the reformates decreased when the olefin to catalyst ratio was increased from 10 to 20.
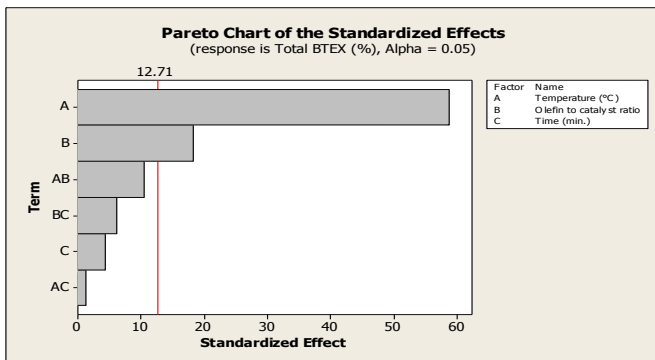
Figure 1. A Pareto chart of the standardized effects for % total BTEX present in OLP. Bars extending beyond the vertical line represent effects that are considered statistically significant.
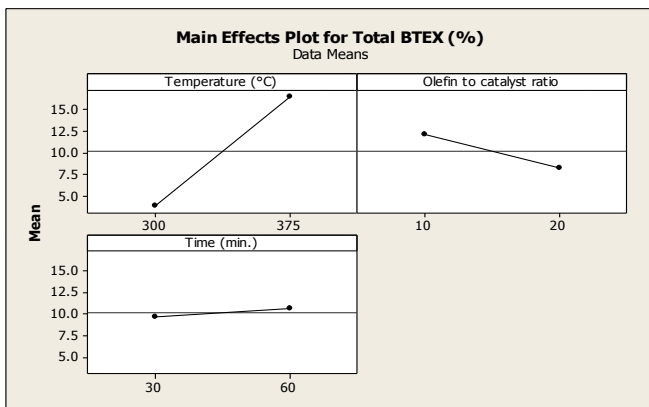
Figure 2. Main effects plots for % total BTEX present in OLP. These plots compare the average value for % yield at the two levels for each factor. Each point represents the average of four experiments.

The Pareto chart and main effects plots for % yield of liquid reformates obtained from 1-tetradecene aromatization are shown in Fig. 3 and 4, respectively. The yield of liquid products was greatly influenced by the reaction temperature and OCR. Increasing the reaction temperature and decreasing OCR significantly reduced the yield of liquid products. A similar trend was observed for the yield of gaseous products, where temperature was the only factor which greatly influenced the response.
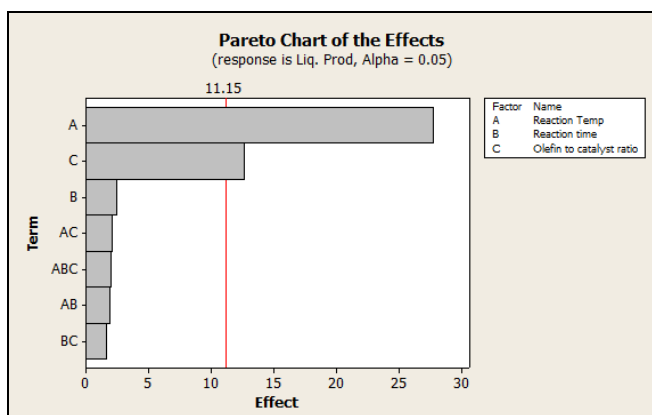
Figure 3. Main effects plots for % total BTEX present in OLP
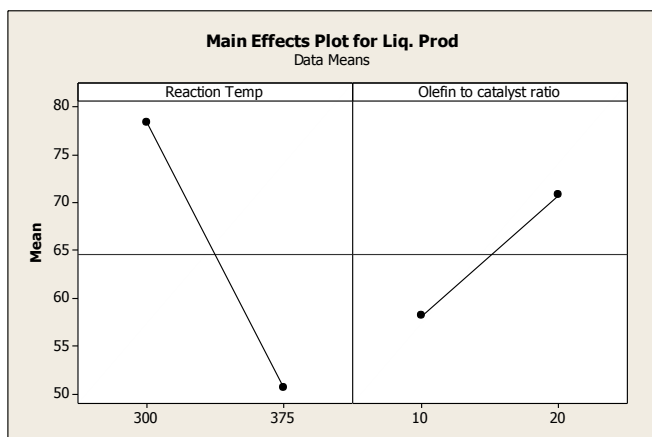
Figure 4. Main effects plots for % yield of liquid products.

Conclusions

Aromatics rich, naphtha - like, liquid products were produced by using HZSM-5 as a catalyst under mild conditions via catalytic cracking of 1-tetradecene. Temperature significantly increased the concentration of total BTEX, while olefin to catalyst ratio significantly decreased the concentration of BTEX in liquid products. These trends were significantly reversed for % yields of liquid products. This study, in future, may open doors for pure or waste 1-tetradecene to be used as a feedstock for the production of value-added aromatic compounds.

PRODUCTION OF BIO-BASED AROMATIC COMPOUNDS FROM CROP OIL

Swapnil Fegade[1], Swastika Bithi[1], Brian Tande[1], Wayne Seames[1], Darrin Muggli[2], Alena Kubátová[3], Evguenii Kozliak[3]

[1]Department of Chemical Engineering, University of North Dakota, 241 Centennial Drive, Stop 7101, Grand Forks, ND 58202-7101, USA

[2]Department of Engineering, Benedictine College, 1020 North 2nd Street Atchison, KS 66002, USA

[3]Department of Chemistry, University of North Dakota, Grand Forks, ND 58202,USA

Abstract

In this work we evaluate the feasibility of producing bio-based aromatic compounds from crop oil via catalytic cracking. Experiments were conducted in a continuous flow reactor by using doped zeolite catalysts. A design of experiments (DOE) strategy was applied and six factors were included. In the DOE analysis, the responses of interest were the selectivities for individual aromatics, such as benzene, toluene, ethylbenzene, and xylenes, as well as the overall yield of BTEX. It was found that reaction temperature and the amount of initial oil charged (oil to catalyst ratio) negatively influenced the overall aromatics yield, while dopant concentration was positively correlated to aromatic yields. A significant interaction between dopant concentration and initial oil charged was found and could be used for controlling toluene yield and thus overall BTEX yield. Our work

suggests that crop oils could be a very effective renewable feedstock for the production of aromatic compounds.

Introduction

Aromatic compounds such as benzenes, toluene ethylbenzene and xylenes (BTEX), are of greatest interest to the petrochemical industries and petroleum refineries because they are starting materials for manufacturing polymers, resins and elastomers. They are also present in gasoline to increase its octane rating. The most common use of BTEX is as solvents and thus they have unlimited applications. The promising method for the production of aromatic compounds (BTEX) is catalytic conversion [1, 2]. Currently, the primary source of BTEX, other aromatics and industrial organic chemicals is petroleum. Considering the limits of availability of petroleum, there is a need and growing interest in exploring the renewable resources for producing aromatics and organic chemicals. As we know that lignins are polymeric materials made of complex aromatic rings. There were several successful attempts made to prepare phenolics by the pyrolysis of lignin present in the wood [3]. In the oxidative environment, the pyrolysis and depolymerization of lignin based polymeric materials produce aromatic aldehydes; while reductive environment was responsible for producing alkyl phenols [4]. Crop oil can be converted into fuels and other hydrocarbons by catalytic cracking over HZSM-5, hydrogen-zeolite Y, silica –alumina, H-mordenite, silica alumina-pillared clay and other solid acid catalysts [5-9]. Among all catalysts, HZSM-5 showed the greatest selectivity to aromatics. Doped and composite catalyst (mesoporous molecular sieves and HZSM-5) and nano size ZSM-5 can also be used for increasing the conversion of crop oil into

aromatics[10-11]. In this present study, our main objective is apply the fractional factorial design of experiments strategy [12-14] for crop oil catalytic cracking process and to screen significant factors and interactions influencing aromatization of crop oils to produce BTEX. The other objective is to prepare a statistical model for this catalytic cracking process for efficient production of renewable aromatics.

Experimental

The experimental apparatus used in catalytic cracking and aromatization is shown in Figure 1. This batch catalyst reaction system contains four main components: an oil flask, a quartz reactor column, two condensers and a product collector.
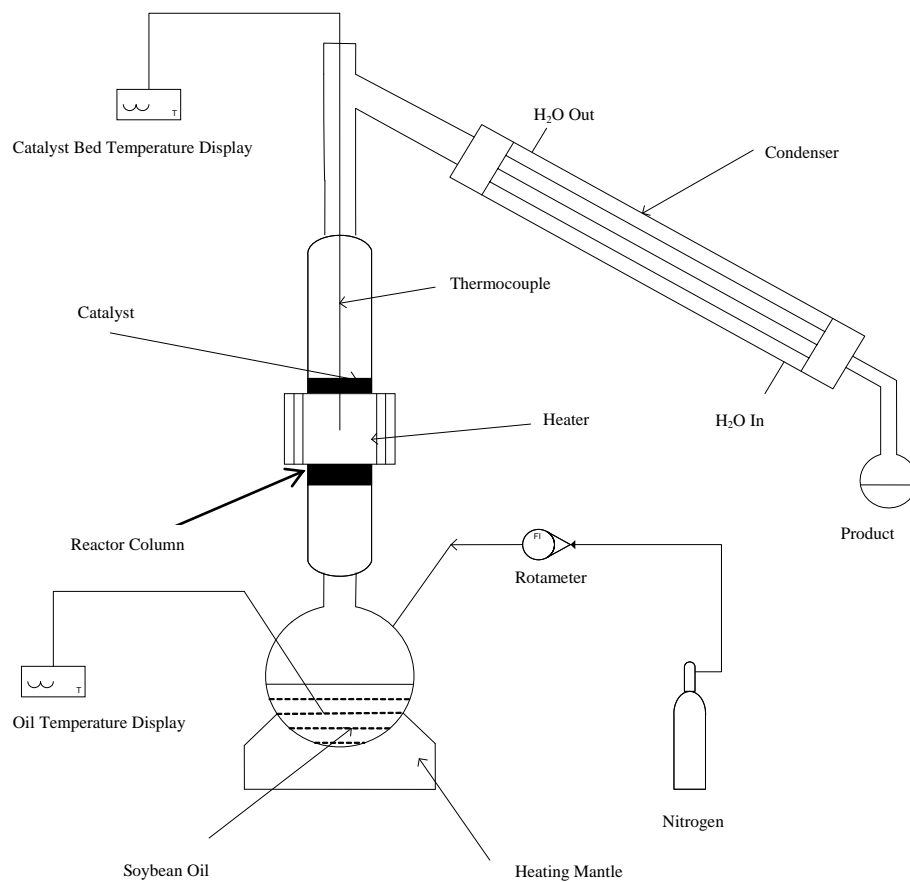
Figure 1. Experimental Setup for Cracking and Aromatization Reaction.

The total length of the quartz reactor column, connected to the center neck of the oil flask, was 300 mm. The reactor had a 24/40 top outer joint, sealed to 25 mm ID tubing and a 24/40 bottom inner joint. There were 5 indents above the inner joint.

Catalysts. Zeolite catalyst, ZSM-5(SiO_2/Al_2O_3 ratio 50) in the NH4–form, was purchased from Zeolyst International. The NH4-form was calcinated in air oven (500°C; 4h) to yield HZSM-5. Zn-ZSM-5 and Ga-ZSM-5 were prepared by a slight modification of the procedure by Saha et al. [15].

Fractional factorial design. A one-quarter (1/4), two level, resolution-IV fractional factorial screening design was constructed. Six factors were studied to determine their effects on seven responses. Because the design is of resolution IV, main effects are clear of two-factor interactions but two factor interactions are confounded with each other. The six factors studied were as follows:

Dopant identity (A); (Zn. Ga)

Dopant concentration (B); (0.5wt%, 3wt%)

Reaction temperature (C), (400, 500°C)

Initial oil charge (D);(37, 64g)

N_2 flow rate (E); (100, 150ml/min)

Reaction time (F); (80, 120 min)

For each experiment, exactly 8.19 g of catalyst was used. The oil heating rate was same for all 16 experiments. Seven responses (% yields of benzene, toluene, ethylbenzene, m-xylene, p-xylene, o-xylene and total BTEX) were measured during the cracking reactions.

The original experimental factors (uncoded units) were transformed into coded units and designated as −1 (low) and +1 (high).The net effect was found out by using a difference between the responses of high and low levels of factors. The relative strength of an estimated effect over the response was determined by its calculated value. Higher the value of the effect higher is the influence over the response. To evaluate the statistical significance of effects of factors, the probability value (p-Value) is used for the effect to be statistically significant, at a 95% confidence level the p-value should be less than or equal to 0.05. The most important part was to study the effect of interactions of factors. We have to define interaction when the effect of one factor relies on the adjustment of one or more other factors. An interaction between two factors is known as 'two way interaction'. The extent of an interaction can be defined as the difference between the average of half the responses and the average of the other half of the responses. For a fractional factorial design, manual estimation of above mentioned tasks becomes complicated and hence we used MINITAB^{TM} 15 as a tool for DOE analysis to obtain significant data, main effects, Pareto, interactions and other charts [13, 15].

Lab scale catalytic cracking and aromatization procedure. The catalyst bed was prepared between the bottom and top quartz wool sections inside the reactor. Then the thermocouple was inserted inside the reactor. The 4-neck flask contained certain weighed amounts of soybean oil. The reactor was then connected to the center neck of the flask.

Then the N_2 flow rate was set according to the experimental design by use of a rotameter. The reaction temperature was set in the temperature controller. Usually the catalyst bed temperature reached the set point within 20-30min. Then the oil started heating at a rate of 9.5°C/min until the oil temperature reached 405±5°C using the heating mantle. The mantle controller maintained this temperature throughout the reaction. Depending on the experiment, a cracking reaction was continued for 80-120 min and the condensed organic liquid product (OLP) was collected in the collection flask. A semi quantitative analysis of OLP was performed by using GC-FID.

Results and Discussion

All experimental runs were carried out according to the fractional factorial design. The analysis of this factorial design data was conducted at 95% confidence level.

Fig. 2a represents the pareto charts for yield of toluene. The vertical red line in this chart represents the line of significance, determined by using the 't' statistics. Any term having the effect/bar beyond this line, is called known a significant term. If a term is combined with another term in pareto chart, then it is known as the interaction term. For example, 'BD' in Fig. 2c shows the effect of the interaction between B (dopant concentration) and D (initial oil charged).

Factors and interactions influencing yield of toluene

From fig. 2a and 2b, it can be clearly seen that initial oil charge, reaction temperature and dopant concentration significantly influence the yield of toluene. Highest yield of toluene was observed when the dopant concentration was at a higher level and when the reaction temperature and initial oil charge were at a lower level. An interaction

211

of the factors, dopant concentration and initial oil charged, was found to have a significant effect on toluene yield. At a higher level of initial oil charge, the yield of toluene was almost the same, regardless of the level of dopant concentration. At a lower level of initial oil charge, toluene yield was increased and was the highest when the dopant concentration was raised to 3 %.

(2 a)
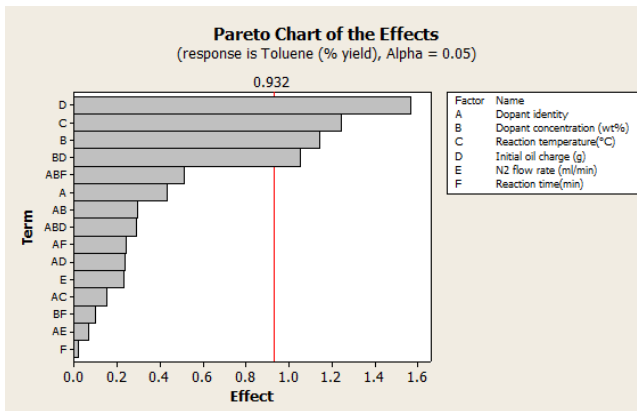
(2 b)
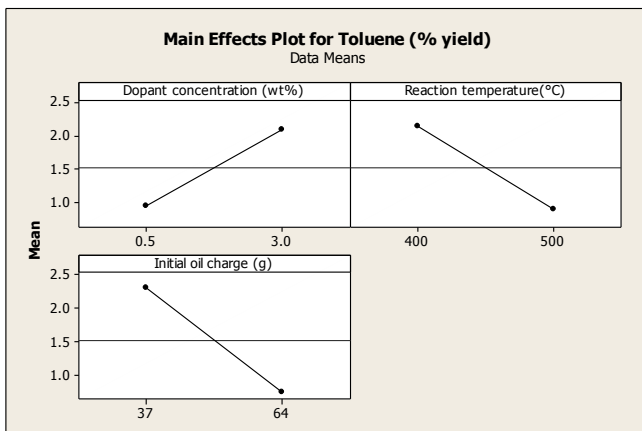
(2 c)
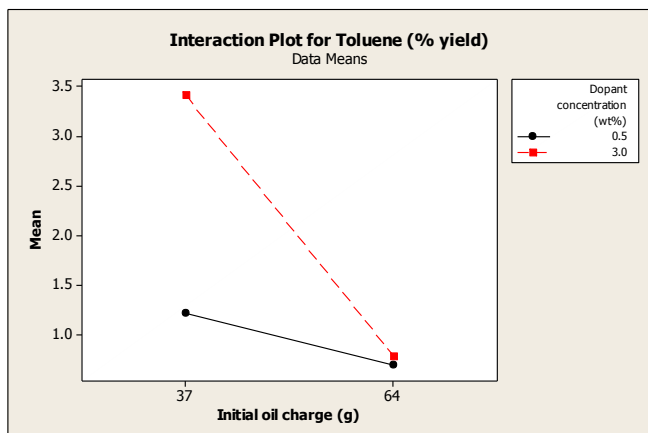
Figure 2. Pareto chart, main effects and interaction plots for toluene (% yield)

Factors and interactions influencing yields of xylenes

Fig. 3a, 3c, 3e represent Pareto charts and Fig. 3b, 3d, 4f represent the main effects plots for individual % yields of m-xylene, p-xylene and o-xylene respectively. It was found that initial oil charged was the only factor showing a significant effect on yields of all the individual xylenes. When the amount of initial oil charged was increased from 37 grams to 64 grams, the % yields of xylenes tend to decrease greatly. There were no interactions affecting the yields of xylenes.

(3 a)

Pareto Chart of the Effects
(response is m-xylene (% yield), Alpha = 0.05)

0.6214

Factor	Name
A	Dopant identity
B	Dopant concentration (wt%)
C	Reaction temperature(°C)
D	Initial oil charge (g)
E	N2 flow rate (ml/min)
F	Reaction time(min)

(3 b)

Main Effects Plot for m-xylene (% yield)
Data Means

(3 c)

Pareto Chart of the Effects
(response is p-xylene (% yield), Alpha = 0.05)

0.2321

Factor	Name
A	Dopant identity
B	Dopant concentration (wt%)
C	Reaction temperature(°C)
D	Initial oil charge (g)
E	N2 flow rate (ml/min)
F	Reaction time(min)

214

(3 d)

Main Effects Plot for p-xylene (% yield)
Data Means

(3 e)

Pareto Chart of the Effects
(response is o-xylene (% yield), Alpha = 0.05)

Factor	Name
A	Dopant identity
B	Dopant concentration (wt%)
C	Reaction temperature(°C)
D	Initial oil charge (g)
E	N2 flow rate (ml/min)
F	Reaction time(min)

(3 f)

Figure 3. Pareto charts and main effects plots for individual xylenes (% yield)

Factors and interactions influencing overall yield of total BTEX

Pareto chart of the effects is shown in Fig. 4a. It was observed that, the reaction temperature, initial oil charge and dopant concentration were the factors those showed a significant effect on the % yield of total BTEX. From Fig. 4b, it can be seen that the highest overall yield of total BTEX was observed when the dopant concentration was at a higher level. This is a clear indication of the fact that doped catalysts help in increasing the aromatics yields.

When the reaction temperature was increased from 400 ^{0}C to 500 ^{0}C, the overall yield of aromatics (BTEX) decreased. This may be because of the increase in coke formation at higher temperature. At higher temperatures, doped catalysts tend to increase the amounts of polycyclic aromatic hydrocarbons, which eventually leads to coke formation.

From Fig. 4b, it can be seen that an increase in amount initial oil charge significantly reduced the overall yield of aromatic compounds. Throughout this study, we kept the amount of catalyst loaded in the continuous reactor, constant for all the experiments. We only changed the amount of oil charged to the reactor and thus there was change in oil to catalyst ratio. Higher the amount of oil charged to the reactor, higher was the oil to catalyst ratio. When we increase amount of oil charged, that means we decreased the amount of catalyst available for the reaction. At a lower catalyst amount, the availability of active sites for the catalytic reaction was less and hence the overall yield of aromatic compounds was lower. We can conclude that lower oil to catalyst ratio was preferred for increasing aromatics yields.

We also found an interesting interaction of the factors, dopant concentration and initial oil charged, showing a significant effect on overall BTEX yield. At a higher level of initial oil charge, the yield of BTEX was almost the same, regardless of the level of dopant concentration. When amount of initial oil charged was decreased, the overall % yield of BTEX was increased and was the highest at increased dopant concentration. The confounding structure was 'BD+CF+ABEF+ACDE', and the factors C (reaction temperature and F (reaction time) were not significant. Both B (dopant concentration) and D (amount of initial oil charged) were significant and hence the BD interaction comes only from significant factors B and D only.

These doped catalysts were found to be very selective towards toluene. Since toluene contributed to the highest among all the aromatics yields, the results for overall BTEX yield and for toluene yield look similar. The dopant concentration-initial oil charged interaction could be used for controlling toluene yield and thus overall BTEX

yield. We found that the statistical approach is the only one best way to study the significant interactions of factors influencing the responses.

(4 a)

Pareto Chart of the Effects
(response is Total BTEX (% yield), Alpha = 0.05)

Factor	Name
A	Dopant identity
B	Dopant concentration (wt%)
C	Reaction temperature(°C)
D	Initial oil charge (g)
E	N2 flow rate (ml/min)
F	Reaction time(min)

(4 b)

Main Effects Plot for Total BTEX (% yield)
Data Means

(4 c)

Interaction Plot for Total BTEX (% yield)
Data Means
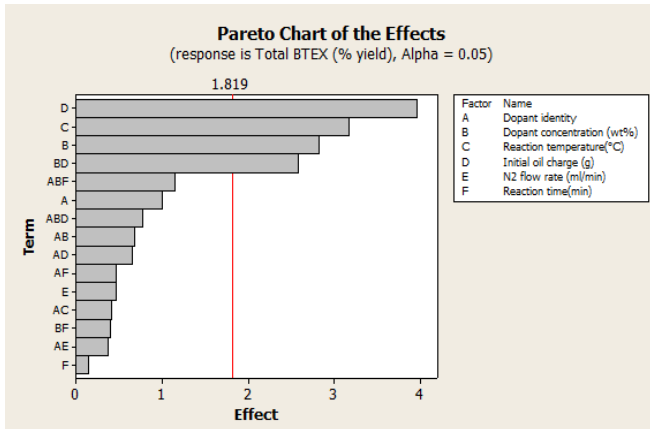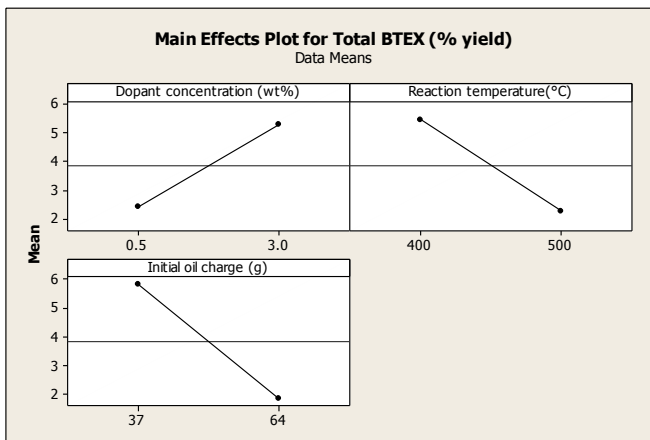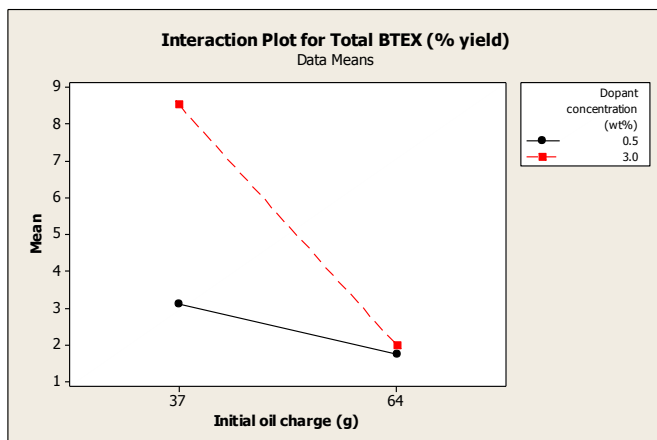
Figure 4. Pareto charts, main effects and interaction plots for total BTEX (% yield)

None of the factors or interactions showed significant effect on the yield of benzene and ethylbenzene.

Statistical model for % yield of total BTX

To propose the statistical model, there are three assumptions we need to prove true. These assumptions are, (1) Residuals should be randomly and normally distributed, (2) residuals should not correlate with the predicted Y, (3) residuals should not exhibit any trends over time [13]. We verified the validity of these assumptions by residual plots.

Based on the above interpretation and coefficients of estimated effects, the statistical model for coded units is as follows:

Total BTEX (% yield) = 3.836 + 1.416 Dopant concentration - 1.591 Reaction temperature - 1.984 Initial oil charged - 1.296 Dopant concentration* Initial oil charged.

Based on the interpretation and coefficients of estimated effects, the statistical model for uncoded units is as follows:

Total BTEX (% yield) = 16.8056 + 5.01030 Dopant concentration - 0.0318129 Reaction temperature - 0.0125981 Initial oil charged - 0.0767802 Dopant concentration* Initial oil charged.

These statistical models are applicable in the dopant concentration range of 0.5 wt %, 3 wt %, temperature range of 400 ^{0}C to 500 ^{0}C and initial oil charge range of 37 g to 64 g. Since there are more than two factors in this statistical model, contour plots were prepared to present this model in a graphical form. Fig. 5 represents the contour plots showing how the % yield of total BTEX relates to two factors (at low settings). The areas of highest BTEX yield are clearly visible in contour plots. A curved nature of contour level lines as shown in Fig. (5 a) confirms that dopant concentration-Initial oil charge interaction is significant.

(5 a)
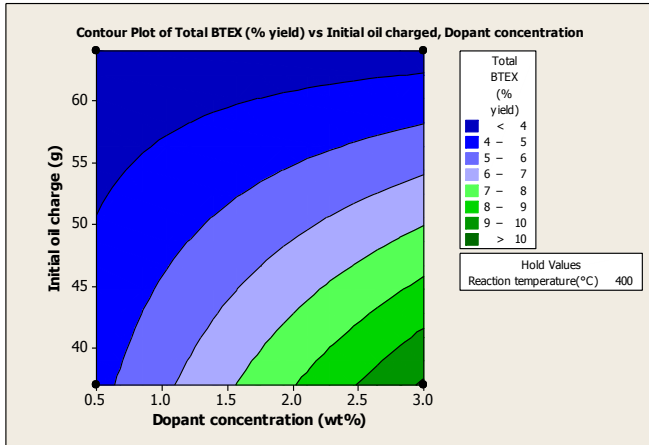
(5 b)
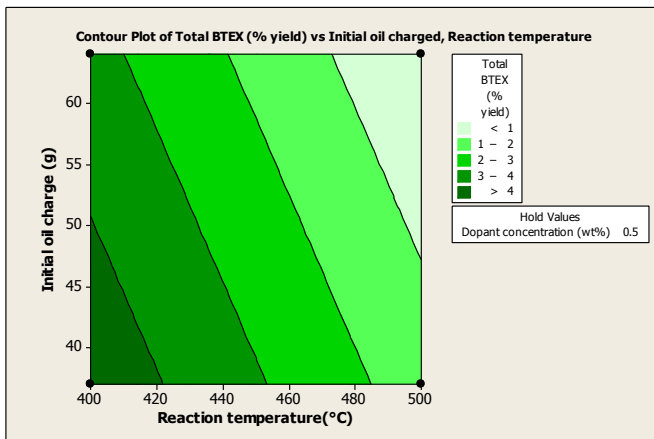
(5 c)
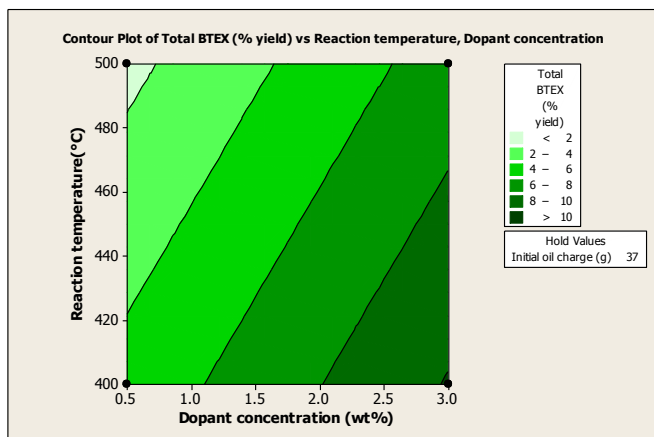
Figure 5. Contour plots for total BTEX (% yield)

Conclusions

Bio-based aromatic compounds can be produced from crop oil via catalytic cracking over doped zeolite catalysts. Reaction temperature, dopant concentration and the amount of initial oil charged to the reactor (oil to catalyst ratio) were the most significant factors for the overall aromatics yield. Dopant concentration positively influenced aromatic yields, while reaction temperature and amount of initial oil charged tend to affect the aromatics yield negatively. An interaction between dopant concentration and initial oil charged was found to be significantly affecting the toluene yield as well as the overall BTEX yield. These factors and interactions could be used for maximizing the yields of aromatic compounds. Crop oil could be very efficiently used as a renewable resource for manufacturing bio-based aromatic compounds.

222

DETERMINATION OF SIGNIFICANT FACTORS INFLUENCING AROMATIZATION OF PROPYLENE VIA STATISTICAL PATH

Swapnil L. Fegade[1], Hyunwook Cho[1], Brian Tande[1], Wayne Seames[1], Darrin Muggli[2], Evguenii Kozliak[3]

[1]Department of Chemical Engineering, University of North Dakota, 241 Centennial Drive, Stop 7101, Grand Forks, ND 58202-7101, USA

[2]Department of Engineering, Benedictine College, 1020 North 2nd Street   Atchison, KS 66002, USA

[3]Department of Chemistry, University of North Dakota, P.O. Box 9024, Grand Forks, ND 58202, USA

Introduction

Short chain, light, aliphatic hydrocarbons are of great interest for petrochemical industries and academic research units. There is a great need of converting these feedstocks into highly valuable products like aromatics. The most important aromatics are benzene, toluene and xylene (BTX) [1, 2]. Propylene (propene) is one of the lighter olefin hydrocarbon having limited applications including polypropylene, acrylics and propylene oxide manufacturing. Currently, the major amount of propylene comes from the petroleum refineries and petrochemical complexes during steam cracking and fluid

catalytic cracking (FCC) processes [3]. We are now moving from conventional fossil fuels to biofuels and it is clear that during the production of gasoline-like biofuels, a lot of propylene is also produced [4]. The catalytic activity tests for propylene on HY zeolites resulted in the formation of intermediates and oligomers [4]. Although the conversion of hydrocarbons to aromatic compounds over zeolite beta was successfully carried out [2], there is a very limited knowledge available on it. Propylene aromatization over ZSM-5 was studied and kinetic models were also developed to explain the steps and routes of aromatics formation [6]. The studies in the space velocity of feed stream and its impact on the product selectivity, and aromatics distribution at atmospheric pressure were successfully done for propylene and other alkanes aromatization reactions over ZSM-5 catalyst [7,8,9]. Although extensive work is being done on the conversion of propylene to aromatics, there is a lack of the use of systematic statistical approach under controlled reaction conditions for this process. In this present study, our main objective is apply the full factorial design of experiments strategy for catalytic reforming process and to screen significant factors and interactions influencing aromatization of propylene to produce BTX. The other objective is to prepare a statistical model for this catalytic reforming process.

Experimental

Zeolite catalysts ZSM-5 having Si:Al ratio of 50 and 80, were obtained in the powder form from Zeolyst International. These catalysts were commercially available in the ammonium forms. The activation of ZSM-5 catalysts was achieved by calcination at

500 ^{0}C for 5 hours to convert ammonium form into hydrogen form known as HZSM-5. High purity propylene gas and nitrogen was obtained from Praxair.

The catalytic activity tests to produce aromatic compounds from propylene were carried out in a continuous, down flow, tubular reactor having inner diameter of 0.4 inches and the length of about 10 inches. The reactor is surrounded by the furnace for the heating purpose. Fig. 1 shows the schematic diagram of the reaction setup.
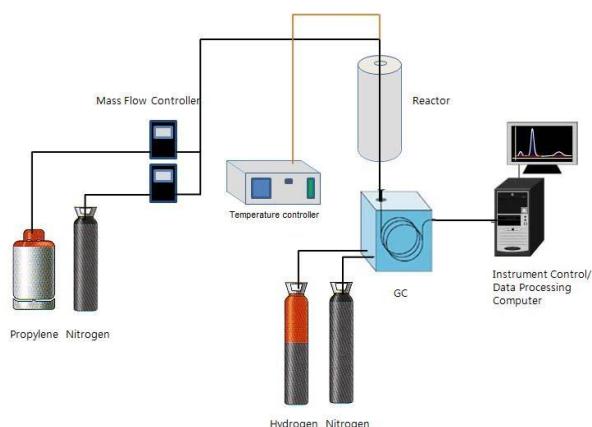
Figure 1. Schematic diagram of the propylene aromatization setup

An appropriate amount of activated catalyst was loaded on a quartz support to make a fixed bed in the reactor. The weight of quartz support was kept constant for all the experimental runs. A type K thermocouple was set at the center of the catalyst bed for proper temperature control. The products were analyzed by a in-line gas chromatograph, fitted with flame ionization detector (GC-FID).

Four factors, catalyst type, catalyst weight, propylene concentration and reaction temperature, were selected to study the responses, benzene, toluene, p-xylene, o-xylene, total xylenes produced. Each response was specified as its % yield calculated on the amount of carbon basis. A full factorial, two level, four factors design of experiments was

created to assess the factors those influence the aromatization of propylene. The low and high values of the factors are shown in Table 1.

Table 1. Factors and Their Low and High Values.

Factors	Si Al ratio of HZSM-5	Catalyst amount	propylene concentration	Reaction Temperature
Low level	50	0.2 (g)	8.9 (%)	400 (^{0}C)
High level	80	1 (g)	12.5 (%)	500 (^{0}C)

Four factors, two level design means minimum of $2^4 = 16$ runs should be performed [10]. No replicates were conducted. Each aromatization reaction run was performed until 400 minutes of reaction time and products were analyzed on GC-FID every 50 minutes.

The full factorial design created by using MINITAB^{TM} 15 was a random order design and the catalytic activity test experiments were conducted in this random order. The experimental data for all the 16 runs was analyzed by using MINITAB^{TM} 15 to obtain significant data, main effects, pareto, interactions and other charts.

Results and Discussion

All experimental runs were carried out according to the full factorial design. All the responses are in terms of the % yields of each aromatic component (BTX) as well as total BTX, calculated on the amount of carbon basis. The analysis of this factorial design data was conducted at 95% confidence level.

Pareto charts of the standardized effects

Fig. 2 represents the pareto charts for all the responses. The vertical red line in each chart represents the line of significance, determined by using the 't' statistics. Any term having the effect/bar beyond this line, is called known a significant term. If a term is combined with another term in pareto chart, then it is known as the interaction term. For example, 'CD' in Fig. 2. shows the effect of the interaction between C (propylene concentration) and D (catalyst amount) [10].

(2 a)

(2 b)

Pareto Chart of the Standardized Effects
(response is Toluene (% yield), Alpha = 0.05)

Factor	Name
A	Si/Al Ratio
B	Temperature (°C)
C	Propylene concentration (%)
D	Catalyst amount (g)

(2 c)

Pareto Chart of the Standardized Effects
(response is p-xylene (% yield), Alpha = 0.05)

Factor	Name
A	Si/Al Ratio
B	Temperature (°C)
C	Propylene concentration (%)
D	Catalyst amount (g)

(2 d)

Pareto Chart of the Standardized Effects
(response is o-xylene (% yield), Alpha = 0.05)

Factor	Name
A	Si/Al Ratio
B	Temperature (°C)
C	Propylene concentration (%)
D	Catalyst amount (g)

(2 e)

Figure 2. Pareto charts for standardized effects for % yields of (a) benzene, (b) toluene, (c) p-xylene, (d) o-xylene, and (e) total BTX.

Thus from Fig. 2, it can be inferred that Si:Al ratio and catalyst amount had the greatest significant effect on aromatization to produce all individual aromatics (benzene, toluene, p-xylene, o-xylene). The effect of reaction temperature is also significant for the yield of individual aromatics except p-xylene. Similarly, it can be seen that the effect of the interaction between propylene concentration and catalyst amount is significant for benzene and toluene production. The yields of p-xylene and o-xylenes are significantly affected by interaction between Si:Al ratio and propylene feed concentration. Apparently, the effect of interaction of Si:Al ratio and catalyst amount is close to be significant. In this study, since the yields of benzene and toluene accounts for more than 60 % yields of total aromatics for all the experiments, the results for total BTX and for individual yields of benzene and toluene are similar.

Effect of the Si:Al ratio of HZSM-5 on aromatization

Currently, there is limited knowledge available on the effect of Si:Al ratio on propylene aromatization. The catalytic activity of the HZSM-5 is mainly due to the Bronsted acid sites present in the bridging hydroxyl groups in the Si-O-Al triad. The active tetrahedral site (T - site) is occupied by tetrahedrally coordinated silicon and aluminum atom. Several theoretical studies have been conducted on locating the active T - site occupied by Al [11]. The feed propylene molecule gets adsorbed on the HZSM-5 at the active acid site and form adsorbed intermediates like alkoxides. The alkoxide formation is a very important step in propylene aromatization because it is responsible for β-scission and hydride transfer reactions. The protonation energy is required to form a protonated molecule when a feed propylene molecule comes in contact with Bronsted acid proton. This protonation energy also depends on the interaction between the zeolite catalyst wall and the protonated molecule. The alkoxide formation energies depend on zeolite structures. The Al sites greatly affect the energy of adsorption of propylene on ZSM-5[12-14]. The location and the number of Al sites change the catalytic activity. The proton affinity, acid strength and the binding energies are greatly influenced by the composition of ZSM-5 and its structure [15-16]. Although a lot of work has been done to study the Al content of the ZSM-5, most of the work was concentrated on the theoretical approaches. In this study we used an experimental approach including the statistical techniques for data analysis. We used HZSM-5 with Si:Al ratios of 50 and 80. For the ratio of 50, the available Al sites are more than that for Si:Al ratio of 80. In the HZSM-5 cluster, there are many active acid sites present near the aluminum atom. Thus it is clear from Fig. 3 that increasing Al content, consequently decreases the Si:Al ratio and

therefore, the catalytic activity increases. Hence, at the lower Si:Al ratio, % yields of BTX are higher and it can be concluded that the aromatization activity of HZSM-5 increases when the Si:Al ratio decreases.
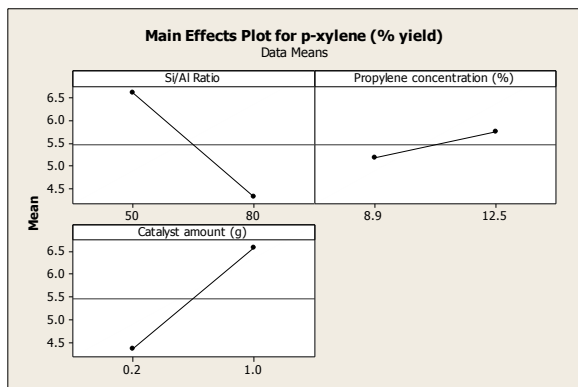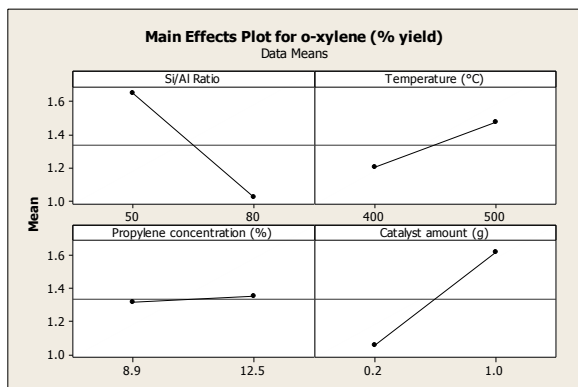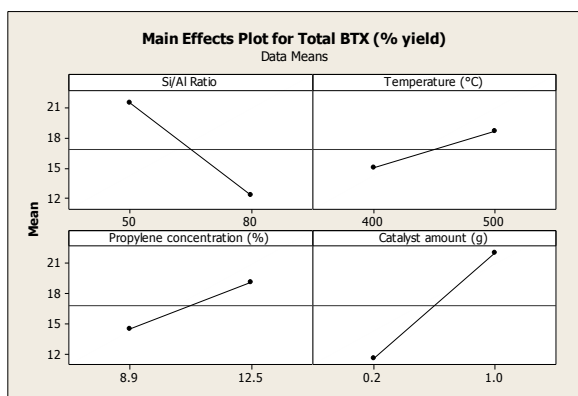
(3 a)
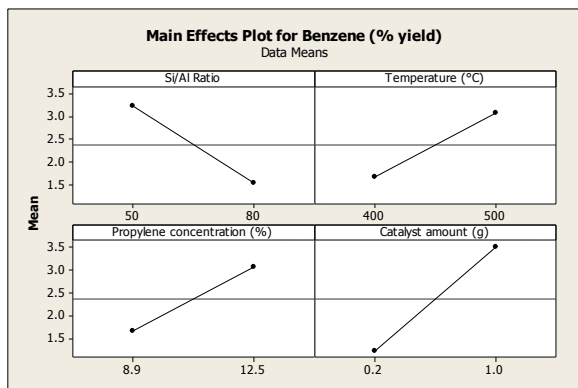
(3 b)
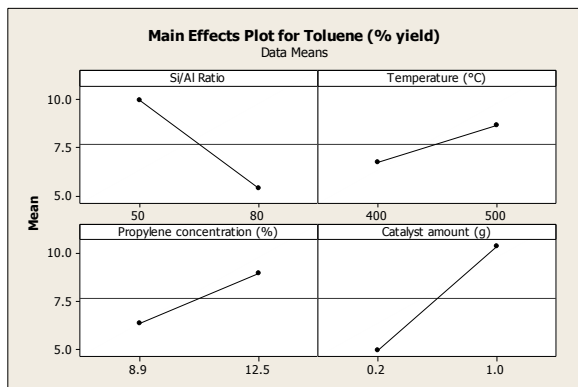
(3 c)

(3 d)

(3 e)

Figure 3. Main effects plots for % yields of (a) benzene, (b) toluene, (c) p-xylene, (d) o-xylene, and (e) total BTX.

Effect of the reaction temperature on aromatization

At lower and moderate temperatures the bridging hydroxyl groups in HZSM-5, form the hydrogen bonds with the neighboring oxygen atoms. With the increase in the temperatures, this hydrogen bond is broken and the availability of free bridging hydroxyl groups increases and thus the acidity and catalytic activity increases. At the higher temperatures, the protons defeat the barrier for activation by acquiring the required energy [17-18]. Thus, the temperature positively affects the acidity of HZSM-5 and hence

there is a significant increase in the aromatics yields at the higher temperature as shown in Fig. 3.

Effect of the propylene feed concentration, catalyst amount on aromatization

When the feed hydrocarbon stream passes through the HZSM-5 pore system, some of the feed molecules fill the straight channels and some fill the sinusoidal channels of the catalyst cluster [19]. In our study, we found that increasing the feed propylene concentration, also increases the yields of all the aromatics as seen in the Fig. 3. At the lower propylene feed concentration, some molecules do not fill the HZSM5 channels and because of the nitrogen, they are pushed through the void spacing between the catalyst particles. When we increase the feed concentration, more propylene molecules are available to fill up both the channels and hence there is an increase in the % yield of benzene, toluene, and xylenes. When we increase the catalyst amount, there is an increase in the number of active protonation and acid sites available; which eventually yields more aromatics. This is confirmed from the main effects plots for catalyst amount shown in Fig. 3.

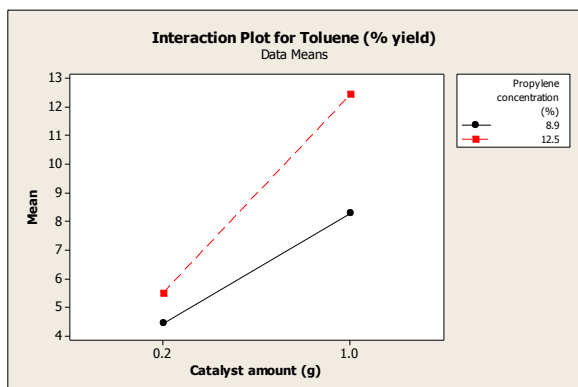**Effects of the significant interactions**

Currently, in the academic as well as industrial research, hydrocarbon feed and catalyst amount are combined into a single factor known as gas hourly space velocity (GHSV). In this present study, we used the 'feed propylene concentration' and 'catalyst amount' as separate factors and found that the effect of interaction between these two factors was also found significant (shown in Fig. 3). The interaction plots for benzene, toluene and total BTX yields, are given in the Fig. 4 (a), 4(b), and 4 (e). It was observed that higher feed concentration is favored for aromatization. There is a little difference in

the responses at 0.2 g of catalyst, but when the catalyst amount is increased to 1 g, the difference between the aromatics yields at 8.9 % and 12.5 % increases abruptly. Thus it can be concluded that a slight increase in propylene concentration and catalyst amount, significantly increases the aromatics yield. Thus the proper balance between the levels of these factors is very important to control the yields of benzene and toluene for process optimization.
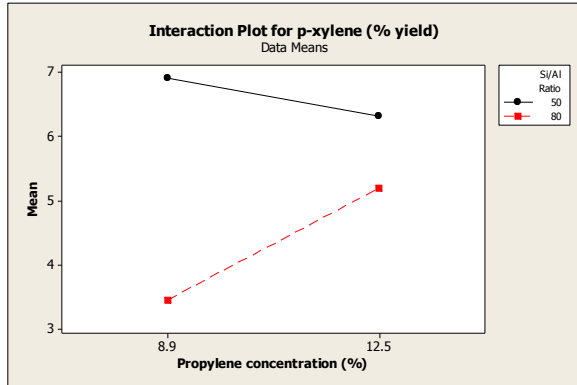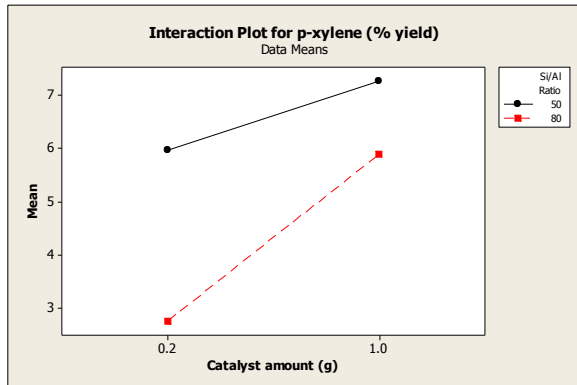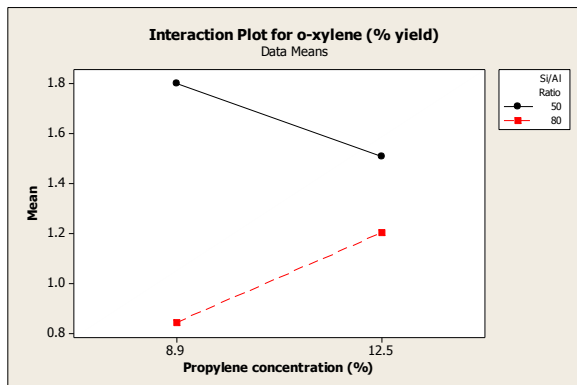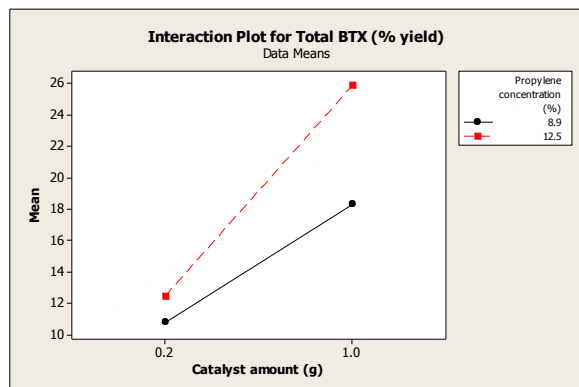
(4 a)
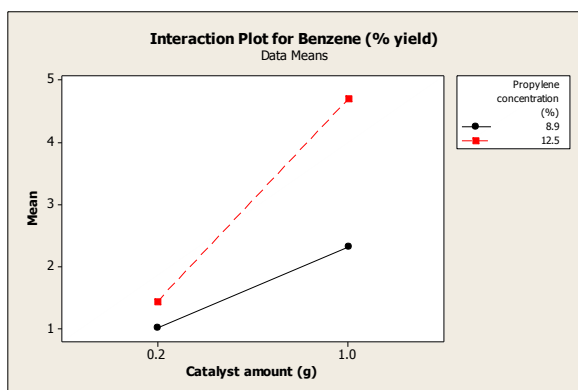
(4 b)

(4 c1)

(4 c2)

(4 d)

(4 e)

Figure 4. Significant interaction effects plots for (a) benzene, (b) toluene, (c1 & c2) p-xylene, (d) o-xylene, and (e) total BTX.

From Fig. 4 (c1) and (d), it was observed that there is a significant interaction effect on xylenes, between the factors Si:Al ratio and propylene feed concentration. For Si:Al ratio of 80, there is increase in response when feed concentration is increased, but for Si:Al ratio of 50, the response is reversed and there are more xylenes produced at lower propylene concentration. Thus it is clear that the increase in the Al content in the catalyst helps in increasing xylene production even at lower feed concentrations. The decrease in the response for xylenes at higher feed concentration may be due to the possible alkylation and isomerization of xylenes in the presence of increased propylene concentration. It looks like that the HZSM-5 having Si:Al ratio of 50 tends to have higher alkylation and isomerization ability than that having ratio of 80.

The interaction of Si:Al ratio with the catalyst amount also had a significant effect on p-xylene yield. When the catalyst amount was kept constant at 0.2 g, the difference in the % yields of p-xylene at Si:Al of 50 and 80 is very large. This difference is very small

when the catalyst amount is 1 g. This concludes that lower amount of catalyst with Si:Al ratio of 50, is required for higher p-xylene selectivity.

We found that the statistical approach is the only one best way to study the significant interactions of factors influencing the responses.

Statistical model for % yield of total BTX

Based on the above interpretation and coefficients of estimated effects, the statistical model for coded units is as follows:

Total BTX (% yield) = 16.8 − 4.59 (Si:Al ratio) + 1.80 (temperature) + 2.32 (propylene concentration) + 5.23 (catalyst amount) + 1.47 (propylene concentration*catalyst amount).

Based on the interpretation and coefficients of estimated effects, the statistical model for uncoded units is as follows:

Total BTX (% yield) = 12.0 − 0.306(Si:Al ratio) + 0.0360(temperature) + 0.0654(propylene concentration) - 8.72(catalyst amount) + 2.04 (propylene concentration*catalyst amount).

These statistical models are applicable in the Si:Al ratio range of 50 to 80, temperature range of 400 ^{0}C to 500 ^{0}C, propylene feed concentration range of 8.9 % to 12.5 %, and catalyst amount range of 0.2g to 1g. Since there are more than two factors in this statistical model, contour plots were prepared to present this model in a graphical

form. Fig. 5 represents the contour plots showing how the % yield of total BTX relates to two factors (at high settings). The areas of highest BTX yield are clearly visible in contour plots. A curved nature of contour level lines as shown in Fig. (5 b) confirms that propylene concentration-catalyst amount interaction is significant.
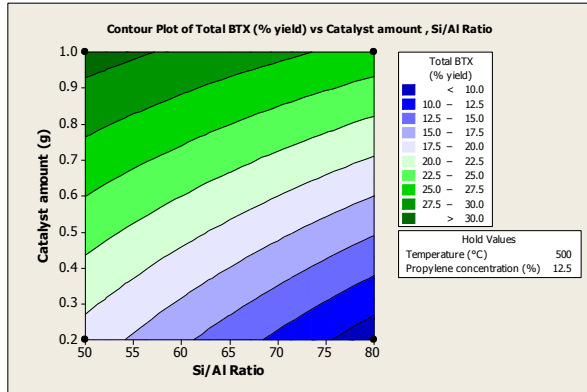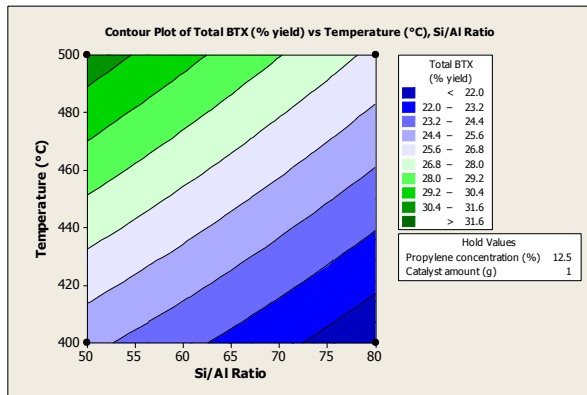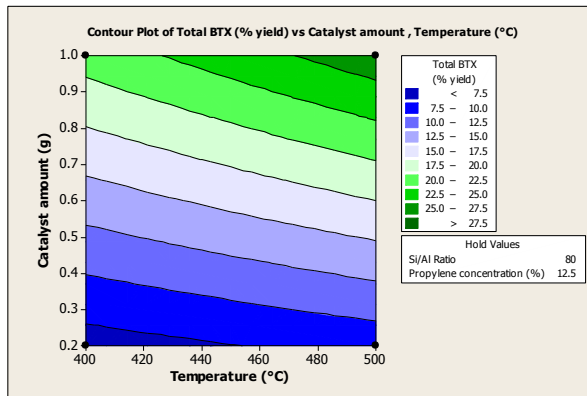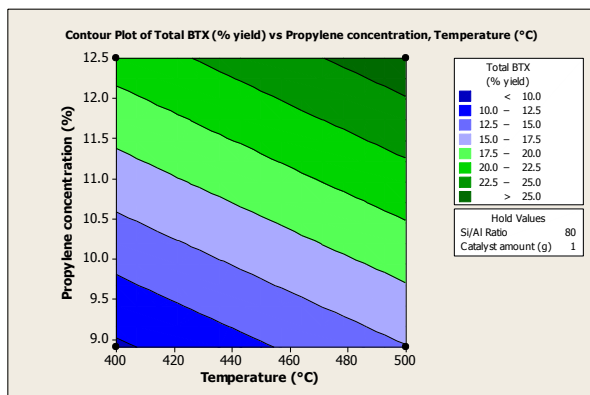
(5 a)

(5 b)

(5 c)

(5 d)

(5 e)

239
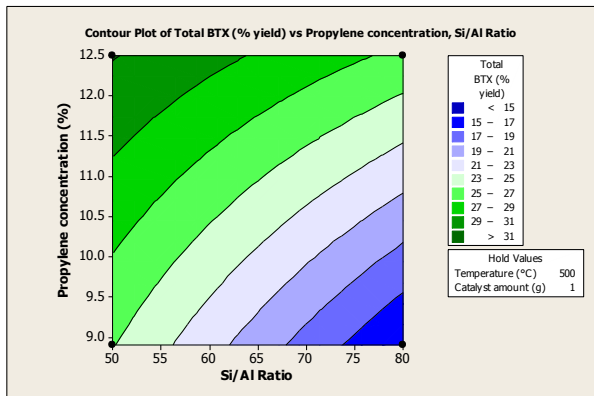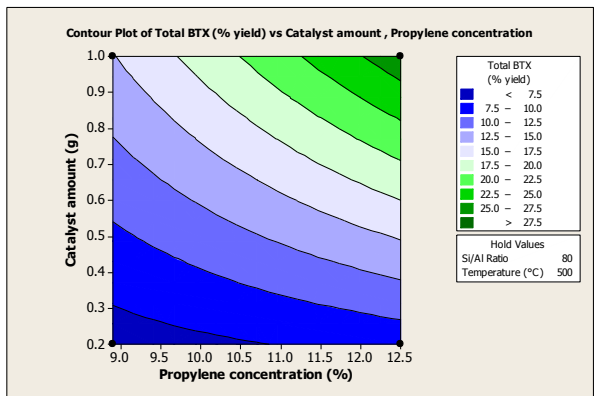
(5 f)

Figure 5. Contour plots for total BTX yield.

Conclusions

For maximizing the yields of all aromatics, the most influential parameters are HZSM-5 Si:Al ratio and the catalyst amount taken for the reforming process. The reaction temperature tends to affect % yields of benzene, toluene, o-xylene and total BTX; while the effect of feed concentration is significant for yielding benzene, toluene and total BTX only. The most striking point found out from this study, was the effect of interaction between initial propylene feed concentration and amount of catalyst, and it is significant for producing benzene, toluene and total BTX. Si:Al ratio-feed concentration interaction only impacts % yields of xylenes. These interactions are important for controlling the yield a particular individual aromatic compound. For maximizing the overall aromatics yields, Si:Al ratio of catalyst should be at lower level, and all the other reaction conditions should be set at higher levels. Statistical models for both the coded as well as uncoded units were successfully proposed for the prediction of total BTX yield and it can be concluded that a statistical approach is necessary for studying the interaction effects of factors.

References

[1] R. A. Meyers. *Handbook of petroleum refining processes*. McGraw-Hill, 2003.

[2] G. J. Antos,, Aitani, A. M. Aitani, J. M. Parera. *Catalytic Naphtha Reforming : Science and Technology*. Dekker, 1995.

[3] A. J. Ragauskas, C. K. Williams, B. H. Davison, G. Britovsek, J. Cairney, C. A. Eckert, W. J. Frederick Jr., J. P. Hallett, D. J. Leak, C. L. Liotta, J. R. Mielenz, R. Murphy, R. Templer and T. Tschaplinski. The path forward for biofuels and biomaterials. *Science 311(5760),* pp. 484-489. 2006.

[4] J. Scott. *Zeolite Technology and Applications : Recent Advances*. Park Ridge, 1980.

[5] A. Kubátová, Y. Luo, J. Štávová, S. M. Sadrameli, T. Aulich, E. Kozliak and W. Seames. New path in the thermal cracking of triacylglycerols (canola and soybean oil). *Fuel 90(8),* pp. 2598-2608. 2011.

[6] Y. Luo. Master's thesis, Chemical Engineering, University of North Dakota. 2006.

[7] B. A.V. Renewable fuels and chemicals by thermal processing of biomass. *Chem. Eng. J. 91(2–3),* pp. 87-102. 2003.

[8] J. Q. Bond, D. M. Alonso, D. Wang, R. M. West and J. A. Dumesic. Integrated catalytic conversion of γ-valerolactone to liquid alkenes for transportation fuels. *Science 327(5969),* pp. 1110-1114. 2010.

[9] L. T. H. Nam, T. Q. Vinh, N. T. T. Loan, V. D. S. Tho, X. Yang and B. Su. Preparation of bio-fuels by catalytic cracking reaction of vegetable oil sludge. *Fuel 90(3),* pp. 1069-1075. 2011.

[10] E. Kozliak, R. Mota, D. Rodriguez, P. Overby, A. Kubátová, D. Stahl, V. Niri, G. Ogden and W. Seames. Non-catalytic cracking of jojoba oil to produce fuel and chemical by-products. *Industrial Crops and Products 43(1),* pp. 386-392. 2013.

[11] R. O. Idem, S. P. Katikaneni, N. N. Bakhshi. Thermal cracking of canola oil: reaction products in the presence and absence of steam. *Energy & Fuels*, 10(6), pp. 1150-1162.1996

[12] W. Seames, Y. Luo, I. Ahmed, T. Aulich, A. Kubátová, J. Št'ávová and E. Kozliak. The thermal cracking of canola and soybean methyl esters: Improvement of cold flow properties. *Biomass Bioenergy 34(7),* pp. 939-946. 2010.

[13] B. Tande, W. Seames, "Production of aromatics from noncatalytically cracked fatty acid based oils," CA 2831485 A1, Oct 26, 2012.

[14] J. Weitkamp, L. Puppe. *Catalysis and Zeolites : Fundamentals and Applications.* Springer, 1999.

[15] J. Ancheyta-Juárez and E. Villafuerte-Macías. Kinetic modeling of naphtha catalytic reforming reactions. *Energy and Fuels 14(5),* pp. 1032-1037. 2000.

[16] G. Zahedi, S. Mohammadzadeh and G. Moradi. Enhancing gasoline production in an industrial catalytic-reforming unit using artificial neural networks. *Energy and Fuels 22(4),* pp. 2671-2677. 2008.

[17] B. Cornils, A. Herrmann, R. Schogl, C. Wong. *Catalysis for A to Z. Concise Encyclopedia.* 2000.

[18] J. G. Speight. *The chemistry and technology of petroleum.* CRC press, 2014.

[19] F. Zaera. Selectivity in hydrocarbon catalytic reforming: A surface chemistry perspective. *Applied Catalysis A: General 229(1-2),* pp. 75-91. 2002.

[20] A. Askari, H. Karimi, M. R. Rahimi and M. Ghanbari. Simulation and modeling of catalytic reforming process. *Petroleum & Coal 54(1),* pp. 76-84. 2012.

[21] P. Tamunaidu and S. Bhatia. Catalytic cracking of palm oil for the production of biofuels: Optimization studies. *Bioresour. Technol. 98(18),* pp. 3593-3601. 2007.

[22] N. S. Gnep, J. Y. Doyemet and M. Guisnet. Conversion of light alkanes into aromatic hydrocarbons. 3. aromatization of propane and propene on mixtures of HZSM5 and of Ga_2O_3. *Studies in Surface Science and Catalysis 46(C),* pp. 153-162. 1989.

[23] J. Ancheyta-Juárez and E. Villafuerte-Macías. Kinetic modeling of naphtha catalytic reforming reactions. *Energy and Fuels 14(5),* pp. 1032-1037. 2000.

[24] B. S. Kwak and W. M. H. Sachtler. Aromatization of propane over zn/HZSM-5 catalysts prepared by chemical vapor deposition. *Korean Journal of Chemical Engineering 13(4),* pp. 356-363. 1996.

[25] B. S. Kwak, W. M. H. Sachtler and W. O. Haag. Catalytic conversion of propane to aromatics: Effects of adding Ga and/or Pt to HZSM-5. *Journal of Catalysis 149(2),* pp. 465-473. 1994.

[26] B. Liu, Y. Yang and A. Sayari. Non-oxidative dehydroaromatization of methane over ga-promoted mo/HZSM-5-based catalysts. *Applied Catalysis A: General 214(1),* pp. 95-102. 2001.

[27] M. Rodrigues, M. Barre, P. Magnoux, V. R. Choudhary and M. Guisnet. Coking, aging and regeneration of zeolites. XVIII coking and deactivation of HZSM-5 and ga/HZSM-5 catalysts during propene aromatization. *J. Chim. Phys. Phys. -Chim. Biol. 93(2),* pp. 317-330. 1996.

[28] X. C. Shen, H. Lou, K. Hu and X. M. Zheng. Non-oxidative aromatization of C1 to C3 hydrocarbons over pd-promoted ga/HZSM-5 catalyst under mild conditions. *Chinese Chemical Letters 18(4),* pp. 479-482. 2007.

[29] A. Smiešková, E. Rojasová, P. Hudec and L. Šabo. Study of the role of zn in aromatization of light alkanes with probe molecules. *Reaction Kinetics and Catalysis Letters 82(2),* pp. 227-234. 2004.

[30] Y. Sun and T. C. Brown. Catalytic cracking, dehydrogenation, and aromatization of isobutane over ga/HZSM-5 and zn/HZSM-5 at low pressures. *Int J Chem Kinet 34(8),* pp. 467-480. 2002.

[31] N. Viswanadham, A. R. Pradhan, N. Ray, S. C. Vishnoi, U. Shanker and T. S. R. Prasada Rao. Reaction pathways for the aromatization of paraffins in the presence of H-ZSM-5 and zn/H-ZSM-5. *Applied Catalysis A: General 137(2),* pp. 225-233. 1996.

[32] H. You. Influence of aromatization reaction conditions in the presence of HZSM-5 catalyst. *Petrol Sci Technol 24(6),* pp. 707-716. 2006.

[33] J. F. Haw, B. R. Richardson, I. S. Oshiro, N. D. Lazo and J. A. Speed. Reactions of propene on zeolite HY catalyst studied by in situ variable-temperature solid-state nuclear magnetic resonance spectroscopy. *J. Am. Chem. Soc. 111(6),* pp. 2052-2058. 1989.

[34] D. B. Lukyanov, N. S. Gnep and M. R. Guisnet. Kinetic modeling of ethene and propene aromatization over HZSM-5 and GaHZSM-5. *Industrial and Engineering Chemistry Research 33(2),* pp. 223-234. 1994.

[35] T. V. Choudhary, A. Kinage, S. Banerjee and V. R. Choudhary. Influence of si/ga and si/al ratios on propane aromatization over highly active H-GaAlMFI. *Catalysis Communications 7(3),* pp. 166-169. 2006.

[36] V. R. Choudhary, D. Panjala and S. Banerjee. Aromatization of propene and n-butene over H-galloaluminosilicate (ZSM-5 type) zeolite. *Applied Catalysis A: General 231(1-2),* pp. 243-251. 2002.

[37] V. R. Choudhary, A. K. Kinage, C. Sivadinarayana and M. Guisnet. Pulse reaction studies on variations of initial activity/selectivity of O2 and H2 pretreated ga-modified ZSM-5 type zeolite catalysts in propane aromatization. *Journal of Catalysis 158(1),* pp. 23-33. 1996.

[38] V. R. Choudhary and P. Devadas. Influence of space velocity on product selectivity and distribution of aromatics and xylenes in propane aromatization over H-GaMFI zeolite. *Journal of Catalysis 172(2),* pp. 475-478. 1997.

[39] H. Lechert, C. Bezouhanova, C. Dimitrov and V. Nenova. Intermediates in the formation of aromatics from propene and 2-propanol on H-zsm-5 zeolites. *Studies in Surface Science and Catalysis 46(C),* pp. 91-98. 1989.

[40] M. Huang and S. Kaliaguine. Propene aromatization over alkali-exchanged ZSM-5 zeolites. *Journal of Molecular Catalysis 81(1),* pp. 37-49. 1993.

[41] A. Bhan and W. N. Delgass. Propane aromatization over HZSM-5 and ga/HZSM-5 catalysts. *Catalysis Reviews - Science and Engineering 50(1),* pp. 19-151. 2008.

[42] R. V. Lenth. Quick and easy analysis of unreplicated factorials. *Technometrics 31(4),* pp. pp. 469-473. 1989.

[43] S. S. Arzumanov, A. A. Gabrienko, D. Freude and A. G. Stepanov. In situ high temperature MAS NMR study of the mechanisms of catalysis. ethane aromatization on zn-modified zeolite BEA. *Solid State Nucl. Magn. Reson. 35(2),* pp. 113-119. 2009.

[44] X. Zhu, S. Liu, Y. Song, S. Xie and L. Xu. Catalytic cracking of 1-butene to propene and ethene on MCM-22 zeolite. *Applied Catalysis A: General 290(1-2),* pp. 191-199. 2005.

[45] J. Lawson and J. Erjavec. *Modern Statistics for Engineering and Quality Improvement.* Duxbury Press, 2000.

[46] J. A. Van Bokhoven, T. Lee, M. Drakopoulos, C. Lamberti, S. Thie and J. Zegenhagen. Determining the aluminium occupancy on the active T-sites in zeolites using X-ray standing waves. *Nature Materials 7(7),* pp. 551-555. 2008.

[47] A. Bhan, Y. V. Joshi, W. N. Delgass and K. T. Thomson. DFT investigation of alkoxide formation from olefms in H-ZSM-5. *J Phys Chem B 107(38),* pp. 10476-10487. 2003.

[48] P. Sarv, C. Fernandez, J. Amoureux and K. Keskinen. Distribution of tetrahedral aluminium sites in ZSM-5 type zeolites: An 27Al (multiquantum) magic angle spinning NMR study. *J. Phys. Chem. 100(50),* pp. 19223-19226. 1996.

[49] G. Krishnamurthy, A. Bhan and W. N. Delgass. Identity and chemical function of gallium species inferred from microkinetic modeling studies of propane aromatization over ga/HZSM-5 catalysts. *Journal of Catalysis 271(2),* pp. 370-385. 2010.

[50] N. O. Gonzales, A. K. Chakraborty and A. T. Bell. A density functional theory study of the effects of metal cations on the brønsted acidity of H-ZSM-5. *Catalysis Letters 50(3-4),* pp. 135-139. 1998.

[51] M. J. Rice, A. K. Chakraborty and A. T. Bell. Al next nearest neighbor, ring occupation, and proximity statistics in ZSM-5. *Journal of Catalysis 186(1),* pp. 222-227. 1999.

[52] K. Sillar and P. Burk. Computational study of vibrational frequencies of bridging hydroxyl groups in zeolite ZSM-5. *Chemical Physics Letters 393(4-6),* pp. 285-289. 2004.

[53] K. Sillar and P. Burk. Hybrid quantum chemical and density functional theory (ONIOM) study of the acid sites in zeolite ZSM-5. *J Phys Chem B 108(28),* pp. 9893-9899. 2004.

[54] M. Firoozi, M. Baghalha and M. Asadi. The effect of micro and nano particle sizes of H-ZSM-5 on the selectivity of MTP reaction. *Catalysis Communications 10(12),* pp. 1582-1585. 2009.

[55] Z. Jing, Z. Liang, C. Guojing, W. Haiyan, W. Min and M. Jun. The aromatization properties of nano-HZSM-5 catalyst. *Petrol Sci Technol 26(5),* pp. 586-592. 2008.

[56] M. Khatamian, A. A. Khandar, M. Haghighi and M. Ghadiri. Nano ZSM-5 type ferrisilicates as novel catalysts for ethylbenzene dehydrogenation in the presence of N2O. *Appl. Surf. Sci. 258(2),* pp. 865-872. 2011.

[57] N. Viswanadham, R. Kamble, M. Singh, M. Kumar and G. Murali Dhar. Catalytic properties of nano-sized ZSM-5 aggregates. *Catalysis Today 141(1-2),* pp. 182-186. 2009.

[58] K. Wang and X. Wang. Comparison of catalytic performances on nanoscale HZSM-5 and microscale HZSM-5. *Microporous and Mesoporous Materials 112(1–3),* pp. 187-192. 2008.

[59] H. Long, X. Wang, W. Sun and X. Guo. Conversion of n-octene over nanoscale HZSM-5 zeolite. *Catalysis Letters 126(3-4),* pp. 378-382. 2008.

[60] P. Zhang, X. Wang and H. Guo. Reducing olefins in FCC gasoline by isomerization and aromatization over modified nano-ZSM-5. *Chinese Journal of Catalysis 24(3),* pp. 159-160. 2003.

[61] Y. Cheng, R. H. Liao, J. S. Li, X. Y. Sun and L. J. Wang. Synthesis research of nanosized ZSM-5 zeolites in the absence of organic template. *J. Mater. Process. Technol. 206(1–3),* pp. 445-452. 2008.

[62] Y. Ni, A. Sun, X. Wu, G. Hai, J. Hu, T. Li and G. Li. The preparation of nano-sized H[zn, al]ZSM-5 zeolite and its application in the aromatization of methanol. *Microporous and Mesoporous Materials 143(2-3),* pp. 435-442. 2011.

[63] J. Zhu, W. T. Wu, Y. Chang, X. H. Sun and H. Y. Wang. Application of nano-HZSM-5 catalyst on aromatization of FCC gasoline. *Petrol Sci Technol 28(1),* pp. 7-12. 2010.

[64] D. Breck. *Zeolite molecular sieves*. Krieger, 1984.

[65] G. Krishnamurthy, A. Bhan and W. N. Delgass. Identity and chemical function of gallium species inferred from microkinetic modeling studies of propane aromatization over Ga/HZSM-5 catalysts. *Journal of Catalysis 271(2),* pp. 370-385. 2010.

[66] S. K. Saha and S. Sivasanker. Influence of Zn- and Ga-doping on the conversion of ethanol to hydrocarbons over ZSM-5. *Catalysis Letters 15(4),* pp. 413-418. 1992.

[67] Y. Zhang, Y. Zhou, A. Qiu, Y. Wang, Y. Xu and P. Wu. Effect of alumina binder on catalytic performance of PtSnNa/ZSM-5 catalyst for propane dehydrogenation. *Industrial and Engineering Chemistry Research 45(7),* pp. 2213-2219. 2006.

[68] J. S. Buchanan, D. H. Olson and S. E. Schramm. Gasoline selective ZSM-5 FCC additives: Effects of crystal size, SiO2/Al2O3, steaming, and other treatments on ZSM-5 diffusivity and selectivity in cracking of hexene/octene feed. *Applied Catalysis A: General 220(1-2),* pp. 223-234. 2001.

[69] Y. Li, S. Liu, S. Xie and L. Xu. Promoted metal utilization capacity of alkali-treated zeolite: Preparation of zn/ZSM-5 and its application in 1-hexene aromatization. *Applied Catalysis A: General 360(1),* pp. 8-16. 2009.

[70] H. Long, X. Wang and W. Sun. Study of n-octene aromatization over nanoscale HZSM-5 zeolite. *Microporous and Mesoporous Materials 119(1-3),* pp. 18-22. 2009.

[71] S. L. Fegade, S. Bithi, B. Tande, W. Seames, D. Muggli, A. Kubátová and E. Kozliak. Production of bio-based aromatic compounds from crop oil. *ACS National Meeting Book of Abstracts*. 2011.

[72] S. L. Fegade, B. Tande, W. Seames, A. Kubátová and E. Kozliak. Triglycerides as an alternative feedstock for manufacturing aromatic compounds. A*CS National Meeting Book of Abstracts*. 2011.

[73] S. L. Fegade, B. M. Tande, H. Cho, W. S. Seames, I. Sakodynskaya, D. S. Muggli and E. I. Kozliak. Aromatization of propylene over hzsm-5: A design of experiments (DOE) approach. *Chem. Eng. Commun. 200(8),* pp. 1039-1056. 2013.

[74] S. L. Fegade, B. Tande, W. Seames, A. Kubátová and E. Kozliak. Catalytic conversion of 1-tetradecene to aromatic compounds over zeolites under mild conditions. *ACS National Meeting Book of Abstracts*. 2011.

[75] S. L. Fegade, H. Cho, B. Tande, W. Seames, D. Muggli and E. Kozliak. Determination of significant factors influencing the aromatization of propylene via statistical path. *ACS National Meeting Book of Abstracts*. 2011.

[76] R. J. Nash, M. E. Dry and C. T. O'Connor. Aromatization of 1-hexene and 1-octene by gallium/H-ZSM-5 catalysts. *Applied Catalysis A: General 134(2),* pp. 285-297. 1996.

[77] Y. Li, S. Liu, Z. Zhang, S. Xie, X. Zhu and L. Xu. Aromatization and isomerization of 1-hexene over alkali-treated HZSM-5 zeolites: Improved reaction stability. *Applied Catalysis A: General 338(1-2),* pp. 100-113. 2008.

[78] G. R. Lappin and J. D. Sauer. *Alpha Olefins Applications Handbook.* CRC Press, 1989.

[79] D. L. Burdick and W. L. Leffler. *Petrochemicals in Nontechnical Language.* Pennwell Books, 2001.

[80] H. Wittcoff, B. G. Reuben, J. S. Plotkin. *Industrial organic chemicals.* John Wiley & Sons, 2012.

[81] ASTM Committee D-2 on Petroleum Products and Lubricants., American Petroleum Institute. Refining Dept. Technical Data Committee., Pennsylvania State University. Dept. of Chemical Engineering. and ASTM Committee D-2 on Petroleum Products and Lubricants. *Physical Constants of Hydrocarbon and Non-Hydrocarbon Compounds* 1991.

[82] J. Koivumäki. Properties of ethylene/1-octene, 1-tetradecene and 1-octadecene copolymers obtained with Cp_2ZrCl_2/MAO catalyst: Effect of composition and comonomer chain length. *Polymer Bulletin 36(1),* pp. 7-12. 1996.

[83] V. Kotzabasakis, N. Petzetakis, M. Pitsikalis, N. Hadjichristidis and D. J. Lohse. Copolymerization of tetradecene-1 and octene-1 with silyl-protected 10-undecen-1-ol using a C_s-symmetry hafnium metallocene catalyst. A route to functionalized poly(α-olefins). *J. Polym. Sci. Part A 47(3),* pp. 876-886. 2009.

[84] A. I. Akhmedov and A. M. Levshina. Copolymers of decyl methacrylate with tetradecene as VI Improvers. *Chem. Technol. Fuels Oils 22(5-6),* pp. 300-301. 1986.

[85] J. Štávová, D. C. Stahl, W. S. Seames and A. Kubátová. Method development for the characterization of biofuel intermediate products using gas chromatography with simultaneous mass spectrometric and flame ionization detections. *Journal of Chromatography A 1224*pp. 79-88. 2012.

[86] P. Qiu, J. Lunsford, M. Rosynek. Characterization of Ga/ZSM-5 for the catalytic aromatization of dilute ethylene streams. *Catalysis letters*. *52(1-2)*, 37-42. 1998.

[87] D. Olson, G. Kokotailo, S. Lawton and W. Meier. Crystal structure and structure-related properties of ZSM-5. *J. Phys. Chem. 85(15),* pp. 2238-2243. 1981.

[88] T. J. Benson, R. Hernandez, M. G. White, W. Todd French, E. E. Alley, W. E. Holmes and B. Thompson. Heterogeneous cracking of an unsaturated fatty acid and reaction intermediates on H+ZSM-5 catalyst. *Clean - Soil, Air, Water 36(8),* pp. 652-656. 2008.

[89] H. E. Jegers and M. T. Klein. Primary and secondary lignin pyrolysis reaction pathways. *Industrial and Engineering Chemistry Process Design and Development 24(1),* pp. 173-183. 1985.

[90] B. Valle, A. G. Gayubo, A. T. Aguayo, M. Olazar and J. Bilbao. Selective production of aromatics by crude bio-oil valorization with a nickel-modified HZSM-5 zeolite catalyst. *Energy and Fuels 24(3),* pp. 2060-2070. 2010.

[91] Y. Cheng, Z. Wang, C. J. Gilbert, W. Fan and G. W. Huber. Production of p-xylene from biomass by catalytic fast pyrolysis using ZSM-5 catalysts with reduced pore openings. *Angewandte Chemie International Edition 51(44),* pp. 11097-11100. 2012.

[92] P. Duan and P. E. Savage. Upgrading of crude algal bio-oil in supercritical water. *Bioresour. Technol. 102(2),* pp. 1899-1906. 2011.

[93] P. A. Horne and P. T. Williams. The effect of zeolite ZSM-5 catalyst deactivation during the upgrading of biomass-derived pyrolysis vapours. *J. Anal. Appl. Pyrolysis 34(1),* pp. 65-85. 1995.

[94] P. A. Horne and P. T. Williams. Upgrading of biomass-derived pyrolytic vapours over zeolite ZSM-5 catalyst: Effect of catalyst dilution on product yields. *Fuel 75(9),* pp. 1043-1050. 1996.

[95] T. P. Vispute, H. Zhang, A. Sanna, R. Xiao and G. W. Huber. Renewable chemical commodity feedstocks from integrated catalytic processing of pyrolysis oils. *Science 330(6008),* pp. 1222-1227. 2010.

[96] Q. Zhang, J. Chang, T. Wang and Y. Xu. Review of biomass pyrolysis oil properties and upgrading research. *Energy Conversion and Management 48(1),* pp. 87-92. 2007.

[97] J. D. Adjaye and N. N. Bakhshi. Production of hydrocarbons by catalytic upgrading of a fast pyrolysis bio-oil. part I: Conversion over various catalysts. *Fuel Process Technol 45(3),* pp. 161-183. 1995.

[98] J. D. Adjaye and N. N. Bakhshi. Production of hydrocarbons by catalytic upgrading of a fast pyrolysis bio-oil. part II: Comparative catalyst performance and reaction pathways. *Fuel Process Technol 45(3),* pp. 185-202. 1995.

[99] J. D. Adjaye, S. P. R. Katikaneni and N. N. Bakhshi. Catalytic conversion of a biofuel to hydrocarbons: Effect of mixtures of HZSM-5 and silica-alumina catalysts on product distribution. *Fuel Process Technol 48(2),* pp. 115-143. 1996.

[100] R. O. Idem, S. P. R. Katikaneni and N. N. Bakhshi. Catalytic conversion of canola oil to fuels and chemicals: Roles of catalyst acidity, basicity and shape selectivity on product distribution. *Fuel Process Technol 51(1-2),* pp. 101-125. 1997.

[101] N. Mo and P. E. Savage. Hydrothermal catalytic cracking of fatty acids with HZSM-5. *ACS Sustainable Chemistry and Engineering 2(1),* pp. 88-94. 2014.

[102] J. Mikulec, J. Cvengroš, Ľ Joríková, M. Banič and A. Kleinová. Second generation diesel fuel from renewable sources. *J. Clean. Prod. 18(9),* pp. 917-926. 2010.

[103] Y. Ooi, R. Zakaria, A. R. Mohamed and S. Bhatia. Catalytic conversion of palm oil-based fatty acid mixture to liquid fuel. *Biomass Bioenergy 27(5),* pp. 477-484. 2004.

[104] S. M. Sadrameli, A. E. S. Green and W. Seames. Modeling representations of canola oil catalytic cracking for the production of renewable aromatic hydrocarbons. *J. Anal. Appl. Pyrolysis 86(1),* pp. 1-7. 2009.

[105] H. M. Teeter, E. W. Bell and M. J. Danzig. Reactions of conjugated fatty acids. VII. catalytic cyclization and aromatization of cis,trans-octadecadienoic acid with selenium. *J. Org. Chem. 23(8),* pp. 1156-1158. 1958.

[106] K. D. Maher and D. C. Bressler. Pyrolysis of triglyceride materials for the production of renewable fuels and chemicals. *Bioresour. Technol. 98(12),* pp. 2351-2368. 2007.

[107] T. Ngo, J. Kim, S. K. Kim and S. Kim. Pyrolysis of soybean oil with H-ZSM5 (proton-exchange of zeolite socony Mobil #5) and MCM41 (mobil composition of matter no. 41) catalysts in a fixed-bed reactor. *Energy 35(6),* pp. 2723-2728. 2010.

[108] S. Gandhi, J. Kadrmas, J. Šťávová, A. Kubátová, D. Muggli, W. S. Seames, S. M. Sadrameli and B. M. Tande. Extraction of fatty acids from noncatalytically cracked triacylglycerides with water and aqueous sodium hydroxide. *Sep. Sci. Technol. 47(1),* pp. 66-72. 2012.

[109] E. Kozliak, R. Mota, D. Rodriguez, A. Kubatova, D. C. Stahl, V. H. Niri, G. Ogden and W. S. Seames. Non-catalytic cracking of jojoba oil to produce fuel and chemical by-products. 20th International Congress of Chemical and Process Engineering and PRES 2012 - 15th Conference PRES. 2012 .

[110] A. Kubátová, Y. Luo, J. Šťávová, S. M. Sadrameli, T. Aulich, E. Kozliak and W. Seames. New path in the thermal cracking of triacylglycerols (canola and soybean oil). *Fuel 90(8),* pp. 2598-2608. 2011.

[111] C. M. R. Prado and N. R. Antoniosi Filho. Production and characterization of the biofuels obtained by thermal cracking and thermal catalytic cracking of vegetable oils. *J. Anal. Appl. Pyrolysis 86(2),* pp. 338-347. 2009.

[112] S. P. R. Katikaneni, J. D. Adjaye, R. O. Idem and N. N. Bakhshi. Performance studies of various cracking catalysts in the conversion of canola oil to fuels and chemicals in a fluidized-bed reactor. *JAOCS, Journal of the American Oil Chemists' Society 75(3),* pp. 381-391. 1998.

[113] J. A. Melero, M. M. Clavero, G. Calleja, A. García, R. Miravalles and T. Galindo. Production of biofuels via the catalytic cracking of mixtures of crude vegetable oils and nonedible animal fats with vacuum gas oil. *Energy and Fuels 24(1),* pp. 707-717. 2010.

[114] T. J. Benson, R. Hernandez, W. T. French, E. G. Alley and W. E. Holmes. Elucidation of the catalytic cracking pathway for unsaturated mono-, di-, and triacylglycerides on solid acid catalysts. *Journal of Molecular Catalysis A: Chemical 303(1–2),* pp. 117-123. 2009.

[115] M. P. Braegelmann, A. D. Azure, D. C. Stahl, A. Kubátová, W. S. Seames and B. M. Tande. Extraction of fatty acids from noncatalytically cracked triacylglycerides using aqueous amines. *Sep. Sci. Technol. 46(14),* pp. 2167-2173. 2011.

[116] Y. Luo, I. Ahmed, A. Kubátová, J. Štávová, T. Aulich, S. M. Sadrameli and W. S. Seames. The thermal cracking of soybean/canola oils and their methyl esters. *Fuel Process Technol 91(6),* pp. 613-617. 2010.

[117] D. M. Bibby, N. B. Milestone, J. E. Patterson and L. P. Aldridge. Coke formation in zeolite ZSM-5. *Journal of Catalysis 97(2),* pp. 493-502. 1986.

[118] K. -. Lee, M. -. Kang and S. -. Ihm. Deactivation by coke deposition on the HZSM-5 catalysts in the methanol-to-hydrocarbon conversion. *Journal of Physics and Chemistry of Solids 73(12),* pp. 1542-1545. 2012.

[119] K. I. Patrilyak, L. K. Patrilyak, V. V. Ivanenko, M. V. Okhrimenko and Y. G. Voloshina. Oscillatory motion of coke in deactivated HZSM-5 zeolite. *Theoretical and Experimental Chemistry 46(4),* pp. 256-262. 2010.

[120] I. Torre, J. M. Arandes, M. J. Azkoiti, M. Olazar and J. Bilbao. Cracking of coker naphtha with gas-oil. effect of HZSM-5 zeolite addition to the catalyst. *Energy and Fuels 21(1),* pp. 11-18. 2007.

[121] H. G. Karge, J. Weitkamp. *Characterization II*, Springer, 2007.

[122] K. D. Maher and D. C. Bressler. Pyrolysis of triglyceride materials for the production of renewable fuels and chemicals. *Bioresour. Technol. 98(12),* pp. 2351-2368. 2007.

[123] K. M. Doll, B. K. Sharma, P. A. Z. Suarez and S. Z. Erhan. Comparing biofuels obtained from pyrolysis, of soybean oil or soapstock, with traditional soybean biodiesel: Density, kinematic viscosity, and surface tensions. *Energy and Fuels 22(3),* pp. 2061-2066. 2008.

[124] C. R. A. Catlow. *Modelling of Structure and Reactivity in Zeolites* 1992.

[125] S. Ernst. *Advances in nanoporous materials.* Elsevier, 2009.

[126] K. Kim and H. Ahn. The effect of pore structure of zeolite on the adsorption of VOCs and their desorption properties by microwave heating. *Microporous and Mesoporous Materials 152*pp. 78-83. 2012.

[127] R. V. Lenth. Quick and easy analysis of unreplicated factorials. *Technometrics Technometrics 31(4),* pp. 469-473. 1989.

[128] B. A. Bodt. *Modern Statistics for Engineering and Quality Improvement*. Technometrics, 2002.

[129] H. E. Jegers and M. T. Klein. Primary and secondary lignin pyrolysis reaction pathways. *Industrial and Engineering Chemistry Process Design and Development 24(1),* pp. 173-183. 1985.

[130] E. Dorrestijn, L. J. J. Laarhoven, I. W. C. E. Arends and P. Mulder. Occurrence and reactivity of phenoxyl linkages in lignin and low rank coal. *J. Anal. Appl. Pyrolysis 54(1),* pp. 153-192. 2000.

[131] C. WANG, Q. HAO, D. LU, Q. JIA, G. LI and B. XU. Production of light aromatic hydrocarbons from biomass by catalytic pyrolysis. *Chinese Journal of Catalysis 29(9),* pp. 907-912. 2008.

[132] J. A. Melero, M. M. Clavero, G. Calleja, A. García, R. Miravalles and T. Galindo. Production of biofuels via the catalytic cracking of mixtures of crude vegetable oils and nonedible animal fats with vacuum gas oil. *Energy and Fuels 24(1),* pp. 707-717. 2010.

[133] S. P. R. Katikaneni, J. D. Adjaye, R. O. Idem and N. N. Bakhshi. Performance studies of various cracking catalysts in the conversion of canola oil to fuels and chemicals in a fluidized-bed reactor. *JAOCS, Journal of the American Oil Chemists' Society 75(3),* pp. 381-391. 1998.

[134] W. Seames, Y. Luo, I. Ahmed, T. Aulich, A. Kubátová, J. Šťávová and E. Kozliak. The thermal cracking of canola and soybean methyl esters: Improvement of cold flow properties. *Biomass Bioenergy 34(7),* pp. 939-946. 2010.